



**HAL**  
open science

## Etude fonctionnelle de la protéine associée aux microtubules XMAP215/ch-TOG

Claudia Paez

► **To cite this version:**

Claudia Paez. Etude fonctionnelle de la protéine associée aux microtubules XMAP215/ch-TOG. Biologie cellulaire. Université de Grenoble, 2011. Français. NNT : 2011GRENV014 . tel-00597065

**HAL Id: tel-00597065**

**<https://theses.hal.science/tel-00597065>**

Submitted on 31 May 2011

**HAL** is a multi-disciplinary open access archive for the deposit and dissemination of scientific research documents, whether they are published or not. The documents may come from teaching and research institutions in France or abroad, or from public or private research centers.

L'archive ouverte pluridisciplinaire **HAL**, est destinée au dépôt et à la diffusion de documents scientifiques de niveau recherche, publiés ou non, émanant des établissements d'enseignement et de recherche français ou étrangers, des laboratoires publics ou privés.

## THÈSE

Pour obtenir le grade de

## DOCTEUR DE L'UNIVERSITÉ DE GRENOBLE

Spécialité : **Biologie cellulaire**

Arrêté ministériel : 7 août 2006

Présentée par

**Claudia PAEZ**

Thèse dirigée par **Monsieur le Professeur François BERGER**

préparée au sein du **Laboratoire Nanomédecine et cerveau.**  
**Grenoble Institut des Neurosciences**  
**INSERM U836**

dans l'**École Doctorale Chimie et Sciences du Vivant**

# Etude fonctionnel de la Protéine associée aux Microtubules XMAP215/ch-TOG

Thèse soutenue publiquement le **29 Avril 2011**  
devant le jury composé de :

**Monsieur le Dr. Marc SAVASTA**

Directeur, Ecole doctorale Chimie et Sciences du Vivant, Grenoble.  
Président du Jury

**Monsieur le Dr. Matthieu PIEL**

Chef d'équipe à l'Institut Curie, Paris. Rapporteur

**Monsieur le Dr. Phong TRAN**

Chef d'équipe à l'Institut Curie, Paris. Rapporteur

**Monsieur le Pr. François BERGER**

Directeur d'équipe au Grenoble Institut des Neurosciences (GIN).  
Examineur





*They (the cosmos explorations) remind us that humans are evolved to wonder, that understanding is a joy, that knowledge is a prerequisite to survival...*

*Those explorations required skepticism and imagination both. Imagination will often carry us to worlds that never were. But without it we go nowhere. Skepticism enables us to distinguish fancy from fact, to test our speculations. The cosmos is rich beyond measure – in elegant facts, in exquisite interrelationships, in the subtle machinery of awe.*

Carl Sagan, *Cosmos*.

*Astrophysicist*



## ACKNOWLEDGMENTS

I would like to thank Professors **Mathieu PIEL** and **Phong TRAN** for refereeing this thesis manuscript. It's a privilege for me that professionals of such international reputation have accepted to judge my work.

I do not have enough words to express my gratitude to the Joseph Fourier University, in particular to its president, **Mr Farid Ouabdesselam**. His helping and fair hand made possible that an objective might come true.

I am really grateful with the members of the Joseph's Fourier Doctoral School CSV (Chimie and Sciences du Vivant). Especially I would like to extend my warmest gratitude to its director, **Dr Marc Savasta**. Thanks a lot for his professional and human support that finally allow me to reach the end.

To Dr **François Berger** at the Grenoble Institut of Neurosciences (GIN), I do express my gratitude. Thanks for accepting me in to your group, an acceptance made with open arms. Thanks for your support and kindness through all this time.

I would like to thank, **Dr Andrei Popov** at the GIN. His accurate guidance through the course of my PhD studies was a key element in my development as a scientist.

Thanks to each one of the members of team 7 at the GIN. These professionals assumed day after day the heroic and courageous effort to deal with my franglais, decorated with an ethnic touch of colombian spanish.

Thanks to the great professionals and scientist that made all this work possible:

Thanks to **Emannuelle Neumann** at the **IBS institute**. A great scientist that made possible the electron microscopy experiments. Thanks for your kindness, professionalism and open minded criteria.

Thanks to **Alexei Grichine**, at the **IAB institute**. A well recognize international authority in the imaging domain, but above all a great human being with a huge sense of humor. The laughs allow me to survive many afternoons of bored and almost never ending imaging analysis. Thanks for your unconditional support.

Thanks to **Dr Didier Grundwald** at the **CEA (Grenoble)**. His help, kindness, enthusiasm and professionalism during the acquisition of the confocal images were determinant for this research.

Thanks to those brave scientists that using the sense of sacrifice and courage read this up-side-down manuscript. Because of their efforts, time, good will and patience, they succeeded to transform all those chaotic pages in to a scientific dissertation. Thanks to Michelle, Jean Paul and Jean-Marc. Please guys, the next time do not forget to check the bibliography...

Next, I must thank infinitely to Catherine Rapin. A generous and open minded angel on earth, that one day decided to give me not only a hand, but also a home, a family and great friends. I must say thanks to each one of the members of this wonderful and giving family that expressed an unlimited generosity, they tolerate an alien among them and this grateful alien was treated as one of them. God bless you all.

Thanks to Constanza, the brain and heart behind this project. Thanks for being so stubborn, not accepting a no for an answer. Thanks for listening, for your prayers, for being there... for so many years already. Thanks for the advices, the trust, the free sharing since the early years of this adventure.

Thanks to Svetlana, pure energy coming from the distant Siberia. Thanks for the inner peace, wisdom and compassion message transmitted systematically through years... *мышь спасибо много велемудрая.*

Thanks to Slaveia... for the adulthood minded criteria, the faith, freedom and for keeping this friendship safe through the distance and time.

Thanks to Mailyn. I just can say: God bless you. You were a light in the dark... only a true friend dares to do so. Gracias

Thanks to the selected members of the Pick-Assietes Grenoble Club. To Vincent, Carmen, Claude, Stephanie, Carole, Fabienne, Nicole and Jean-Jacques. Thanks for accepting my modest candidature to enjoy your taxes....

Thanks to Nicole. Thanks for the free thinking and the open minded sharing, the unlimited generosity, the freedom, the solidarity, the complexity and simplicity of the friendship... thanks for everything.

Thanks to Soline, that funny little and generous fairy that made this manuscript and my thesis defence possible... 100% pure handcraft. Thanks to Aurelien, Jao and Eliseo... for their laughs.

I must thank my beloved third world. Thanks a lot for the ever lasting hope, for the wisdom of the chaos, for the never-ending positivism, for the short term memory law, for the warm and friendly no reason every day smile...

I must thank to my beloved ones. Thanks to Mom and Dad, my angels. You encouraged me to follow my dreams at my way. Thanks for the freedom to growing up as a wild-type human being, thanks for the respect for each one of my projects and for the non question inner law. Thanks to every single member of this loving and mad family that excerced individually or collectively as a hybrid among Sigmund Freud and a Tibetan monk... thanks a lot for the brightest words in the darkest times.

At the end, it is time to say thanks to my beginning. Thanks to the light, thanks to the love, thanks to Abba...

# CONTENTS

ACKNOWLEDGEMENTS	I
LIST OF ABBREVIATIONS	III
CONTENTS	IV
FIGURES LIST	XI
TABLES LIST	XII
SUMMARY	1
RESUME	3
<b>GENERAL INTRODUCTION</b>	<b>5</b>
<b>1. The cell and its cell cycle</b>	<b>7</b>
<b>1.1 The cell</b>	<b>7</b>
<b>1.2 The cell cycle</b>	<b>7</b>
<b>1.3 Mitosis phases</b>	<b>9</b>
1.3.1 Interphase	9
1.3.2 Prophase	9
1.3.3 Prometaphase	9
1.3.4 Metaphase	10
1.3.5 Anapahase	10
1.3.6 Telophase	10
1.3.7 Cytokinesis	10
<b>2. Cytoskeleton</b>	<b>13</b>
<b>2.1 Microtubules</b>	<b>15</b>
2.1.1 The dynamic instability model	17
2.1.2 Tubulin post-translational modifications	18



<b>3. MAPs and the Plus-end-tracking proteins (+ TIPS)</b>	<b>21</b>
<b>3.1 Differential mechanism</b>	<b>23</b>
<b>3.2 EB1 (Ending Binding Protein 1)</b>	<b>25</b>
3.2.1 EB1 Structure	26
3.2.2 EB1 Interactions	27
<b>3.3 CLIP170 (Cytoplasmic Linker Protein 170)</b>	<b>28</b>
3.3.1 CLIP170 structure	28
3.3.2 CLIP170 interactions	29
<b>3.4 p150<sup>Glued</sup></b>	<b>30</b>
3.4.1 p150 <sup>Glued</sup> structure	32
3.4.2 p150 <sup>Glued</sup> interactions	32
<b>3.5 Regulation of + TIPS interactions</b>	<b>33</b>
3.5.1 Specific sequences	33
3.5.2 Phosphorylation	34
3.5.3 Mechanical implications	36
3.5.4 $\alpha$ -tubulin tyrosination-detyrosination	36
3.5.5 The GTP cap	37
3.5.6 Autoinhibition complexes or co-regulation?	38
<b>4. The XMAP215/Dis1family</b>	<b>41</b>
<b>4.1 Protein Structures: conserved repeat motifs</b>	<b>42</b>
<b>4.2 Cellular localization of XMAP215/Dis1 proteins</b>	<b>44</b>
<b>4.3 XMAP215</b>	<b>46</b>
4.3.1 XMAP215 and tubulin dimmers	48
<b>4.4 ch-TOG</b>	<b>49</b>
<b>4.5 XMAP215/ch-TOG mapping</b>	<b>50</b>
<b>RESEARCH AIMS</b>	<b>55</b>

<b>METHODS</b>	57
<b>5. Anti XMAP215/ch-TOG mcAB production</b>	57
<b>5.1 XMAP215 characterization</b>	57
5.1.1 mcAB antibodies obtention	57
5.1.2 Cell Fixing and Immunofluorescence	58
<b>5.2 mcAB Characterization</b>	61
5.2.1 mcAB Specificity	61
5.2.1.1 mcAB specificity: egg extract obtention	61
5.2.1.2 mcAB specificity: XMAP215 depletion	63
5.2.1.3 mcAB Class	64
5.2.1.4 mcAB epitopes cartography	64
5.2.1.5 Fixed cells imaging	65
<b>5.3 XMAP215 <i>in vitro</i> interaction</b>	66
5.3.1 Co-sedimentation Assays	66
5.3.1.1 Tubulin/XMAP215-his7 interaction	66
5.3.1.2 Tubulin / XMAP215-his7 / mcAB	66
5.3.1.3 Microtubules/XMAP215-his7 / mcAB	67
<b>5.4 XMAP215 5D12 <i>in vivo</i> behavior</b>	68
5.4.1 5D12 mcAB labeling	68
5.4.2 Microscopy assay visualization of MTs/XMAP215 interaction: Total Internal Reflection Fluorescence Microscopy (TIRF)	69
<b>5.5 XMAP215/MT ultrastructural behaviour: Electron         microscopy</b>	70
5.5.1 Negative staining	71
5.5.2 Specimen preparation and cryo-electron microscopy	71
5.5.3 Image analysis	72

<b>5.6 XMAP215 <i>in vitro</i> inhibitor research</b>	<b>72</b>
5.6.1 Screening	72
5.6.2 Experimental approach	73
5.6.2.1 Molecules collection	73
5.6.2.2 Tubulin	73
5.6.2.3 Rhodamine conjugated to Tubulin	74
5.6.2.4 XMAP215-his7 Protein	75
5.6.2.5 Ni-NTA saturation by XMAP215-his7	75
5.6.3 MTs nucleation by XMAP215-his7 immobilized on Ni-NTA beads	76
5.6.3.1 Principle and first part of the aster nucleation test	76
5.6.4 Second round. Hits evaluation on the tubulin Assembly	77
5.6.5 Third part: Final activity test for the positive molecules	78

## RESULTS

<b>6. Anti-XMAP215 mcAB</b>	<b>79</b>
6.1 Anti-XMAP215 mcAB production and Characterization	79
6.1.1 Anti-XMAP215 mcAB production: Three selected clones identifying the XMAP215/ ch-TOG cell localization	79
6.1.2 anti XMAP215 mcAB characterization	81
6.1.2.1 mcAB Specificity	81
6.1.2.2 mcABs staining activity on fixed cells	82
6.1.2.3 mcAB isotyping, class	86

6.1.2.4	mcAB epitops Cartography	87
6.1.2.5	mcAB technical data sheet	90
<b>6.2</b>	<b>XMAP215/ch-TOG cellular localizations</b>	<b>92</b>
6.2.1	Two cellular localizations for XMAP215/ ch-TOG	92
6.2.2	The +TIP XMAP215/ch-TOG and EB1 Colocalize	94
6.2.3	+TIP XMAP215 and other +TIPs, a hierarchy	95
6.2.4	XMAP215/ch-TOG is at the top of the +TIPs hierarchy. Our plus end complex hypothesis	97
<b>6.3</b>	<b>+TIP XMAP215 does exist <i>in vivo</i></b>	<b>100</b>
<b>6.4</b>	<b>XMAP215 is a travelling protein. From the tubulin dimer addition at the MT + TIP trough the controlled depolymerization?</b>	<b>102</b>
<b>6.5</b>	<b>XMAP215 travels from the mitotic + TIP to the lattice of interphasic MTs. Is XMAP215 a multi-task protein?</b>	<b>104</b>
<b>6.6</b>	<b>XMAP215-MT interaction does exist <i>in vitro</i>. Cosedimentation essay</b>	<b>106</b>
<b>6.7</b>	<b>XMAP215 and the MT ultrastructure</b>	<b>108</b>
6.7.1	XMAP215 builds differentially the MT tip	108
6.7.2	Does XMAP215 builds the MT lattice?	115
<b>6.8</b>	<b>XMAP215 inhibitors research</b>	<b>116</b>
6.8.1	Screening first part: MTs Nucleation by immobilized XMAP215-his7	118
6.8.2	Screening second part: Molecules effects on the tubulin assembly	119
6.8.3	Dose activity test and screening partial	

results: 3 stabilizing molecules and five depolymerizing molecules	120
<b>DISCUSSION</b>	123
<b>7.1 XMAP215/ch-TOG, a new +TIP protein</b>	128
<b>7.2 The N-terminal domain related activity</b>	134
<b>7.3 Our plus end hierarchy complex hypothesis</b>	136
<b>7.4 Microtubular XMAP215/ch-TOG: RNA trafficking     and other cellular activities.</b>	
<b>Another protein-protein interaction?</b>	141
<b>7.5 Centrosomal XMAP215/chTOG and MT     Anchoring</b>	144
<b>7.6 ch-TOG, from the functional theory to the fact     theory</b>	147
<b>7.7 The XMAP215/ch-TOG future</b>	153
<b>CONCLUSION</b>	157
<b>BIBLIOGRAPHY</b>	159
<b>Appendix: Buffers and solutions</b>	179
<b>Table of solutions, buffers, and chemicals I</b>	179
<b>Table of solutions, buffers, and chemicals II</b>	180
<b>Table of solutions, buffers, and chemicals III</b>	181
<b>Table of solutions, buffers, and chemicals IV</b>	182

## FIGURES LIST

### 1. The cell and its cycle

- Figure 1** Overview of the cell cycle 8  
**Figure 2** Mitotic cycle and cytokinesis 11

### 2. Cytoskeleton

- Figure 3** Interphasic and mitotic MT polymer organization 15  
**Figure 4** Microtubules structure 16  
**Figure 5** Polymerization dynamics in the GTP mechanism 17  
**Figure 6** MT dynamic instability model 18  
**Figure 7** Tubulin post-translational modifications 19

### 3. MAPS and the + TIPs

- Figure 8** Described mechanism for the MT plus-end localization 24  
**Figure 9** EB1 cell localization, structure and domain organization 27  
**Figure 10** CLIP170 cell localization and structure 29  
**Figure 11** p150<sup>Glued</sup> cellular localization and domain organization in the dynactin complex 31  
**Figure 12** Schematic +TIPs hierarchy 34  
**Figure 13** Protein kinases and tip tracking 35  
**Figure 14** MT GTP-cap theoretical model 37  
**Figure 15** CLIP170 autoinhibition model 38

### 4. XMAP215/Dis1 family

- Figure 16** Phylogenetic tree of the MAP215/Dis1- family 41

<b>Figure 17</b>	Architecture of the MAP215/Dis1 family of MAPs	43
<b>Figure 18</b>	TOG domain sub-classification	44
<b>Figure 19</b>	XMAP215 cellular localization	47
<b>Figure 20</b>	XMAP215 behaviour <i>in vitro</i>	49
<b>Figure 21</b>	XMAP215/ch-TOG schematic representation	51
<b>Figure 22</b>	XMAP215/ch-TOG domains described to bind cyclin B1	53

## 5. Experimental procedures

<b>Figure 23</b>	<i>Xenopus laevis</i> Egg extract obtention	62
<b>Figure 24</b>	Mitotic spindle assembly <i>Xenopus laevis</i> egg Extract	63
<b>Figure 25</b>	XMAP215 cloned fragments	65
<b>Figure 26</b>	Labelling of mcAB 5D12	69
<b>Figure 27</b>	Tubulin purification and quantification	74
<b>Figure 28</b>	Rhodamine labelled tubulin spectrum	75
<b>Figure 29</b>	Ni-NTA saturation by XMAP215-his7	76
<b>Figure 30</b>	Microtubule nucleation test on magnetic beads saturated by XMAP215-his 7	77

## Results

<b>Figure 31</b>	Immunization evolution of the BALB/c mice	80
<b>Figure 32</b>	ch-TOG single staining in PHF	81
<b>Figure 33</b>	mcAB anti XMAP215/ch-TOG specificity	82
<b>Figure 34</b>	4B6 mcAB staining on PHF	83
<b>Figure 35</b>	5A6 mcAB staining on PHF	84
<b>Figure 36</b>	5D12 mcAB staining on PHF	85
<b>Figure 37</b>	mcAB isotyping, indirect immunofluorescence	86

<b>Figure 38</b>	mcAB isotypification	87
<b>Figure 39</b>	XMAP215 antigen cartography for the mcAB	88
<b>Figure 40</b>	4B6 mcAB technical data sheet	90
<b>Figure 41</b>	5D12 mcAB technical data sheet	91
<b>Figure 42</b>	Two different intracellular localizations for ch-TOG in PHF	92
<b>Figure 43</b>	+TIP ch-TOG co-localizes with EB1	94
<b>Figure 44</b>	+TIPs in the PHF model: ch-TOG and EB1	95
<b>Figure 45</b>	+TIPs in the PHF model: CLIP170 and p150 <sup>Glued</sup>	96
<b>Figure 46</b>	Analysis method of a « comet like » structure	97
<b>Figure 47</b>	+TIPs proteins hierarchy	98
<b>Figure 48</b>	Astral MTs +TIPs in the Egg extract are marked by mcAB 5D12- Atto 488	101
<b>Figure 49</b>	+TIP XMAP215 presence is confirmed at the + TIPs of growing MTs in the mitotic egg extract	103
<b>Figure 50</b>	+TIP XMAP215 is part of the <i>in vivo</i> depolymerization mechanism	104
<b>Figure 51</b>	XMAP215 travels on the tubulin polymer	105
<b>Figure 52</b>	Cosedimentation assays of XMAP215-his 7 using the mcAB 5D12 and 4B6	107
<b>Figure 53</b>	MT ends in cryo-EM	109
<b>Figure 54</b>	MT tips conformation at the cryo-electron microscopy	111
<b>Figure 55</b>	Cryo-electron images of MT tips and their trajectories	113
<b>Figure 56</b>	XMAP215 longitudinal binding model	114
<b>Figure 57</b>	XMAP215 organizes MT into ordered bundles	115
<b>Figure 58</b>	Screening approach general diagram	117



<b>Figure 59</b>	Aster nucleation test	118
<b>Figure 60</b>	Examples of the different effects of the molecules on tubulin assembly	119
<b>Figure 61</b>	Dose activity test	120
<b>Discussion</b>		
<b>Figure 62</b>	XMAP215/ch-TOG isoforms comparison	126
<b>Figure 63</b>	Different + TIPs XMAP215 activity models	132
<b>Figure 64</b>	Hypothetical model of the + TIP XMAP215/ch-TOG tubulin dimmers addition	134
<b>Figure 65</b>	<i>In vitro</i> XMAP215 behaviour	138
<b>Figure 66</b>	+TIPs hierarchy theory	139
<b>Figure 67</b>	Hypothetical model of MT-XMAP215/ch-TOG participation in complex protein formation	143
<b>Figure 68</b>	Model for XMAP215/ch-TOG activity in the microtubular environment	144
<b>Figure 69</b>	A XMAP215 activity at the centrosome in M phase	147
<b>Figure 70</b>	Identified genes in chromosome 11p and their possible implication in cancer	151
<b>Figure 71</b>	Clonal mechanism of cancer	153

## TABLES LIST

<b>Table I</b>	Eukaryotic cytoskeletal polymers	14
<b>Table II</b>	Properties of mammalian MAPs	22
<b>Table III</b>	Cellular localization for some of the proteins of the MAP215/Dis1 family	45
<b>Table IV</b>	XMAP215/ch-TOG domains and their interactions	52
<b>Table V</b>	Immunization schedule of BALB/c mice for the XMAP215 mcAB production	58
<b>Table VI</b>	Cell lines used in this study	59
<b>Table VII</b>	Primary and secondary antibodies used in the IF	60
<b>Table VIII</b>	mcAB anti-XMAP215/ch-TOG in vitro immunoreactivity	88
<b>Table IX</b>	mcAB anti-XMAP215/ch-TOG characterization	89
<b>Table X</b>	+ TIPs comets lengths	99
<b>Table XI</b>	Screening final list of active chemical compounds	121



## SUMMARY

XMAP215/ch-TOG are members of an evolutionary conserved family of microtubule-associated proteins (**MAPs**), the XMAP215/Dis1 family. This family of proteins plays a key role in the regulation of the microtubule (**MT**) cytoskeleton, particularly during the cell division. In humans, ch-TOG is the colon-hepatic tumor overexpressed gene, a protein whose sequence was originally reported from blastic cells and from several forms of cancer. A few members of the XMAP215/ch-TOG family have been found to be present in different cell localizations, always MT-related, perhaps providing in this way a selected activity. However, the XMAP215/ch-TOG exact localization and activity has remained as a theory to be probed.

In this scientific context, we developed a series of monoclonal antibodies (**mcABs**) that allow us to identify two different populations of the XMAP215/ Dis1 family of proteins. Confocal images of fixed cells revealed a first and well known XMAP215/ch-TOG population, a microtubular-XMAP215 (**MT-XMAP215**), co-localizing with microtubules (**MTs**) in interphase and mitotic spindle. A second localization was identified at the tips of growing MTs, placing XMAP215/ch-TOG as one more member of the known microtubule plus end tracking proteins (**+TIPs**). This second population was identified as the **+TIP XMAP215/ch-TOG**.

The + TIP XMAP215 is the most distal +TIP protein at the tip of MTs. The + TIPs hierarchy was established comparing the XMAP215/ch-TOG localization with other well known + TIPs proteins such as **EB1**, **CLIP170** and **p150<sup>Glued</sup>**. In the *Xenopus laevis* mitotic egg extract, the Total Internal Reflection Fluorescence (TIRF) *In vivo* images, identified a **+TIP XMAP215** that is present at the tip of polymerizing and depolymerising MTs.

Cryo-electron microscopy (**Cryo-EM**) images probed a selective activity for the +TIP XMAP215 population. In pure tubulin solutions XMAP215 shown to promote the formation of outwardly sheet structures at the tip of MTs, compatible with growing mechanisms in MTs.

Based in our results we propose a model where free XMAP215 is previously loaded with tubulin dimers to become a protofilament-like structure. This structure joins the MT tip using its C-terminal domain, not only adding the tubulin dimers but also perhaps participating in the MT sheet closure. The possibility that the protein participates in the MT depolymerization could be associated to a “controlled” depolymerization mechanism. Once the tubulin addition has taken place, the +TIP XMAP215 protein could evolve to a MT-XMAP215, the well know form of the protein that has been related to the RNA granules traffic.

**Key words:** XMAP215, ch-TOG, microtubules, monoclonal antibodies.

## RESUME

Les protéines XMAP215/ch-TOG appartiennent à une famille de protéines associées aux microtubules (**MAPs**), dont la séquence génétique a été conservée tout au long de l'évolution, il s'agit de la famille XMAP215/Dis1. Cette famille joue un rôle dans la régulation du cytosquelette des microtubules (**MT**), en particulier pendant la division cellulaire. Chez l'humain, ch-TOG est la protéine surexprimée dans les tumeurs du colon et du foie. Certaines protéines XMAP215/ch-TOG ont été retrouvées dans différentes localisations cellulaires, toujours reliées aux MTs, à l'origine d'une activité spécifique. Cependant, la localisation exacte de XMAP215/ch-TOG ainsi que son activité restait à être déterminées.

Dans ce contexte scientifique, nous avons développé une série d'anticorps monoclonaux (**mcAB**) qui nous ont permis d'identifier deux populations différentes de XMAP215/ch-TOG. Les images de microscopie confocale des fibroblastes humaines primaires et de *xenope* ont montré une première localisation microtubulaire. C'est la colocalisation établit XMAP215-microtubulaire (**MT-XMAP215**) qui s'observe pendant l'interphase et pendant la mitose cellulaire. Une deuxième localisation a été identifiée sur le bout *plus* des MTs, donnant XMAP215/ch-TOG comme faisant parti de la famille des protéines de bout *plus* (+TIPs). Cette deuxième colocalisation a été identifiée comme **+TIP XMAP215/ch-TOG**.

La +TIP XMAP215 est la protéine la plus distale du bout des MTs. La hiérarchie a été établie en faisant la comparaison de la localisation de XMAP215/ch-TOG avec les protéines les plus connues du bout *plus*, telles qu'**EB1**, **CLIP170** et **p150<sup>Glued</sup>**. Dans l'extrait mitotique de *Xenopus laevis*, les images obtenues *in vivo* par la microscopie de fluorescence par réflexion totale interne (TIRF) ont permis d'identifier une **+TIP XMAP215** présente au bout des MTs qui polymérisent et dépolymérisent.

Les images de microscopie cryo-électronique (Cryo-EM) ont montré une activité spécifique de la population +TIP XMAP215. Dans les solutions de tubuline pure, XMAP215 induit la formation de structures au bout des MTs, cette activité est compatible avec les mécanismes de croissance des MTs.

Sur la base de nos résultats, nous proposons un modèle où XMAP215 sert de transporteur des dimères de tubuline en devenant une structure de type protofilament. Cette structure se lie au bout du MT en utilisant son domaine C-terminal, en rajoutant les dimères de tubuline et probablement en participant à la fermeture de la structure microtubulaire même. La protéine interviendrait donc dans la dépolymérisation et aurait un rôle dans le mécanisme de dépolymérisation contrôlée. Une fois que l'addition de tubuline a eu lieu, la +TIP XMAP215 pourrait évoluer en MT-XMAP215, forme la plus connue de la protéine associée au trafic des granules d'ARN.

**Mots clés** : XMAP215, ch-TOG, microtubules, anticorps monoclonaux.

## GENERAL INTRODUCTION

Cell support, organization function and division rely on cell cytoskeleton. It is composed by microtubules (**MTs**), actin and intermediate filaments. MTs are dynamic and polar polymers that develop a complex rearrangement process going from the interphasic MT net until the mitotic spindle in the cell cycle. Once the cell enters mitosis, the interphasic MT network reorganizes and forms a bipolar mitotic spindle, the resulting structure is a well organized “mitotic machine”, able to separate the chromosomes between the two daughter cells.

The increased dynamics of MTs in mitosis is an essential prerequisite for spindle formation. These changes are executed by subtle modifications in the balance of the activities of MT stabilizing and destabilizing factors. This highly synchronized mechanism is the product of the coordinated activity of different classes of proteins including microtubule-associated proteins (**MAPs**) and molecular motors.

Among many others, a MAP that takes part in the MT dynamics is XMAP215. XMAP215 is the founding member of a highly conserved family of proteins, the **XMAP215/Dis1** family of microtubule-associated proteins (MAPs), originally was identified in 1987 in the *Xenopus laevis* egg extract. **Ch-TOG**, the human homologue was described eight years later, sharing an 80% homology in their sequence. Both proteins promote MT assembly *in vitro* and localize to spindle MTs and centrosomes *in vivo*. XMAP215 in particular can affect the MT plus end.

Eventhough the XMAP215 activity at the MT +TIP has been predicted and its possible role in the conformation in the MT tip ultrastructure has been proposed, the XMAP215/ch-TOG functional activity remains to be probed or denied. Based on the different theories available, our research is focused on the establishment of the functional XMAP215/ch-TOG activity *in vivo* and *in vitro*.



This thesis has been divided into four general parts: Introduction, experimental procedures, results and discussion.

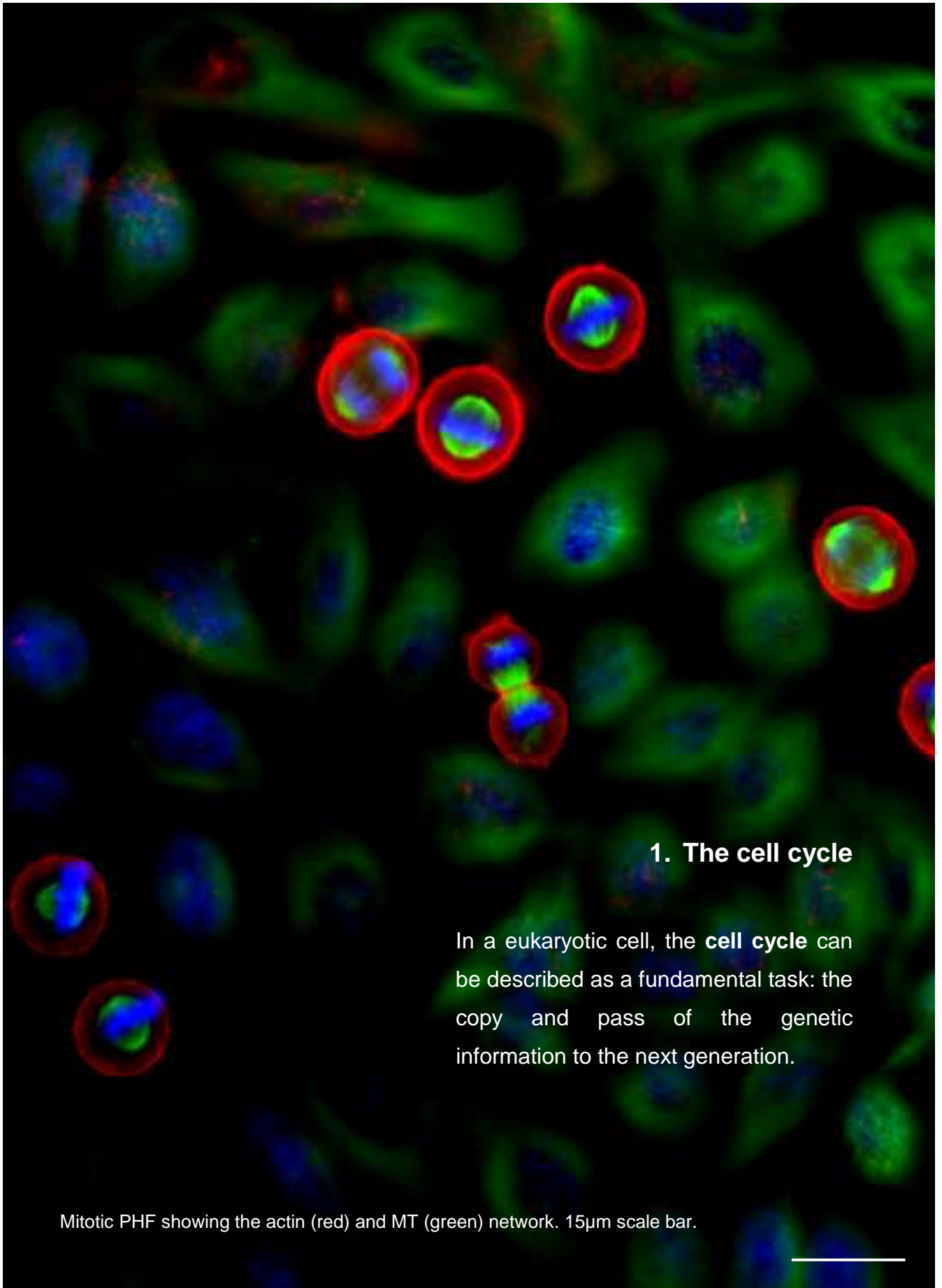
The introduction concerns the first four chapters. The **first** one discusses the generalities of the cell cycle and its biological mechanism. The **second** chapter discusses the cytoskeleton nature, with particular reference to the MT structure, properties and activity in the cellular context. A **third** chapter introduces and develops the +TIPS concept. In it, three of the most well known +TIPs proteins are described (EB1, CLIP170 and p150<sup>Glued</sup>) from their structure until reaching their potential (or predicted) cellular activity. A **fourth** chapter introduces the reader to the XMAP215/Dis1 family of proteins, focusing in particular on XMAP215 and ch-TOG.

The employed methods in this work are explained in the **fifth** chapter. The different approaches go from the fixed cells imaging in the confocal microscopy domain, through the physical principle of the TIRF until finally reaching the Cryo- electron microscopy analysis. This chapter is composed of six sub-chapters: the mAb production and characterization (**5.1**), the XMAP215 / ch-TOG over-expression (**5.2**), the *in vitro* interaction tubulin or MT/XMAP215 (**5.3**), the XMAP215 *in vivo* interactions (**5.4**), the MT ultrastructure related to the XMAP215 effects (**5.5**) and finally the *in vitro* research for a XMAP215 inhibitor is described (**5.6**).

The **sixth** chapter lists the results obtained through the experimentation phase. The interpretation is realized with reference to the cell localization, MT ultrastructure and XMAP215/ch-TOG predicted activity.

An **seventh** chapter addresses the results discussion and to the different conclusions and theories that can be extracted from this work.





## 1. The cell cycle

In a eukaryotic cell, the **cell cycle** can be described as a fundamental task: the copy and pass of the genetic information to the next generation.

Mitotic PHF showing the actin (red) and MT (green) network. 15 $\mu$ m scale bar.





## 1. The cell and its cell cycle.

### 1.1 The cell.

The cell is the functional unit of life and is often described as the building block of life. It was discovered by Robert Hooke, an English natural philosopher (from Latin *philosophia naturalis*, the study of nature). Hooke published in 1665 *Micrographia*, a book that described microscopic observations. He coined the term **cell**, a word derived from the Latin “*cellula*”, which means small compartment.

In 1673 the Dutch microscopist Anthonine van Leeuwenhoek, known as the father of microbiology, described in his letters to the Royal society of London the single celled structures, today known as protist. Later in 1839, the Germans Mathias Schleiden (botanist) and Theodor Schwann (zoologist) elucidate the principle that plants and animals are made of cells, concluding that cells are a common unit of structure and development, funding the cell theory.

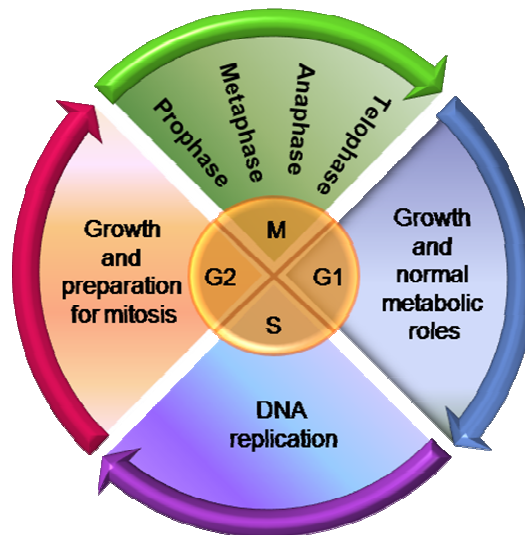
Rudolf Virchow completed the cell theory in 1858, publishing the epigram *Omnis cellula e cellula* (every cell originates from another existing cell like it), originating the concept of cell multiplication by cell division.

### 1.2 The cell cycle

The cell cycle is the mechanism by which a parent cell divides into two daughter cells. The cell division is a small part of a larger cell cycle. In eukaryotes this type of cell division is known as **Mitosis**.

The basic function of the cell division is to **duplicate** cellular DNA and to **segregate** the copies in two identical daughter cells in an ordered process. These processes define the two major phases of the cell cycle (**Fig.1**). DNA duplication occurs during **S phase** (Synthesis), which requires 10 -12 hours. After S phase, chromosome segregation and cell division occur in **M Phase** (Mitosis), which requires about 1 hour. **G1** is the gap between M phase and S

phase, while **G2** is the gap between S phase and M phase (Scholey *et al.*, 2003).



**Figure 1. Overview of the cell cycle.**

The cell cycle is an ordered set of events in eukaryotic cells. They are designed: **G1**, **S**, **G2** and **M**. **G1 (GAP1)** the cell grows and produce the enzymes needed for future DNA replication. **S** stage (**Synthesis**) involves the DNA replication and occurs until the cell DNA has doubled. **G2 (GAP2)** protein synthesis occurs preparing the cell for mitotic events. During the **M** stage (**Mitosis**) the nuclear and cytoplasmic division occurs producing two daughter cells. Mitosis is divided into 4 phases: Prophase, Metaphase, Anaphase and Telophase.

G1, S and G2 together are called **Interphase**. The two gap phases allow the cell to grow and monitor the internal and external environment to ensure that the conditions are suitable and preparations are complete before mitosis.

These cell cycle events are regulated by the activation of a complex family composed of cyclin-dependent kinases (**CDK**) and cyclin subunits, CDK1/cyclin B being the universal cell cycle regulator implicated in the **G2/M** transition (Le Breton *et al.*, 2005). This mechanism is only possible using the highly synchronized cellular machine that divides the cell using cytoskeletal proteins as the key tools to accomplish mitosis (**Fig.2a**). **MTs** (mitotic spindle) and actin (contractile ring), molecular motors and MAPs coordinate their activities driving the cell through mitosis and cytokinesis.

## 1.3 Mitosis phases.

### 1.3.1 Interphase

Eventhough the cell prepares itself for cell division during interphase, the interphase is not part of the mitosis mechanism. Interphase is divided into three phases: **G1** (first gap), **S** (synthesis), and **G2** (second gap). During these three phases the cells grows producing proteins and cytoplasmic organelles. The cell grows (**G1**), keeps growings duplicating the chromosomes (**S**), prepares for mitosis (**G2**), and finally divides (**Mitosis**).

### 1.3.2 Prophase

The genetic material is condensed into ordered structures, the chromosomes. During the S phase, the genetic material was duplicated, now the replicated chromosomes have two sister chromatids, bounded by the centromere.

The cell centrosome is located close to the nucleus and is made of a pair of centrioles, a centrosome is duplicated before the new mitosis. This structure nucleates MTs to form the spindle and the molecular motor proteins push each centrosome to opposite sides of the cell, forming microtubular asters.

### 1.3.3 Prometaphase

The nuclear envelope disassembles and MTs invade the nuclear space. Chromosomes keep condensing and the spindle MTs develops several different organizations: Astral, polar and kinetochore MTs. The Kinetochore MTs will be attached to proteic structures of each chromosome centromere.

Each chromosome forms two kinetochores at the centromere, one attached at each chromatid. When a MT connects to the kinetochore, some molecular motors activate, using energy from ATP to “crawl” up the MT to the originating centrosome. Is the molecular motor activity who added to the MT polymerization-depolymerization, providing the pulling force necessary to later separate the two sister chromatides.

### 1.3.4 Metaphase

As the prometaphase evolves, the highly condensed chromosomes of centrosomes arrive to the metaphase plate (equatorial plane), they are finally aligned. The resulting alignment is the consequence of the different pulling forces generated by the opposing kinetochores.

### 1.3.5 Anaphase

During the early anaphase, the proteins that bind sister chromatids together are cleaved, allowing them to separate. Doing this, each sister chromatid is pulled apart. The mechanistic method consists in a shortening of the kinetochore MTs, allowing the movement to the respective centrosomes.

In the late anaphase the non kinetochore MTs elongate, pulling the centrosomes (and the attached centrosomes) to the opposite poles of the cell. At the end of anaphase, the cell has separated successfully the two identical copies of the genetic information in two different groups.

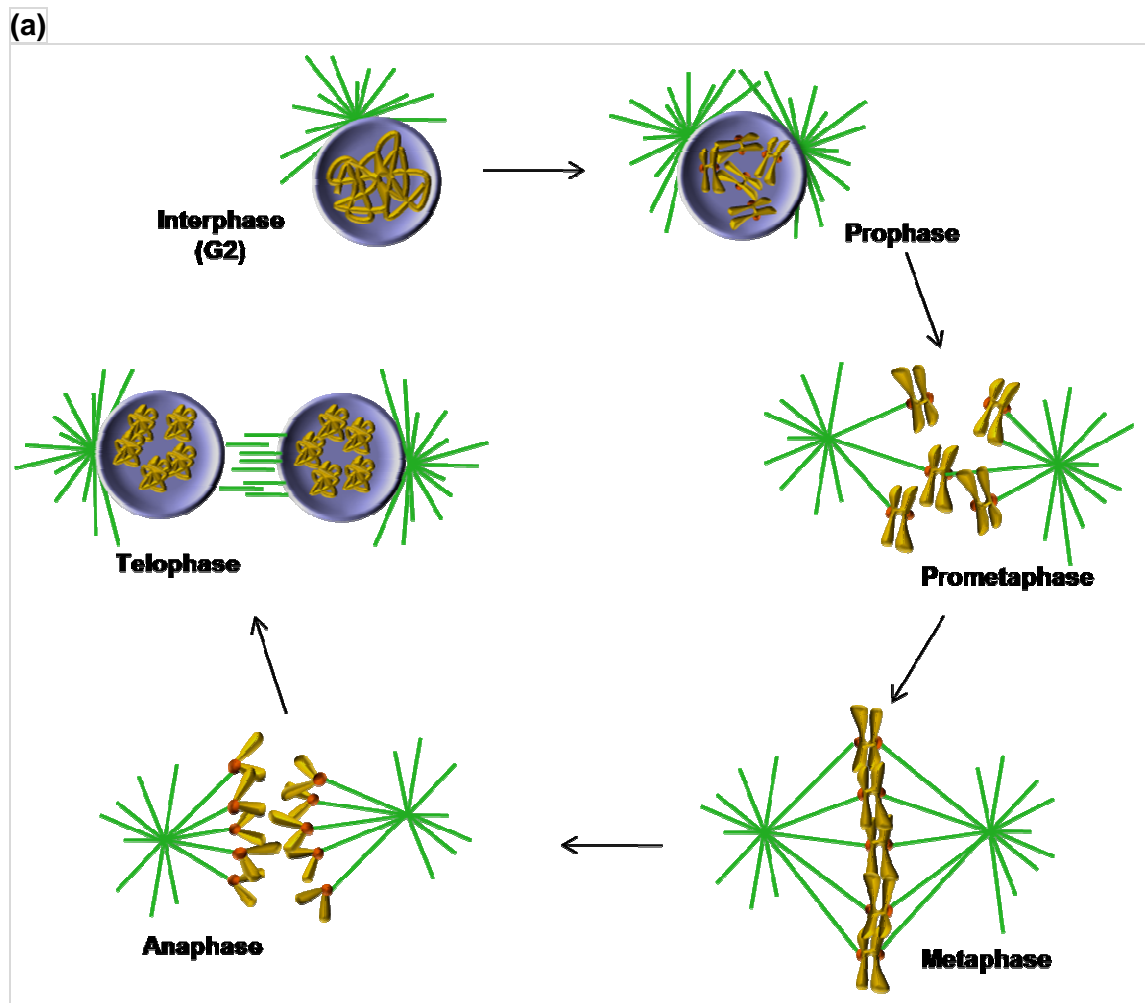
### 1.3.6 Telophase

The nonkinetochore MTs continue to lengthen, elongating the cell even more. Corresponding sister chromosomes attach to each other and a new nuclear envelope is created from the "parent" fragments of the cell's nuclear membrane. The chromosomes unfold back into chromatin.

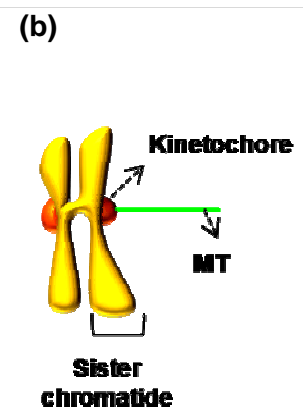
### 1.3.7 Cytokinesis

Even though cytokinesis is not a phase of mitosis, but is a necessary process to complete cell division. The cleavage furrow containing the contractile ring at the metaphase plate level. Each daughter cell has a complete copy of the genome of its parent cell. The end of cytokinesis marks the end of the M-phase (Scholey *et al.*, 2003, Cheeseman *et al.*, 2008).





**Figure 2. Mitotic cycle and cytokinesis.** (a) During **Interphase** (G1,S and G2), the cell is engaged in metabolic activity previous to mitosis. **Prophase**, the chromatin in the nucleus begins to condense and the duplicated centrosomes begin to migrate to opposite poles of the cell. **Prometaphase**, the nuclear membrane dissolves; chromosomes are attached by MTs through the kinetochore, moving the chromosomes to the cell equator. **Methaphase**, sister chromatids face opposite poles. **Anaphase**, sister chromatids moves to opposite poles of the cell. **Telophase**, chromatids arrive to opposite poles of the cell and nuclear envelopes reassemble around. The contractile ring creates the spindle mid-zone called the midbody. Finally, the furrow “seals” separating the daughter cells. (b) **Mitosis general vocabulary.** Sister chromatids, kinetochores, spindle equator, centromeres, poles

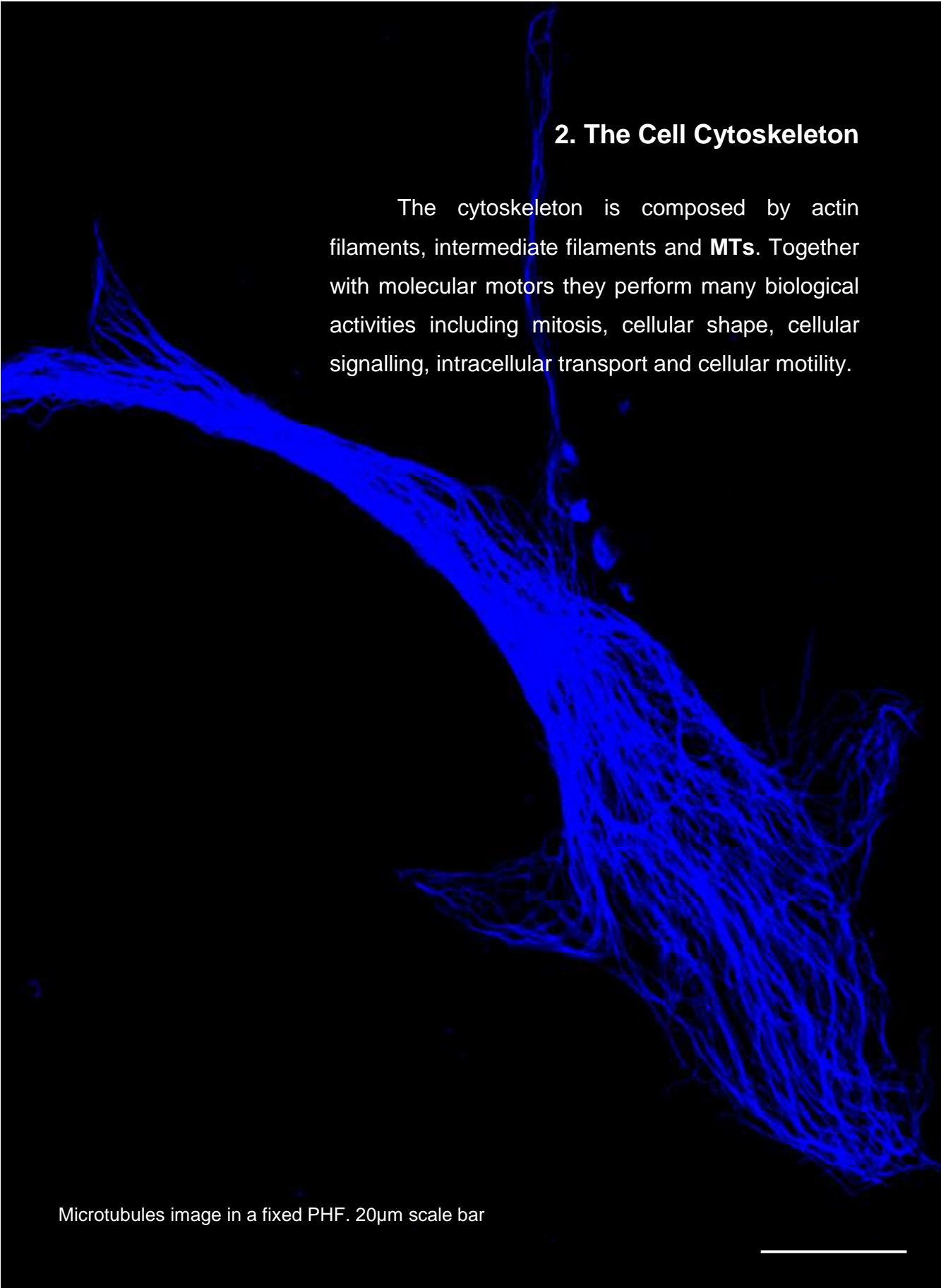




## 2. The Cell Cytoskeleton

The cytoskeleton is composed by actin filaments, intermediate filaments and **MTs**. Together with molecular motors they perform many biological activities including mitosis, cellular shape, cellular signalling, intracellular transport and cellular motility.

Microtubules image in a fixed PHF. 20 $\mu$ m scale bar



A fluorescence microscopy image showing a dense network of microtubules (MTs) in a fixed PHF. The microtubules are stained blue and form a complex, interconnected structure. A white scale bar is located in the bottom right corner of the image.



## 2. Cytoskeleton

The term cytoskeleton (cytosquelette) was first introduced in 1931 by the French embryologist Paul Wintrebert. There are three types of cell cytoskeletal polymers: actin filaments, **MTs** and intermediate filaments (**Table I**).

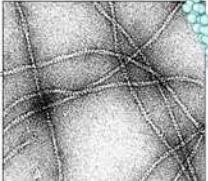
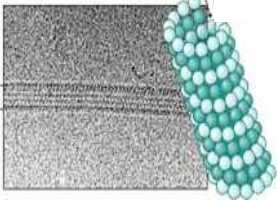
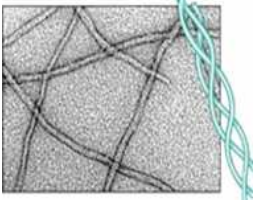
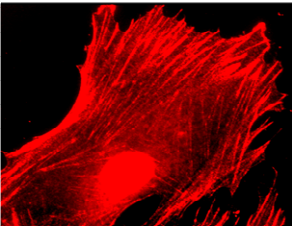
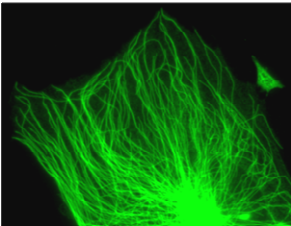
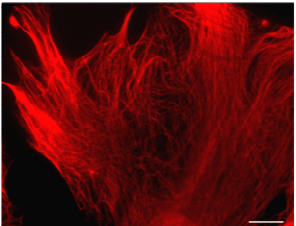
Actin was described for first time by Straub in 1943. In 1948 De Robertis and Schmitt described intra-axonal fibers, with a tubular shape. These structures were known years later as “microtubules” (Slautterback, 1963). Ishikawa and collaborators identified filaments possessing a calibre “intermediate” between MTs and actin filaments, thus the intermediate filaments concept was born in 1968 (Frixione, 2000).

Cytoskeletal polymers are in highly dynamic structures that possess a rapid reorganization mechanism. They are capable of polymerizing, depolymerising and moving within the cytoplasm only in a few seconds. **MTs** are implicated in movement, using polymerization for pushing and depolymerization by pulling (Desai and Mitchinson, 1997).

**MTs** are polar and linear polymers, built from 13 strands of  $\alpha/\beta$ -tubulin heterodimers. Actin filaments (F-actin) are built by two strands of globular actin (G-actin) monomers. Intermediate filaments assemble through the association of antiparallel dimers into oligomers, generating apolar filaments that confer strength to the cell. Each one of these polymers can generate pushing and pulling forces as they grow and shrink by addition and loss of subunits from their ends. They also serve as tracks for motor proteins that use **GTP** or **ATP** hydrolysis to generate force and motility whereas intermediate filaments use accessory proteins, such as kinases and phosphatases (Scholey *et al.*, 2003; Galjart *et al.*, 2005).

In the interphasic cell, the cytoskeletal proteins generate multiple forces, at the piconewtons scale producing movements at the nanoscale. During cell

division they work as a unique machine, able to generate forces in the nanonewtons scale, moving the cellular components and rearranging the cell structure in a surface of many microns.

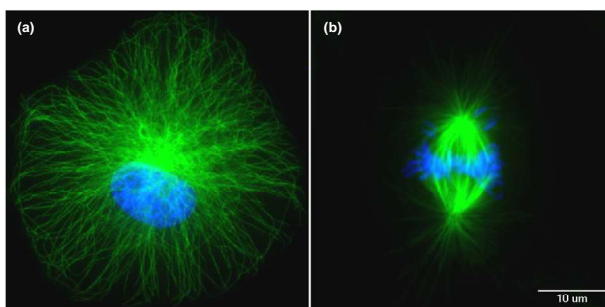
Polymer	Actin filament	Microtubule	Intermediate filament
<b>Protein subunit</b>	Actin monomer	Tubulin heterodimer	Various proteins with $\alpha$ -helical coiled-coil
<b>Polymerization</b>	yes	yes	Probably
<b>Bound nucleotide</b>	ATP	GTP	None
<b>Dynamic instability</b>	No	Yes, dramatic	No
<b>Track for motors</b>	Yes, 20 families of myosins	Yes, several dyneines and many families of kinesins	No
<b>Electron micrographs of polymers</b>			
<b>Fluorescence micrographs of cell polymers</b>			

**Table 1: Eukaryotic cytoskeletal polymers.** Electron micrographs and 3D illustrations: migration.wordpress.com. Fluorescence images showing PHF stained for each one of the cytoskeletal polymers. 10  $\mu\text{m}$  scale bar. Modified from Pollard *et al.*, 2003.

## 2.1 Microtubules.

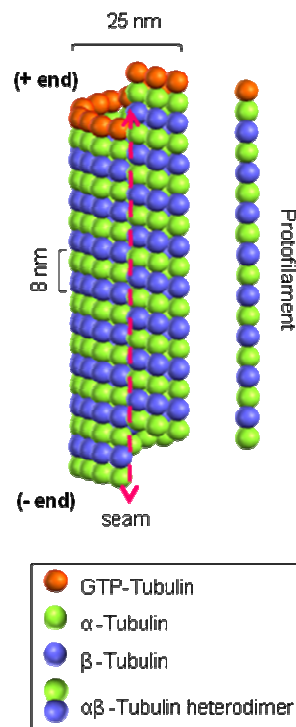
The **MTs** are a key component of the cell cytoskeleton. They allow a variety of tasks in the different cell state. During interphase they are responsible for the cell shape, vesicle and mitochondria movement and cell signalling. In mitosis build the mitotic spindle that segregates the duplicated chromosomes, providing support to the organelle organization and also orienting the cell plane of cleavage (Desai and Mitchinson, 1997; Jordan and Wilson 2004).

As the cell enters mitosis, a radial array of long interphase MTs (**Fig.3a**) is disassembled and converted to a bipolar spindle composed of much shorter MTs (**Fig.3b**). This reorganization is accompanied by changes in MT assembly dynamics; entry into mitosis corresponds with a 10-fold increase in the rate of MT turnover (Cassimeris *et al.*,1999).



**Figure 3. Interphasic and mitotic MT polymer organization** . The MT polymer organization at **interphase (a)** and **mitosis (b)** is a consequence of both MT dynamics regulated by accessory proteins and additional organization provided by the actin cytoskeleton or motor proteins (Cassimeris *et al.*,1999). Scale bar 10 $\mu$ m

MTs are hollow polymers assembled from  $\alpha/\beta$ -tubulin heterodimers. These heterodimers are arranged linearly into protofilaments; 13 protofilaments typically form the MT wall. The organization of heterodimers in the MT lattice is polarized, resulting in structural polarity and kinetic differences at the MT ends. The faster growing end is designated the **plus end (+ end)**, close to the cell cortex) and has the  $\beta$ -tubulin subunit of each heterodimer exposed, whereas the slower growing end (from the centrosome) has an  $\alpha$ -tubulin subunit exposed and is designated the **minus end (- end,)** (**Fig.4**) (Cassimeris *et al.*,1999; Siegrist *et al.*, 2007).



**Figure 4. Microtubules structure.**

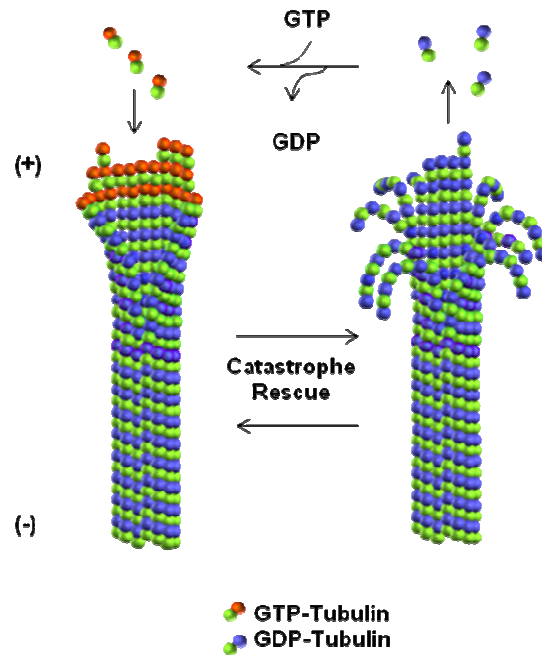
Typically a MT is composed of 13 individual protofilaments consisting of  $\alpha/\beta$ -tubulin heterodimers, this organization forms a hollow tube of 25 nm diameter.

An  $\alpha/\beta$ -tubulin heterodimer measures 8 nm has an exchangeable GDP/GTP binding site on the  $\beta$  subunit. The MT is a polar structure where, the  **$\beta$ -tubulin** is exposed at the growing end (**+ end**) and the  **$\alpha$ -tubulin** is exposed at the slower growing end (**- end**). A **GTP- tubulin cap** (orange) stabilizes MT growth by keeping individual protofilaments close to each other. (Gardner *et al.*, 2008)

In interphase cells the MT polarity is a key issue, it permits the motor proteins the unidirectional movement on the MT lattice executing their diverse functions. In this case they function as tracks for intracellular transport of vesicles and cellular organelle distribution (Dammermann *et al.*, 2003 ; Siegrist *et al.*, 2007). In interphasic cells the network shows a slow growing end (**- end**), localized at the cell centrosome. The faster growing end (**+ end**) is close to the cell cortex.

Growing MT **+ ends** are composed of **GTP-tubulin**, which helps to stabilize them (more mature sections of MTs typically bind **MAPs**, which promotes stability). In this region, where the tubulin dimers are exchangeable that is known as the **GTP cap**. Here the polymerization dynamics is created by the gain and loss of tubulin-GTP or tubulin-GDP and inorganic phosphate (Pi) at the MT end. Tubulin-bound GTP is hydrolyzed to tubulin GDP and Pi at the time that tubulin is added to the MT end. The tubulin-GDP remains non-dissociable and non-exchangeable from the MT tip until the tubulin subunit dissociates from the MT (**Fig 5**). The cycles of MT growth and collapse are termed “dynamic instability” (Jordan and Wilson 2004; Siegrist *et al.*, 2007).



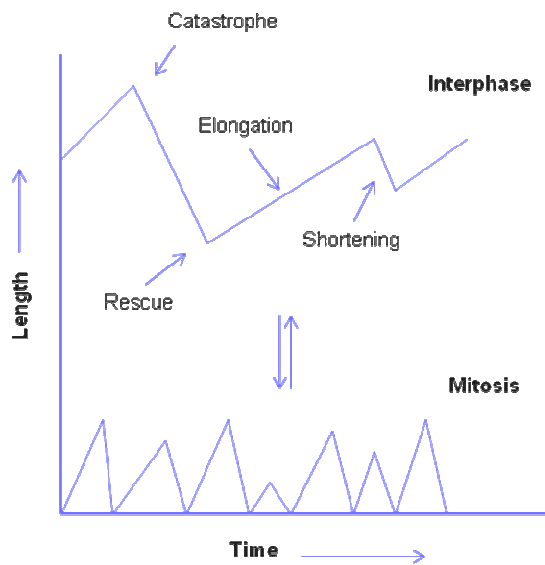


**Figure 5. Polymerization dynamics in the GTP-cap associated mechanism.** GTP-tubulin is incorporated at polymerizing MT ends, the bound GTP is hydrolyzed and inorganic phosphate (Pi) is released. Thus, the MT lattice is basically composed of GDP-tubulin. Cassimeris *et al.*, 1999.

### 2.1.1 The dynamic instability model.

The observation of MT assembly from purified preparations *in vitro* of tubulin has led to the description of dynamic instability. MTs exist in continuous alternation phases of growth (**elongation**) and shrinkage (**shortening**) with stochastic switches between these states (**Fig.6**) (Desai and Mitchinson, 1997; Shiina *et al.*, 1999; Carvalho *et al.*, 2003).

During the growth and shrinkage tubulin heterodimers are added or lost at the filaments ends. The switch from elongation to shortening is termed **catastrophe**, and the switch from shortening to elongation, **rescue** (Cassimeris *et al.*, 1999). MTs ends can also exhibit a “**pause**” state, showing no significant growth or shrinkage, behaviour often observed in living cells, but its functional significance is yet to be understood (Dammermann *et al.*, 2003)



**Figure 6. MT dynamic instability model.**

MT dynamics length changes by dynamic instability during interphase and mitosis. (Cassimeris *et al.*, 1999)

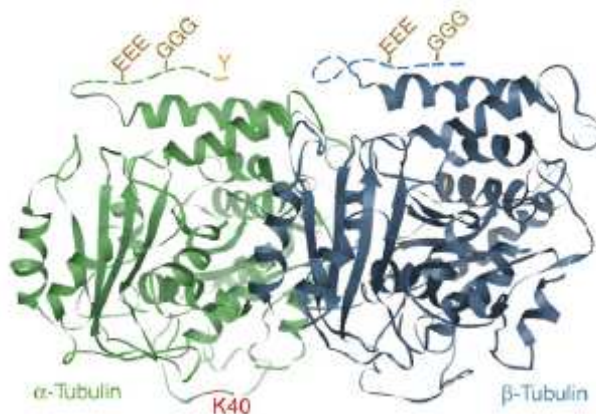
MTs within cells display similar behaviours, but the specific parameters of dynamic instability are influenced by a variety of MAPs that allow the cell to assemble and modify an extensive MT network (Morrison *et al.*, 2006).

### 2.1.2 Tubulin post-translational modifications.

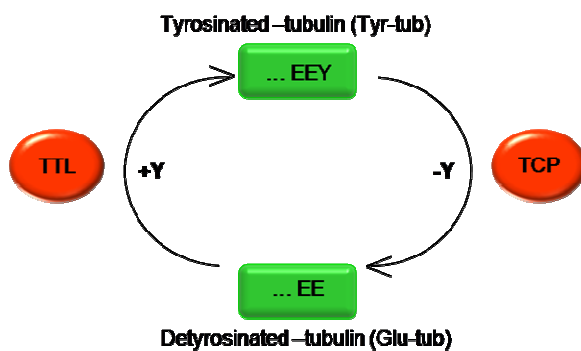
The  $\alpha/\beta$  tubulin dimers are used to generate a variety of MT structures with organelle-specific properties and functions. This characteristic can be achieved in the post-translational modifications (**PTMs**) of the tubulin dimer (**Fig.7a**). These modifications may allow the recruitment of different protein complexes, regulating in this way the MT specific properties (Hammond *et al.*, 2007).

One of the most studied tubulin post-translational modifications is the **tyrosination cycle of the  $\alpha$ -tubulin**. The carboxy-terminal tyrosine is removed by a tubulin tyrosine carboxypeptidase (**TTCP**), giving origin to the Glu-tubulin. The addition of the tyrosine residue to the  $\alpha$ -tubulin occurs on soluble tubulin heterodimers, a reaction catalyzed by tubulin tyrosine ligase (**TTL**). The resulting Glu-MTs seems to be stabilized by suppression of the dynamics at the **+ end** through a capping complex of unknown composition (**Fig. 7b**).

(a)



(b)



### Figure 7. Tubulin post-translational modifications.

(a) Crystal structure representation showing the different PTM on an  $\alpha/\beta$ -tubulin dimer.

**Tyrosination/Detyrosination cycle (Y)** is considered to be involved in cell differentiation. **Polyglutamylation (EEE)** is proposed to participate in the centriole maturation and MAPs interaction. **Acetylation** occurs on the lysine 40 (**K40**), it is supposed to participate in the regulation of cell motility and the binding of MAPs to MTs. **Polyglycylation (GGG)** participates in Tetrahymena: axonemal organization, ciliary motility and cytokinesis. **Phosphorylation (Ser 441/444  $\beta$ -tubulin subunit)**, could participate in neuronal differentiation.

#### (b) $\alpha$ -tubulin tyrosination cycle.

Detyrosination/tyrosination cycle of the  $\alpha$ -tubulin C-terminal tyrosine. The Tyr-tub from  $\alpha$ -tubulin is removed by a tubulin tyrosine carboxypeptidase (**TTCP**), producing a Glu-tubulin. The tyrosine is restored by the action of the tubulin tyrosine ligase (**TTL**). (Modified from Westerman *et al.*, 2003; Hammond *et al.*, 2007)

Detyrosination/ tyrosination cycle recruits differentially two types of MAPs, molecular motors and microtubule plus-end tracking proteins (**+TIPs**). For example the motor protein Kinesin-1 binds preferentially to detyrosinated MTs. In contrast, tyrosinated MTs are involved in the recruitment of + TIP proteins that contain a CAP-Gly domain (e.g. CLIP170 and p150<sup>Glu<sup>ed</sup></sup>). The basic region contained in the CAP-Gly domain is required for targeting to the acidic EEY/F sequence present at the C-terminus of the  $\alpha$ -tubulin. Also, CAP-Gly domains and EEY/F motifs contribute to the binding interactions between +TIPs proteins. Thus, multiple interactions among tyrosinated  $\alpha$ -tubulin, +TIPs and the dynein/dynactin complex contribute to MT-based functions during mitosis and interphase (Rosenbaum *et al.*, 2000; Westermann *et al.*, 2003; Hammond *et al.*, 2007).





### 3. +TIPS

In living cells, a large number of protein factors regulate the MT dynamic instability and the MT based transport, having profound effects on the shape of the MT network during cell division, motility and morphogenesis. Particularly, a group of proteins specifically and dynamically track the tips of growing MTs, they are known as **Microtubule plus-end-tracking proteins (+TIPS)**.

EB1 staining on PHF. 10 $\mu$ m scale bar.

---



### 3. MAPs and the Plus-end-tracking proteins (+TIPs)

*In vivo*, the cellular MT dynamics is the product of a large variety of microtubule associated proteins (**MAPs**). These proteins play an important role in the MT dynamic instability either stabilizing or destabilizing the MT. MAPs function by targeting soluble, non polymerized tubulin subunits, the MT wall lattice and/or MT ends (Akhmanova and Steinmetz., 2008).

Among the different MAPs we found the ones who bind to the length of MTs, and others able to regulate the MT plus-end dynamics. The last ones are known as the microtubule plus-end-tracking proteins (**+TIPs**). Their functions include regulation of MT + end dynamics, providing the MT-to-cortex attachment necessary for vesicle delivery, force generation, and signalling for cortical cell polarity (Carvalho *et al.*, 2003; Galjart *et al.*, 2005).

The +TIPs are a highly diverse group of MT-associated proteins, found in species from yeast to humans. These include both MT-dependent motors and non-motor proteins (**Table II**). The particularity of +TIPs compared to other MT-associated proteins is their specific accumulation at the plus-ends of growing MTs, with a characteristic localization described as “comet-like” structures, coinciding at the end of polymerizing MTs (Akhmanova *et al.*, 2005).

The +TIPs comprise a combinations of a limited set of evolutionary conserved modular binding domains, repeat sequences and linear motifs. An increasing number of proteins have been identified so far, a short list of +TIPs includes the end binding proteins **EB1**, **EB2** and **EB3**; the cytoplasmic linker protein **CLIP170** and **CLIP 115**; the dynein/dynactin MT motor complex, in particular the **p150<sup>Glued</sup>** subunit of dynactin, the adenomatous polyposis coli tumour suppressor protein, APC; the CLIP-associating proteins, CLASPs; and the Mitotic Centromere-Associated Kinesin, MCAK; among many others. The EB family, the CLIPs and P150<sup>Glued</sup> are found at growing MT ends and are the best

<b>+ Tip family</b>	<b>Structural domains</b>	<b>Interaction partners among + TIPs</b>	<b>Main Functions</b>
<b>NON-MOTOR PROTEINS</b>			
<b>EB Family</b> (EB1,EB2,EB3)	CH, coiled coil, EBH, EEY/F	CAP-Gly domains, basic/serine rich stretches)	Promotion MT growth and dynamicity Catastrophe activity Targeting of other + TIPs to MT ends
<b>CAP-Gly family</b> (CLIP 170 CLIP 115)	CAP-Gly, Coiled coil, basic serine rich, zinc finger, EEY/F (CLIP170)	EB proteins CLASPs CLIP170 P150 <sup>Glued</sup> Stu2 XKCM1	MT rescue and stabilization Targeting of dynein to MT ends MT interaction with the cell cortex, kinetochores and vesicles.
p150 <sup>Glued</sup>		Cytoplasmic dynein CLIP170	Binding dynein cargo Regulation of dynein processivity
<b>CLASPs</b> CLASP1 and 2	TOG-like, Basic serine rich	EB proteins CLIP170 CLIP115	MT rescue and stabilization MT interaction with kinetochores, cell cortex and Golgi
<b>APC</b>	Armadillo, SAMP repeats, coiled coil, basic serine rich	EB1 proteins XKCM1	MT stabilization, anti catastrophe activity Interaction with the cell cortex and kinetochores MT-unrelated functions in Wnt signalling, etc
<b>XMAP215/Dis1 family</b> ch-TOG	TOG	EB proteins XKCM1	MT stabilization, promotion of MT growth MT-cortex interactions
<b>MICROTUBULE MOTOR PROTEINS</b>			
<b>Cytoplasmic dynein</b> Dynein heavy chain	AAA-ATPase, coiled coil	Dynactin (p150 <sup>Glued</sup> ) LIS1	MT - end directed transport of macromolecular complexes and organelles, pulling MTs at the cortex.
<b>Kinesin 13</b> MCAK	Kinesin motor, coiled coil, basic/ serine rich	EB proteins XMAP215, CLIP170, APC ( <i>Xenopus laevis</i> )	MT depolymerization, induction of catastrophes

**Table II. + TIPs proteins according to their structural properties.** Main families of Microtubule plus-end tracking proteins (+TIPs). They are grouped according to their structural characteristics. Modified from Akhmanova and Steinmetz, 2008



candidates to be considered as the core component of the MT + TIP complexes (Mimori *et al.*, 2005, Morrison *et al.*, 2006, Siegrist *et al.*, 2007).

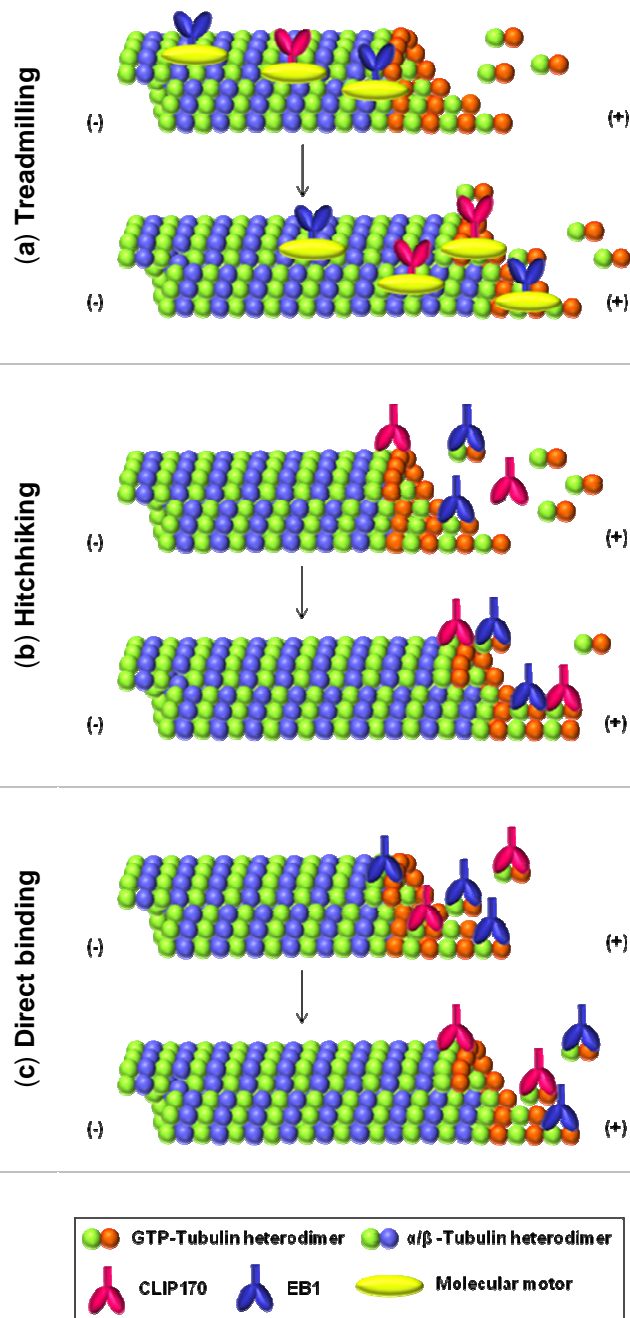
### 3.1 Differential mechanism

The dynamic accumulation of +TIPs at the ends of polymerizing MTs is a poorly understood mechanism. There are three described mechanisms: **Treadmilling** kinesin-mediated transport (**Fig.8a**); **Hitchhiking** on other proteins already localized at the plus-end (**Fig.8b**) and by **direct binding** to the MT plus-end itself by copolymerizing with tubulin (**Fig.8c**) (Wu *et al.*, 2006; Siegrist *et al.*, 2007; Slep and Vale, 2007; Dragestein *et al.*, 2008).

**Treadmilling** (known also as motor driven) refers to the specific association of +TIP proteins at the new formed MT tip by a high affinity mechanism. In the case of CLIP170 the mechanism was described as a “riding on a plus-end directed motor” (Folker *et al.*, 2005). They are coupled to be quickly released from the older part of the MT within a half-life of 1-3 seconds. This mechanism results in a transient concentration of proteins at the growing MT end (Komarova *et al.*, 2005, Dragestein *et al.*, 2008).

In contrast, **Hitchhiking** (or surfing) refers to a MT plus-end-directed transport through an association with microtubule-binding partners (other +TIPs). This interaction might be sufficient to target preferentially some proteins to MT ends (Komarova *et al.*, 2005, Akhmanova and Steinmetz 2008).

The **direct binding to the MT plus-end** (also refers as end loading) mechanism is based on the *in vitro* interaction among +TIP proteins with tubulin dimers in solution. This result suggest a model in which +TIPs bind tubulin, once the +TIP protein has been charged, it joins the MT plus end and the co-assembling takes place. By itself it is a mechanism that provides physically additional interactions for tubulin dimers that finally join the MT tip (Folker *et al.*, 2005; Slep *et al.*, 2007).



**Figure 8. Described mechanism for the MT plus-end localisation.**

Three possible mechanisms that can explain the plus end tracking behaviour.

**(a) Treadmilling**, the plus end directed motor drives the + TIP protein to the MT end.

**(b) Hitchhiking**, the + TIP protein respond to an end-specific conformation or another +TIP protein.

**(c) Direct binding**, the + tip protein binds directly to the MT + end and dissociates a few seconds later. The protein could be pre-loaded with tubulin dimers followed by a MT co-polymerization or by association of the free protein to the MT “cap recognition”, providing a “tubulin free” surface available for the dimers loading.

The + TIPs dissociation has been suggested to occur either by decreased affinity after incorporation into the mature MT lattice or by release due to phosphorylation (Carvalho *et al.*, 2003; Folker *et al.*, 2005; Slep and Vale, 2007)

**Molecular motors** (yellow), **EB1** (blue), **CLIP170** (pink),  **$\alpha/\beta$ -tubulin hetero dimer** (green/orange).

Besides interacting with the MT ends, some + TIPs can bind to tubulin dimers and oligomers *in vitro*. This finding led to the idea that CLIPs reach MT ends by co-polymerizing with tubulin, and are then gradually released from the older lattice. Both EBs and CLIPs are dimers and seems to require at least two tubulin binding domains (calponin homology-CH or CAP-Gly respectively) to track MT ends, which suggest that the affinity of individual sites for MTs or

tubulin is relatively weak. The arrangement of these sites with respect to each other does not seem to be important because an artificial combination of a CH domain and a CAP-Gly domain is capable of plus-end tracking (Akhmanova and Steinmetz.,2008).

In the case of CLIP170, co-assembly with tubulin dimers or oligomers together with quick release from the MT has been proposed. Alternatively, proteins may have an increased affinity for a specific structure of the MT polymerizing end, such as tubulin sheets or the GTP cap (Akhmanova *et al.*, 2005).

Another unresolved aspect of plus-end tracking is the mechanism of protein release from the older part of the MT lattice. Many + TIPs proteins have a high affinity for MTs and decorate the whole MTs *in vitro*, for CLIP170 it was shown that it dissociates from the MTs *in vitro* much slower than *in vivo* (Lansberggen *et al.*, 2006). This preferential dissociation of the + TIPs from the older part of the MT could be the result of their phosphorylation by a MT-bound kinase. This theory remains not proved because the knowledge of + TIPs directed kinases remains fragmentary (Akhmanova *et al.*, 2005).

The most characteristic +TIPs (CLIP170, p150<sup>Glued</sup> and EB1) share certain structure domains such as the CAP-Gly domain (CLIP170 and p150<sup>Glued</sup>) and the dimerization domain, common to the three of them (Galjart *et al.*, 2005; Ligon *et al.*, 2006)

### **3.2 EB1 (Ending Binding Protein 1)**

EB family members are MAPs conserved in plants, yeast and mammals. In general all EB-like proteins share a common role in keeping the MT dynamic. In all species, EB1 homologues promote polymerization by increasing the MT rescue frequencies and decreasing the rate of depolymerization and the time MTs spend pausing (Lansbergen *et al.*, 2006).

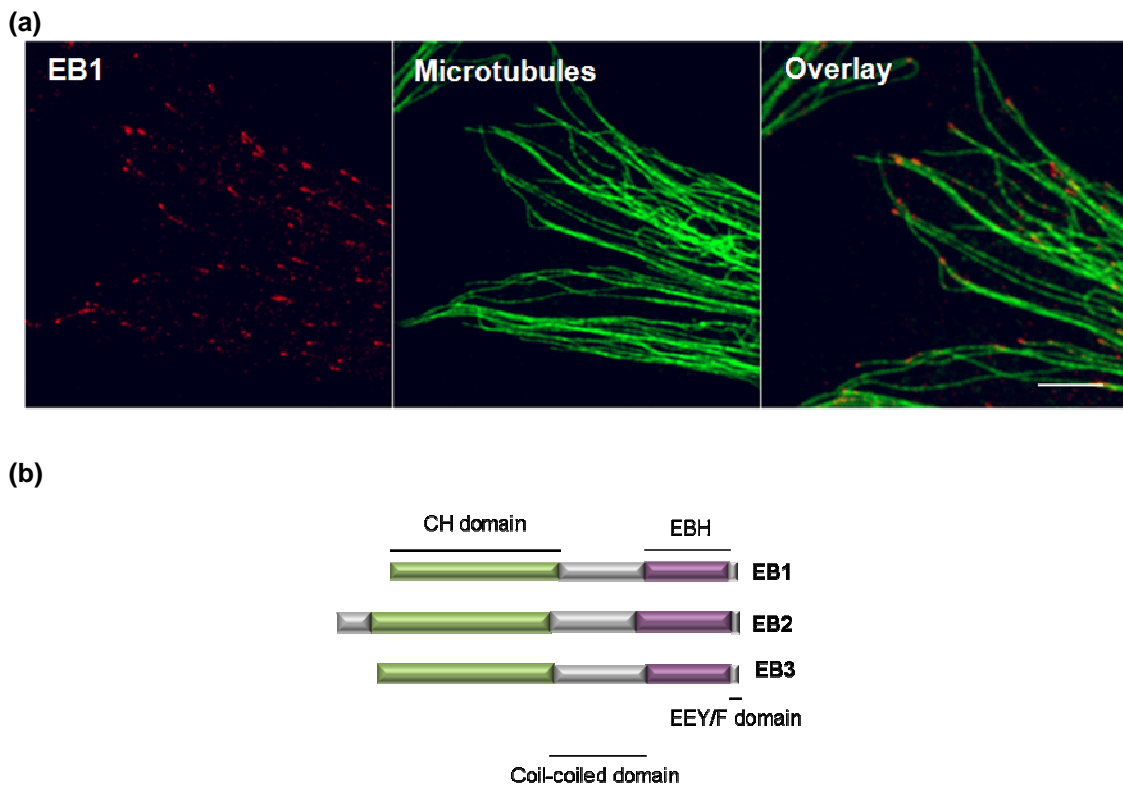
EB1 was first described as an adenomatous polyposis coli (APC) – interacting protein whose binding domain was affected by APC mutations implicated in colorectal cancer. EB1 contributes to the accumulation of APC at the MT ends, where EB1-APC complex can promote MT polymerization and stability.

The EB1 gene was predicted to encode a 268 amino acid protein (Su *et al.*, 1995). Later, Morrison described the EB1 preference for the MT + TIP (1998). Further experiences showed the EB1 tendency for the elongating MTs, and appear to “track with the MT end”, since they are known as “tip tracking” (**Fig.9a**) (Vaughan *et al.*, 2005).

### 3.2.1 EB1 Structure

EB proteins (EB1, EB2 and EB3) contain a highly conserved N- and C-terminal domains that are separated by a linker sequence (**Fig.9b**). The MT binding domain of EB1 is localized at the N-terminal region of the protein, whereas the C-terminal regions contributed to its localizations at the MT +TIP (the dynactin binding domain) and centrosome (Askham *et al.*, 2002; Ligon *et al.*, 2003).

EB proteins exert a growth promoting or stabilizing function in *Xenopus laevis* egg extracts (Su *et al.*, 1995; Tirnauer *et al.*, 2002). They form homodimeric complexes composed of two calponin homology (CH) domains (Gimona *et al.*, 2002), essential for MT association (Hayashi and Ikura, 2003). The MT plus ends recognition is realized via its CH domain through its residues 55-102, the CH domain of EB1 contains a highly basic area that is predicted to form the interface to MT (Hayashi and Ikura, 2003; Sandblad *et al.*, 2006).



**Figure 9. EB1 cell localization and structure. (a)** Immunostaining showing **EB1** localization on primary human fibroblast (PHF) at the tip of MTs. Cells are coimmunostained for MTs (green) and EB1 (red). Scale bar 5  $\mu$ m. **(b)** EB family of proteins general domain structure. EB1 (268aa), EB2 (327aa) and EB3 (281). **CH domain**, Calponin homology domain; **EBH**, End-binding protein homology. Modified from Bu *et al.*, 2003.

The EB1 CH domain is spherical and approximately half the size of a tubulin monomer. Mutagenesis suggests that several residues around one hemisphere contribute to tubulin binding (Slep *et al.*, 2007). Previous studies have suggested that the locus of interaction is near the carboxyl terminus of  $\alpha$ -tubulin (Honnappa *et al.*, 2006).

The C terminal region of the EB proteins contains a coiled-coil domain, which mediates the parallel dimerization of EB monomers. The  $\alpha$ -helical coiled-coil is a universal protein oligomerization motif that is frequently found in +TIPs (Akhmanova and Steinmetz., 2008)

### 3.2.2 EB1 Interactions

EB1 binds to and labels a subset of the total MT population, specifically, the tips of MTs undergoing elongation. Immunofluorescence microscopy images

suggest that native EB1 is punctuate, resembling large protein complexes. This would be consistent with the extensive co-localization with other membrane-associated proteins such as CLIP170 and dynactin.

Direct interactions between EB1 and other proteins (p150<sup>Glued</sup> and CLIP170) have been interpreted as recruitment mechanisms. The fact that these binding partners can also bind tubulin directly suggests some transition or sequential loading process at the plus-ends (Vaughan *et al.*, 2005).

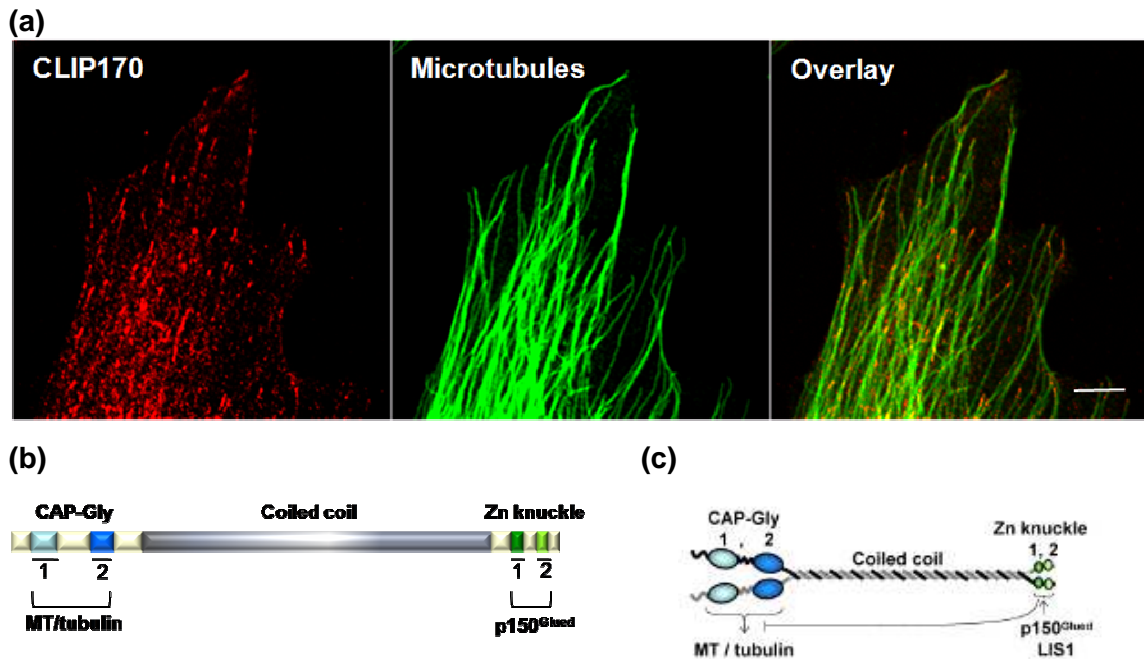
A detailed electron microscopy study showed that the yeast EB1 homologue Mal3 can specifically bind to the MT seam (**Fig.4**), proposing that EB proteins might recognize tubulin sites that are normally shielded by contacts between protofilaments (Sandblad *et al.*, 2006; Akhmanova and Steinmetz, 2008)

### 3.3 CLIP170 (Cytoplasmic Linker Protein 170)

The term CLIP was proposed for a new class of MT-binding protein that mediated specific interactions between organelles and growing MTs. The first identified member of this family is CLIP170, a linker between endosomes and MTs (Galjart *et al.*, 2005; Ligon *et al.*, 2006) who presents a classical comet-like pattern at the tips of growing MTs (**Fig.10a**).

#### 3.3.1 CLIP170 structure

Structurally, consist of a central  $\alpha$ -helical, coiled-coil domain that separated an N-terminal microtubule-binding region from a C-terminal binding motif (**Fig.10b**). This C-terminal domain was presumed to be the cargo binding domain that was responsible for the interaction of CLIP170 with endocytic vesicles. (**Fig. 10c**) (Galjart *et al.*, 2005).



**Figure 10. CLIP170 cell localization and structure.** (a) Primary human fibroblast Immunostaining showing CLIP170 comet like staining at the end of the MTs. Scale bar 5  $\mu\text{m}$ . (b) CLIP170 domains and protein-protein interaction regions. Coiled-coil region (grey), Cap-gly domains (blue), zinc knuckles (green). (c) CLIP170 dimerization model. Modified from Galjart *et al.*, 2005, Mishima *et al.*, 2007.

The N-terminal domain of each monomeric subunit of CLIP170 contains two similar cytoskeleton-associated protein glycine rich (CAP-Gly) domains (Fig.10b) (Galjart *et al.*, 2005). These domains mediate their interaction with MTs and EB proteins. They are also found in the structurally related large subunit of the dynein complex, p150<sup>Glued</sup>. The coiled-coil domains mediate their homotypic association and result in the formation of parallel dimers (Fig.10c) (Akhmanova and Steinmetz., 2008).

The C-terminus of CLIP170 contains Cys and His residues, which are predicted for a metal binding domain. Two of these domains, called Zinc Knuckles are present in each monomer (Fig.10b) (Galjart *et al.*, 2005).

### 3.3.2 CLIP170 interactions

The CAP-Gly structural resemblance among CLIPs and p150<sup>Glued</sup> raises the possibility that CLIPs are involved in aspects of dynein-dynactin function. In interphase HeLa cells, CLIP170 have been reported to accumulate in “patches”

along the MT network (although the nature of the patches is not clear) and at the plus-ends of MTs. In mitotic cells, CLIP170 localizes to prometaphase kinetochores, which indicates its role in chromosome segregation. Overexpressed mammalian GFP-CLIP170 interacts with MT ends by a treadmilling mechanism. In this manner, CLIP170 binds with high affinity to the newly synthesized, distal end of a polymerizing MT, is transiently immobilized and subsequently dissociates from the MT lattice (Galjart *et al.*, 2005).

How CLIP170 recognizes the MT end and how it dissociates from the MT lattice is not yet clear. However, some essays showed that CLIP170 binds the acidic tails of EB1/EB3 as well as those of  $\alpha$ -tubulin (Honnappa *et al.*, 2006). This fact suggests that EB1/EB3 that localized at the MT plus end contribute to the CLIP170 recruitment to the plus end. This positively charged binding surface is not necessarily preserved in other CAP-Gly domains, suggesting that the CAP-Gly domain is a common structural module found in cytoskeletal proteins but may participate in other protein-protein interactions. The p150<sup>Glued</sup> CAP-Gly domain has a less positively charged surface only weakly interacts with the  $\alpha$ -tubulin acidic tail (Mishima *et al.*, 2007).

CLIP170 but not EB1 fails to recognize the ends of detyrosinated MTs in cultured cells (Peris *et al.*, 2006), showing that C-terminal tyrosine of  $\alpha$ -tubulin is essential for the accumulation of CLIP170 on MT ends and that the presence of EB1 is not enough.

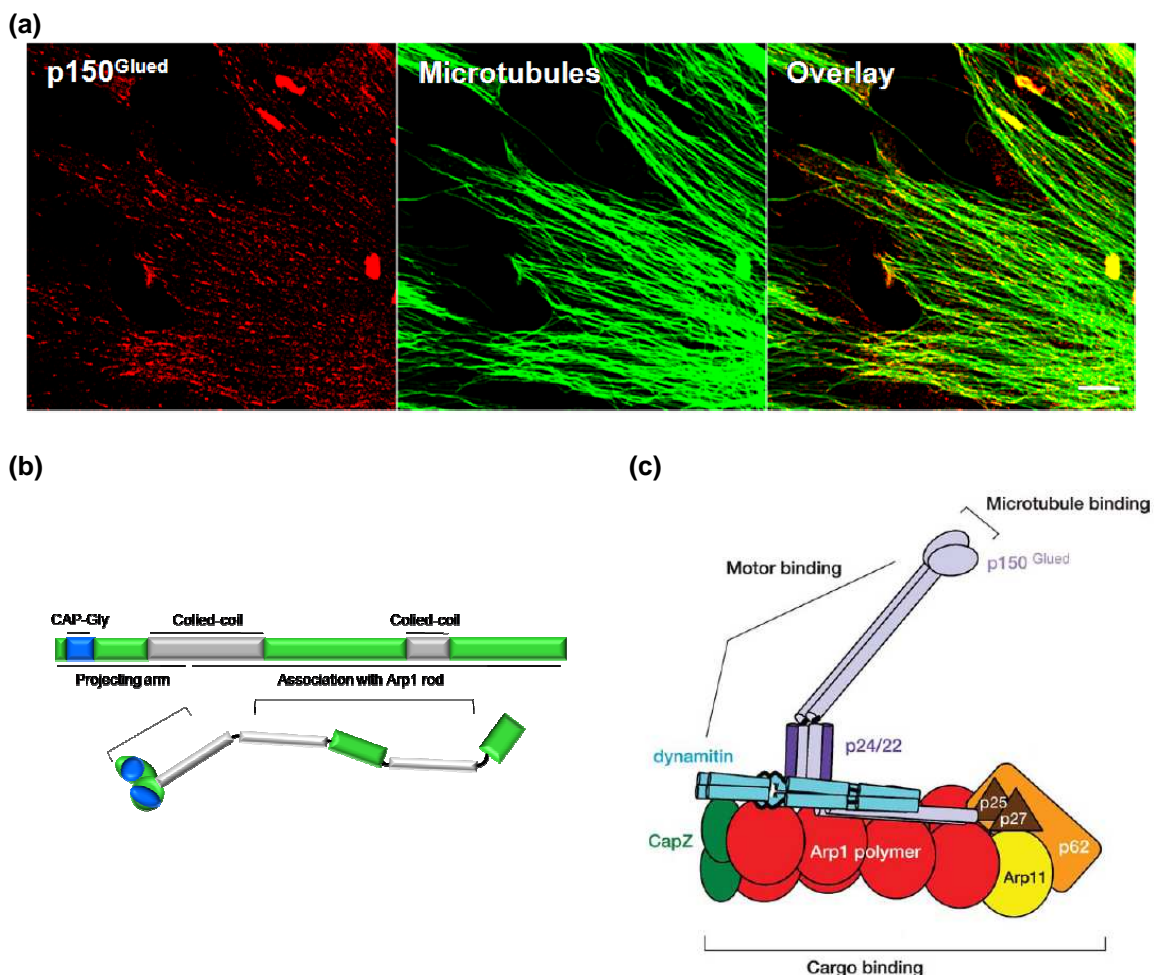
### 3.4 p150<sup>Glued</sup>

p150<sup>Glued</sup> own its name in reference to the *Drosophila* homologous gene *Glued* (Holzbaur *et al.*, 1991; Gill *et al.*, 1991) and was first described as a polypeptide of 150kDa, which co-purifies with the microtubule-activated mechanochemical ATPase, the cytoplasmic dynein (Collins and Vallee., 1989). p150<sup>Glued</sup> exists as part of the stable macromolecular dynactin complex



conformed by: Arp1 polymer, Arp11, p62, p27, p25, p24/22, CapZ and dynactin (Waterman-Storer *et al.*, 1995).

Dynactin is required for mitosis in multicellular organisms and is thus essential for viability. The dynactin largest sub-unit is p150<sup>Glued</sup>, and plays an important role, as it participates in motor binding and enhancement of motor processivity (Schroer *et al.*, 2004). It localizes at the tip of growing MTs forming the classical comet-like structures (Fig. 11a).



**Figure 11. p150<sup>Glued</sup> cellular localization and domain organization in the dynactin complex**  
**(a)** Primary human fibroblast immunostaining showing p150<sup>Glued</sup> comet like staining at the end of the MTs. scale bar 5 $\mu$ m. **(b)** p150<sup>Glued</sup> domain organization and proposed functions. **(c)** Dynactin complex schematic conformation. CAP-Gly domain (blue), Coiled-coiled regions (green). Modified from Schroer *et al.*, 2004

### 3.4.1 p150<sup>Glued</sup> structure

p150<sup>Glued</sup> is the largest of all dynactin subunits (**Fig.11b**). It assembles into an elongated dimer that contains two central coiled coils of approximately ~50 and ~20 nm in length respectively. Each of the two globular heads at the very tip of the dynactin arm contains a conserved CAP-Gly (Cytoskeleton-Associated Protein, Glycine-rich) motif.

The CAP-Gly motif is contained within the extreme N-terminus (aa 1-110) (Schroer *et al.*, 2004), these domains mediate their interaction with MTs and EB proteins (Akhmanova and Steinmetz., 2008), the presence of coiled-coil domains allow the formation of dimers, the same mechanisms as CLIP170 (**Fig.11c**).

### 3.4.2 p150<sup>Glued</sup> interactions

The CAP-Gly motif plays a very important role in dynactin function. N-terminal fragments of p150<sup>Glued</sup> bind MTs *in vitro* and *in vivo*. MT binding by p150<sup>Glued</sup> is necessary for its ability to enhance the processivity of the dynein motor. The CAP-Gly domain may also contribute to MT minus end anchoring at interphase centrosomes and mitotic spindle poles (Schroer *et al.*, 2004).

In addition to MTs, the p150<sup>Glued</sup> CAP-Gly domain binds proteins such as EB1 and CLIP170, both of which are themselves microtubule-binding proteins (Schroer *et al.*, 2004). p150<sup>Glued</sup> binds to the flexible C-terminal tail (20 aa) of EB1 through its N-terminal CAP-Gly domain. The N-terminal CAP-Gly domain of p150<sup>Glued</sup> forms a complex with EB1 of moderate stability consisting of two molecules of p150<sup>Glued</sup> and one molecule of EB1 dimer (Manna *et al.*, 2008).

Even though the CAP-Gly motif is generally considered to function as a tubulin-binding module, most recently CAP-Gly module of +TIPs have been implicated in the tubulin Detyrosination-tyrosination cycle (Erck *et al.*, 2005; Peris *et al.*, 2006). The p150<sup>Glued</sup>-CLIP170 interaction links CLIP170 to the dynein-dynactin pathway and is essential for the efficient recruitment of the

dynactin to growing MT plus ends. It has been suggested that the C-terminal EEY/F sequence motif contained by the EB proteins and the  $\alpha$ -tubulin can activate CLIP170 by targeting the CAP-Gly domains. Activation of +TIPs through their associations with other members of this family represents a common issue in their function: the CAP-Gly domain of p150<sup>Glued</sup> activates EB1 by binding the EB1 EEY/F sequence motif (Weisbrich *et al.*, 2007).

### 3.5 Regulation of +TIPs interactions

The +TIPs specificity can be given by different mechanisms, some of them MT-related. This specificity can be the product of motor-based loading, local control of post-translational modifications or intramolecular actions. Using this strategy different processes can have place such as cell division, cell polarity and cell differentiation (Akhmanova and Steinmetz., 2008).

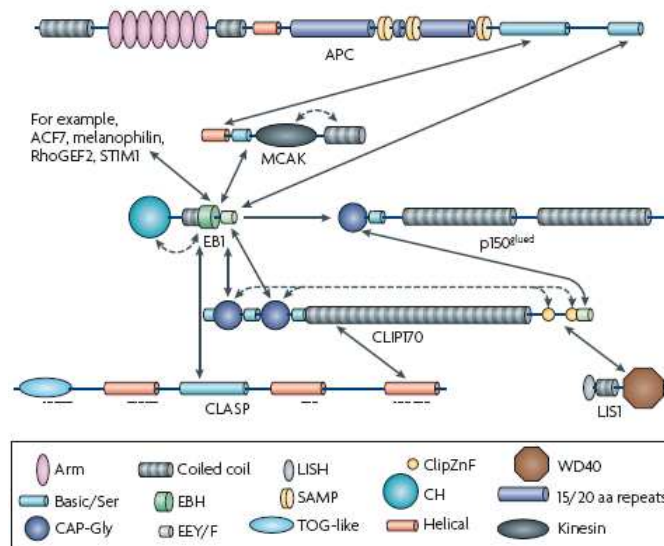
Proposed mechanisms for higher affinity plus-end binding include a selection of different conserved sequences, phosphorylation related activity, autoinhibition among one or many proteins,  $\alpha$ -tubulin detyrosination-tyrosination at the MT +TIP conformation, preferential binding to the GTP cap region and recognition of a unique structural feature of the growing plus-end can be cited as a few among many strategies.

#### 3.5.1 Specific sequences

A **first** mechanism to be considered includes the specific +TIP mechanism developed for each +TIP protein. Each plus-end proteins so far identified have different microtubule-binding-domains (CH domain for EB1, CAP-Gly domain for CLIP170 and p150<sup>Glued</sup>) as part of a final strategy: to be targeted to MTs and to load and transport tubulin dimers.

The *in vitro* interactions among the +TIPs have been previously subject of study. For example the **p150<sup>Glued</sup> N-terminal** domain (the CAP-Gly domain) interacts with the **EB1 C-terminal** domains (Honnappa *et al.*, 2006) allowing

p150<sup>Glued</sup> to recruit the soluble EB1. In the other hand **p150<sup>Glued</sup>** also recruits the free **CLIP170** through its C-terminal zinc knuckle domain (**Fig. 12**) (Akhmanova and Steinmetz., 2008). EB1 could also contribute to the +TIPs tracking to the MT growing end mainly through its interactions with p150 and MCAK (Carvalho *et al.*, 2003). Additionally, **EB1** could positively regulate **XMAP215** by promoting its binding to MTs. EB1 binds throughout the cell cycle to MT ends, but it affects MTs growing only during mitosis, when it interacts with XMAP215 (Kronja *et al.*, 2009).



**Figure 12. Schematic +TIPs hierarchy.** The established relationship among each protein domain constitutes by itself a +TIP mechanism of targeting. An example of the +TIPs interaction is illustrated; each domain has been identified by a symbol. Arrows indicate the interactions among domains; pointed arrows indicate auto-inhibition processes described for CLIP170 (Akhmanova and Steinmetz, 2008).

This domain-selective interaction among +TIPs proteins make us think in a “sequential interaction mechanism”; where one protein recruits the next one, guaranteeing the tubulin dimers addition using their different “active domains” in this physico-chemical chain reaction.

### 3.5.2 Phosphorylation

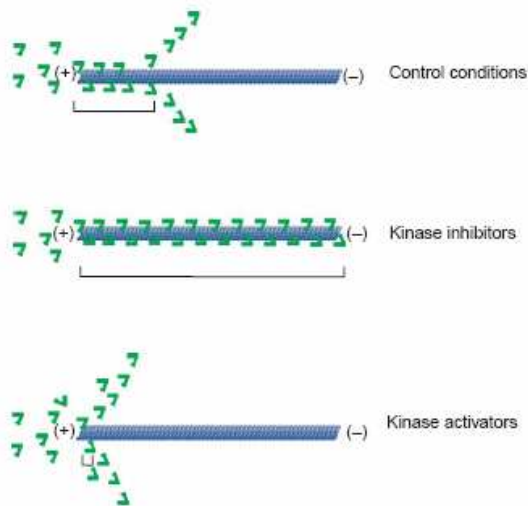
A **second** mechanism to consider could involve **phosphorylation**. Most identified MAPs are known to be regulated by this mechanism, and the more phosphorylated forms are inhibited in the ability to stabilize MTs. The binding of

MAPs to MTs is predominantly electrostatic, involving the highly acidic C-terminal domains of both  $\alpha$  and  $\beta$  tubulin (Desai and Mitchinson, 1997).

Some of the +TIPs proteins are phosphorylation “sensitive”, being the case for CLIP170 (Perez *et al.*, 1999), p150<sup>Glued</sup> (Wu *et al.*, 2006; Kardon *et al.*, 2009) and APC (Zumbrunn *et al.*, 2001).

The +TIP behaviour could be related to the serine-rich regions, originating a basic sequence. Given the negative charge of the MT, phosphorylation of the +TIPs proteins in this specific region might reduce their affinity, regulating in this way the tubulin-+TIP loading-unloading mechanism.

The use of kinase inhibitors suggest that kinase activity could be responsible for the MT +TIP targeting (Fig.13). This is the most favoured mechanism for selective release from the MT wall, which is known to inhibit the binding of CLIP170 and p150<sup>Glued</sup> to MTs through the phosphorylation of their targets (rapamycin and protein kinase A respectively) (Carvalho *et al.*, 2003).



**Figure 13. Protein kinases and tip tracking.** The +TIP proteins recruitment at the MT growing end could be controlled by kinases. The +TIPs presence have been evaluated in presence or absence of kinase inhibitors or activators. The **kinase inhibitors** promote the +TIP protein binding with a slow release, leading to a larger +TIP comet-like structure, in comparison to the control conditions. In contrast, **kinase activators** boost the +TIPs proteins release, inducing to a highly limited MT plus-end binding. The length of the +TIP comet like structure is indicated in each case by the scale. Modified from Vaughan *et al.*, 2004

Additionally, the cell cycle MT dynamics indicate that many +TIPs might be substrates of mitotic kinases. It is tempting to think that CDK1 alters the balance between kinases and phosphatases that modulate the dynamics of interactions between MAPs (Niethammer *et al.*, 2007).

### 3.5.3 Mechanical implications.

The biological response of the + TIPs proteins to a **mechanical change** has been considered as a mechanism in itself. Could the classic + TIP distribution be a consequence of binding to a tubulin conformation, such as flat sheets of tubulin polymer that is only present at the MT +TIP?. This is an attractive idea as it provides a mechanism for the dissociation of + TIPs from older MT polymer, where the + TIPs proteins release is triggered by conformational change when the MT sheet curves into a hollow tube (Morrison *et al.*, 2006) and the MT conformation changes from a deep-long structure to a linear one.

### 3.5.4 $\alpha$ -tubulin tyrosination-detyrosination

The post-translational tubulin modification identified as **tyrosination** and **detyrosination** could be considered as one possible mechanism of +TIPs proteins targeting to the MT growing end.

A specialized subset of stable detyrosinated MTs accumulates markedly fewer CAP-Gly proteins at their plus ends. In most eukaryotic cells, the EEY/F tail of  $\alpha$ -tubulin is subjected to an enzymatic detyrosination-tyrosination cycle in which the C-terminal tyrosine is repeatedly cleaved and added back (**Fig. 7**). Suppression of this cycle leads to defects in spindle positioning, abnormal cell morphology, disorganized neuronal networks and tumor progression.

Recently the  $\alpha$ -tubulin tyrosination has been linked to the ability of the MT end to recruit p150<sup>Glued</sup>, CLIP170 and CLIP115, consistent with the fact that most CAP-Gly domains specifically recognize C-terminal EEY/F motifs. This strategy could provide a molecular basis of the detyrosination/tyrosination cycle in controlling CAP-Gly proteins (Weisbricht *et al.*, 2007).

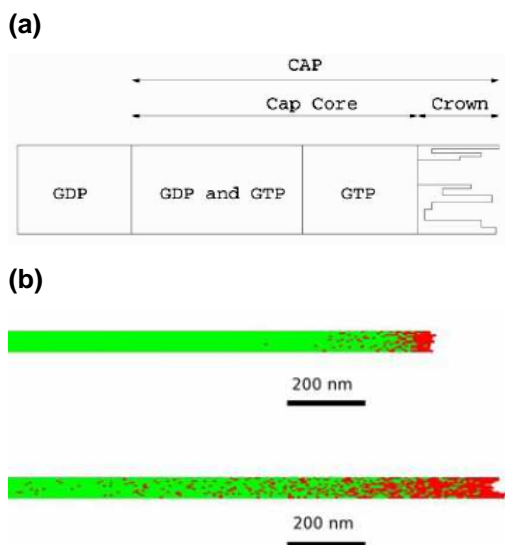
In this case, the fundamental role of the tubulin detyrosination-tyrosination cycle would be to regulate the binding of CAP-Gly proteins to a specific population of MTs, the ones that are polymerizing in a highly changing

environment and the ones that are anchored to the cellular focal adhesion points.

### 3.5.5 The GTP cap.

Proteins accumulation at the MT growing end could be related to the structural difference provided by the GTP hydrolysis, the **GTP cap** (Fig. 14). In mammals this cap has an average length of 0.5-2 $\mu$ m (Akhmanova and Steinmetz, 2008).

In pure tubulin solutions, the GTP tubulin dimer is proportional to the concentration of the free tubulin going from ranges of 20 to 80nm length. The cap is formed from two components: a crown consisting of incomplete protofilaments and the core that forms the MT and include the GDP tubulin dimers (Piette *et al.*, 2009)



**Figure 14. MT GTP-cap theoretical model. (a)** For structural studies the GTP cap is divided into two components: a **crown** consisting of new added protofilaments and the **core** that forms the body of the complete MT. The core would contain a mixture of GDP and GTP tubulin dimers. **(b)** MT cap structure model. Under two different tubulin concentrations (lower and higher respectively) the GTP-cap structure is calculated. The cap length is considered to be the distance from the MT tip to the last GTP tubulin dimer; this distance (the GTP-cap) is proportional to the concentration of free tubulin in the solution. GDP-tubulin (**Green**), GTP-tubulin (**Red**). From Piette *et al.*, 2009

Each one of these mechanisms have an effect from the very +TIP to a range of nm of distance on the already created and sealed MT. The combination of each one of the could create the general picture that we can see, a highly dynamic MT that grows and shrinks thanks to the collective activity of several proteins and physicochemical interactions that make of the MT growing end a re-encountering point for the +TIPs proteins.

### 3.5.6 Autoinhibition complexes or co-regulation?

The different complex that produce a +TIP comet structure could be the result of protein complexes that regulates its self or that could be regulate for other proteins. These mechanisms might have as objective the regulation and dynamics of the activity among the different proteins.

CLIP170 can fold on it self, acquiring an auto-inhibiting conformation. Here, the C-terminal region of the protein bind and blocks the N-terminal one, blocking the protein activity. The blocked mechanism would be released only if EB1 intervention takes place (Fig. 15) (Lansbergen *et al.*,2004).

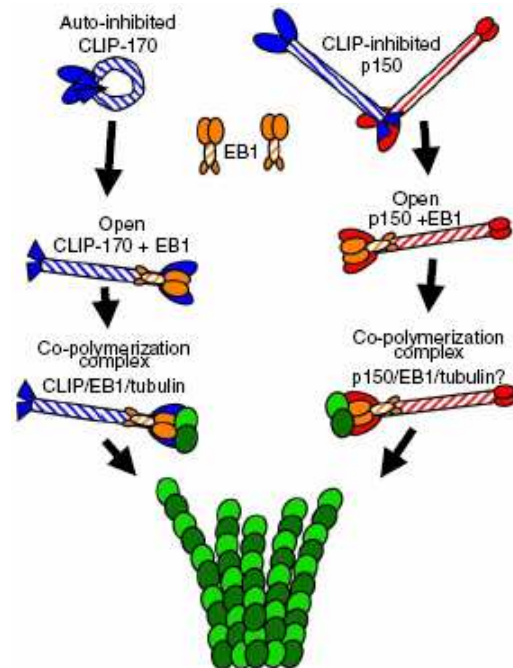
**Figure 15. CLIP170 autoinhibition model.**

The +TIPs comet-like structure could be the result of different complex at the end of growing MTs.

CLIP170 auto-inhibition could have place by the binding of the C-terminal domain to its N-terminal portion of the protein. Another strategy to reach inhibition could take place through the CLIP170-p150<sup>Glued</sup> complex (C-terminal and N-terminal region respectively).

Then, and to load tubulin dimers, the EB1 N-terminal domain can bind to CLIP170 and p150<sup>Glued</sup> N-terminal domains, the inhibitory complex is released to create a complex of their own, where the tubulin dimer is captures and added at the MT growing plus-end.

CLIP170 (blue), p150<sup>Glued</sup> (red), EB1(orange), tubulin dimers (green). From Ligon *et al.*, 2006.



Another approach would indicate that the +TIPs proteins could co-regulate each other. EB1 can bind directly the CAP-Gly domain of CLIP170 and/or p150<sup>Glued</sup>, both contained in the N-terminal regions of the proteins. The two different complexes: EB1/CLIP170 and EB1/p150<sup>Glued</sup> may bind to tubulin dimers to finally target the MT growing end *in vitro*. Further studies suggest that the EB1/CAP-Gly domain interaction could be involved in the activation of this



complex to MT binding (Ligon *et al.*, 2006; Hayashi *et al.*, 2007; Manna *et al.*, 2008).

The inter-dependent interaction among p150<sup>Glued</sup> and EB1 has been probed through the siRNA approach. p150<sup>Glued</sup> depletion leads to EB1 mislocalization along the length of the MT, over-expression can produce the same mislocalization as well (Ligon *et al.*, 2006; Hayashi *et al.*, 2007)





#### 4. XMAP215/ch-TOG

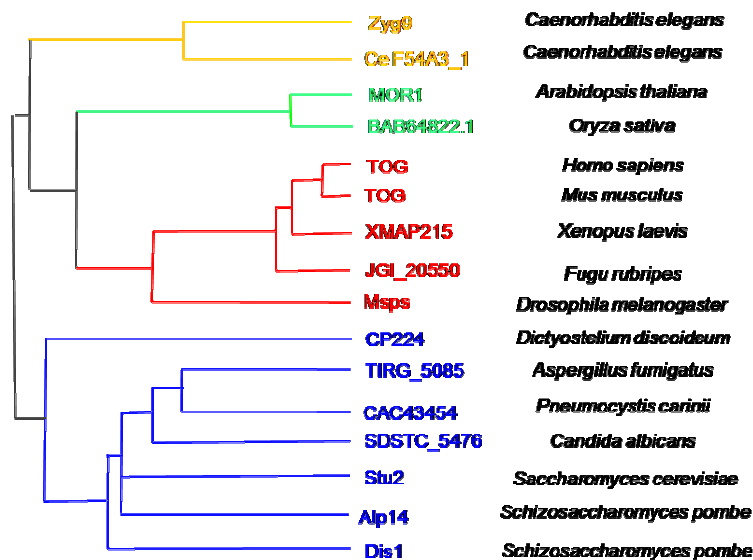
In 1987 David Gard and Marc Kirshner from the University of California, reported the isolation of a protein factor from *Xenopus* eggs that promoted microtubule assembly *in vitro*. This assembly promotion was associated with a 215-kDa protein, termed ***Xenopus* Microtubule Assembly Protein (XMAP)** (From Gard and Kirshner 1987).

XMAP215 staining in PHF. Scale bar 10  $\mu\text{m}$



#### 4. The XMAP215/Dis1 family.

During the cell cycle the MTs change their distribution in order to provide the dynamics to the different cell states. A class of proteins called microtubule-associated proteins (**MAPs**) which includes MT motors plays a key role in the regulation of MTs *in vivo*. A highly conserved family of non motor MAPs, the **XMAP215/Dis1** family has been described in various organisms, including yeast, animals and plants (**Fig. 16**), been the only known family of MAPs common to plants and animals (Ohkura *et al.*, 2001; Brittle and Ohkura, 2005).



**Figure 16. Phylogenetic tree of the XMAP215/Dis1-family.**

The conserved XMAP215 family of proteins has been described in plants, animals and yeast, reflecting in this way the high conservation level through evolution. Mostly of them were described through genetic screens. Abbreviations: human **TOG** (Tumour Over expressing Gene, Charrasse *et al.*, 1998), mouse **TOG** (Tumour Over expressing Gene, Kawai *et al.*, 2001), **XMAP215** (*Xenopus laevis* Microtubule Associated Protein of apparent molecular weight of 215 kDa. Gard and Kirschner, 1987), **Msp1** (Mini Spindles, Cullen *et al.*, 1999) **MOR1** (Microtubule Organization gene 1. Whittington *et al.*, 2001), **CP224** (Centrosomal Protein of 224 kDa. Gräf *et al.*, 2000), **Zyg9** (Zygote defective, Vanderslice, 1976), **Dis1** (Defect in Sister chromatid disjoining. Ohkura *et al.*, 1988) / **Alp14** (Altered Polarity loci 14. Garcia *et al.*, 2001) and **Stu2** (Suppressor of a tubulin mutation contain 2 TOG repeats. Wang and Huffaker, 1997). Modified from Ohkura *et al.*, 2001; Kinoshita *et al.*, 2002, Gard *et al.*, 2004

These MAPs associate with various MT structures in a dynamic way and appear to be involved in a range of different aspects of MT function – kinetochore activity, spindle formation and cell morphogenesis, for example.

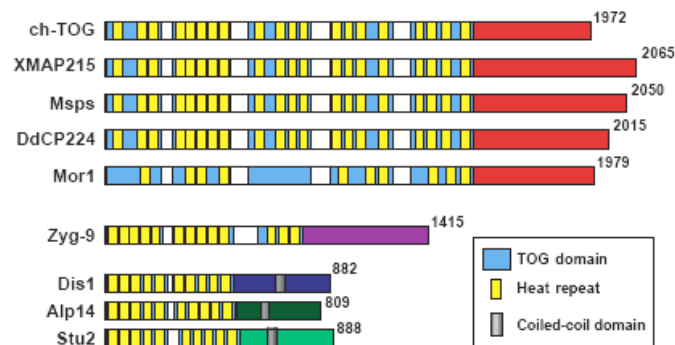
The fact that XMAP215/Dis1 family members were isolated by various approaches -genetic, biochemistry, cell biology and molecular cloning- reflects their multiple roles (Ohkura *et al.*, 2001).

#### 4.1 Protein Structures: conserved repeat motifs.

The most characteristic feature of this family is an N-terminal repeating structure (**Fig. 17**). The N-terminal regions contain two to five repeats of ~200 amino acid residues so called “**TOG domains**” named after their initial identification in the human ortholog, **ch-TOG** (Ohkura *et al.*, 2001; Al-Bassam *et al.*, 2007). Each one of these TOG domain repeats consists of up to five **HEAT** motifs.

The HEAT repeats are thought to be protein-protein interaction domains (Ohkura *et al.*, 2001). They derive their name from four diverse eukaryotic proteins in which they were first identified: **Hungtintin** (involved in Huntington’s disease), **Elongation factor 3**, **PR65/A** (a subunit of protein phosphatase A), and the **TOR** the target of rapamycin (Andrade *et al.*, 2001).

The significance and function of the repeats that define the XMAP215/Dis1 family are not yet understood. The TOG domain is structurally predicted:  $\alpha$ -helical zig-zags that form elongated, sometimes spirally curved domains, this diversity of conformations are the result of the HEAT repeat structures contained in it (Al-Bassam *et al.*, 2007). Given the diverse function of proteins that possess HEAT repeats, it is likely that this is the protein-protein interaction domain for each member of the XMAP215/Dis1 family (Ohkura *et al.*, 2001).



**Figure 17. Architecture of the XMAP215/Dis1 family of MAPs.** TOG domains can be numbered (TOG1, TOG2, etc) from left to right based on their positions in the protein. The C-terminal region of the yeast protein (Dis1, Alp14 and Stu2) has a coiled-coil domain followed by a basic region that has been shown to bind MTs. In higher eukaryotes homologues the sequence is unique and has a C-terminal domain implicated in MT association (Ohkura *et al.*, 2001)

The family can be divided into three groups based on the number of TOG domains they contain.

The **first** group, the higher eukaryotic homologs that contain five repeats the N-terminal region and a conserved C-terminal non-repeat domain. This group includes the human ch-TOG, *Xenopus laevis* XMAP215, *Drosophila melanogaster* Mini spindles, *Dictyostelium discodeum* (amoeba) DdCP224 and *Arabidopsis thaliana*, MOR1.

The **second** group consist of only one known protein, *Caenorhabditis elegans* Zyg-9, which has three repeats in the N-terminal region and a C-terminal non repeat region that has no apparent similarity to the other proteins.

The **third** group, the lower eukaryotic homologs, such as *Saccharomyces cerevisiae* Stu2p, *Schizosaccharomyces pombe* Dis1 and Alp14, which have two repeats in the N-terminal region and form homodimers at a C-terminal non repeat region. The non-repeat regions in the yeast proteins contain a predicted coiled-coil region, followed by a basic region that has been shown to bind MTs (Ohkura *et al.*, 2001; Al-Bassam *et al.*, 2007).

Individual XMAP215 family members exhibit a high diversity of functional properties. For example, Stu2 and higher eukaryotic XMAP family members bind free tubulin, meaning that the capture of tubulin heterodimers is a TOG domain-related activity. They increase MT plus-end growth rates, suggesting that they facilitate plus-end addition of  $\alpha/\beta$ -tubulin heterodimers, they can have also a destabilizing activity, for example Stu2p, ch-TOG and XMAP215 (Kerssemakers *et al.*, 2006; Al-Bassam *et al.*, 2007).

Detailed comparisons based on the alignment of the TOG domains from Stu2p, XMAP215 and Zyg9 proteins suggest that they have diverged into types based on their position in the protein. TOG domains have been classified after their physiological pH (**Fig 18**). The **Type A** domains are composed by the even-numbered TOG domains that display a negative charge (TOG2 and TOG4) and bind  $\beta$ -tubulin preferentially, the **Type B** domains are composed by the TOG odd-numbered domains (TOG1 and TOG3) that bind  $\alpha$ -tubulin preferentially; and the TOG domain 5 is **Type C** because its part of a basic region that has been shown to bind MTs (Al-Bassam *et al.*, 2007; Slep and Vale, 2007).



**Figure 18. TOG domains subclassification.** Classification of TOG domains 1 to 5 for the XMAP215/ch-TOG homologue in *Drosophila melanogaster*, Mini spindles (**Msp**). **CTD**, C-terminal domain; Type A TOG domain (light green); Type B TOG domain (dark green). Modified from Slep *et al.*, 2007

## 4.2 Cellular localization of XMAP215/Dis1 proteins.

Functional studies of the XMAP215/Dis1 family of proteins including *S. pombe*, *S. cerevisiae*, *D. melanogaster*, *C. elegans*, *H. sapiens*, *X. laevis* and *D. discoideum* revealed a role for the proteins in the organization and function of the mitotic spindle (Charrasse *et al.*, 1998; Gräf *et al.*, 2000; Tournebize *et al.*, 2000; Garcia *et al.*, 2001; Nakaseko *et al.*, 2001). Further studies showed that they were all associated with the MT network and centrosomes or spindle pole bodies in some or all stages of the cell cycle (**Table. III**) (Popov *et al.*, 2001).



<i>Found on</i>	<i>P93dis1</i>	<i>STU2</i>	<i>Msp</i> s	<i>Zyg-9</i>	<i>ch-TOG</i>	<i>XMAP215</i>	<i>DdCP224</i>
<b>MTs in interphase</b>	+GFP	+/- GFP	-IF	-IF	+IF	+IF, GFP	+IF, GFP
<b>MTCO interphase</b>	- ?GFP	+GFP	-IF	-IF	-IF	-IF, GFP	+IF, GFP
<b>MT mitotic spindle</b>	+/- GFP	+/- GFP	+IF	+IF	+IF	+IF, GFP	+IF, GFP
<b>Spindle poles</b>	+GFP	+GFP	+IF	+IF	+IF	+IF, GFP	+IF, GFP

**Table III. Cellular localization for some of the proteins of the XMAP215/Dis1 family.** **Dis1**, *Schizosaccharomyces pombe*; **Stu2**, *Saccharomyces cerevisiae*; **Msp**s, *Drosophila melanogaster*; **Zyg-9**, *Caenorhabditis elegans*; **ch-TOG**, *Homo sapiens*; **XMAP215**, *Xenopus laevis*; **DdCP224**, *Dictyostelium discoideum*. **MT**, microtubule; **MTCO**, MT organization center; **IF**, Immunofluorescence; **GFP**, Green fluorescent protein expression. Popov *et al.*, 2001; Gard *et al.*, 2004

Dramatic spindle defects are seen in mutants of the *Drosophila* homologue, mini spindles (*msps*) (Cullen *et al.*, 1999; Cullen and Okhura, 2001) and in *ch-TOG* depletion (Gergely *et al.*, 2003; Holmfeldt *et al.*, 2004). Defects in astral MTs are seen in budding yeasts *Stu2* mutants and the worm homologue *zyg-9* (Matthews *et al.*, 1998; Usui *et al.*, 2003). A functionality Kinetochore-related has been described for *Dis1*, *Alp14*, *Stu2* (Garcia *et al.*, 2001; Nakaseko *et al.*, 2001; Severin *et al.*, 2001).

The functions of the XMAP215 family in regulating MT behaviour have been conserved through evolution. It is possible that a three component system: XMAP215/Dis1 family, Kin I family and tubulin have coevolved to maintain a highly dynamic state of MT plus-ends during cell proliferation. In addition, there is evidence that the XMAP215/Dis1 protein family might have a second role in kinetochore activity. *Dis1*, *Alp14* and *Stu2* localize to kinetochores and the mutation of *dis1* and *stu2* reveals that the dynamic behaviour of sister centromeres during early mitosis requires *Dis1/Stu2* function (Kinoshita *et al.*, 2002).

### 4.3 XMAP215

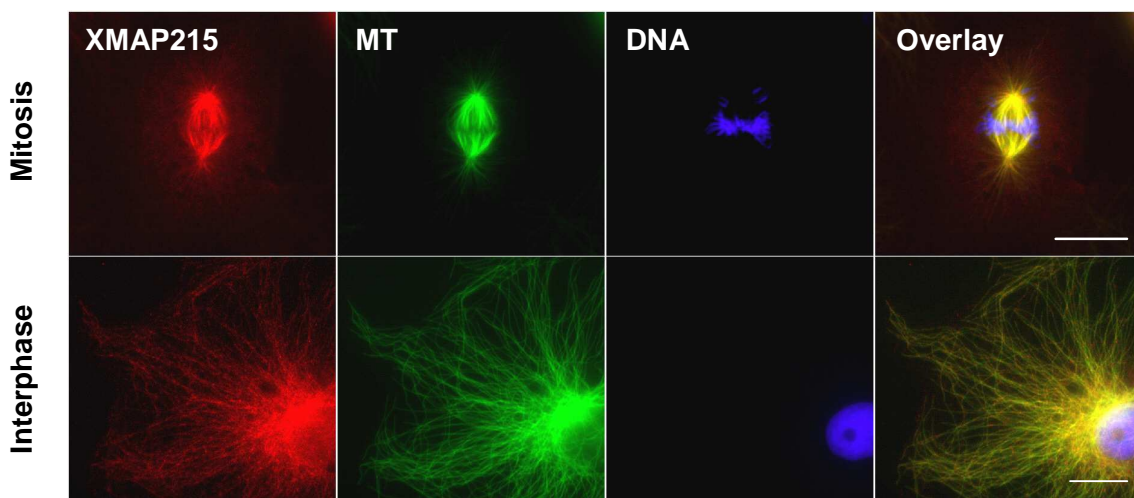
**XMAP215** it's named after the *Xenopus laevis* microtubule associated protein of apparent molecular weight of 215 kDa. It was reported for the very first time in 1987 by Gard and Kirschner. They described it as a major MT assembly factor based on its ability to promote assembly in a *Tetrahymena* axonemes-nucleated MT assay *in vitro*. Further analysis did show a specific promotion of assembly at the MT plus-end by 7-10 folds and rapid shortening by 3 fold, suggesting in this way the increase of the rate-on constant of tubulin addition and a decrease in the off-rate constant (Vasquez *et al.*, 1994; Gard and Kirschner, 1987).

XMAP215 is the primary MAP that stabilizes MTs in *Xenopus* egg extracts. The protein has a predicted molecular mass of 228 kDa. It belongs to a conserved family of proteins required for the growth of MTs and mitotic spindle assembly. In extracts XMAP215 stimulates the rapid assembly of MT plus ends and protects plus ends from XKCM1, a catastrophe factor member of the kinesin-13/KinI family. These two proteins are proposed to be the principal regulators of MT dynamics (Gard and Kirschner., 1987; Kinoshita *et al.*, 2001; Popov *et al.*, 2001; Cassimeris and Morabito, 2004).

The XMAP215 sequence is highly similar to those of the human homologue ch-TOG (78.4% identity) (Tournebize *et al.*, 2000), with a specific cellular localization through the cell cycle. In interphase XMAP215 localizes along the MT lattice and in centrosomes; during mitosis it localises on mitotic spindle and spindle pole bodies (**Fig.19**). In addition, XMAP215 also appears to be required for centrosomes-independent aster formation induced by Ran, a ubiquitous GTP-binding protein that is essential for spindle formation (Popov *et al* 2001, 2002).

Two different XMAP215 proteins are present during the *Xenopus laevis* early embryos. The transcripts differ in the presence or absence of 108-bp (aa

1136 to 1171) insert. The transcript expressing the insert is named **XMAP215<sub>M</sub>** (XMAP215 **maternal** form). The XMAP215<sub>M</sub> form is expressed from oogenesis through gastrulation (from the egg stage until stage 13, the early gastrula). In contrast, the transcript lacking the insert is named, **XMAP215<sub>Z</sub>** (XMAP215 **zygotic** form) is first observed from gastrulation onward. Because the XMA215<sub>M</sub> isoform is expressed before the zygotic gene expression (mid-blastula transition), it is possible that this isoform could be the product of the maternal transcription (Becker *et al.*, 2000).



**Figure 19. XMAP215 cellular localization.** XL177 *Xenopus laevis* cells showing the XMAP215 localization in mitotic and interphasic cells. **XMAP215** (red), **MTs** (green) **DNA** (blue). Scale bar 10  $\mu$ m.

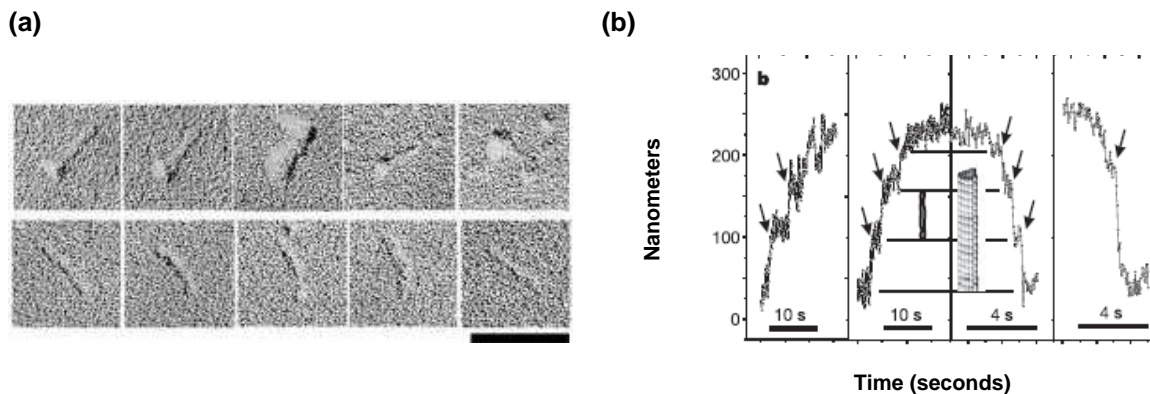
XMAP215 did also show to be a phosphoprotein, whose level of phosphorylation is regulated during the cell cycle, been strongest in metaphase of both meiotic and mitotic cell cycles being a substrate for CDK1 (Gard and Kirschner, 1987; Vasquez *et al.*, 1999). These observations suggest a regulation by phosphorylation during the transition from interphase to M-phase perhaps by contributing to changes in MT length (Andersen *et al.*, 1994; Vasquez *et al.*, 1999). The phosphorylated XMAP215 is less able to promote MT growth, although it is able to bind to MTs. The MT alterations during the cell cycle could be the result from changes in the down regulation and up regulation among MT stabilizing and destabilizing factors (Andersen *et al.*, 2000).

The model that could explain the turnover of MTs between interphase and mitosis is that XMAP215 promotes MTs growth in interphase, thus exerting a dominant MT-stabilizing activity over the MT destabilizing factors such as OP18/Stathmin, katanin and **XKCM1**. In mitosis it does not stimulate MT growth, allowing catastrophe factors to act more efficiently (Tournebize *et al.*, 2000; Popov *et al.*, 2001; Kinoshita *et al.*, 2002).

#### 4.3.1 XMAP215 and tubulin dimers

XMAP215 is a long thin monomer molecule in solution with an average length of  $60.0 \pm 17.7$  nm. In pure tubulin solutions the XMAP215 length suggests that it could span seven to eight dimers along a protofilament and can bind to a single protofilament of MTs (Spittle *et al.*, 2000; Cassimeris *et al.*, 2001). The length of a XMAP215 TOG domain is closely matched to a tubulin monomer ( $\alpha$  or  $\beta$ ) and likely makes an extensive contact through a combination of hydrophobic and electrostatic interactions (Slep *et al.*, 2007).

*In vitro* XMAP215 activity on the MT assembly is known to promote the MT growth rate, increase the frequency and duration of rapid MT plus end length changes at the nanoscale. In the *in vitro* MT polymerization, the XMAP215 presence produced step size polymerizations of 40-60 nm long, facilitating in this way the tubulin dimers addition (instead of the 20-30 nm length in a pure tubulin solution). The event size can correspond to the XMAP215 already predicted length (**Fig 20**). This activity could be explained from two different hypotheses. One where XMAP215 could template the tubulin heterodimers in solution, finally joining the MT end. A second approach could include a previous XMAP215 binding to the MT end, and then allowing the building-up of oligomers along the length of the XMAP215 molecule. During the shrinkage events it is possible that the XMAP215 molecule remains attached to the MT lattice some time after arrival (Kerssemakers *et al.*, 2006).



**Figure 20. XMAP215 behaviour *in vitro*.** (a) XMAP215 is a long rod shaped molecule that remains as a 60 nm monomer, scale bar 100 nm (Cassimeris *et al.*, 2001) (b) High resolution of tubulin polymerization in presence of XMAP215. Arrows indicate the length changes during growth (left) and shrinkage (Kerssemakers *et al.*, 2006)

#### 4.4 ch-TOG

The colonic, hepatic tumor over-expressed gene protein was originally described 1995. As part of a tissue based screening, the ch-TOG was identified as a 6.449 kb messenger that encoded a putative protein of 1972 amino acids with a predicted molecular mass of 218 kDa. Ch-TOG was found over-expressed in human hepatocellular carcinomas and colonic tumors, showing an ubiquitous expression in healthy tissues (Charrasse *et al.*, 1995, 1996, 1998).

The gene is located on the human chromosome 11, in the p11.2 band. This locus has been previously associated with neoplastic events related to molecular and cytogenetic data (Kaname *et al.*, 1993; Dong *et al.*, 1995). This could indicate that the short arm of chromosome 11 contains genes involved in tumor development (Charrasse *et al.*, 1995).

Ch-TOG is a resident protein of the centrosome, been responsible for the mitotic spindle bipolar morphology, centrosome integrity and MT anchorage. Ch-TOG has showed to be associated with the endoplasmic reticulum (ER) during interphase and with centrosomes during mitosis (Charrasse *et al.*, 1998).

Ch-TOG role in cell division and cell proliferation was concluded from its over-expressed presence in tumours. It is possible that this ch-TOG overexpression can be necessary for the rapid remodelling of the cytoskeleton-spindle assembly in highly rate dividing cells such as the tumour cells or the early embryos (Charrasse *et al.*, 1998).

Two different sequences have been reported, they are known as **TOG 1 (isoform a)** and **TOG2 (isoform b)**. The “isoform a” is a 1972 aa sequence, reported from the human hepatomas and colonic tumours. The “isoform b” is 2032 aa long reported from a group of precursor and tumour cells. The difference among them is a 59 aa gap present at the C-terminal region of the protein.

The mRNA ch-TOG over-expression in tumour cells and the XMAP215 higher expression during early embryogenesis could explain the presence of the two isoforms in human tissues. The preferential presence of the “earlier” ch-TOG isoform might indicate a de-differentiation of the tumor cells to up-regulate genes that are normally highly expressed in development stages (Charrasse *et al.*, 1998).

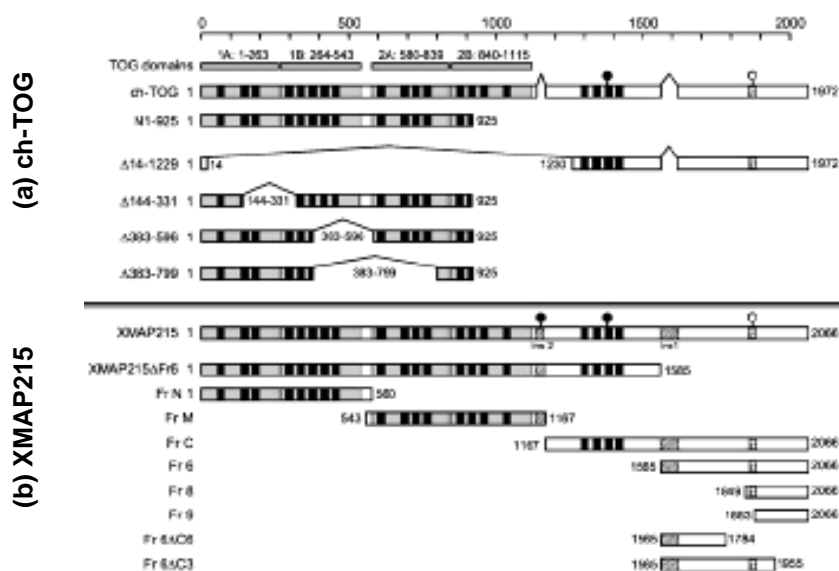
The ch-TOG identification as a MAP was made considering that (1) it localizes to MTs, (2) co-pellets with taxol stabilized MTs and (3) promotes rapid MT assembly *in vitro* (Charrasse *et al.*, 1998). The ch-TOG phosphorylation by the p110 kinase has been suggested due to the XKGS sequence in the C-terminal region of the protein (**Fig. 21**). This region is known as a MT binding domain and is present in other MAPs (Charrasse *et al.*, 1998).

#### **4.5 XMAP215/ch-TOG mapping**

Mapping of XMAP215 and ch-TOG has permitted the establishment of a parallel among the most complex members of the XMAP215/Dis1 family of proteins. Both proteins bind MTs *in vivo* and *in vitro* (Charrasse *et al.*, 1998; Tournebize *et al.*, 2000), they are characteristically related to the centrosome

during the interphasic state and to the appropriate development of the spindle pole when cells reach mitosis (Charrasse *et al.*, 1998; Tournebize *et al.*, 2000; Popov *et al.*, 2001).

Experimentally, and to determinate the MT-binding domain of **XMAP215** responsible for targeting centrosomes and MTs, the protein was divided into three fragments, termed **FrN** (aa 1-560), **FrM** (aa 543-1167) and **FrC** (aa 1168-2065) for fragment N-terminal, Middle and C-terminal respectively (Fig.21b) (Popov *et al.*, 2001). FrN and M contains two TOG domains each (TOG domains 1A-1B and 2A-2B respectively) and the fifth and last TOG domain is contained in the FrC.



**Figure 21. XMAP215/ch-TOG schematic representation.** XMAP215/ch-TOG mapping based on the existing homology among other family members. Several fragments were produced. **Fr N-ter**; XMAP215 N terminal fragment, **Fr M**; XMAP215 fragment of the middle and **FrC-ter**; XMAP215 C terminal fragment, **aa**; amino acid. The TOG domains from 1 to 4 are indicated at the top of the image. From Gard *et al.*, 2004

Also, **ch-TOG** was mapped and different fragments were produced. There, the protein was basically divided in two fragments: an **N-terminal** (containing three TOG domains) and a **C-terminal** fragment (one TOG domain) (Fig. 21a). The ch-TOG N-terminal fragment probed to bind the subtilisin treated MTs, meaning that the ch-TOG MT-binding activity is independent of the extreme C-terminus of  $\alpha$  and  $\beta$  tubulin, suggesting that the ch-TOG binding site on tubulin differs from MAP2, MAP4 and tau (Spittle *et al.*, 2000).

For the two proteins and through the *in vitro* interactions, the identification of the MT binding domain in N-ter region of the protein was realized. (Table IV) The XMAP215 fragments FrN and FrM cosedimented with MTs *in vitro* and in the egg extract, the N-ter fragment of XMAP215 was able to regulate MT dynamics suppressing catastrophes and restoring the spindle assembly in the XMAP215 depleted egg extract, substituting successfully the full length XMAP215 in the experiments. In contrast, the C-terminal fragment (FrC) of the XMAP215 protein was distributed along MTs and centrosomes, while a shorter fragment of the C-terminal region (aa 1565-2066) was restricted to centrosomes only (Popov *et al.*, 2001). Finally, each fragment that contained a TOG domain in their sequence succeeded in the MT-fragment interaction, however the absence of the fifth TOG domain sequence (fragments 1565-1784 and 1565-1955) probed to be determinant for the identification of the C-terminal region as a centrosomal targeting sequence.

	Sequence (aa)	MT binding (Kd)		Centrosome binding
		<i>In vitro</i>	<i>In vivo</i>	
ch-TOG Spittle <i>et al.</i> , 2000	1-1972	~5 $\mu$ M	ND	ND
	1-925	~5 $\mu$ M	ND	ND
	1230-1972	>25 $\mu$ M	ND	ND
	1-144 / 331-925	>25 $\mu$ M	ND	ND
	1-383 / 596-925	>25 $\mu$ M	ND	ND
	1-383 / 799-925	>25 $\mu$ M	ND	ND
	XMAP215 Popov <i>et al.</i> , 2001	1-2066	++	++
1-1585		ND	+	-
1-560 (FrN)		+	-	-
543-1167(FrM)		+	-	-
1167-2066 (FrC)		+	++	+++
1565-2066		ND	ND	+++
1849-2066		ND	ND	+
1883-2066		ND	ND	-
1565-1784		ND	ND	-
1565-1955	ND	ND	++	
XMAP215 Gard <i>et al.</i> , 2004	1-2066	<1 $\mu$ M	ND	ND
	1504-2066	>20 $\mu$ M	ND	ND
	225-999	~2-5 $\mu$ M	ND	ND
	952-1314	<1 $\mu$ M	ND	ND

**Table IV. XMAP215/ch-TOG domains and their MT interactions.** ND, non determined. Each cross symbolises a positive interaction, the strongest interaction is denoted by three crosses.



Thus, and based on the functional domains mapping, XMAP215 has shown to be a resident centrosomal protein who contributes to the MT-nucleating activity of centrosomes (Popov *et al.*, 2001, 2002). The centrosome targeting sequence could be located in a region among the amino acids 1565-1955 of the protein sequence. This particular region contains the tau sequence (50% identity) founded in the MT-binding sequence of tau, MAP2 and MAP4.

The tau repeat could play a role in the XMAP215 targeting to the centrosome and the further MT anchoring. There is a little sequence homology existing between XMAP215, ch-TOG and other stabilizing MAPs such as tau, MAP4 and MAP2b. The only sequence homology existing among this group of proteins is present in an 18 aa sequence located in the known as the XKGS motif in their C-terminus region (Fig. 22). The substitution of this sequence for an unrelated one diminished the MT centrosomal targeting by as much as 50%, suggesting that specifically the tau sequence play a role in the XMAP215 targeting to the centrosome. Although the XMAP215 C-fragment can bind MTs, the C-terminal fragment of ch-TOG was not found to bind MTs *in vitro* (Spittle *et al.*, 2000; Popov *et al.*, 2001).

The mapping of the MT binding domain and the centrosome targeting domains for XMAP215 and ch-TOG has indicated that these two activities are independent functions in the proteins, and that the sequences responsible are located in different functional domains. The ch-TOG MT binding domain has been mapped to aa 144-799 (Gard *et al.*, 2004).

aa	Sequence	aa	MAP
1964	L A E M F K <b>K I G S</b> K E N T K E G L	1985	XMAP215
1773	L A E I F K <b>K I G S</b> K E N T K E G L	1790	ch-TOG
195	L K N V K S <b>K I G S</b> T E N L K H Q P	212	tau
932	L K N V R S <b>K V G S</b> T E N I K H Q P	949	MAP4
1669	L K N V K S <b>K I G S</b> T D N I K Y Q P	1687	MAP2b

**Figure 22. XMAP215/ch-TOG domains described to bind cyclin B1.** Common features among MAPs. Modified from Charrasse *et al.*, 1998

XMAP215 is the only member of this family that has shown to be phosphorylated in a cell-cycle dependent manner (Gard and Kirschner, 1987). The XMAP215 phosphorylation has been probed during the M phase of meiosis in *Xenopus* oocytes and in the mitotic cycles of early *Xenopus* embryos (Gard and Kirschner, 1987).

The members of the XMAP215/Dis1 family of proteins possess a conserved sequence TPAK (aa 1361-1364 of the XMAP215 sequence), corresponding to the target sequence for the cell cycle kinase CDK1. Further studies shown that XMAP215 is a substrate for CDK1 *in vitro*, additionally this phosphorylation probed to regulate XMAP215 activity producing as a final result the reduced MT elongation. However, the XMAP215 phosphorylation by CDK1 did not affect its MT-binding to taxol stabilized MTs (Vasquez *et al.*, 1999).

XMAP215 has the sequence particularity to contain two copies of the CDK1 target sequence in its maternal isoform. The first one is located from aa **1361** to aa **1364** of the sequence (TPAK), and the second one from aa **1155** to aa **1158** (TPSK), contain in a 30 amino acid insert. This kind of insert is not present in any other member of the family identified so far (Becker and Gard, 2000; Tournebize *et al.*, 2000). These structural characteristics might provide XMAP215 of a particular behaviour in the protein regulation during the rapid turn over in the cell cycles of the *Xenopus* embryo development.

## **RESEARCH AIMS**



## RESEARCH AIMS.

XMAP215/ch-TOG are proteins that have been described as key elements for the establishment and dynamics of the MT cell cytoskeleton. The *Xenopus laevis* (**XMAP215**) and its human homologue (**ch-TOG**) share an 80% identity, allowing in this way the development of parallel experiments. Studies along this time has shown the structural complexity of the proteins in terms of multiple TOG domains containing several HEAT repeats, predicted CDK1 target regions, and centrosome targeting sequences, among many others. This complexity is perhaps the evidence of a highly evolved protein, with multiple activities up on the targeted domain.

Software simulator programs have previously allowed the prediction of their potential cellular activity (van Buren *et al.*, 2002 and 2004). Additionally, the XMAP215/ch-TOG effect on the MT ultrastructure has been analyzed from several scientific approaches. Different protein fragments have been used counting on the protein homology among species. Their affinity for tubulin dimers and the MT structure have revealed a region-dependent activity (Al-Bassam *et al.*, 2007; Popov *et al.*, 2001, 2002), placing the protein to a high degree of specialization. However, the biological evidence of its activity in the cellular context and in the *in vitro* environment has not yet been fully understood.

The aim of our work is to explore the XMAP215 cellular activity in the *in vivo* and *in vitro* context. With this purpose a panel of mcAB was developed using the full length recombinant XMAP215-his7 as antigen. The mcAB cloning was followed by its isotyping, characterization and production. The selected mcABs were used to identify different XMAP215/ch-TOG localizations and activity in fixed primary human fibroblast, *Xenopus laevis* cells and egg extracts.



## **METHODS**





## METHODS

### 5. Anti XMAP215/ch-TOG mcAB production

The XMAP215/Dis1 family of proteins presents preserved structural characteristics with possibly common cellular activities as well. Based on the localizations reported for some of the members of this family, we decided to explore the cellular localizations for XMAP215/ch-TOG, counting on their 80% homology. Our experimentation concerning the XMAP215/ch-TOG precise cellular localization required the development of monoclonal antibodies (mcAB) and their further characterization.

#### 5.1 XMAP215 characterization

The mcABs production is described from the very early steps of the processes, starting from the mice immunization through the antibody production, purification, isotyping, immunofluorescence reactivity on fixed cells (human and frog cells) and labelling.

##### 5.1.1 mcAB antibodies obtention

Three females BALB/c mice were immunized following the typical immunization schedule ([Table V](#)).

After the third injection we tested the reactivity of seric antibodies against XMAP215 by immunofluorescence (IF). The best responder mouse (number 1) was sacrificed and its spleen cells were fused to myeloma cells. Serial dilutions of the fused hybridomas were necessary to obtain one cell by well in a sterile 96 multi well plate.

The obtained hybridomas multiplied at 37°C, 5% CO<sub>2</sub> in a medium containing : 10% NCTC-109 (Gibco®) , 10% fetal bovine serum (FBS) (Gibco®), penicillin/streptomycin 100 U/μg (Gibco®), sodium pyruvate (Gibco®), 50μM 2Mercaptoethanol (Gibco®), 1% Non essential amino acids (Gibco®) and RPMI 1640 (Gibco®).

Three clones were identified as positives by IF and its specificity was confirmed by western blot.

<i>Day</i>	<i>Step</i>
0	IP injection of 50 µg of recombinant XMAP215-7his in 250 µl of PBS mix with 250 µl of complete Freund's adjuvant.
14	Same dose but using incomplete Freund's adjuvant.
24	Tail bleeds were collected. Immunofluorescences were realized on PFA fixed PHF (Paraformaldehyde 4%, glutaraldehyde 0,1%, Triton 100 0,5% in BRB80, final pH 6,8). As secondary antibody a goat anti-mouse IgG Alexa fluor 488® was used.
35	Animals were injected IP with incomplete Freund's adjuvant.
45	Tail bleeds tested by IF on PHF as described before.
56	Best responder (mouse number 1) injected (50µg recombinant XMAP215) 100µl IV and 100 µl IP. The other mice got an IP injection with incomplete Freund's adjuvant.
59	Best responder splenocytes were fused with myeloma cells.
66	First test of hybridomas supernatant to be tested.

**Table V. Immunization Schedule of BALB/c mice for the XMAP215 monoclonal antibodies production.** IF, immunofluorescence. IP, Intraperitoneal. IV, Intravenous. PFA, Paraformaldehyde. PHF, Primary Human Fibroblast.

### 5.1.2 Cell Fixing and Immunofluorescence

Primary human Fibroblast (PHF) and XL177 cells (*Xenopus laevis* epithelial cells) (Table VI) were allowed to grow on pre-cleaned and sterilized coverslips (12 mm). Cells were kept in culture for at least 48 hours before fixing in order to have a mitotic population. Fixation of slides containing at 50% confluence cells was realized following an established fixing method upon the mcAB to analyze.

Cell line	Origin	Description	Author	Propagation		
				Growth	Media	CO <sub>2</sub>
<b>PHF</b>	Primary human fibroblast	Surgery	Tissue simple Kindly donated by a CHU (Grenoble) patient.	Donation	Adherent	
<b>HeLa</b>	Human epithelial cells		Adenocarcinoma cell line	Scherer <i>et al.</i> , 1953	Adherent	RMPI, FBS 10%, PS 5% 5%
<b>NEK37</b>	Human T cell	Dr Popov's collection	Lymphoblastoid cell line	Mayer <i>et al.</i> , 1982	Non adherent	
<b>NSO</b>	Mouse Lymphoblast		Myeloma cell line	Köhler G and Milstein C, 1975	Non adherent	
<b>XL177</b>	<i>Xenopus laevis</i> epithelial cell line		Cell line derived from <i>Xenopus</i> stage 40 tad poles	Miller and Daniel, 1977; Ellison <i>et al.</i> , 1985	Adherent	Levovitz 60% ; FBS 10% ; PS 5%, HEPES 10 mM Air

**Table VI. Cell lines used in this study.** CHU, Centre Hospitalier de Grenoble ; RPMI, Roswell Park Memorial Institute medium; FBS, Fetal Bovine Serum ; PS, Penicillin and streptomycin; HEPES, 4-(2-hydroxyethyl)-1-piperazineethanesulfonic acid.

Cells designated to be stained with the clones identified as **mcAB 5D12** and **mcAB 5A6** required liquid nitrogen (LN) fixation. The fixation method was realized as described: the slides were air dried at 37°C for 2 seconds to eliminate the residual humidity. Next, the slide was put in to LN for 1 minute and the post-fixation had place in methanol (**MetOH**) at -80°C for 5 minutes. The slides were washed three times with PBS (GIBCO®) and then washed three times in a solution containing PBS/Triton 100, 0.1% (**PBS/Tx 0.1%**). At this stage the cells were ready to be stained with the mcAB used as primary antibodies.

	Antibody	Species	Type	Fluoro- chrome	Producer	Dilution	
Primary antibodies	5D12	mouse	mcAB	----	This research	SN	
	5D12	mouse	mcAB	Atto-488	This research	1/100	
	4B6	mouse	mcAB	----	This research	SN	
	5A6	mouse	mcAB	----	This research	SN	
	anti $\alpha$ -tubulin	rat	pcAB	----	CEA, Grenoble	1/1000	
	anti - EB1	rabbit	pcAB	----	Andrei Popov collection	1/100	
	anti - Clip170	rabbit	pcAB	----	EMBL, Heidelberg	1/100	
	anti – p150 <sup>Glued</sup>	mouse	mcAB	----	BD Biosciences	1/100	
Secondary antibodies	anti-mouse	goat	pcAB	Cy-3	Jackson Immunoresearch	1/1000	
	anti-mouse	goat	pcAB	Al488	Molecular Probes	1/1000	
	anti-rabbit	goat	pcAB	Al 488	Molecular Probes	1/1000	
	anti-rat	donkey	pcAB	Cy-5	Jackson Immunoresearch	1/1000	
	anti-rat	goat	pcAB	Al488	Molecular Probes	1/1000	
	anti-rabbit	goat	pcAB	Al 355	Molecular Probes	1/250	
	F(ab)2 fragment to mouse IgM ( $\mu$ chain)	goat	pcAB	Rhodamine conjugated	Cappel	1/1000	
	F(ab)2 fragment to mouse IgG ( $\gamma$ -chain)	goat	pcAB	Rhodamine conjugated	Cappel	1/1000	
	WB	anti-mouse	goat	pcAB	Peroxidase conjugated	SIGMA	1/5,000

**Table VII. Primary and secondary antibodies used in IFs.** mcAB, monoclonal antibody; pcAB, polyclonal antibody; SN, supernatant; AI, Alexa fluor®; WB, Western blot.

For the clone identified as **4B6 mcAB** the cell fixation slides established method was as follows: the media was removed and the slides were covered

with a BRB80 solution containing PFA 4%, Triton 100 0.5% and glutaraldehyde 0.1% (Sigma) for 20 minutes at 37°C. The slides were washed three times with PBS. Next, free aldehydes were quenched by incubation in 0.1% NaBH<sub>4</sub> in PBS. Finally, slides were washed three times with PBS and three times PBS/Tx 0.1%, the slides were ready for the mcAB used as primary antibody.

The already fixed and permeabilized cells were then incubated with 100µl mcAB anti-XMAP215 supernatant (100 µl at an mcAB concentration of 5 µg/ml), for 30 minutes at room temperature followed by PBS/Tx 0.1% washing. The secondary antibody of choice was diluted in PBS/Triton 100 0.1% as indicated in [Table VII](#), followed of 15 minutes incubation. A second washing PBS/triton 100 0.1% was realized. Stained cells were preincubated 20 minutes in 2µg/ml Hoechst 3352 to stain DNA and washed once more with PBS/Tx 100 0.1%, finally the cover slide was mounted using Fluorsave reagent (Carlbiochem). The preparation was allowed to dry at 4°C overnight before the images acquisition.

## 5.2 mcAB Characterization

The XMAP215 presence in the *Xenopus laevis* egg extract becomes an invaluable tool in the *in vivo* experimental procedures development. The egg extract has been used for several years in the cell biology domain as it represents a concentrated cytoplasm open to biochemical manipulation, having always the possibility to reconstitute many cellular events in a test tube.

### 5.2.1 mcAB Specificity

#### 5.2.1.1 mcAB specificity: egg extract obtention

Eggs are obtained from *Xenopus laevis* females. To induce ovulation the female frogs are injected subcutaneously with 100 units of PMSG (Pregnant Mare Serum Gonadotropin) at least three days before their utilisation. To induce the laid of eggs, they are injected 16-18 hours before utilisation with 500 units of HCG (Human Chorionic Gonadotropin). Frogs are placed in individual boxes and they are kept at 16°C.

The eggs were collected and washed in 800 ml MMR buffer. All possible contaminants were removed in this process. Once the dejelling buffer is removed eggs were washed once more in MMR buffer, four times with XB buffer and twice with the CSF-XB buffer.

Eggs were transferred to a Beckman tube containing 0.5 ml of CSF-XB buffer containing the protease inhibitors and cytochalasin B. Eggs were centrifuged one minute at 500g at 4°C. The supernatant (excess of CSF-XB) was eliminated.

Finally the eggs were crashed at 17,000g 16 minutes at 16°C. Xenopus egg extract is removed with the a needle, then is transferred to a tube on ice, aliquoted and freezed in liquid nitrogen and stored at -80°C (Fig.23)

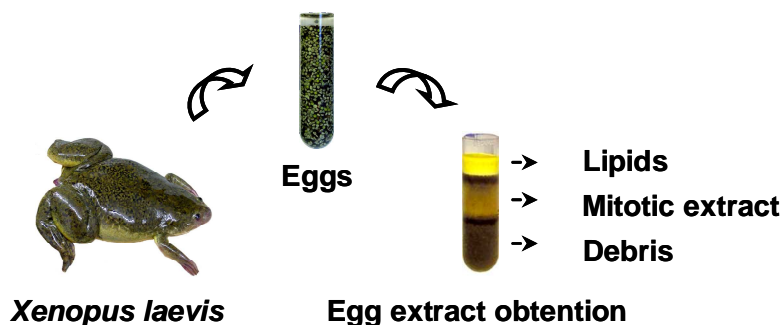
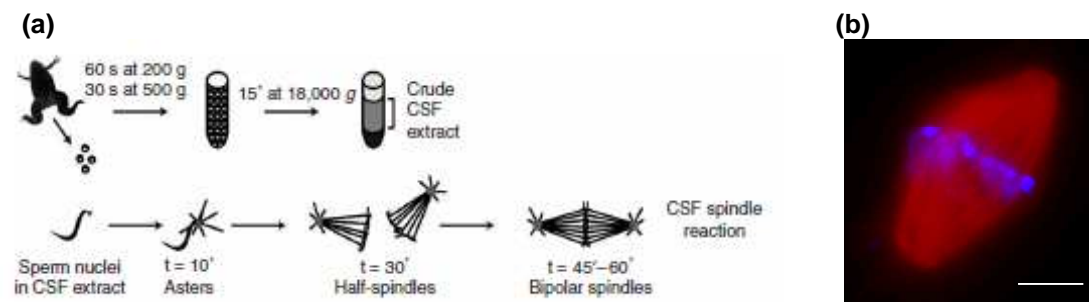


Figure 23. *Xenopus laevis* egg extract obtention.

In order to guarantee the quality and activity of the egg extract we promoted the formation of mitotic spindle. 1  $\mu$ l of sperm nuclei is added to 20  $\mu$ l mitotic egg extract containing 0.2  $\mu$ l rhodamine labelled tubulin. Reaction was kept at 20°C among 30 and 60 minutes. 2  $\mu$ l of fixing agent (containing Hoescht) and 2  $\mu$ l of the tested extract was drop on a slide and analyze at the microscope (Fig. 24).



**Figure 24. Mitotic spindle assembly in the *Xenopus laevis* egg extract. (a)** Schematic representation of spindle assembly reaction. Sperm nuclei are added to a mitotic egg extract (metaphase arrested), promoting first the formation of half spindle and then bipolar spindle structures. **(b)** Mitotic spindle observed at the microscope. Addition of rhodamine labelled tubulin allows the visualization of mitotic spindle (**red**) and the sperm nuclei are stained with hoechst (**blue**), scale bar 10 $\mu$ m. Modified from Hannak *et al.*, 2006.

### 5.2.1.2 mcAB specificity: XMAP215 depletion

*Xenopus laevis* egg extracts where XMAP215 depleted as follows. 40  $\mu$ l of Dynabeads® Protein A where washed and charged with 10  $\mu$ g of antibody anti-XMAP215 fragment 1, corresponding to aa 1 to 560 of the protein (Popov *et al.*, 2001) during 60 minutes on ice in presence of PBS/Tx 0.1%. After binding the beads where washed in a solution containing PBS/Tx 100 0.1%, then resuspended in 100 $\mu$ l PBS/Tx 0.1% and finally divided in two samples.

The beads (first sample) were washed in CSF-XB and 50 $\mu$ l of mitotic egg extract was added, the reaction took place on ice for one hour ( **$\Delta$ -XMAP215 egg extract**). Beads were removed from the extract and were replaced by the second beads sample. This gave origin to a  **$\Delta\Delta$ -215XMAP215 egg extract**. After one hour reaction on ice, beads were removed. Beads charged by antibody/XMAP215,  $\Delta\Delta$ -215XMAP215 egg extract and a non depleted egg extract were putted into LB loading buffer (2 minutes at 100°C) and stored at -20°C.

The samples of the XMAP215 depletion were run in a 6% SDS-PAGE gel at 90 volts during 2 hours. The proteins were transferred to a nitrocellulose membrane (0.3 amps, 2 hours) using the Mini PROTEAN 3 Cell (BIO-RAD) system.

Immunodetection of the XMAP215 protein was realized using the three monoclonal antibodies (as primary antibodies) and a goat anti-mouse IgG peroxidase conjugate (SIGMA) as secondary antibody. Detection was achieved using ECL kit (Amersham).

### 5.2.1.3 mcAB Class

The idiotype identification of the different mcAB produced was realized using immunofluorescence (IF) staining. The cell fixation was realized after the specific fixation established for each antibody and the IF was realized following the previously described method.

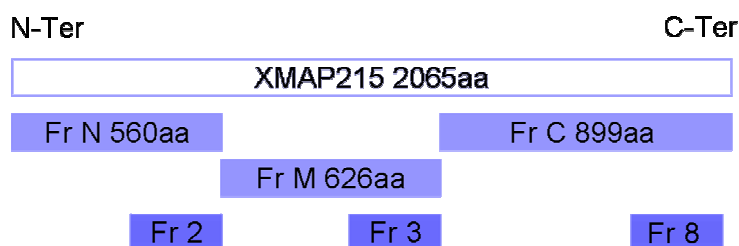
The mcAB idiotype initial identification was based on the targeting of the  $\mu$ - or  $\gamma$ -chains of the mcAB. The antibodies used were the goat anti mouse IgM F(ab')<sub>2</sub> fragment and the goat anti mouse IgG  $\gamma$ -chain F(ab)<sub>2</sub> fragment (Cappel catalogue number 55536 and 55534 respectively), both rhodamine-conjugated.

Further and more precise mcAB isotype characterization was realized using the mouse monoclonal antibody isotyping kit IsoStrip (Roche applied Science). Briefly, the latex beads contained in the kit bears kappa and anti-mouse lambda antibodies, once they have captured the monoclonal antibody to test, the beads migrate to immobilized bands of goat-anti mouse antibodies corresponding to the common mouse antibody isotypes (IgG<sub>1</sub>, IgG<sub>2a</sub>, IgG<sub>2b</sub>, IgG<sub>3</sub>, IgM and IgA) and to the kappa and lambda light chains, producing a blue line on the strip.

### 5.2.1.4 mcAB epitopes cartography

The identification of the potential domains recognized by the mcABs was realized through the development of an ELISA test (Enzyme Linked ImmunoSorbent Assay). Here, we used the XMAP215 cloned fragments (**Fig.25**) described previously (Popov *et al.*, 2001) as antigens of the reaction.





**Figure 25. XMAP215 cloned fragments.** Popov *et al.* 2001

Serial dilutions of the fragments (from 100 to 1 ng/ml) were made in a 10 mM sodium phosphate buffer pH 7.2, allowing the fragments adsorption to the multiwell plate (Falcon ref 353912) overnight at 4°C. After washing (PBS/Tx 100 0.1%) the blocking was made using a 5% serum in sodium phosphate 10mM solution for 10 minutes. The excess was washed with running water and finally each one of the supernatants was added (50 µl of each supernatant antibody) for 40 minutes, the procedure was followed by washing with a PBS/Tx100 0.1%.

An anti-mouse IgG HRPO (1/10.000 in PBS/Tx 100 0.1%, 15 minutes) was used as secondary antibody. As positive control of the reaction we used a monoclonal antibody anti-fragment 2 (Popov *et al.*, 2001). Revelation was made using 100 µl per well of a Citric Buffer (20ml cold Citric buffer, ABTS 0.1 µM; H<sub>2</sub>O<sub>2</sub> 0.001%). The plate reaction was read at 405 nm using the SPECTRAMax® PLUS 384 microplate spectrophotometer (Molecular Devices).

### 5.2.1.5 Fixed cells imaging

Images acquisition was performed using a Zeiss Axiovert 200M inverted microscope equipped with a CCD camera (COOLSNAP HO, Photometrics). Images were analyzed using the MetaMorph software version 6.2 (Universal Imaging Corp).

Confocal images were acquired using the Leica confocal microscope TSC-SP2. The fluorescence emissions of Alexa 488 were collected among 500 and 530 nm (488 nm excitation wave length), Cy-3 among 555 and 620 nm (543 nm excitation wave length) and Cy-5 among 660 and 680 nm (633 nm excitation wave length). Parameters are acquired sequentially and the images analysis were made using Leica Confocal Software:

### 5.3 XMAP215 *in vitro* interaction

XMAP215 is a protein that contains five TOG domains in its sequence; these domains are potentially responsible for the tubulin dimers loading. The studies of the interactions were designed to establish the *in vitro* reactivity of the mcAB and the XMAP215-his7 protein.

#### 5.3.1 Co-sedimentation Assays

Different cosedimentation assays were developed in order to establish the mcAB/XMAP215/tubulin or mcAB/XMAP215/MT interaction.

##### 5.3.1.1 Tubulin/XMAP215-his7 interaction

To determine de tubulin binding affinities of recombinant XMAP215 (XMAP215-his7) 2.5 µg XMAP215-his7 were added to a tubulin solution at a concentration of 10 µM in BRB80 and with a final concentration of GTP 1mM. After 20 minutes incubation at 5°C the reaction was centrifuged in the Beckman TLA100.2 rotor at 50000 rpm for 30 minutes at 5°C. Supernatants and pellets were considered as independent samples.

SDS-PAGE electrophoresis was performed using a 6% gel in a BIO RAD mini-gel electrophoresis system using the precision Plus Protein Standards (10-250KDa) for molecular weight markers (Biorad). Gels were stained with Coomassie Brilliant Blue R-250.

##### 5.3.1.2 Tubulin / XMAP215-his7 / mcAB

20 µl of Dynabeads® Protein A where saturated with 5 µg of each mcAB (5D12 or 4B6) or mouse IgG (control) in a solution containing NaCl 3 M pH 8.5. After antibodies binding, the solution containing tubulin 10 µM and XMAP215-his7 (2.5 µg) was added and incubated in BRB80 containing GTP 1 mM for one hour on ice.

After the time of the reaction, beads with the mcAB/XMAP215-his7/tubulin complex were recovered. Each sample was loaded in a 6% SDS-PAGE gel and ran at 90 volts during 1 hour in a BIO RAD mini-gel electrophoresis system. Gels were stained with Coomassie Brilliant Blue R-250.

### **5.3.1.3 Microtubules/XMAP215-his7 / mcAB**

Microtubule assembly was realized in presence of GTP 1mM at 37°C during 20 minutes. 2 µg of XMAP215-his7 was allowed to react in the presence of 20 µg of taxol-stabilized MTs and 1 µg of each antibody (5D12, 4B6). Mouse IgG was used as control of the reaction.

Samples were centrifuged using a TL-100 Beckman ultracentrifuge with a TLA 100.2 rotor during 10 minutes at 50000 rpm at 37°C in order to pellet the MTs/XMAP215/mcAB complex. SDS-PAGE electrophoresis was performed using a 6% gel in a BIO RAD mini-gel electrophoresis system. Gels were stained with Coomassie Brilliant Blue R-250.

## 5.4. XMAP215 5D12 *in vivo* behaviour

Once the existence of the XMAP215/ch-TOG presence was probed in fixed cells, the evidence of its *in vivo* activity became the next step. The +TIP mcAB was coupled (Atto 488) in order to minimize the complex XMAP215-mcAB during the MT polymerization in the *Xenopus laevis* egg extract.

### 5.4.1 5D12 mcAB labelling

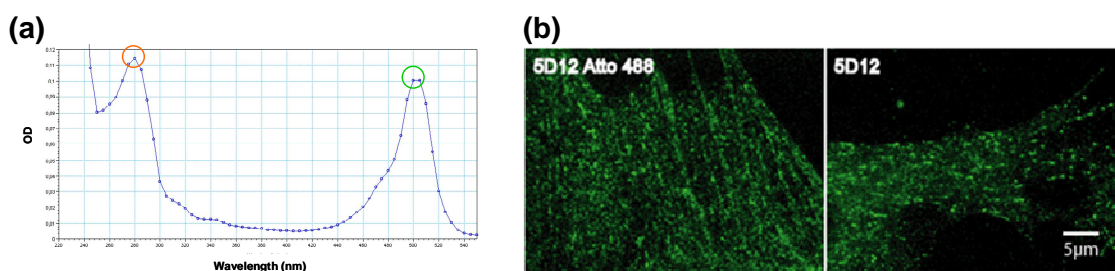
900 µl of a 2 mg/ml of mcAB 5D12 (or 4B6 mcAB) were dissolved in 100 µl bicarbonate buffer 0.1 M pH 8.3. The Atto NHS ester (Fluka ref 41698) was diluted in DMSO at 2 mg/ml concentration. 20 µl Atto NHS was added to the reaction. The reaction took place 1 hour at room temperature. Finally 200 µl of monoethanol amine pH 8.3 (100µM final) were added during 10 minutes.

For the separation of labelled antibodies we used a NHS-activated sepharose™ column (GE Healthcare Bio-Sciences AB), using the XMAP215 cloned fragment 8 as antigen of the reaction. The column was equilibrated with phosphate buffer 0.5 M pH 7.2 to be charged with the antibody. The reaction was allowed to take place during 2 hours at 4°C under agitation.

Elution was made with Glycine 0.1M pH 2.3. The eluted antibody (7 ml) was concentrated using Vivaspin 15R ultrafiltration spin columns (Vivascience) until a final concentration of 0.71 mg/ml of recovered mcAB 5D12-Atto 488. The concentration recovery was estimated using the SPECTRAMax® PLUS 384 microplate spectrophotometer (Molecular Devices) using a spectra among 220 and 580 nm.

**Figure 26a** shows the optical density at 280 nm (mcAB absorption) and the maximal absorption at 488 nm (Fluorophore emission wave length). A rapport 1:4 was obtained. The activity of the stained 5D12-Atto488 was tested on fixed cells using the antibody in a direct IF (**Fig. 26b**). The founded reactivity

was identical to the one obtained through the conventional indirect immunofluorescence method.



**Figure 26. Labelling of mcAB 5D12.** Spectrum of the 5D12 labelling (a). The maximal optical density for the protein (mcAB) is observed at 280nm (red circle), the fluorophore emission is observed at 523 nm (green circle).

#### 5.4.2 Microscopy assay visualization of MTs/XMAP215 interaction: Total Internal Reflection Fluorescence Microscopy (TIRF)

In TIRF, the excitation light is restricted to a narrow region near the cover glass. The thickness of the evanescent field is about 150 nm providing much higher axial resolution and signal-to-noise ratio than epifluorescence or confocal microscopy. Here we used an objective-based multilaser TIRF module (Carl Zeiss) coupled with dynamic acousto-optical splitter (Errol) and spot illumination system (Rapp Optoelectronics) to study a single microtubule growth dynamics in solution. We used the egg extract *in vivo* model for the aster formation and MT/XMAP215 at +TIP interaction. Ni-NTA beads coated by recombinant XMAP215 (XMAP215-his7) were used to nucleate MT aster formation.

In a first approach we used two colour sequential acquisitions. MTs were visualized in red adding Cy3B labelled tubulin to the egg extract. The +TIP XMAP215 was visualized using the mcAB 5D12-Atto 488, providing a signal in green. To keep the MT within the excitation field we used rhodamine labelled tubulin (2.5  $\mu$ M), Ni-NTA beads (Ni-NTA/XMAP215-his7) and mcAB 5D12-Atto 488 (0.3  $\mu$ M) in *Xenopus laevis* mitotic egg extract at 20°C for 5 minutes.

TIRF images were collected using a CCD N/B (CoolSnap HQ2, Roper Scientific) camera on a Zeiss Aviovert 200M inverted microscope using a 100x/1.46 Plan-Apochromat objective and a 488 nm or a 514 argon laser lines. The excitation wavelength and intensity was chosen by the computer controlled acousto-optical tunable filter. Standard 38HE and 43HE epifluorescence filter sets were modified by removing the excitation bandpass in order to avoid laser absorption and coherent interference pattern in TIRF field. The angle of incidence was adjusted to be higher than the critical value (ca. 64°) for both wavelengths. Atto488 (exc 501/ em 523 nm) and CY3B (exc 550/ em 570 nm) were detected in time lapse sequences at a continuous rate of one frame each two seconds with 300 ms exposure for each channel. Acquisition of image was performed using MetaMorph® v.7.5.6 software (Universal Imaging).

In a “single colour” mode only mcAB 5D12-Atto 488 was detected with an 488 nm excitation at a rate of two frames per second with 300 ms exposure. All TIRF image processing and analysis was performed with the MetaMorph software version 6.2 (Universal Imaging).

## **5.5 XMAP215/MT ultrastructural behaviour: Electron microscopy**

Electron microscopy technology can provide an insight in to the MT tip architecture mechanism under the potential effects of XMAP215 at the tip of MT. Two approaches were considered in this domain. The negative staining permits to create a general view of the MT-XMAP215 behaviour in an immediate period of time.

The final XMAP215/MT ultrastructural detail was obtained through the cryo-electron microscopy approach.

### 5.5.1 Negative staining

MTs were assembled at 37°C during 10 minutes from a tubulin solution 20  $\mu$ M and 1mM GTP in BRB80 buffer. The test had place in the presence and absence of recombinant XMAP215-his7. A final working concentration of 20  $\mu$ M tubulin and 0.4  $\mu$ M XMAP215-his7 was established. 4  $\mu$ l of the MT suspension was dropped on a carbon coated electron microscope grid; the solution excess was removed using filter paper following a twice washing with BRB80 at 37°C. Finally, grids were negative stained by applying 4  $\mu$ L of a 1% uranyl acetate solution over a period of 30 s and were allowed to dry at room temperature.

Micrographs were taken with a Phillips CM 120 microscope (FEI Eindhoven, The Netherlands) operating at 120 kV and a nominal magnification of 45.000x at under focus values ranging from 1.6 to 2.1  $\mu$ m. Micrographs were recorded on Kodak SO-163 film and were developed for 12 min in full-strength Kodak D19. Images were digitized on a Photoscan TD scanner (Z/I imaging, Belgium).

### 5.5.2 Specimen preparation and cryo-electron microscopy

Microtubules were assembled in a tube at 37°C during 10 minutes from a 20  $\mu$ M tubulin solution, containing GTP 1mM and Taxol 10 $\mu$ M in a BRB80 buffer. The tubulin was both polymerized in the absence and presence of recombinant XMAP215 0.4  $\mu$ M.

Microtubules (with or without XMAP215) were studied by cryo-electron microscopy on a CM200 microscope with an LaB<sub>6</sub> electron source operating at 200 kV and magnification of 38,000x (FEI Eindhoven, The Netherlands). About 2  $\mu$ l of sample was deposited onto a holey carbon grid (Quantifoil R 2/1, Quantifoil Micro Tools GmbH, Germany), blotted to remove excess liquid, and frozen by plugging rapidly into liquid ethane at the temperature of liquid nitrogen. Grids were transferred to a Gatan 626 cryoholder and imaged by low-dose techniques. Images were recorded on Kodak SO-163 film and were developed for 12 minutes in full-strength Kodak D19

To observe other effects of XMAP215 at the very tip of the microtubules we run additional experiments where 2.5  $\mu\text{l}$  of pre-polymerized MTs (20  $\mu\text{M}$ ) were dropped onto the grid, then 0.4  $\mu\text{l}$  of XMAP215 (2.6  $\mu\text{M}$ ) was added. 10 seconds later, the grid was blotted, and frozen into liquid ethane.

### 5.5.3 Image analysis

Images were digitized on an Epson Expression 1680 Pro scanner at a resolution of 800 dpi. Microtubule end structures were analyzed using Adobe Photoshop CS3 software. The “+ TIPS” structures have been classified into three different categories: blunt ends, curled ends and sheet ends. The percentage of each type of microtubule “+ TIP” structure was calculated with respect to the total number of structures analyzed for a specific condition.

## 5.6 XMAP215 *in vitro* inhibitor research

The XMAP215/Dis1 family of proteins express a mitotic profile, in particular its human orthologue ch-TOG, the Colon Hepatic Tumour Overexpressed Gene Protein has been related to cancer. This mitotic implication makes of XMAP215/ch-TOG a target of choice in the search for new antiproliferative molecules.

### 5.6.1 Screening

A random selected collection of molecules were tested. The screening had XMAP215-his7 as main target with only a possible secondary target, tubulin. Disrupting the MT anchoring by the centrosome will reduce dramatically the cell proliferation.



## 5.6.2 Experimental approach

The test was based on the XMAP215-his7 property to bind the NiNTA beads to allow the MT anchoring and final development of bead-nucleated asters. NiNTA beads-XMAP215his7 were added to a pure tubulin-GTP solution, the targeted molecule activity would be expected to be expressed in terms of absence of aster formation.

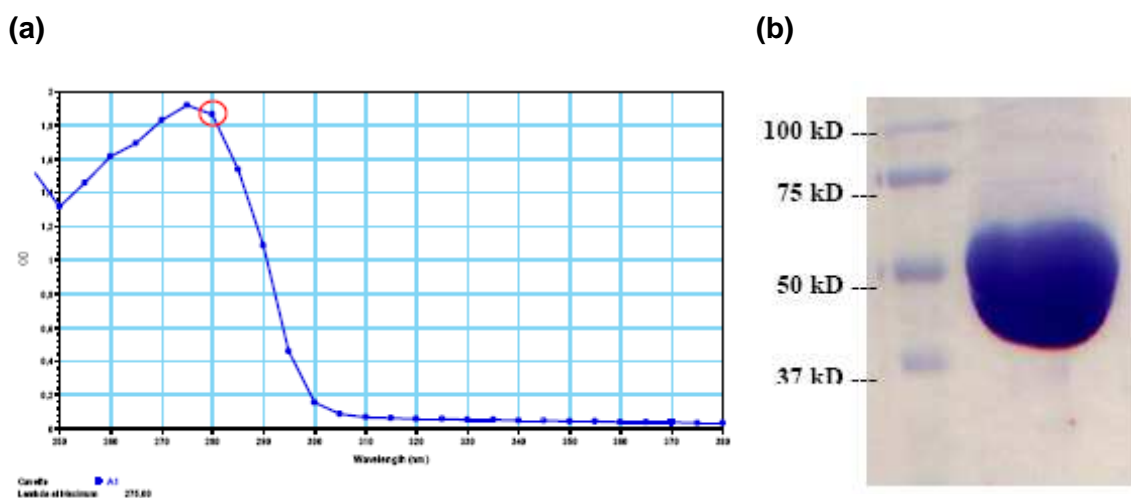
### 5.6.2.1 Molecules collection

The molecule collection to be tested is composed by Molecule Collection from Curie Institute, one sub-population of 2,640 molecules; Joseph Fourier University collection LEDSS, 960 molecules and the ChemBridge Research Laboratories collection (DIVERSet™), 10,000 molecules.

### 5.6.2.2 Tubulin

Tubulin purification from bovine brain was realized as described (Castoldi and Popov, 2003). Brains were cleaned (meninges elimination) and broyes in a MES Buffer MES 50 mM (2-N-Morpholino ethanesulfonic acid). Two cycles of polymerization and depolymerization were made in presence of a high molarity PIPES buffer (Piperazine -1,4-bis(2-ethanesulfonic acid)) to eliminate the contaminant proteins like MAPs and molecular motors. Tubulin concentration was determined at an absorbance of 280nm in the SpectraMax Plus spectrophotometer (Molecular Devices).

The tubulin from cow brain was quantified and analyzed by a SDS PAGE electrophoresis. Tubulin concentration was calculated measuring the 280nm absorbance (**Fig. 27a**), and using the tubulin molar extinction coefficient ( $A_{280\text{ nm}}=115.000\text{ M}^{-1}\text{cm}^{-1}$ ). The final concentration was estimated at 207 $\mu\text{M}$ . The purity of the obtained tubulin is showed in a 10% SDS PAGE gel Coomassie blue stained (**Fig. 27b**).



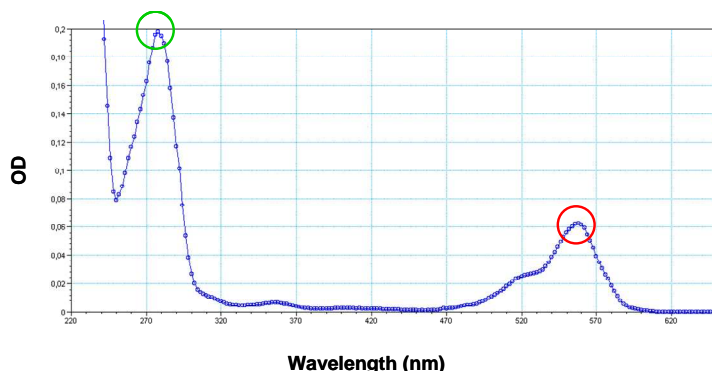
**Figure 27. Tubulin purification and quantification.** (a) Optic density of a tubulin sample diluted 1:20, the red circle indicates the 280nm absorption of the sample; (b), 10% SDS-PAGE gel (Sodium Dodecyl Sulphate-Polyacrylamide Gel Electrophoresis) Blue Coomassie stained. The 50kD band (s) corresponds to  $\alpha$  and  $\beta$ -tubulin. **MW**, Molecular Weight Markers.

### 5.6.2.3 Rhodamine conjugated to Tubulin

Rhodamine-labelled tubulin was prepared as described by Hyman AA., 1991 with modifications made by E. Donadieu and A. Popov. The purified tubulin was labelled by TAMRA (5-(and 6)-carboxytetramethylrhodamine, succinimidyl ester) (Molecular Probes C1171) dissolved in DMSO (Dimethyl sulfoxide) at 37°C in the presence of GTP. The cycles of polymerization and depolymerization allow the TAMRA incorporation and the final obtention of the rhodamin-labelled tubulin. The spectrum at an optical density among 220 and 600nm allowed us to establish the rhodamine and tubulin concentrations.

Tubulin was labelled using a ratio 2:1 rhodamine/tubulin. After labelling, we obtained 3 ml of Rho-tubulin. The final Rhodamine content was calculated measuring the solution optic density at 560nm (Fig.28), and using the rhodamine molar extinction coefficient ( $A_{560 \text{ nm}} = 95000 \text{ M}^{-1}\text{cm}^{-1}$ ) for a final concentration of 153 $\mu\text{M}$ .

The final tubulin concentration (245  $\mu\text{M}$ ) was estimated at 280nm. Considering the rhodamine and tubulin final concentration the obtained ratio was 0.62 molecules of tubulin by each tubulin molecule.



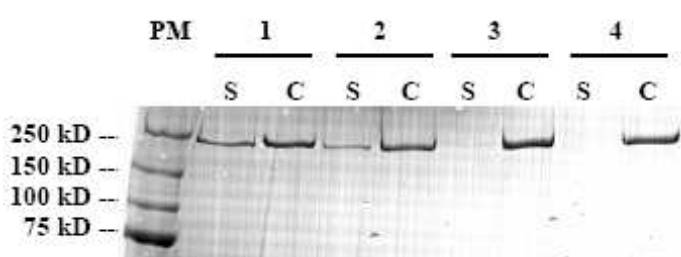
**Figure 28. Rhodamine labelled tubulin spectrum.** Two maximal optical densities (OD) were obtained: at 280nm the protein absorption is marked by the green circle, at 560nm the red circle indicates the rhodamine emission.

#### 5.6.2.4 XMAP215-his7 Protein

The XMAP215-7his recombinant protein was kindly provided by Sonja Rybina (EMBL, Heidelberg). This recombinant protein is produced using the baculovirus protein expression vector system. The addition of 7 histidines to the C-terminal extremity of the protein allow the use of the affinity of histidine chains for some metals as nickel ( $\text{Ni}^{2+}$ ), metal composing the magnetic beads. The presence of some chelators as the nitrilotriacetic acid (NTA) permits a specific protein binding to the magnetic bead and more stable (Hainfeld *et al.*, 1999).

#### 5.6.2.5 Ni-Nta saturation by XMAP215-his7

The saturation of NiNTA beads by XMAP215-his7 was realized to determine the quantity of the protein necessary for the experiment. Different quantities of magnetic beads were incubated in presence of a constant quantity of XMAP215-his7 (10 $\mu\text{l}$ , 0.6mg/ml). After incubation on ice and centrifugation, samples corresponding to supernatant (**S**) and pellet (**P**) were analyzed by a 6% SDS-PAGE gel. XMAP215-his7 disappearing from the supernatant shows the amount of magnetic beads that adsorbs the total XMAP215-his7 protein. **Figure 29** shows the simple number 3, at the saturation quantity of beads/protein: 4  $\mu\text{l}$  magnetic beads and 10 $\mu\text{l}$  XMAP215-his7 0.6 mg/ml.



**Figure 29. Ni-NTA saturation by XMAP215-his7.** MW, Molecular weight markers; (S), Supernatant; (P), Pellet; (1,2,3,4), Different volumes of magnetic beads tested: 1 $\mu$ l, 2 $\mu$ l, 3 $\mu$ l, 4 $\mu$ l respectively. 6% SDS-PAGE gel, Blue Coomassie stained.

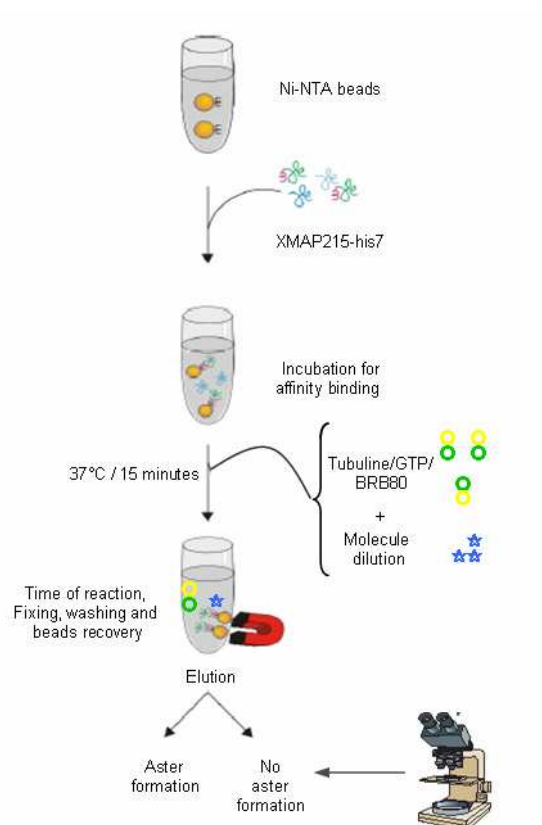
### 5.6.3 MTs nucleation by XMAP215-his7 immobilized on Ni-NTA beads

#### 5.6.3.1 Principle and first part of the aster nucleation test

The test was based on the XMAP215 property to allow the MT nucleation by centrosomes, without XMAP215 the MT nucleation does not take place (Popov *et al.*, 2001). The centrosomes were replaced by with Ni-NTA beads, to obtain a controlled nucleation mechanism, XMAP215 was the only nucleating target and at the same time the Ni-NTA beads are an easily and proper recover product using only a magnet for that purpose. Once the Ni-NTA beads were saturated by XMAP215-his7, the tubulin, GTP and the diluted molecule were added to fulfill the reaction.

The test was realized on 96 multiwell plates, each well corresponded to a defined molecule. The molecule final concentration was 65 $\mu$ M in a 20 $\mu$ l solution containing 0.05  $\mu$ l of beads saturated by XMAP215-his7, tubulin 14  $\mu$ M, Rhodamine labelled tubulin 6  $\mu$ M, GTP 1 mM in BRB80.

The reaction was incubated 15 minutes at 37 $^{\circ}$ C to allow tubulin polymerization. The asters were fixed on a buffer solution containing 0.5% glutaraldehyde and 10 $\mu$ M taxol in BRB80. The test was evaluated by the presence or absence of nucleation (asters formation), the visual evaluation was made using a microscope Axiovert 200M (Zeiss), camera CCD COOLSNAP HO. Images were taken using MetaMorph software version 6.2 (Fig 30).



**Figure 30. Microtubule Nucleation test on magnetic beads saturated by XMAP215-7his.**

### 5.6.4 Second round. Hits evaluation on the tubulin assembly

This second test was realized only for the molecules that showed a positive result in the nucleation test (asters absence). It remained possible that the absence of asters (understood as positive result) was the result of a molecule effect on the tubulin dimers addition. So, the objective of this second test is to determine if the molecule is active against the tubulin dimer.

The molecules were added at a final concentration of 100  $\mu\text{M}$  in a solution containing 40  $\mu\text{M}$  tubulin, GTP 1 mM in BRB.

The kinetics of tubulin polymerization was realized measuring the absorbance at 350 nm in the spectrophotometer using a 96 multi well plate (Costar® Corning Incorporated 3695) during an hour at 37°C. The control was

made using dimethyl sulfoxide (DMSO) 4%, the same substance in which the molecules were preserved.

### **5.6.5 Third part: Final activity test for the positive molecules**

The considered positive molecules retained after the two consecutive selection test were analyzed to determinate their title activity.

The test realized was a modification of the initial aster formation test. In this case the molecule concentration varies in a range among 6 and 100 $\mu$ M. Colchicine, a well known depolymerising molecule was used as the control of the reaction. No positive control is possible because to the actual absence of an XMAP215 specific inhibitor.

## **RESULTS**





## RESULTS

### 6. Anti-XMAP215 mcAB

#### 6.1 Anti-XMAP215 mcAB production and characterization

The reported cellular localization of XMAP215 and ch-TOG is characterized mostly by their colocalization with centrosomes in interphase and with the mitotic spindle. In interphase XMAP215 has shown previously to colocalize with MTs (Popov *et al.*, 2001) and ch-TOG has been found colocalizing with the endoplasmic reticulum (Charrasse *et al.*, 1998).

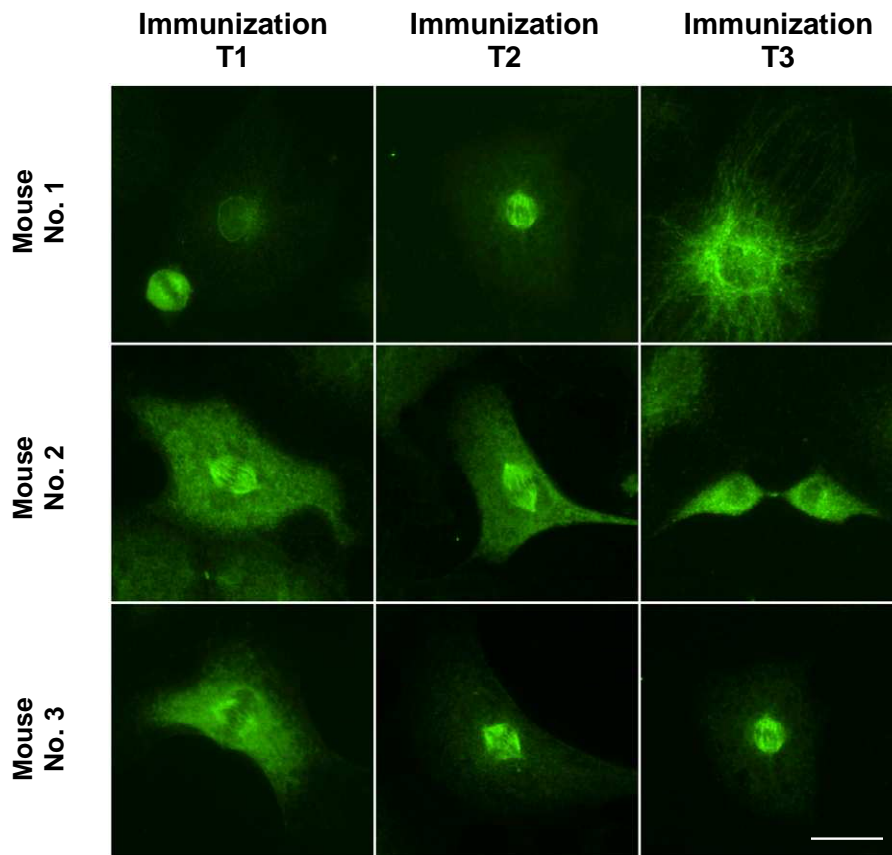
Having in mind the fact that both proteins share an 80% identity and the different cell localizations reported for some of their homologues, we direct our objective to re-evaluate the XMAP215/ch-TOG cell localization. For this purpose we developed a set of mcABs using the full length recombinant protein XMAP215-his7 as antigen.

##### 6.1.1 Anti-XMAP215 mcAB production: Three selected clones identifying the XMAP215/ch-TOG cell localization.

The mice immunization evolution was followed by single IF on PHF and XL177 cells (**Fig. 31**). The chosen fixing methods were PFA 4% and the -80°C cold methanol. Before each immunization, each serum sample was analyzed for reactive antibodies against XMAP215/ch-TOG.

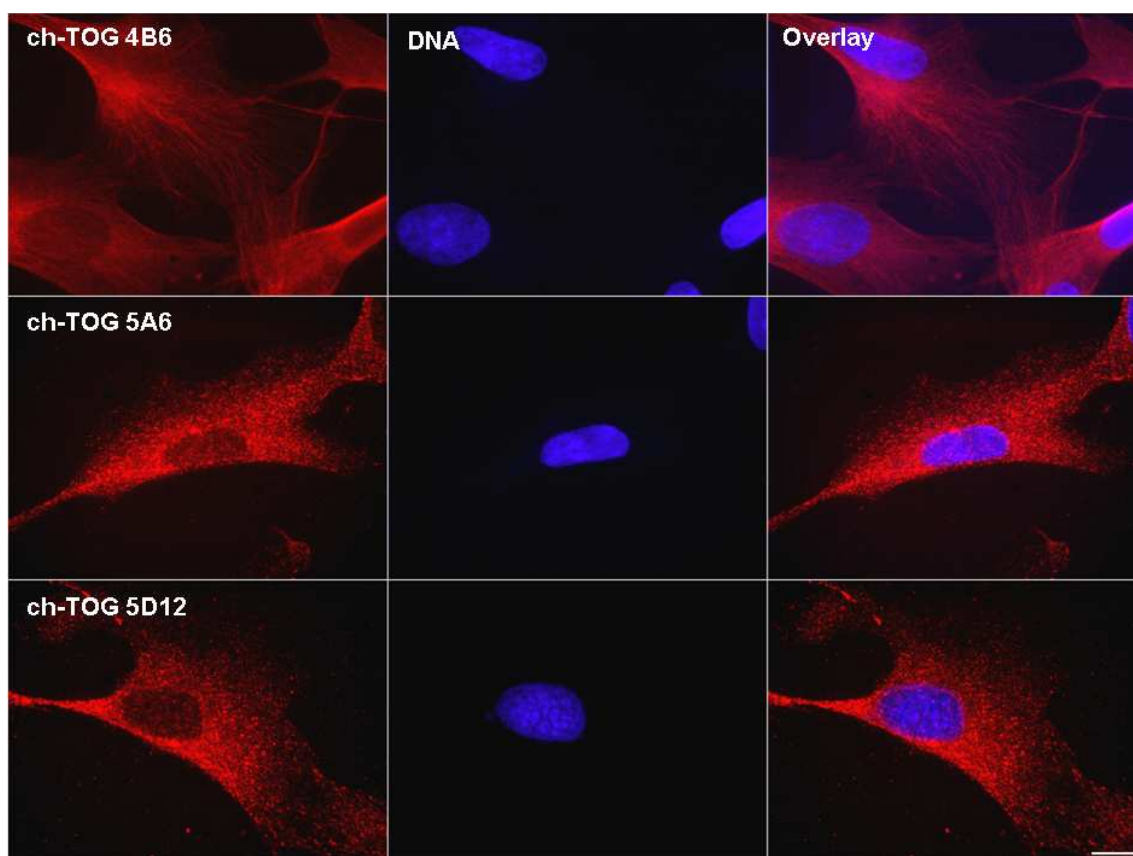
The reactive IF antibodies selection criteria were established after the future imaging scheduled experiments. Other antibodies selection criteria such as western blot or ELISA were not considered during the primary approach due to the possible mcAB non-cross reactivity among the different techniques. After the third immunization, the reactivity of the serum antibodies against XMAP215/ch-TOG were tested one last time by IF, the resulting images showed a clear and strong potential positive reaction at the IF. The mitotic spindle staining was considered as the visual evaluation criteria for a positive

immunological response. After three serial immunizations with the recombinant XMAP215/ch-TOG, the best responder mouse was sacrificed for the further splenocytes fusion with myeloma cells.



**Figure 31. Immunization evolution of the BALB/c mice.** The selection of the clones took place using the IF single staining on PFA or methanol fixed PHF and XL177 cells. The selection method of the responding mouse antiserum was based on the search for a signal defining the cell mitotic spindle, being the strongest known signal for XMAP215/ch-TOG. Scale bar 20 $\mu$ m.

Three clones were selected. After fixation an indirect immunofluorescence showed two different patterns. The first one, the **4B6 clone** was reactive to a PFA fixing method, producing an IF staining with the “classical” microtubular type pattern already reported for XMAP215 (Popov *et al.*,2001). Other two clones (**5A6** and **5D12**) supernatants responded to a methanol fixing procedure, the resultant signal showed a “dot” staining, similar to the staining observed previously for proteins present at the tips of growing MTs, such as **EB1** (Fig. 32).

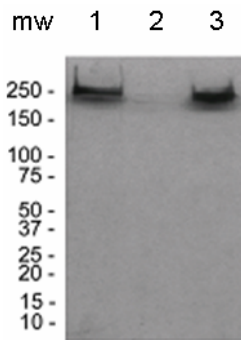


**Figure 32. ch-TOG single staining in primary human fibroblast (PHF).** Fixed PHF and XL177 (images not shown) cells were used to select the clone mcAB production. Images show a single staining IF using the clone supernatant as source of mcAB, as secondary antibody a goat anti-mouse alexa fluor 548 (red) was used; DNA staining was obtained using Hoescht 355. Scale bar 10  $\mu$ m.

## 6.1.2 anti XMAP215 mcAB characterization

### 6.1.2.1 mcAB Specificity

After fusion, the hybridomas were cloned. Three positive clones were identified using IF on PHF and XL177 cells. Using the hybridomas supernatant as source, each one of the three obtained mcAB was confirmed for their specificity in western blot (**Fig. 33**). With this purpose, *Xenopus laevis* egg extract was XMAP215 depleted.



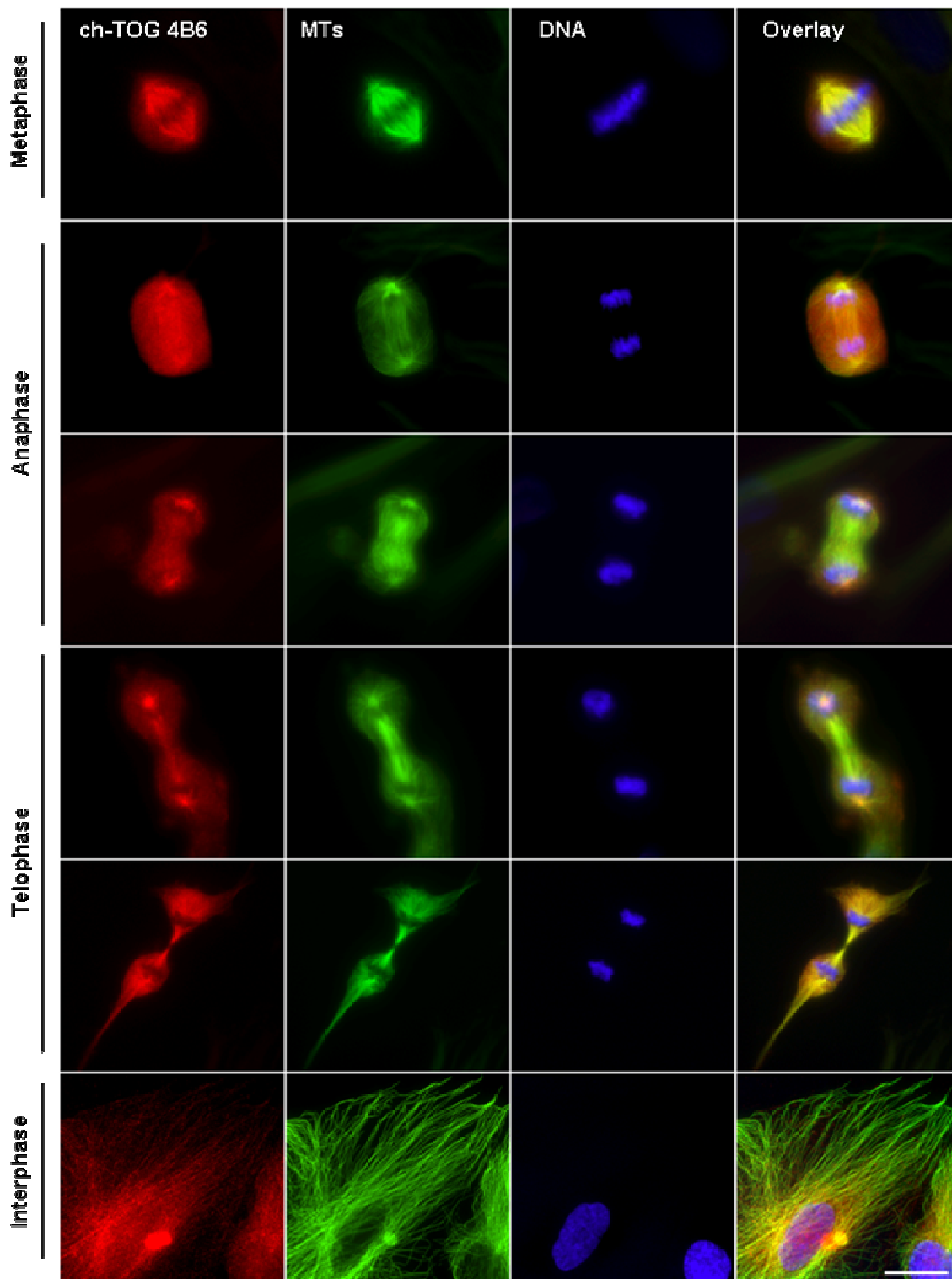
**Figure 33. mcABs anti XMAP215/ch-TOG specificity.** The specificity of the anti XMAP215/ch-TOG mcAB was assessed by immunoblotting against the no depleted and depleted ( $\Delta\Delta$ XMAP215) *Xenopus laevis* mitotic egg extract. The image shows the non depleted egg extract (**lane 1**) and the depleted one (**lane 2**). XMAP215 depleted egg extract ( $\Delta\Delta$ XMAP215) was obtained using polyclonal antibodies directed against the N terminal fragment of the protein (Popov *et al.*, 2001). **Lane 3**, Protein A beads used for depletion. The specificity of the selected mcABs was confirmed by IF. IB realized for the three cloned mcAB in parallel. **mw**, molecular weight markers.

Once the primary clone's selection was made, and the specificity of the obtained antibodies was confirmed, our next step consisted on the confirmation of the staining with a double staining IF. In this case, we use the cell cytoskeleton as known reference. Microtubules **MT/ch-TOG** or **MT/XMAP215** double staining IF were analyzed. Each mcAB was tested on PHF and XL177 cells (data not shown) under the fixation method established for each case.

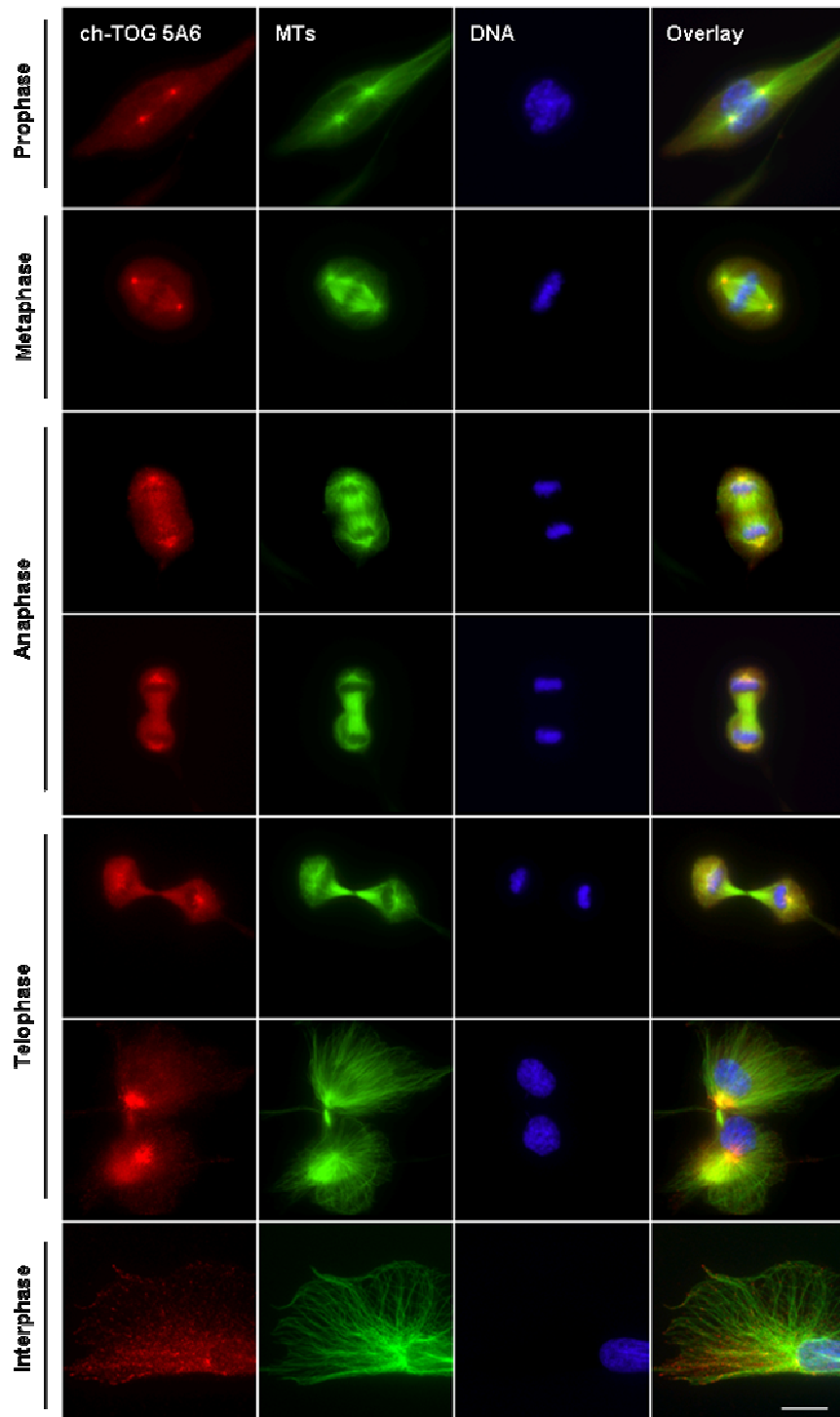
#### 6.1.2.2 mcABs staining activity on fixed cells

Each one of the obtained mcABs stained interphasic and mitotic cells. Clearly the different phases of the cell cycle are identified. **Figure 34** shows the **4B6 mcAB** IF reactivity. This mcAB responds to a **PFA 4%** fixing method, identifying the ch-TOG conformation that colocalize with MTs. In these images the **centrosome** is clearly identified by the mcAB. Once the cell is entering in **Metaphase**; mitotic spindle, centrosome and astral MTs are stained. As the cell cycle keeps going, the **4B6 mcAB** identifies the mitotic spindle evolution through **anaphase**, with the DNA staining showing the chromosomes movement in direction to the opposite poles. MTs and cells contractile ring are present classically during the **telophase**. Finally the **4B6 mcAB** staining identifies **interphasic** ch-TOG that colocalize perfectly with the MT signal.

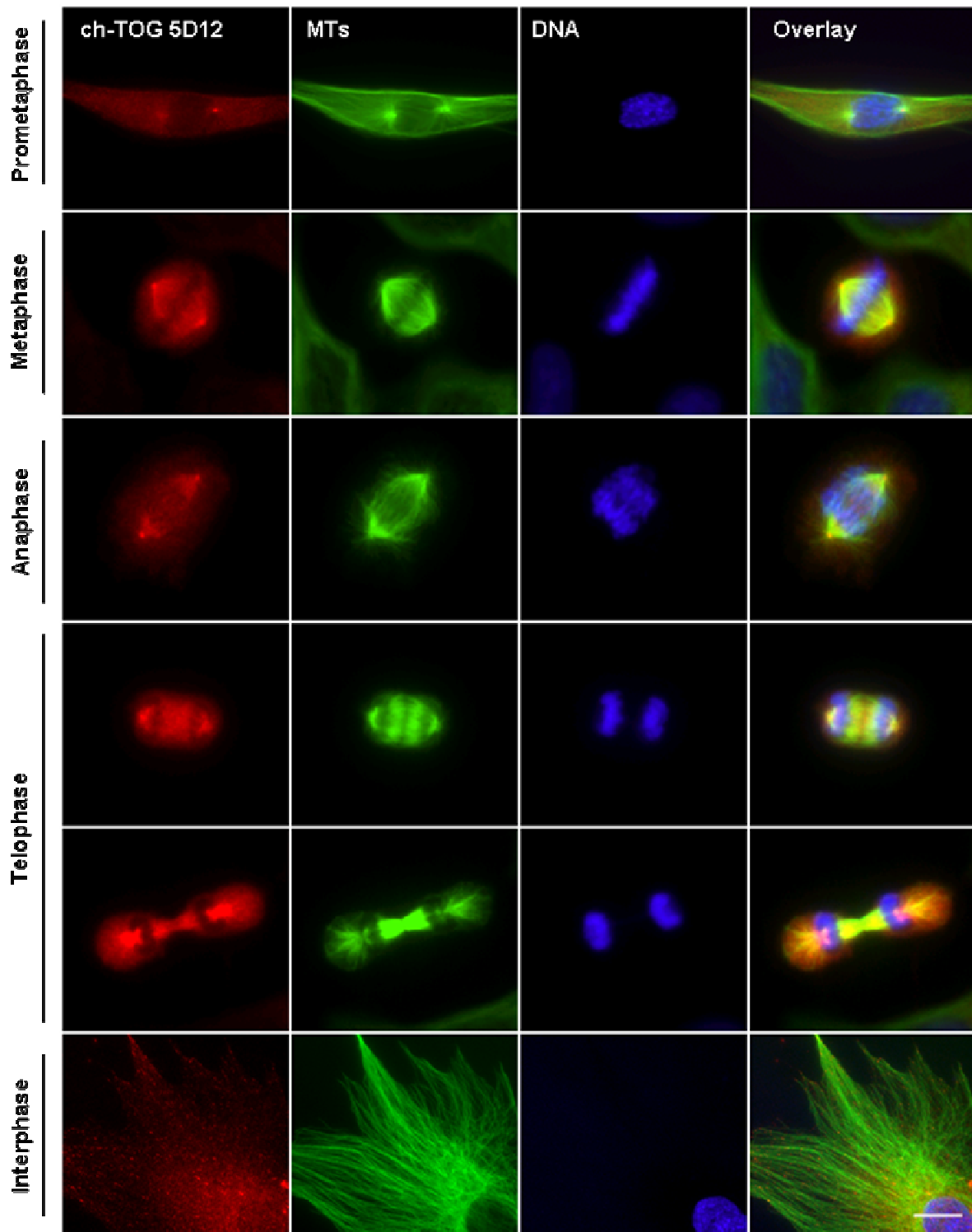
Both methanol fixing responders mcAB (**5A6** and **5D12**) (**Fig. 35** and **Fig. 36** respectively) identified the XMAP215/ch-TOG present in the different stages of the cell cycle until the cell reaches the interphase.



**Figure 34. 4B6 mcAB staining on PHF.** The entire mitotic cycle can be followed in the PFA fixed PHF. Images show the mitotic evolution from **metaphase** to **telophase**, until the furrow is sealed and the cell finally reaches the interphase. **ch-TOG 4B6**, mcAB directed against the colon-hepatic tumor overexpressed gene protein, clone 4B6 (**red**); **MTs**, Microtubules (**green**); **DNA** (**blue**). 10 µm scale bar.



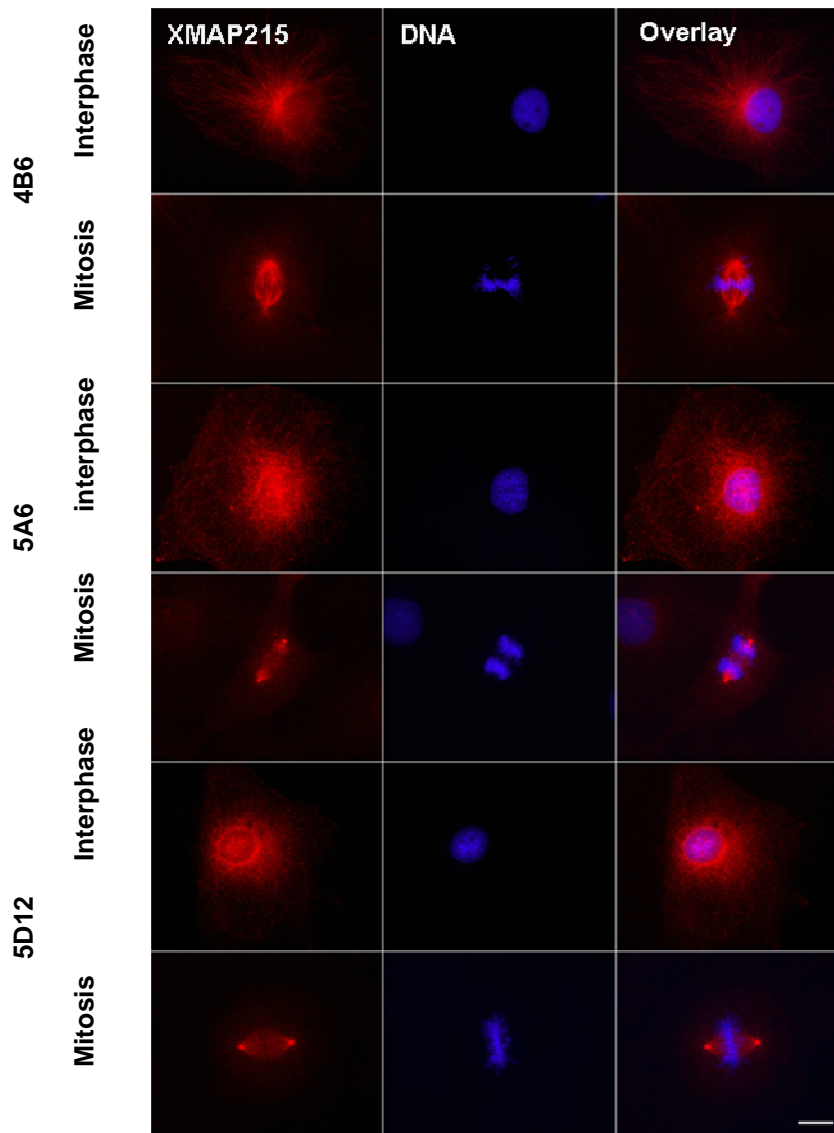
**Figure 35. 5A6 mcAB staining on PHF.** Methanol fixed PHF in a double staining ch-TOG/MT image. 5A6 mcAB identifies ch-TOG co-localizing with mitotic spindle and the interphasic microtubular cytoskeleton. All stages of the cell cycle can be identified from **prophase** until the cell reaches the **interphasic** state. Microtubules and ch-TOG colocalize during each event. **MTs**, microtubule (**green**); **ch-TOG 5A6**, mcAB directed against the colon-hepatic tumor overexpressed gene protein, clone 5A6 (**red**); **DNA** (**blue**). Scale bar 10  $\mu$ m.



**Figure 36. 5D12 mcAB staining on PHF cells.** PHF fixed methanol -80°C and stained with the 5D12 mcAB supernatant. The cell cycle can be followed after the 5D12 staining. Centrosomes, mitotic spindle, cell furrow and the final interphasic ch-TOG localization can be identified. **MTs**, microtubule (**green**); **ch-TOG 5D12**, mcAB directed against the colon-hepatic tumor overexpressed gene protein, clone 5D12 (**red**); **DNA** (**blue**). Scale bar 10  $\mu\text{m}$ .

### 6.1.2.3 mcAB isotyping, class

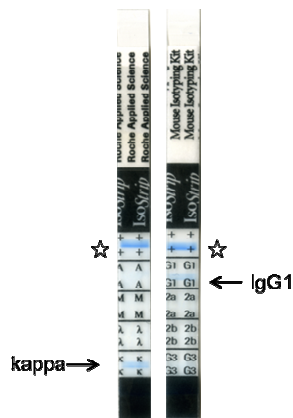
Supernatant from each of the propagated clones were tested with anti-mouse immunoglobulin class-specific reagents. The three produced mcAB were identified as immunoglobulins of type IgG by the goat F(ab)2 fragment anti-mouse IgG ( $\gamma$  chain). **Figure 37** shows the immunofluorescence staining result using anti-  $\gamma$  chain antibodies on PHF fixed cells.



**Figure 37. mcAB isotyping.** mcAB staining using an anti gamma antibody rhodamine conjugated (**red**). Culture supernatants were used as primary antibodies source on PFA or methanol fixed *Xenopus laevis* cells (XL177). DNA staining was obtained using Hoescht 355 (**blue**). Scale bar 10 $\mu$ m.



To precise the isotyping characterization, the three produced mcAB were analyzed using IsoStrip, Mouse monoclonal antibody isotyping kit (Roche applied Science). The three antibodies were identified as immunoglobulins type G I (IgG) subclass (IgG1) kappa light chain (**Fig.38**).



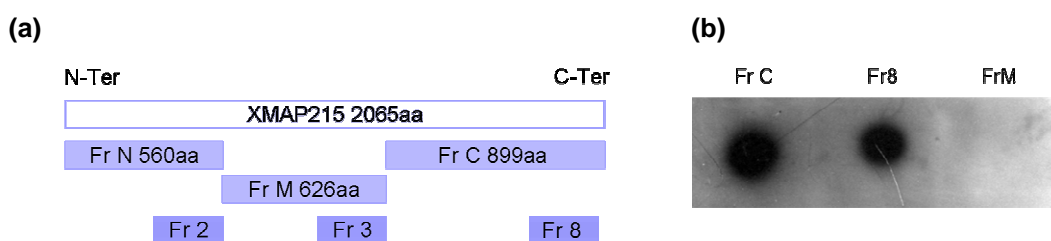
**Figure 38. mcAB isotyping.** Each one of the mcAB was analyzed. The three different clones were confirmed as IgG immunoglobulins and identified as IgG<sub>1</sub>(κ) antibodies. The star symbol represents the reaction positive control

#### 6.1.2.4 mcAB epitops Cartography

The ELISA test showed that the produced mcABs recognized an epitope present in the C-terminal domain of the XMAP215 sequence. In previous studies Popov and collaborators, 2001 divided the full length protein (2,065 aa) in several fragments.

Here, the fragment 8 (Fr8) constitute a short fragment of 218 aa contained in the C-terminal region of the XMAP215 protein, the epitope recognized by the produced mcAB is contained in this sequence. No specificity was detected against the XMAP215 recombining fragments N (FrN), Fragment 2 (Fr2), Fragment (Fr M) or Fragment 3 (Fr3) (**Fig. 39a**).

A confirmation Dot-blot test was run, showing the same reaction using fragments C (FrC) as a positive control, fragment M (FrM) as negative control and fragment 8 as tested sample (**Fig. 39b**).



**Figure 39. XMAP215 antigen cartography for the anti-XMAP215 mcAB.** (a) Schematic representations of XMAP215 fragments. Fragment N (**FrN**), Fragment M (**Fr M**), Fragment C (**FrC**) and other three derived sub-fragments: Fragment 2 (**Fr2**), Fragment 3 (**Fr3**), Fragment 8 (**Fr8**). Modified from Popov *et al.*, 2001 (b) Dot blot showing the mcAB immunoreactivity identified for the C-terminal domain of the XMAP215 protein. More precisely the epitope recognized by the mcAB was located in the fragment 8 (aa 1847-2065)

The mcAB immunoreactivity was also established for the three mcAB. Three different species (human, frog and mouse) were considered counting on the different identity observed among species (Table VIII).

	<i>Identity (%)</i>	<i>Length (aa)</i>	<i>IB</i>	<i>IF</i>	<i>IP</i>	<i>ELISA</i>
<i>Xenopus laevis</i>	100	2065	+	+	+	ND
<i>Homo sapiens</i>	82.4	2031	+	+	ND	ND
<i>Mus musculus</i>	80.1	2010	+?	+	ND	ND

**Table VIII. mcAB antibodies anti XMAP215/ch-TOG *in vitro* immunoreactivity.** The identity considered for the Homo sapiens (CKAP5) isoform a. **IB**, Immunoblotting; **IF**, Immunofluorescence; **IP**, Immunoprecipitation; **ELISA**, Enzyme-Linked ImmunoSorbent Assay; **ND**, Non determined.

For the immunoblotting (IB) we used the *Xenopus laevis* egg extract and the HeLa cell lysate for the frog and human analysis respectively. The immunoreactivity was established using PHF (human), XL177 cells (*Xenopus laevis*) and 3T3 cells (mouse). The characterization of the produced antibodies is resumed in Table IX.

mcAB	5D12	4B6	5A6
<b>Class/ Sub-class</b>	IgG <sub>1</sub> K	IgG <sub>1</sub> K	IgG <sub>1</sub> K
<b>Antigen</b>	XMAP215-his7	XMAP215-his7	XMAP215-his7
<b>IB reactivity</b>	230 kD	230 kD	230 kD
<b>Target on XMAP215</b>	C-terminal region (aa 1847-2065)	C-terminal region (aa 1847-2065)	C-terminal region (aa 1847-2065)
<b>Possible epitope on XMAP215</b>	Contained in Tau sequence? (aa 1866-1883)	Contained in Tau sequence? (aa 1866-1883)	Contained in Tau sequence? (aa 1866-1883)
<b>Fixation (IF productive)</b>	Methanol (-80°C)	PFA	Methanol (-80°C)
<b>Staining (Co-localization)</b>	+ TIPs, centrosomes, mitotic spindle	Microtubule, centrosomes, mitotic spindle	+TIPs, centrosomes, mitotic spindle
<b>IF Immunoreactivity</b>	Human, mouse, frog.	Human, mouse, frog.	Human, mouse, frog.
<b>Functional assays</b>	+TIPXMAP215 tracking in mitotic <i>Xenopus laevis</i> egg extracts, Absence of MT anchoring?	MTXMAP215 tracking in mitotic <i>Xenopus laevis</i> egg extracts	+TIPXMAP215 tracking in mitotic <i>Xenopus laevis</i> egg extracts
<b>Experimental Applications</b>	IF, WB, IP using protein A and protein G beads, ELISA.	IF, WB, IP using protein A and protein G beads, ELISA.	IF, WB, IP, using protein A and protein G beads, ELISA.
<b>Human Diagnostic Applications</b>	Immunohistochemistry (to be determined)	Immunohistochemistry (to be determined)	Immunohistochemistry (to be determined)
<b>Patent</b>	Pending	Pending	Pending

**Table IX. mcAB anti-XMAP215/ch-TOG characterization.** mcAB, monoclonal antibody; kD, kilodalton; aa, aminoacid; PFA, Paraformaldehyde; +TIPs, MT plus ends tracking proteins; MT, Microtubule; ELISA, Enzyme Linked ImmunoSorbent Assay; IF, Immunofluorescence; WB, Western Blotting; IP, Immunoprecipitation.

### 6.1.2.5 mcAB technical data sheet

Due to the potential use of the mcAB in the scientific research and/or the human diagnosis domain the patenting and commercialization of the mcAB has been considered. A “Technical Information Data Sheet” was produced for each one of the obtained mcAB (**Fig. 40** and **Fig.41**).

**Figure 40. 4B6 mcAB technical data sheet.**

<b>mouse anti-microtubular XMAP215 (MT-XMAP215/ch-TOG mcAB)</b>
<b>Clone: 4B6 C-Ter</b>
<b>Background</b>
<b>XMAP215</b> is a microtubule Associated Protein of 228 kDa that belongs to a highly conserved family of proteins, been the only known family of MAPs common to plants and animals. Its human ortholog is <b>ch-TOG</b> , the Colon-Hepatic Tumour Overexpressed Gene protein. <b>XMAP215</b> is required for the growth of microtubules and mitotic spindle assembly. In extracts, <b>XMAP215</b> exerts its microtubule growth-promoting activity mainly by antagonizing the activity of XKCM1. In interphasic cells, <b>XMAP215 co-localizes</b> with <b>microtubules</b> and the centrosome. In mitotic cells <b>XMAP215</b> localize to the spindle pole bodies and spindle microtubules, also XMAP215 co-localizes with MT in the interphasic network.
<b>References</b>
Gard, D., M, Kirschner. 1987. A Microtubule-assembly in cytoplasmic extracts of <i>Xenopus</i> oocytes and eggs. <i>J. Cell Biol.</i> 105:2191-2201 Kinoshita, K., <i>et al.</i> 2002. XMAP215: a key component of the dynamic microtubule cytoskeleton. <i>Trends Cell Biol.</i> 12 (6):267-273 Popov, A., <i>et al.</i> 2002. XMAP215 is required for the microtubule nucleating activity of centrosomes. <i>Curr Biol.</i> 12:1326-1330
<b>Chromosomal localisation</b>
Genetic locus: Human mapping to 11p11.2
<b>Source</b>
Monoclonal anti <b>MT-XMAP215/ch-TOG</b> C-ter (mouse IgGk1) is derived from the hybridoma cells produced by the fusion of mouse myeloma cells and splenocytes from a BALB/c mouse immunized with the full length recombinant XMAP215-his7.
<b>Product</b>
The antibody is supplied as purified mouse immunoglobulin at 1mg/ml in phosphate buffered saline, pH 7.2-7.4 with 0.1% sodium azide.
<b>Precautions and disclaimer</b>
Due to the sodium azide content, a material safety data sheet (MSDS) has been sent with the product. Consult the MSDS for information regarding hazardous and safe handling.
<b>Storage</b>
Store at -20°C. For extended storage, freeze i n working aliquots. Repeated freezing and thawing is not recommended.
<b>Applications</b>
4B6 mcAB is recommended for the detection of <b>MT-XMAP215</b> ( <i>Xenopus laevis</i> ), ch-TOG (CKAP5-human) and ckap5 (mouse) conformation by Western blotting (1:1000 dilution), immunofluorescence (1:100 dilution), immunoprecipitation and ELISA. For IF purposes a PFA fixation is recommended: PFA 4%, Triton 100 0.5% in BRB80.

Each data sheet contains the technical specifications for the different set of experiments where the antibody can be used successfully, as the

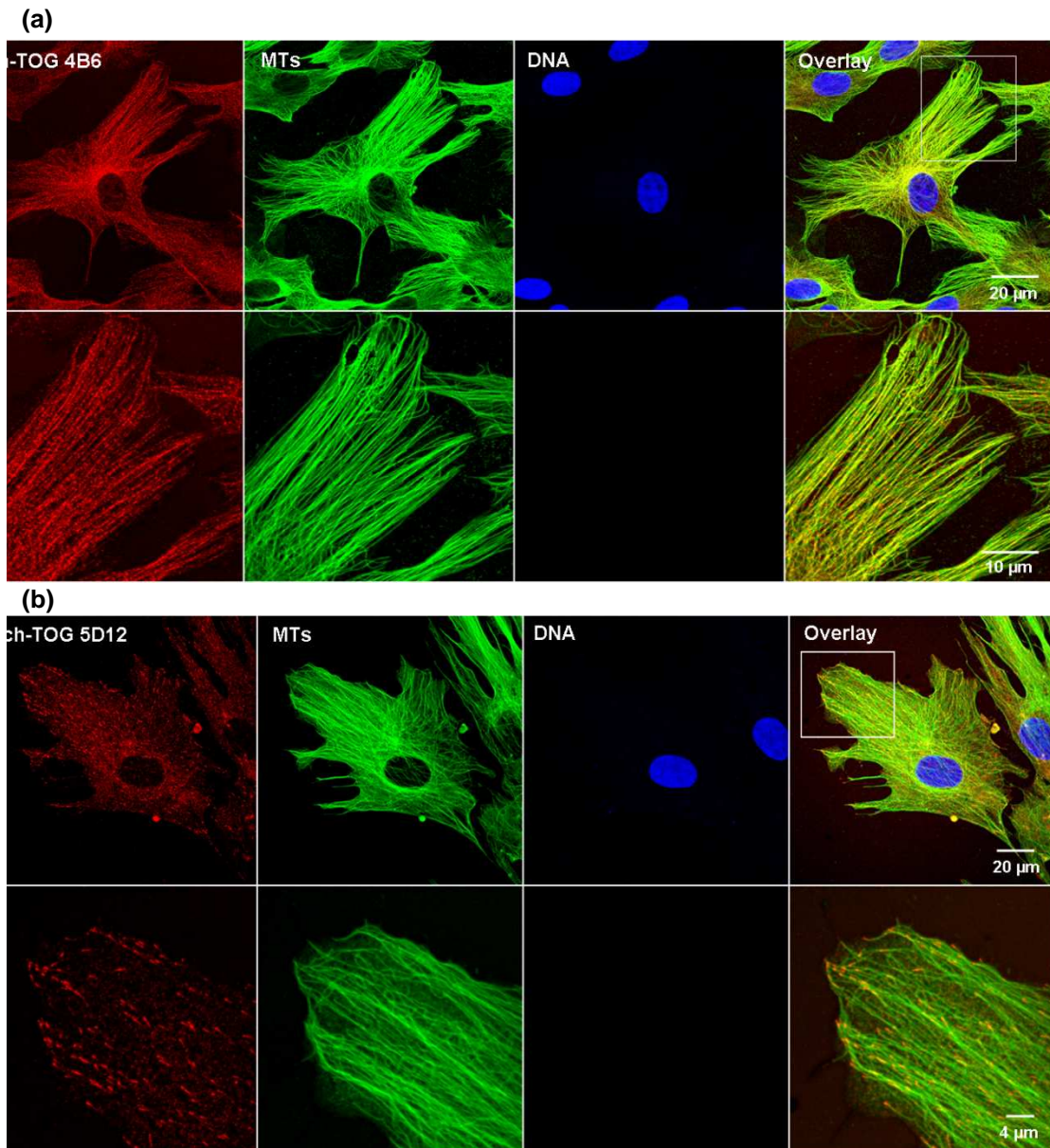
experimentation phase goes on; the technical data sheet is actualized. The clone stability and mcAB quality are guaranteed through a serial hybridoma re-cloning and a subsequent series of functional test.

**Figure 41. 5D12 mcAB technical data sheet.**

<b>mouse anti +TIP XMAP215 (+TIP XMAP215/ch-TOG mcAB) Clone: 5D12 C-Ter</b>
<b>Background</b>
<b>XMAP215</b> is a microtubule Associated Protein of 228 kDa that belongs to a highly conserved family of proteins, been the only known family of MAPs common to plants and animals. Its human ortholog is <b>ch-TOG</b> , the colon-hepatic tumour overexpressed gene protein. XMAP215 is required for the growth of microtubules and mitotic spindle assembly. In extracts, <b>XMAP215</b> exerts its microtubule growth-promoting activity mainly by antagonizing the activity of XKCM1. In interphasic cells, <b>XMAP215 co-localizes</b> with <b>microtubules growing ends (+TIP XMAP215)</b> and the centrosome. In mitotic cells <b>XMAP215</b> localize to the spindle pole bodies and spindle microtubules. Other XMAP215 orthologs such as Stu2 ( <i>S. cerevisiae</i> ) and Msps ( <i>D. melanogaster</i> ) have been also reported as +TIPs proteins.
<b>References</b>
Gard, D., <i>et al.</i> 1987. A Microtubule-associated protein from <i>Xenopus</i> eggs that specifically promotes assembly at the plus-end. <i>J. Cell Biol.</i> 105:2203-2215 Kinoshita, K., <i>et al.</i> 2002. XMAP215: a key component of the dynamic microtubule cytoskeleton. <i>Trends Cell Biol.</i> 12 (6):267-273 Popov, A., <i>et al.</i> 2002. XMAP215 is required for the microtubule nucleating activity of centrosomes. <i>Curr Biol.</i> 12:1326-1330
<b>Chromosomal localisation</b>
Genetic locus: Human mapping to 11p11.2
<b>Source</b>
Monoclonal anti <b>+TIP XMAP215/ch-TOG C-ter</b> (mouse IgGk1) is derived from the hybridoma cells culture. The antibody is the result of the fusion of mouse myeloma cells and splenocytes from a BALB/c mouse immunized with the full length recombinant XMAP215-his7.
<b>Product</b>
The antibody is supplied as purified mouse immunoglobulin at 1mg/ml in phosphate buffered saline, pH 7.2-7.4 with 0.1% sodium azide.
<b>Precautions and disclaimer</b>
Due to the sodium azide content, a material safety data sheet (MSDS) has been sent with the product. Consult the MSDS for information regarding hazardous and safe handling.
<b>Storage</b>
Store at -20°C. For extended storage, freeze in working aliquots. Repeated freezing and thawing is not recommended.
<b>Applications</b>
<b>5D12 mcAB</b> is recommended for the detection of <b>+TIP-XMAP215</b> ( <i>Xenopus laevis</i> ), ch-TOG (CKAP5-human) and ckap5 (mouse) conformation by Western blotting (1:1000 dilution), immunofluorescence (1:100 dilution), immunoprecipitation and ELISA. For IF purposes a methanol -80°C fixation is recommended.

## 6.2 XMAP215/ch-TOG cellular localizations.

### 6.2.1 Two cellular localizations for XMAP215/ch-TOG



**Figure 42. Two different intracellular localizations for ch-TOG in PHF. (a) Microtubular ch-TOG localization (red) using the 4B6 mcAB.** ch-TOG is localized along the MT lattice (vert) in PFA fixed interphasic cells. This type of staining has been already described for mostly of the XMAP215/Dis1 family members. **(b) + TIP ch-TOG localization (red) revealed using the 5D12 and 5A6 mcAB.** ch-TOG is localized at the plus tips of the MTs (vert). This localization has been described only for two other members of the MAP215/Dis1 proteins family (*S. cerevisiae*, **Stu2** and *Drosophila melanogaster*, **Msp5**). DNA staining was obtained using Hoescht 355 (blue). PHF were fixed in methanol -80°C as described previously. Images were acquired using the Leica TCS-SP3 confocal microscope. An identical reactivity have been obtained for the mcAB 4B6 and 5D12 in *Xenopus laevis* cells XL177 (images not shown).

The cellular localization of XMAP215/ch-TOG was analyzed on fixed cells such as PHF (**Fig. 42**) and *Xenopus laevis* XL177 cells (Images not shown).

Two intracellular localizations of XMAP215/ch-TOG were confirmed depending only on the mcAB used. A first localization obtained with the 4B6 mcAB (**ch-TOG 4B6**) shown ch-TOG colocalizing with **MTs**. This localization was denominated microtubular XMAP215/ch-TOG (**MT-XMAP215/ch-TOG**) (**Fig. 42a**). A second localization was observed with the 5D12 mcAB (**ch-TOG 5D12** and **5A6**). The methanol fixation procedure showed a ch-TOG localization at the MTs + **TIPs**, a localization named **+TIP XMAP215/ch-TOG** (**Fig. 42b**). XMAP215/ch-TOG has two localizations in fixed cells, one following the MT lattice and another one at the growing MT end, the MT + TIP.

### 6.2.2 The +TIP XMAP215/ch-TOG and EB1 colocalize

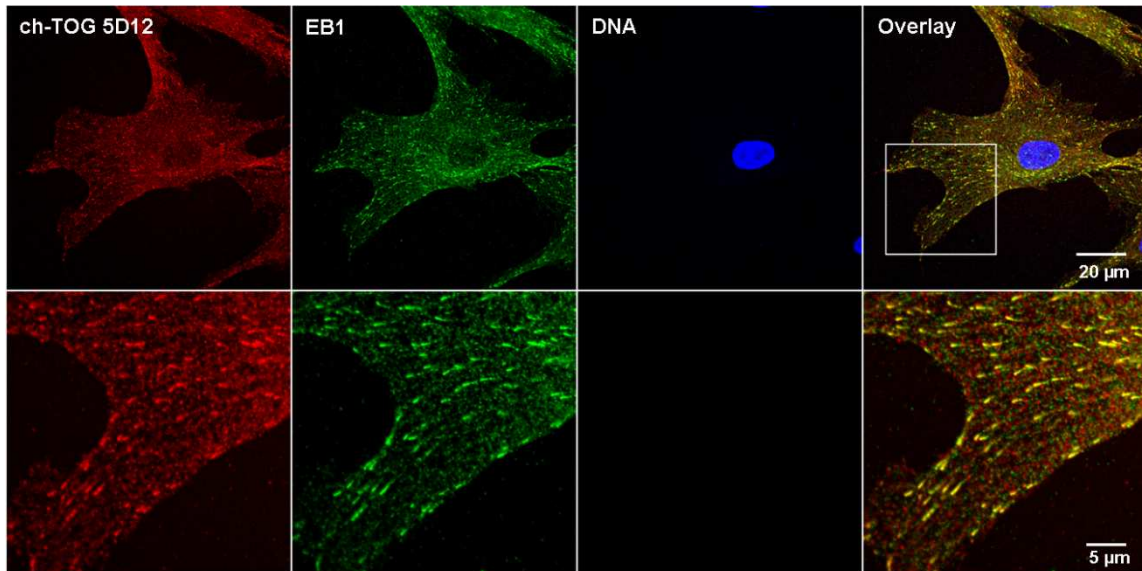
The new XMAP215/ch-TOG localization shown by **mcAB 5D12** and **mcAB 5A6** was analyzed using the confocal microscopy technology. The XMAP215/ch-TOG signal has the characteristic “comet-like” structure and localization at the end of growing MTs, a similar staining to the one obtained for the **+ Tips proteins** such as **EB1**.

To confirm this discovery, the **colocalization** of **+TIP ch-TOG 5D12** with **EB1** at the plus tips of the MTs was observed and analyzed (**Fig.43**) using the same methods and acquisition characteristics previously cited. ch-TOG 5D12 and ch-TOG 5A6 do clearly colocalize with EB1 on fixed PHF (**Fig.43a**) and *Xenopus laevis* XL177 cells (images not shown). Additionally, the triple staining for **ch-TOG 5D12**, **EB1** and **MTs** confirms the + TIP localization of **XMAP215/ch-TOG**.

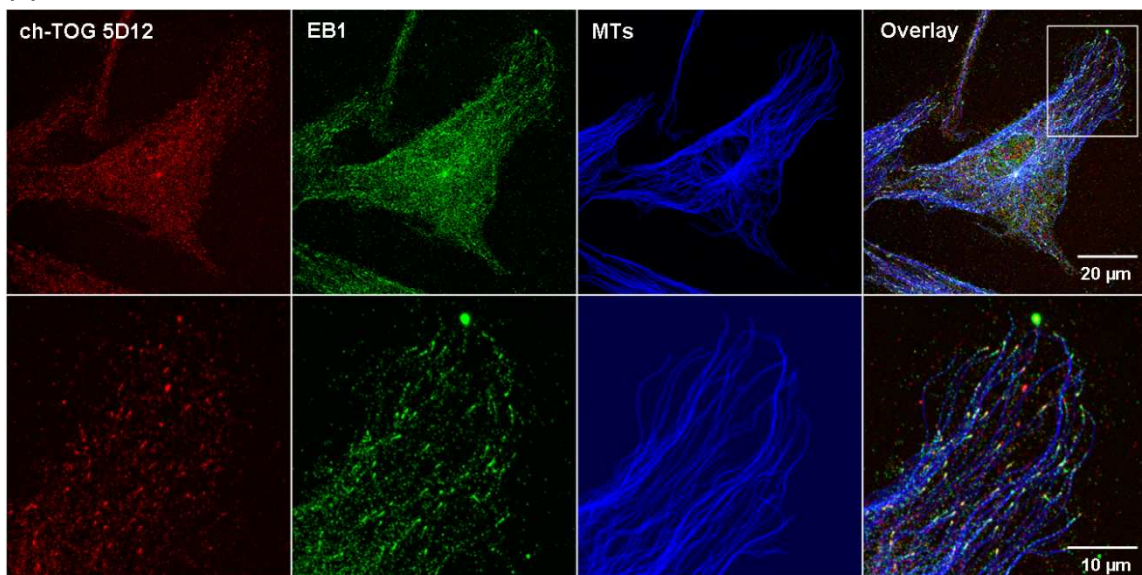
XMAP215/ch-TOG does exist as a + TIP protein in the different species of the fixed cells analyzed. In addition to its co-localization with EB1, XMAP215/ch-TOG seems to precede EB1 at the tip of the MT. Further

experiments were oriented to establish the XMAP215/ch-TOG exact localization at the tip of the MT.

(a)



(b)



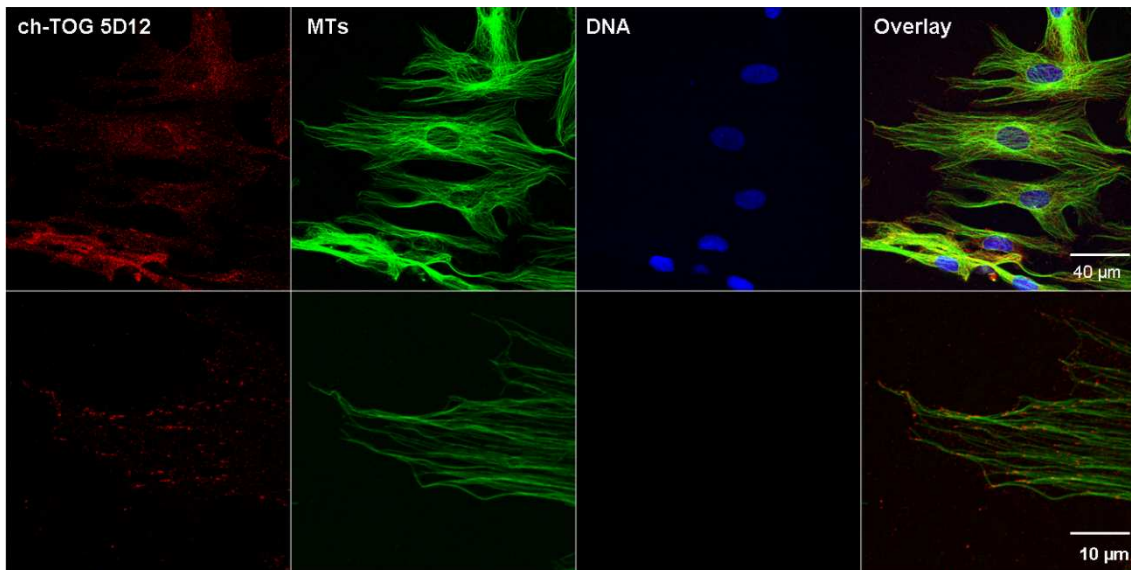
**Figure 43. + TIP ch-TOG co-localizes with EB1.** (a) + TIP ch-TOG (red) and a well known plus tip protein: EB1 (green). ch-TOG is identified by the mcAB 5D12. (b) + TIP ch-TOG triple staining localization, ch-TOG (red), EB1 (green) and MTs (blue). Indirect immunofluorescence realized on methanol fixed PHF. The primary antibodies (mouse anti-ch-TOG, rabbit anti-EB1 and rat anti  $\alpha$ -tubulin) were visualized using goat anti-IgG mouse Cy3, goat anti-IgG rabbit Alexa 488 and a goat anti-IgG rat Cy5 as the secondary antibodies respectively. In the double and triple staining + TIP ch-TOG showed not only the ch-TOG-EB1 colocalization, but also confirm the localization at the tip of the growing MTs.



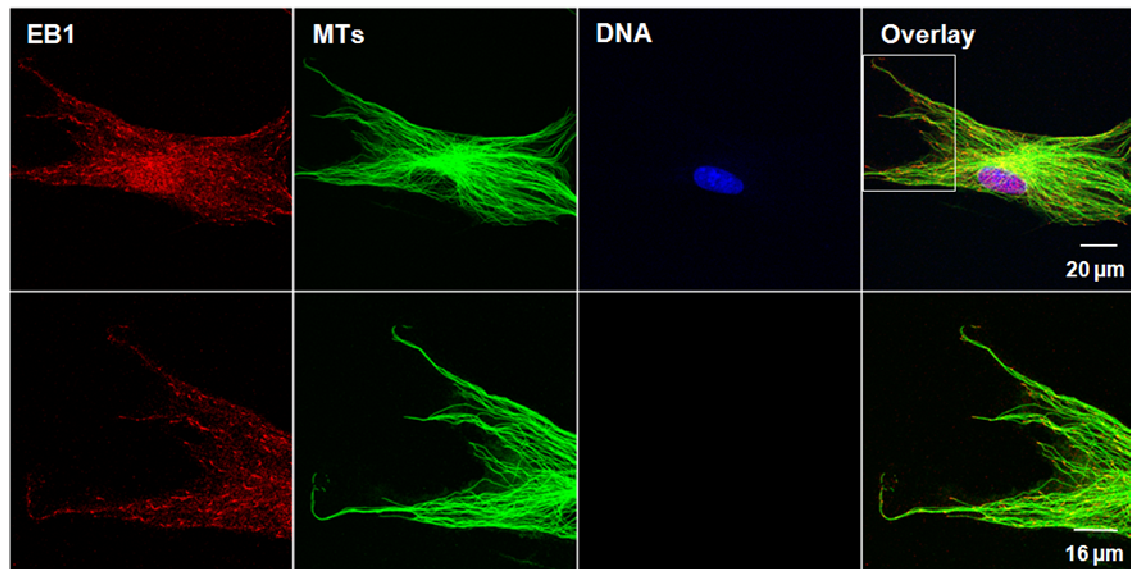
### 6.2.3 +TIP XMAP215 and other +TIPs, a hierarchy

In order to establish the +TIP ch-TOG 5D12 labelling exact localization in comparison to the other +TIPs proteins; we developed our own **analysis method** for the “comet-like” structures measurement.

(a)



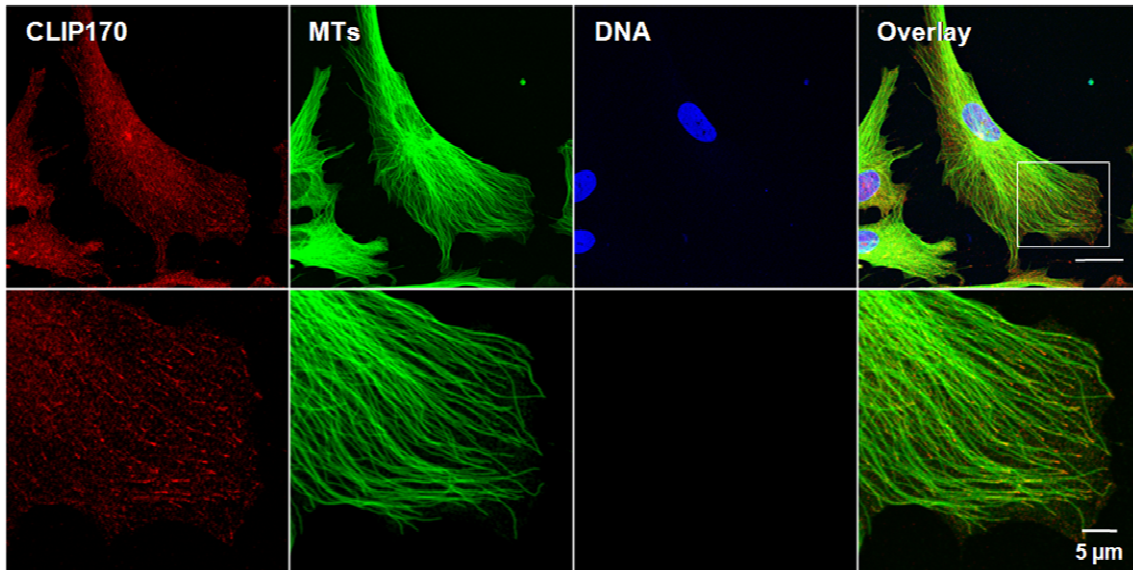
(b)



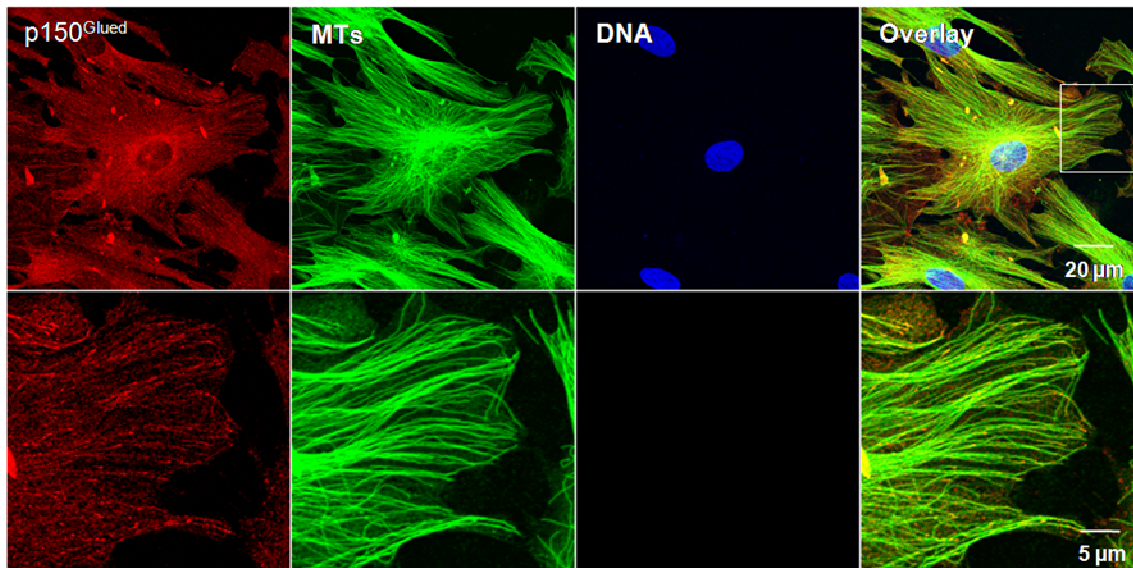
**Figure 44. +TIPs in the PHF model: ch-TOG and EB1.** ch-TOG and EB1 localization at the plus tips of the MTs. Analysis of the +TIPs comets using a mouse anti ch-TOG (or a rabbit anti EB1) and a rat anti  $\alpha$ -tubulin primary antibodies in confocal fluorescence microscopy images acquisitions. Superposition of the corresponding +TIP image (red) and the MT (green) demonstrate a co-localization at the tip of interphasic MTs that finally was used for measurement purposes. DNA staining was obtained using Hoescht 355 (blue).

An analysis of double staining indirect immunofluorescences for the most representative +TIPs proteins was produced: **EB1** (End Binding protein 1), **ch-TOG 5D12** (colon-hepatic Tumor Over-expressed Gene) (Fig. 44), **CLIP170** (Cytoplasmic Linker Protein) and **p150<sup>Glued</sup>** (the largest component of the dynactin complex) (Fig. 45).

(a)

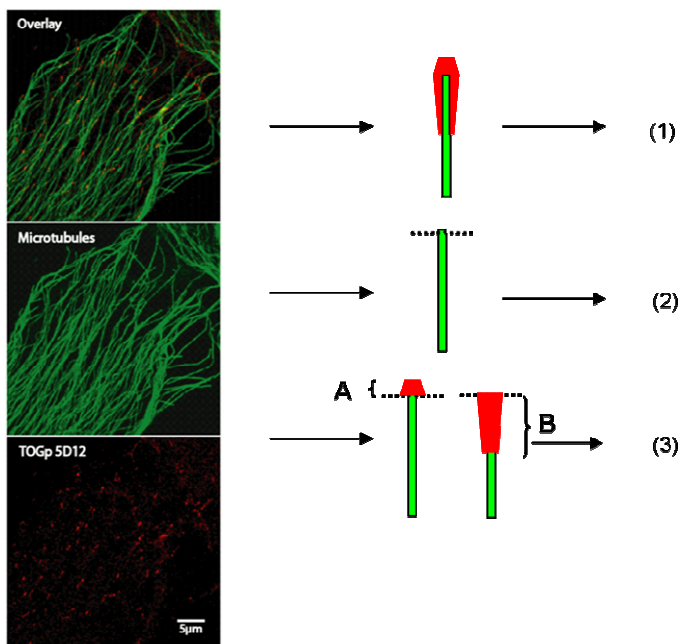


(b)



**Figure 45. +TIPs in the PHF model: CLIP170 and p150<sup>Glued</sup>.** Colocalization of **CLIP 170** (or **p150<sup>Glued</sup>**) and **MTs** in fixed cells. Analysis of the +TIPs comets using a rabbit anti CLIP170 (or a mouse anti p150<sup>Glued</sup>) and a rat anti  $\alpha$ -tubulin as primary antibodies. Confocal fluorescence microscopy images where the final superposition corresponds to +TIP image (**red**) and the MT (**green**,) demonstrating a colocalization at the tip of interphasic MTs. DNA staining was obtained using Hoescht 355 (**blue**).

As showed in the **figure 46** a double staining of confocal microscopy image was chosen. First, a MT was selected at high magnification (1). Then, the tip of the MT was established as the point zero of the measurement (2). At that point, each one of the regions (A, forward length) and (B, back length) of the comet was measured (3), and finally the size of the comet was calculated.

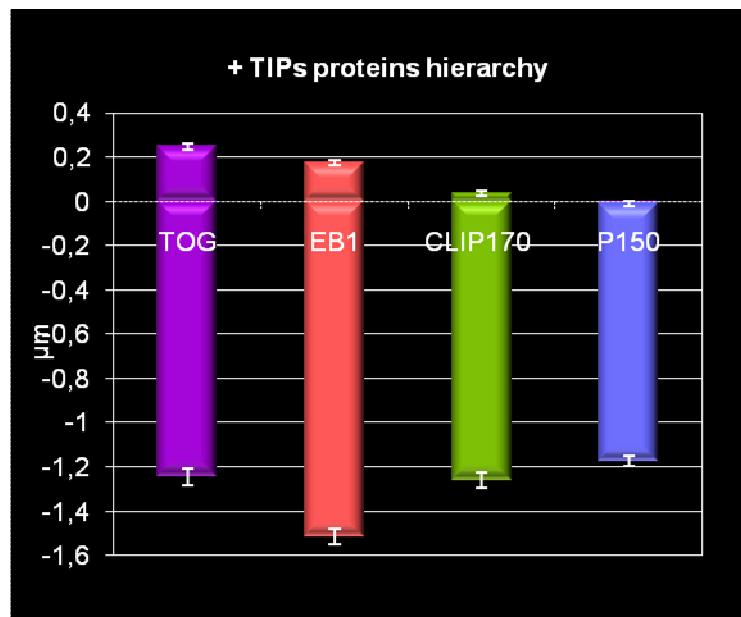


**Figure 46. Analysis method of +TIP “comet-like” structure.** Forward length comet (A), back length comet (B). ch-TOG (red); MTs (green). Methanol fixed PHF image. Scale bar 5 µm.

#### 6.2.4 XMAP215/ch-TOG is at the top of the +TIPS hierarchy. Our plus end complex hypothesis

The +TIPS proteins hierarchy was established: ch-TOG presents the most distal localization in comparison to the other MTs +TIPS proteins analyzed in the fixed PHF confocal images (**Fig. 47**).

Based on the MT tip as the point zero of the measurement we could establish the + TIP hierarchy. The comet-like structure for the four analyzed proteins present a sequential conformation at their forward length (the part of the comet who remains tubulin free), been **ch-TOG** the most distal comet of all the +TIPS analyzed.



**Figure 47. +TIPs proteins hierarchy.** ch-TOG localization in comparison to the other MT +TIPs proteins. Analysis realized from indirect IFs double staining (+TIP protein vs. MT) for the following proteins: **ch-TOG**, **EB1**, **CLIP170** and **p150<sup>Glued</sup>**. The tip of the MT is identified by the point zero of the scale. Same results were obtained analyzing triple staining images (ch-TOG, EB1 and MTs. Data not shown). Confocal images analysis of images realized using METAMORPH and LEICA confocal software simulator.  $\mu\text{m}$ , micrometer.

**Ch-TOG** 5D12 comets exceed the MT tip by  $0.24\mu\text{m}$ ,  $0.07\mu\text{m}$  more than the average measurements obtained for EB1. For each protein, the analysis was realized for at least 100 MTs tips in a random selection.

Confocal microscopy analysis of the fixed PHF + TIPs comets revealed an average comet length of  $1.1787\mu\text{m}$  (**Table X**). After our measurements, **p150<sup>Glued</sup>** is the + TIP protein that remains below the MT tip limit ( $-0.0098$  to  $-1.1621\mu\text{m}$ ), remaining logical considering that is a molecular motor that is able to “move on” the MT structure. Then, and above the MT tip **p150<sup>Glued</sup>** is followed sequentially by **CLIP170** ( $0.037$  to  $-1.26\mu\text{m}$ ), **EB1** ( $0.17$  to  $-1.51\mu\text{m}$ ) and finally by **ch-TOG** with a MT tip localization among the  $0.2472$  and  $-1.2445\mu\text{m}$ .

This +TIPs comet hierarchy could be the result of highly selective protein-protein interactions turning around a common objective: the tubulin dimmers addition and even the MT sheet closure mechanism could be implicated.

<b>+ TIP protein</b>	<b>Forward length (<math>\mu\text{m}</math>)</b>	<b>Back length (<math>\mu\text{m}</math>)</b>	<b>Total length (<math>\mu\text{m}</math>)</b>	<b>n</b>
<b>ch-TOG</b>	0.2472	-1.2445	0.9973	110
<b>EB1</b>	0.1760	-1.5148	1.3388	139
<b>CLIP170</b>	0.0370	-1.2627	1.2257	102
<b>p150<sup>Glued</sup></b>	-0.0098	-1.1621	1.1531	117
<b>Average</b>	0.1175	-1.2960	1.178725	117

**Table X. +TIPs comets lengths.** 468 MTs tips were random selected in a double staining image (MTs vs. +TIP protein) of fixed PHF. Measurements were made using the Leica confocal software.  $\mu\text{m}$ , micrometers; n, total number of MT tips analyzed for each protein.

All plus-end proteins so far identified have different microtubule-binding-domains (**CH** domain for EB1, **CAP-Gly** domain for CLIP170 and p150<sup>Glued</sup>) as part of a final and very well composed strategy: to be targeted to MTs. It has been demonstrated that each protein can provide a support surface for tubulin dimers, add the tubulin dimers to the structure and interact among each other to join the MT growing end.

In the case of **XMAP215/ch-TOG** multiple MT binding sites have been described. Two binding regions have been described, a first one (aa ~250 to aa~800) that presents a moderate MT affinity ( $\sim 2\text{-}5 \mu\text{M}$ ), and a second one (aa ~1,150 to ~1,325) with a high MT binding affinity ( $< 1 \mu\text{M}$ ). Also a centrosome targeting domain (aa~1,850 to aa ~1,950) represent crucial elements for the mechanism underlying preferential MT plus end targeting that provide one protein with many tubulin affinities in an independent way.

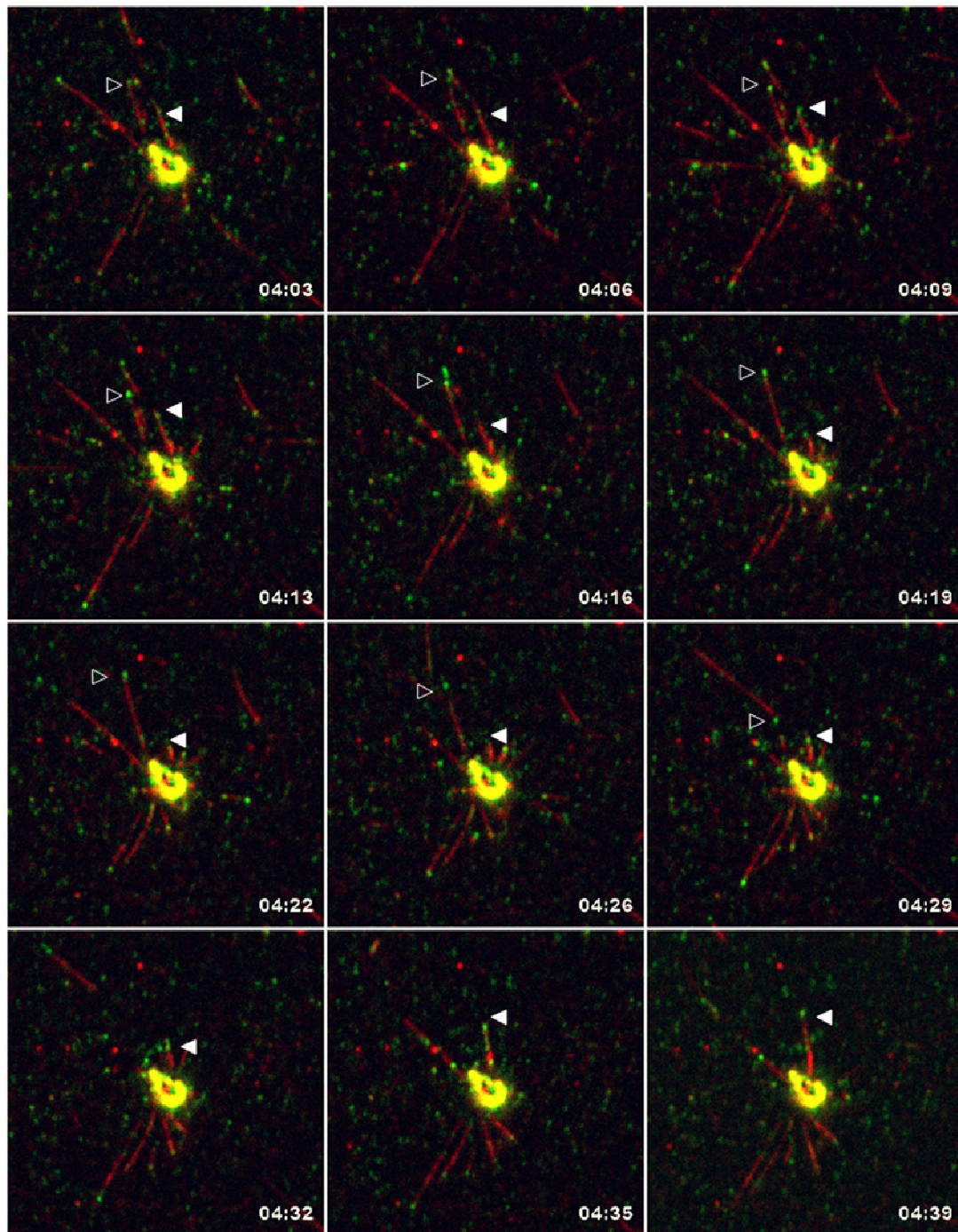
XMAP215/ch-TOG has been identified as a + TIP protein, present in fixed cells and even most important: it is the most distal + TIP protein among the analyzed + TIPs proteins. The nature of its + TIP conformation and exact activity remains unknown, but the ch-TOG most distal localization suggests that this population is directly implicated in the MT growing and stabilization.

We have identified so far two XMAP215/ch-TOG populations: the **MT-XMAP215/ch-TOG (4B6 mcAB)** and the **+TIP XMAP215/ch-TOG (mcAB 5D12)**. To explain the two identified staining we hypothesize that: **(1)** XMAP215/ch-TOG modifies its conformation in the presence of soluble tubulin and/or adopts a specific conformation at the MT + TIP. **(2)** The XMAP215/ch-TOG populations at the + TIP and on the MT lattice present a different conformation, product of a post-translational modification. **(3)** The interaction with other proteins (other than tubulin) could change the XMAP215/ch-TOG conformation *in vivo*, without any molecular change. To confirm or deny our hypothesis we did choose to probe the existence of the XMAP215 5D12 conformation *in vivo*.

### 6.3 +TIP XMAP215 does exist *in vivo*

We use the Total Internal Reflection Fluorescence (**TIRF**) microscopy to determine the **+ TIP XMAP215** activity *in vivo*. The restriction of light only to the nearest region of the cover glass produces a background free image that facilitate the acquisitions in the egg extract preparation with a minimal background signal (Brouhard *et al.*, 2008; Asbury *et al.*, 2008)

For the *in vivo* experiments we produced Ni-NTA based asters in the *Xenopus laevis* egg extract. Ni-NTA beads saturated by XMAP215-his7 allowed MT nucleation (Popov *et al.*, 2002). Dual-color TIRF imaging was used to visualize MTs and the + TIP XMAP215 in one “composed image”. **MTs** were visualized adding **Cy3** labelled tubulin to the reaction (**red**) and the + TIP XMAP215 configuration was observed using the **5D12 mcAB** labelled by the **Atto-488** fluorophore (**green**).



**Figure 48. Astral MTs + TIPs in the egg extract are marked by mcAB 5D12- Atto 488.** Ni-NTA nucleated asters formed in the *Xenopus laevis* mitotic egg extract. MTs were visualized adding Cy3B labelled **tubulin (red)** and +TIP XMAP215 is identified using the **5D12-Atto488** labelled mcAB (**green**). Time lapse video showing the XMAP215 + TIP presence at the tip of mitotic MTs. **+TIP XMAP215** conformation is present during MT **polymerization**. Surprisingly, the + TIP XMAP215 is also present at the tip of **depolymerizing** MTs. Fulfilled and empty arrow heads show two examples of the observed MT dynamics, each MT can go from polymerization to depolymerization processes. Scale bar 20  $\mu$ m.

The two colours microscopy assay visualization of **MTs** (red)/ **XMAP215** (green) interaction showed a XMAP215 detected by the 5D12-Atto488 antibody at the tip of **growing** mitotic MTs. Surprisingly, 5D12 -Atto488 also detects the same + TIP XMAP215 configuration at the tips of **shrinking** MTs (**Fig. 48**). The fulfilled arrowhead and the empty arrowhead follow two different MTs that go through polymerization-depolymerization states.

+TIP XMAP215 identified by the mcAB5D12-Atto488 produce a traceable signal at the MT tip during their polymerization and depolymerization states.

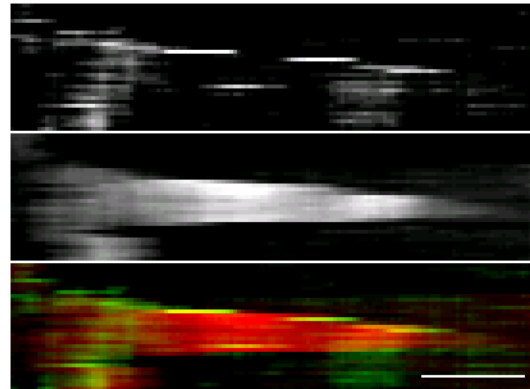
#### **6.4 XMAP215 is a travelling protein. From the tubulin dimer addition at the MT + TIP trough the controlled depolymerization?**

The Presence of XMAP215 is confirmed at the tip of a polymerizing and depolymerizing MTs. Produced kymographs were the final optical microscopy evidence of the XMAP215 presence at the tips of growing MTs.

We used two approaches for our FRAP acquired time lapse videos. **First**, two colour images (**MTs**-red, **XMAP215**-green) were produced at an interval of two seconds with an exposure time of 300 ms each one. The resulting sample consisted of 256 MTs from Ni-NTA based asters in the *Xenopus laevis* egg extract. In the obtained two colour images 92.18 % of the analyzed MTs showed a 5D12-Atto488 **traceable signal** at the **growing** and **shrinking** tip of the MT (**Fig. 49**).



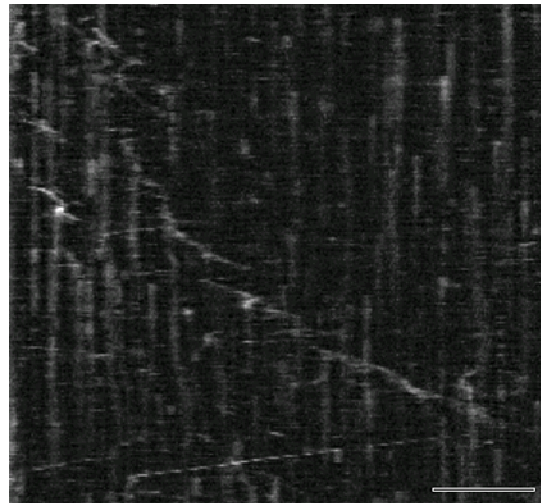
**Figure 49. +TIP XMAP215 presence is confirmed at the +TIPs of growing MTs in the mitotic egg extract.** Kymograph representing the +TIP XMAP215 (green) and MT (red) in a 0.3 seconds acquisition in a 2 seconds time interval. +TIP XMAP215 is traceable at the tip of polymerizing and depolymerising MTs. Scale bar 5  $\mu\text{m}$ .



In a **second** approach, a single colour and faster acquisition was made. This time the acquisition for 5D12-Atto488 signal was made at 300 ms interval each. Kymographs from 236 MTs were analyzed confirming the + TIP XMAP215 presence at the + TIP of growing MTs in 216 of them (**Fig. 50**). Under our experimental conditions MTs polymerize at 11.826  $\mu\text{m}/\text{sec}^{-1}$ , being an average speed for the previous MT polymerizations reports. On the contrary, the MT depolymerization speed obtained is 47,34  $\mu\text{m}/\text{sec}^{-1}$ ; being almost 4 times faster than the previous reported average (Tournebize *et al.*, 2000; Tirnauer *et al.*, 2004).

Is the increasing speed in the depolymerization mechanism induced by our mcAB-XMAP215 complex? The mcAB emplacement at the XMAP215 C-terminal domain could perturb the possible XMAP215/MT interactions. This possibility could be taken in to account if we keep in mind the fact that the possible interactions described previously for other +TIPs are a kind of chain-reaction: the **N-ter** region of one +TIP protein interacts with the **C-Ter** region of the next one, our mcAB placed at the C-terminal region could block the possibility of new protein interactions.

**Figure 50. +TIP XMAP215 its part of the *in vivo* depolymerization mechanism.** Kymograph obtained from a line drawn over a single MT trajectory. The Ni-NTA based aster in the mitotic egg extract in a time lapse microscopy acquisition. 300ms single colour acquisition for **5D12-Atto488** mcAB. Scale bar **10  $\mu$ m**.

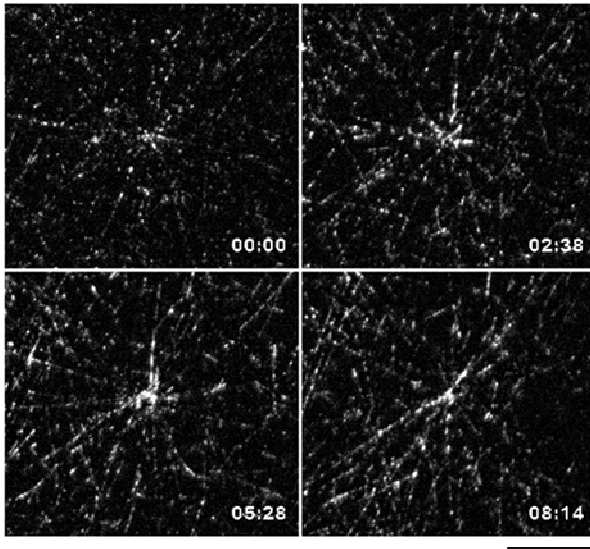


The XMAP215 constant presence during the growing events shows a molecule being an active part of the polymerization mechanism at the + TIP of the MT. The surprisingly presence of XMAP215 during the shrinkage events, shows not only a molecule that has already a polymerization activity, but also can have a key localization during the depolymerization process. This mechanism could provide a MT depolymerization process in a “MAP controlled” way.

Taken together these results indicate that **+ TIP XMAP215** conformation does exist *in vivo* and it is present during the **polymerization** and **depolymerization** of MTs in the mitotic *Xenopus laevis* egg extract.

## **6.5 XMAP215 travels from the mitotic + TIP to the lattice of interphasic MTs. Is XMAP215 a multi-task protein?**

As the *Xenopus laevis* mitotic egg extract becomes an interphasic egg extract, we observed the 5D12-Atto488 “evolution” pattern from a highly dynamic dot signal (**Fig. 49**) to a stable MT staining pattern signal (**Fig. 51**). This observation could indicate the + TIP XMAP215 arrival to the MT + tip to finally become a constitutive MT component. Are we watching the XMAP215 transformation from the +TIP XMAP215 to a microtubular form of XMAP215?



**Figure 51. XMAP215 travels with the tubulin polymer.** As the mitotic *Xenopus laevis* egg extract became an interphasic egg extract, the XMAP215 pattern changed. The pointy dynamics dots changed for a stable and “microtubular” signal with the 5D12 Atto488 mcAB. The possible biological or mechanical objectives of this XMAP215 evolution remain to further analysis. The main question that remains is what would be the biological purpose of this mechanism?, is structural/mechanical or functionally related? Scale bar 20 $\mu$ m.

As the cell cycle goes on, the XMAP215 localization may possibly evolve from the mitotic and highly dynamic +TIP XMAP215 to a final interphasic MT XMAP215. This observation could explain the XMAP215 “pointy” behaviour observed on the MT colocalizations in the interphasic fixed cells.

## 6.6 XMAP215-MT interaction does exist *in vitro*. Cosedimentation essay

A configurational change made by +TIP XMAP215 in response to the tubulin dimers presence have been considered to be at the origin of the 5D12 epitope expression. We created the *in vitro* cosedimentation test for the developed mcAB in the presence or absence of XMAP215, free tubulin or pre-assembled MTs.

In a **first** approach, the XMAP215 configurational modification as the result of the tubulin dimers loading was studied. An *in vitro* pull-down reaction took place using the two possible sensors of the differential conformation: **5D12mcAB**, allowing the identification of the **+TIP XMAP215**; and the **4B6 mcAB**, identifying the **MT-XMAP215**. XMAP215 charged with its tubulin cargo was recognized and captured by the mcAB adsorbed to paramagnetic protein A beads.

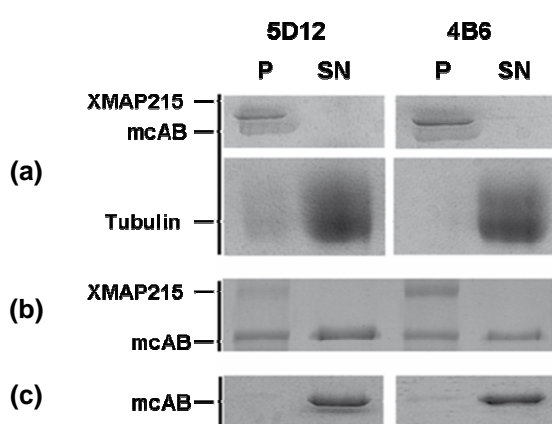
A **second** possibility considered a selective XMAP215 conformation acquired only when it is actively being part of the MT structure. With this purpose the mcABs adsorbed to protein A beads were incubated in the presence of a pre-incubated mix of XMAP215-his7 and pre-formed taxol stabilized **MTs**.

We have found that the 5D12 and 4B6 mcAB identify the XMAP215-his7 charged by tubulin (**Fig. 52a**). Also, the two produced antibodies recognize the recombinant XMAP215 epitopes once the XMAP215 is present on the surface of pre-assembled MTs (**Fig. 52b**).

We did not identify any difference among the amount of 5D12 mcAB or 4B6mcAB that recognize the growing + end or the MT lattice it self. If the XMAP215 recognized epitope would be available only at the conformational change, the amount of pelleted **+ TIP 5D12 mcAB** would be inferior to the

amount of **MT- 4B6 mcAB** recovered due to its preferential presence at one place or the other on the MT surface.

In a MT absence, the mcABs remains in the supernatant, eliminating in this way its presence in the pellet as an artefact. XMAP215 do not pellet in absence of MTs, the interaction XMAP215- taxol stabilized MT is specific (Spittle *et al.*, 2000).



**Figure 52. Cosedimentation assays of XMAP215-his7 using the mcAB 5D12 and 4B6.**

Protein A beads mcAB saturated recognize identify the tubulin charged XMAP215 **(a)**. The mcAB 4B6 and 5D12 recognize the XMAP215 present on taxol stabilized MTs**(b)**. Control showing that in the MTs absence, the mcAB 4B6 and 5D12 remains in solution, in the supernatant (SN) **(c)**. SDS PAGE electrophoresis in absence of 2-Mercaptoethanol, IgG migration in one 150 kDa band. 6% SDS-PAGE gel coomassie blue stained.

In the pure tubulin or MT conditions, recombinant XMAP215 is capable of binding taxolized MTs, as described previously for ch-TOG (Charrasse *et al.*, 1998; Gard *et al.*, 2004). Both mcAB identify the XMAP215 epitopes indiscriminately, when XMAP215-his7 is charged by tubulin dimers or when XMAP215 localizes on the MTs lattice. The obtained result probes that the XMAP215 and the exposed epitope that produces a differential conformation is not the result of a XMAP215-tubulin or XMAP215-MT interaction.

Our results reinforce the possibility that the distinctive epitope conformation identified by the +TIP XMAP215 is the product of a posttranslational modification mechanism, or the result of its interaction with other proteins.

## 6.7 XMAP215 and the MT ultrastructure

### 6.7.1 XMAP215 builds differentially the MT tip

Our previous results indicated the XMAP215 activity and presence at the tip of growing MTs *in vivo*. To explore the XMAP215 structural activity on the *in vitro* MT tip architecture, we used the transmission electron microscopy and the cryo-electron microscopy (**cryo-EM**).

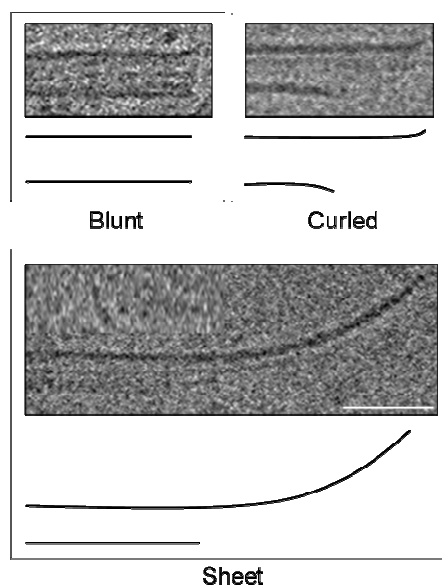
The potential architectural effects at the MT tips permit to associate them to the growing MTs + ends, or to the transitional events among growing and shrinking. This ultrastructural MT behaviour has giving origin to the theory by which the MT and its 13 protofilaments GTP-capped, could have growing and shrinking protofilaments at the same time (van Buren *et al.*, 2005). Arnal and collaborators in 2004 proposed a MT TIP classification, giving origin to the following categories: **blunt ends**, **curled ends** and **sheets** (Fig. 53). We adopted this classification for our images analysis.

The **blunt end** conformation has characteristically straight protofilaments that terminate simultaneously, producing flat ended MT tips. The blunt ends are considered to be metastable pausing ends; they are in transition among shrinkage or growth, depending on the cell circumstances (Zovko *et al.*, 2008).

The **curled end** MT tip corresponds to a combination of sheet and blunt conformation, is the transition among them. The curled structure has a straight extension and a curved part that extends away from the MT axis. These two different extensions give origin to short and lightly curved MT tips. The splayed protofilaments undergoing the MT rapid shortening (GDP-tubulin, the short and curved protofilament) (Chrétien *et al.*, 1995; Zovko *et al.*, 2008).

Finally, the **sheet conformation** presents a deep curled curvature of protofilaments, producing deep curled MT tips. This conformation has been found to be associated with the MT growth *in vitro* and *in vivo* in cryo-EM

studies (Chrétien *et al.*, 1995; Zovko *et al.*, 2008). These sheet-like structures are thought to represent MTs undergoing elongation (GTP-tubulin, the sheet structural side).



**Figure 53. MT ends in cryo-EM.** Three different structures were studied in our analysis data: blunt, curled and sheet ends. **Blunt** ends are associated to pausing ends, in contrast to the **sheet** ends described as part of the MT growing mechanism. The curled end are considered as a transition among the other two (Zovko *et al.*, 2008; Vitre *et al.*, 2008).

For our **primary approach** we evaluated the **XMAP215-his7** activities as part of the MT polymerization process, **tubulin** polymerization took place in presence of XMAP215. The resultant structures of the tubulin dimers/GTP/XMAP215 interaction produced two predominant phenotypes: **blunt** and **sheet** end conformations (39.7 and 40.4% respectively). The curled conformation (the transition among the other two structures) remained stable with a  $\approx 20\%$  expression for all the conditions analyzed (**Fig. 54**).

In a **secondary** approach the **XMAP215-his7** activity on the tip of preformed **MT** was evaluated. The obtained conformations from the MT/GTP/XMAP215 produced one predominant phenotype: the **sheet** ends (49.6%). This time the sheet ends acquired an enormous importance, being almost twice more expressed than the same structure in the control (22.9%) (**Fig.54**). After the XMAP215 localization at the MT tip using the fluorescent

microscopy, the Cryo-EM results might possibly allow us to hypothesize that the tubulin dimer addition is the objective.

The MT Tip structure results obtained for our *in vitro* cryo-EM are comparable to the MT Tip structures founded previously in the periphery of interphasic 3T3 cells. For our *in vitro* cryo-EM conditions, and counting on the growing MT tip population, we reach a **60.3%** of curled and sheet structures for the **tubulin+XMAP215** group and **69.8%** of the same structures in the **MT+XMAP215** group, with a 43.6% obtained for the control (**Fig. 54**). In the cryo-EM analysis on 3T3 cells, Zovco (2008) founded a **63%** expression of growing MTs (**curled and sheet structures**) in an area 2-5  $\mu\text{m}$  away from the cell border, a finding that shows the preferential presence of this conformation in the *in vivo* condition, in regions where the cell architectural changes are required the most.

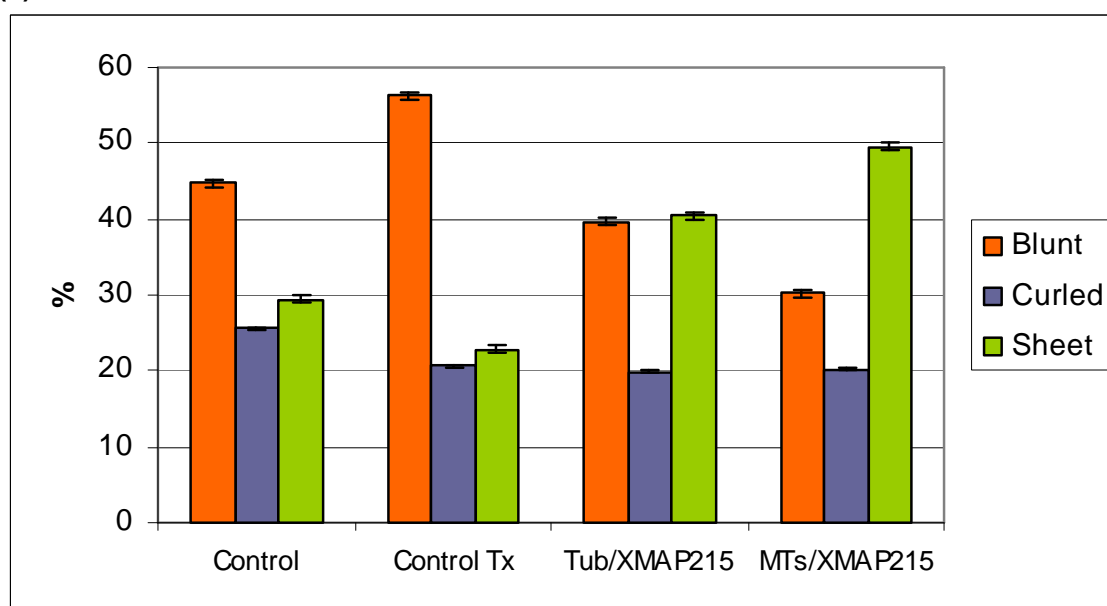
The observed transition at the MT end shown the evidence of the XMAP215 activity at the MT tip, delivering the tubulin dimmers. The preferential presence of sheet conformation could be associated to the MT elongation mechanism, through the addition of the predicted 60nm length protofilament-like structures at the MT growing end. Also, MT ends produces sheet lengths (distance between the long and short side of the MT lattice) and angels differently in each one of the tested preparations: one in presence of XMAP215 during the MT polymerization and another one, where XMAP215 was allowed to be active in presence of pre-polymerized MTs, at the very TIP of the growing MT.



(a)

MT tip type	Tubulin	Tubulin Tx	Tubulin + XMAP215	MTs + XMAP215
<b>Blunt</b>	44.8% (47)	56.3% (76)	39.7% (66)	30.2% (82)
<b>Curled</b>	25.7% (27)	20.7% (28)	19.9% (33)	20.2% (55)
<b>Sheet</b>	29.5% (31)	22.9% (31)	40.4% (67)	49.6% (135)
<b>MT tips analyzed (n)</b>	105	135	166	272

(b)



**Figure 54. MT tips conformation at the cryo-electron microscopy.** (a) Quantification of tubulin/XMAP215 or MT/XMAP215 activity at the tip of *in vitro* polymerized MTs. As control conditions we used tubulin 20 $\mu$ M that was polymerized for 10 minutes at 37°C in presence (Tubulin-Tx) and absence (Tubulin) of taxol 10 $\mu$ M. We did not observed any changes in the MT tip sheet structures. A total amount of 678 MT tips were analyzed. (b) Diagram of the different MT tips conformations observed for the established experimental conditions.





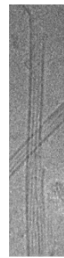

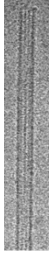
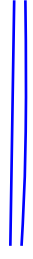


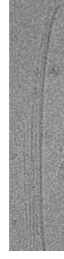
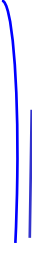




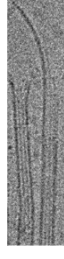




XMAP215 might be also involved in the MT sheet closure. The MTs that polymerized in the constant presence of XMAP215 show a more linear configuration at their growing ends (Fig. 55). The possible explanation to this phenomenon has been analyzed from the MT mechanical dynamics point of view. The tubulin-GTP polymerization into protofilaments would produce a

straight conformation structure, but once the GTP hydrolysis follows, the MT conformation would change to a curved form then, the MT would tend to shrink due to the lack of lateral contacts of the outer layer of protofilaments in the extension. Using this strategy, **XMAP215** could not only participate in the tubulin dimers addition, but also could facilitate and guaranteed the closure and **mechanical stabilization** of the new created structure (Jordan and Wilson 2004; van Buren *et al.*, 2005).

Even though the presence of sheet-like structures or splayed protofilaments can be considered as a probe of MT elongation, it can also be interpreted as a MT tip that is undergoing a rapid shortening event (Chretien *et al.*, 1995). The full length XMAP215 and its N-terminal fragment can promote disassembly of GMPPCP-stabilized MTs. The tips of GMPPCP MTs are blunt; representing MTs going through a paused state. Shirasu-Hiza, 2003 proposed a model where XMAP215 intervention provokes either growth or shortening, inhibiting the pause state. Using this mechanism, **XMAP215** could contribute to the two-three fold enhancement of the rapid shortened observed in its presence.

It remains unclear the directionality of the **XMAP215/ch-TOG** attachment to the MT lattice. We can think in two possible models. A first one the **longitudinal binding** model in which a XMAP215 binds along protofilaments. The second one is the **lateral binding model**, where a molecule of XMAP215 wraps around the MT structure (Gard and kirschner, 1987).

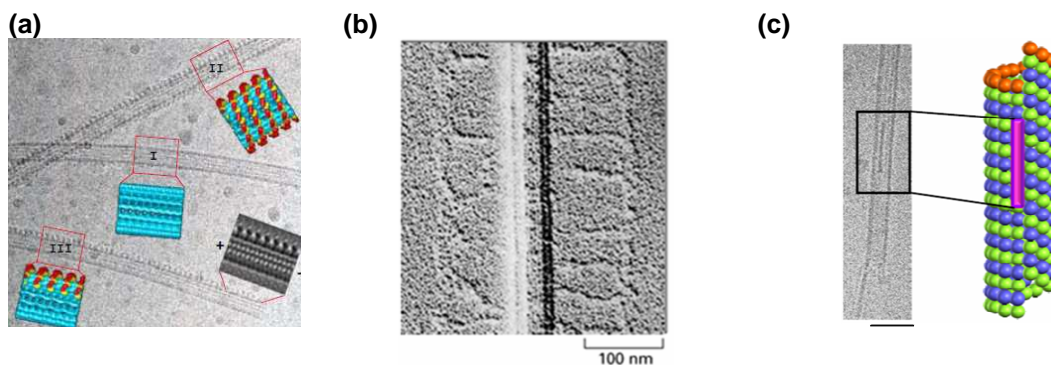
The **longitudinal binding model** could produce a double effect: a protofilament-like addition to the MT growing tip (tubulin dimers addition) and at the same time could provide an increased MT stability by strengthening the  $\alpha/\beta$  tubulin interactions along the protofilament. On the other way, the **lateral binding model** would provide a safer mechanism to prevent protofilaments separation (Al-Bassam *et al.*, 2002).

	Blunt ended tips		Curled ended tips		Curled sheet tips	
	Cryo-EM	Tr	Cryo-EM	Tr	Cryo-EM	Tr
Control						
Tubuline/XMAP215						
MTs/XMAP215						
Overlay						

**Figure 55. Cryo-electron images of MT tips and their trajectories.** MTs trajectory was traced on the images of each one of the different experimental groups analyzed. Overlay images shows the difference on the MT ultrastructure among the XMAP215 activity during polymerization (tubulin/XMAP215) and XMAP215 activity at the tip of MTs (MTs/XMAP215). **MTs**, microtubules; **Cryo-EM**, cryo electron microscopy; **Tr**, trajectory. 50 nm scale bar.

The theory that XMAP215/ch-TOG remains bounded in a longitudinal sense has been proposed previously and can fit our observations. In our cryo-

EM images we can observe a perceptible linear figure, of around 60nm length that is present in the images originated under the tubulin/XMAP215 conditions (**Fig.56**). If the final MT/XMAP215 pattern would be different, the final XMAP215 conformation would be traceable, as is the case for other MAPs



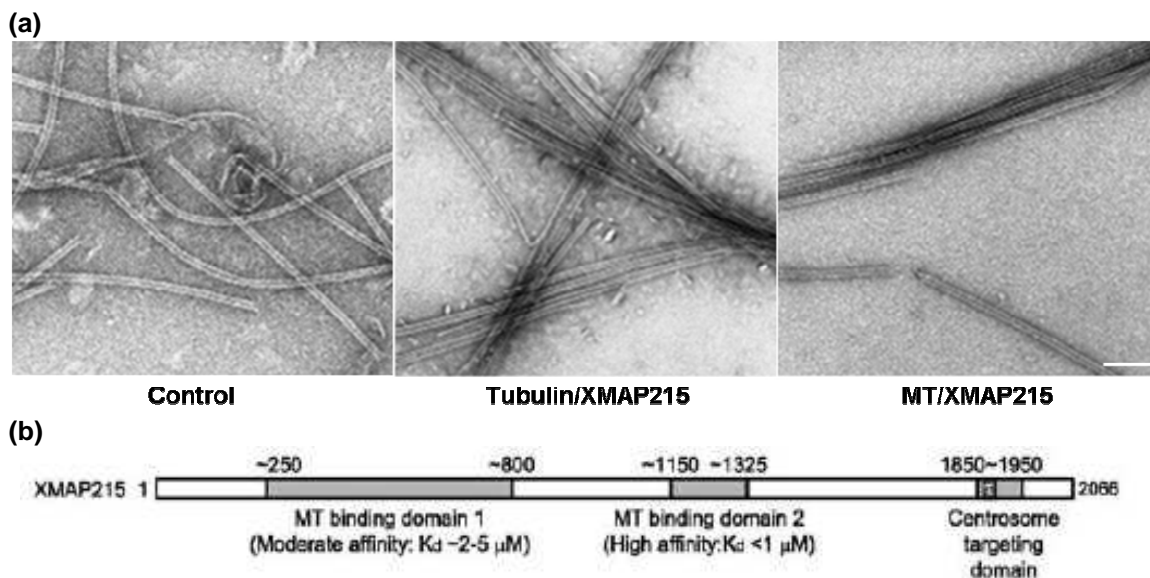
**Figure 56. XMAP215 longitudinal binding model.** Different cryo-electron microscopy images showing the patterns observed for some MAPs, relating their architectural association to the MT structure. **(a)** cryo-EM example of different MT binding patterns and the visual result of a kinesin effect on the MT structure. From Hoenger *et al.*, EMBL Research Reports 2001. **(b)** MAP2 cryo-EM and its lateral localization on the MT ultrastructure. **(c)** In our cryo-EM images obtained during the **tubulin/XMAP215** experiment it is possible to trace a 60nm structure on the MT surface. Scale bar 50 nm.

**Ch-TOG** is able to bind to protofilament rings and tubulin Zn-sheets, where the protofilaments are antiparallel, these results place ch-TOG along protofilaments on the MT lattice rather than circumferentially around them (Spittle *et al.*, 2000). If we keep in mind the activity of the protein and the different regions identified in it, it would be possible that the XMAP215/ch-TOG protein arrives to the MT lattice with a predicted orientation: the **C-terminal** region would be oriented to the minus growing end of the MT (a region of the protein that points the centrosome direction), leaving the **N-terminal** region directed to the MT growing end (Popov *et al.*, 2001). This sense of orientation is compatible with the fact that the XMAP215 N-terminal fragment has been considered to be responsible of growing (+) end and MT destabilization (Shirasu-Hiza *et al.*, 2003).

### 6.7.2 Does XMAP215 builds the MT lattice?

In negative staining observations single MTs were observed in the control reactions lacking XMAP215. In contrast, ordered MT bundles were observed after the addition of XMAP215 (Fig. 57a). The ordered nature of these bundles has been already associated as a possible XMAP215 longitudinal interaction with the MTs (van Buren *et al.*, 2002).

The association among the MT cross-linking and MT bundling by XMAP215 in electron microscopy has been observed previously. The answer could relay in the XMAP215 binding along the entire MT length, either longitudinally or circumferentially (Gard and Kirshner, 1987). Moreover, is a constant finding that at high stoichiometry, the full length XMAP215 is able to bundling MTs *in vitro* (Shirasu-Hiza *et al.*, 2003; Gard *et al.*, 2004)



**Figure 57. XMAP215 organizes MT into ordered bundles.** (a) Negative stained images of tubulin 20 $\mu$ M assembled in absence or presence of XMAP215-his7 0.4  $\mu$ M. From left to right control (tubulin 20  $\mu$ M/GTP); Tubulin polymerization in presence of XMAP215, **Tubulin/GTP/XMAP215** (center) and pre-polymerized MTs in presence of XMAP215 **MT/GTP/XMAP215** (right). Reaction samples were negatively stained with uranyl acetate and visualized by electron microscopy. Scale bar, 100 nm. (b) XMAP215 schematic model. XMAP215 might include two MT binding domains, potentially responsible for the MT bundling. Gard *et al.*, 2004.

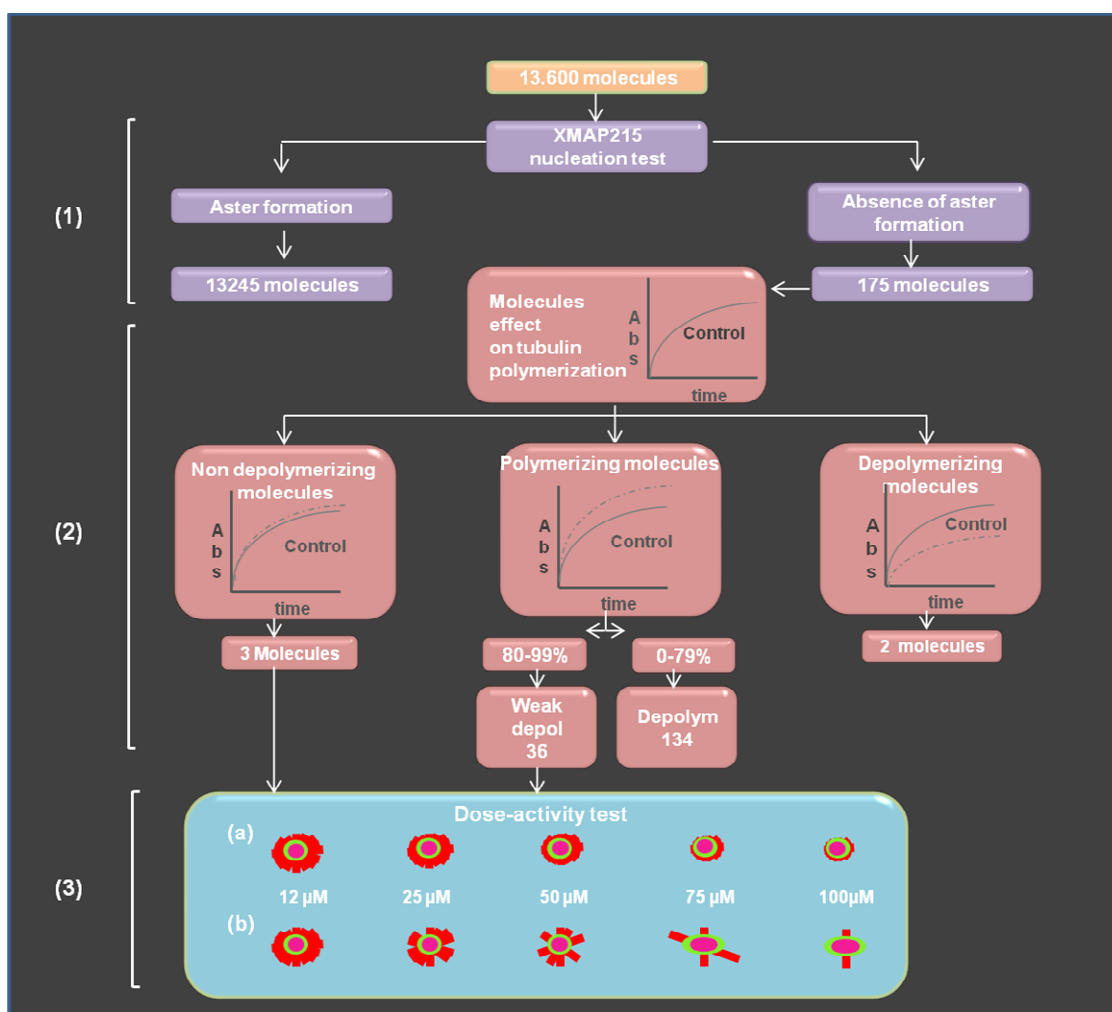
Other structural properties of XMAP215 using its 60 nm surface and directionality could include the development of several tasks: **(1)** permit the load of tubulin dimers, **(2)** bind MTs assuring the bond among protofilaments and **(3)** target the molecule to the cell centrosome. These activities could be given by structural properties that could make of XMAP215 a linear protein. Some protein regions express a higher affinity for the MT lattice than the others, these regions are known as the MT binding domains. Based on their apparent dissociation constant ( $K_d$ ) of different XMAP215 fragments, two domains have been predicted. One would be contained in the N-terminal region, the **MT binding domain 1** correspond to aa ~**250-800** expressing a MT moderate affinity ( $K_d$  ~2-5  $\mu$ M, pI 8.45); and a second one, a central domain, the **MT binding domain 2** that binds MTs with a higher affinity at the aa ~**1,150-1,325** ( $K_d$  <1 $\mu$ M; pI 7.85); these domains are contained in a protein that co-sediments with MTs with a  $K_d$  of <1 $\mu$ M (Gard *et al.*, 2004). Additionally, a single centrosome-targeting domain (aa ~**1,850-1,950**) overlaps the Tau repeat (aa ~**1,866-1,863**) in the XMAP215 sequence (Popov *et al.*, 2001) (**Fig.57b**), a repeat that by itself is considered to be part of the centrosome targeting sequence (Gard *et al.*, 2004).

The multiple MT binding domains in XMAP215 could be responsible for the *in vitro* MT bundling in the electron micrographs, corresponding to the protein constitution itself, functionality and possible interactions.

## 6.8 XMAP215 inhibitors research, a screening approach

A XMAP215 inhibitor could provide a highly selective antiproliferative molecule, with a limited toxicity. Ch-TOG, its human homologue has been found overexpressed in several cancer forms. Thus, and taking into account their homology, XMAP215 is an innovative target and candidate in the battle against cancer. The potential inhibitor effect of the molecules on the MT nucleation XMAP215 activity was evaluated using a 14,000 molecules collection. **Figure 58** illustrates the general approach for each of the screening parts: **(1)** The MT nucleation on NiNTa beads by XMAP215-7his, **(2)** The effect

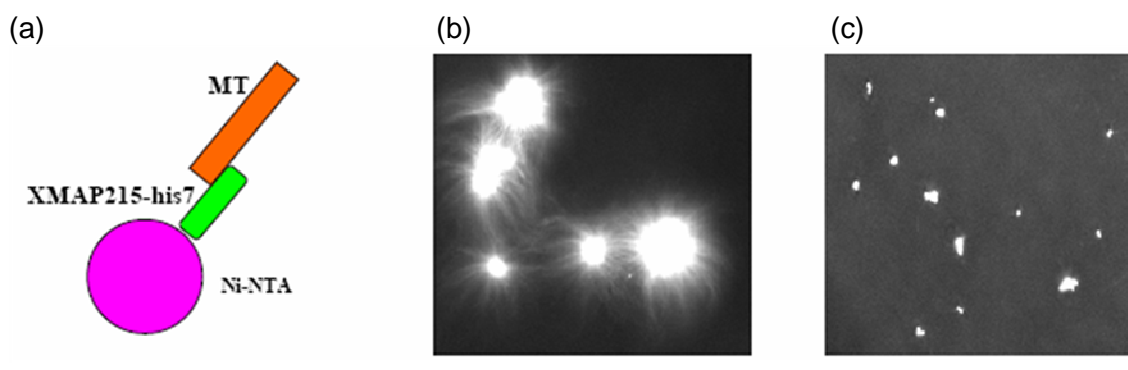
of the molecules in the tubulin *in vitro* polymerization and **(3)** the candidate molecules dose-activity test. In this last approach we considered the effect of a known molecule, the colchicine and the effect on the aster phenotype through depolymerization **(3a)**. In contrast, an XMAP215 inhibitor would influence the number of MTs anchored, this particularity would provide its pharmaceutical advantage **(3b)**.



**Figure 58. Screening approach general diagram.** Each one of the developed methods are illustrated **(1)** The MTs nucleation test. **(2)** In vitro tubulin assembly and **(3)** dose activity test. **(3a)** illustrates the effect of a known depolymerizant molecule: the colchicines; In contrast **(3b)** illustrates the expected effect of an XMAP215 inhibitor.

### 6.8.1 Screening first part: MTs Nucleation by immobilized XMAP215-his7.

The test explores the XMAP215 MT nucleation activity on the centrosome. In this case, centrosomes are replaced by Ni-NTA beads, limiting the molecule targeting to a one protein only.



**Figure 59. Aster Nucleation test.** (a) General diagram of asters formation from Ni-NTA beads charged by XMAP-his7; (b) aster formation after incubation and fixing is considered to be a negative result; (c) the absence of aster formation, is positive result. The positive selected molecules followed a second screening test. **Ni-NTA**, Nickel-Nitriloacetic Acid; **XMAP215-his7**, recombinant XMAP215; **MT**, microtubule. Scale bar 10 $\mu$ m.

Once the XMAP215-7his/Ni-NTA beads nucleation had taken place, the tubulin and the GTP were added to the reaction. The final result is a Ni-NTA based aster under control conditions. For experimentation conditions, the diluted sample of the molecule is added to the reaction previously cited; the ideal molecule would be able to produce a “blocking” effect of the XMAP215 MT nucleation activity.

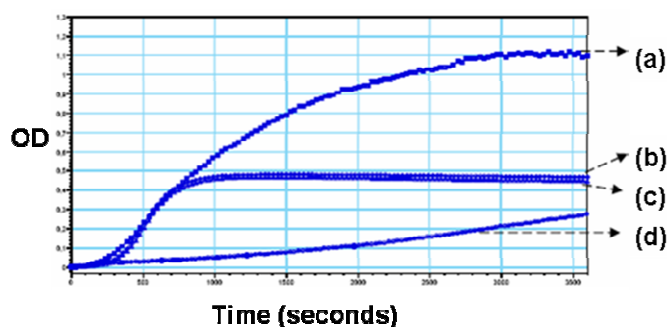
The developed test produced a positive result understood as the absence of aster formation. A total of 175 molecules were listed as potential XMAP215 inhibitors (**Fig.59**).



## 6.8.2 Screening second part: Molecules effects on the tubulin assembly

A possible activity on the tubulin polymerization could be behind the positive results obtained during the first part of the screening. In order to analyze the effect of the hits on the *in vitro* tubulin polymerization the second part of the screening was developed in absence of XMAP215-his7.

As the **figure 60** shows, the molecules present a well defined profile. A **stabilizing** molecule shows a maximal optical density (**OD**) of 1.1 in comparison to the control (0.45 OD) at 20 minutes of the test (800 seconds). A **depolymerising** molecule has a maximal OD of 0.28 after 60 minutes test without arriving to a stationary phase. In contrast, a **non depolymerising molecule** (having no effect on polymerisation) shows a similar OD to the one observed for the control (DMSO 4%).



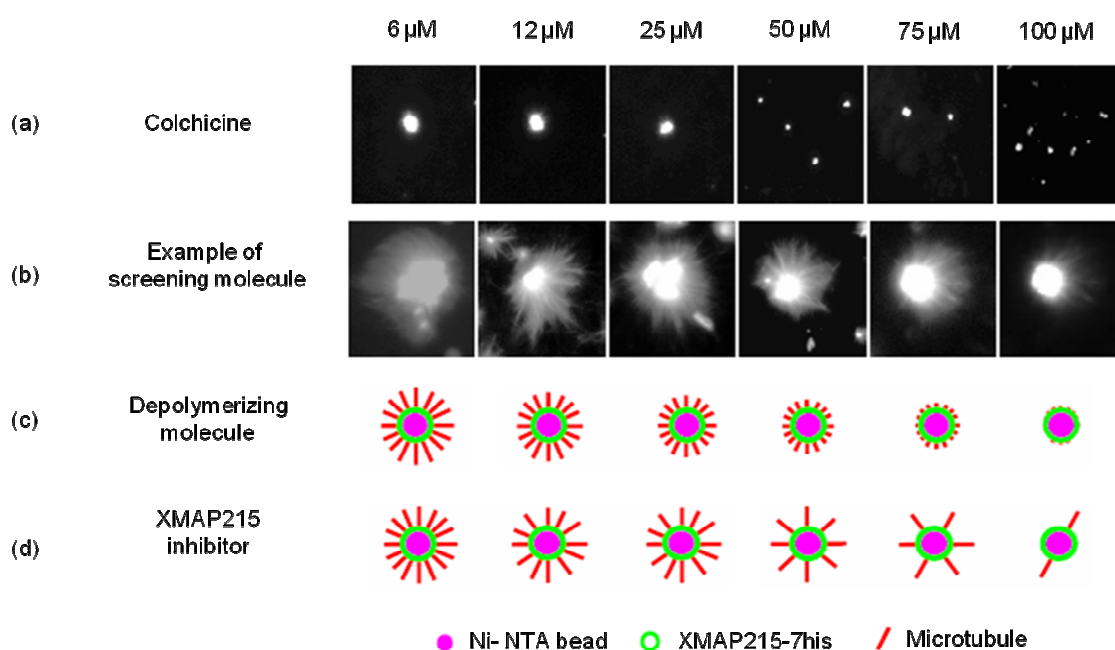
**Figure 60.** Example of the different effects of the molecules on tubulin assembly. (a), stabilizing molecule; (b), Control; (c), No depolymerising molecule in comparison to control; (d) Depolymerizing molecule,.

The kinetic test of *in vitro* tubulin polymerization allows us to classify the molecules having their effect on tubulin as a parameter. Three different groups of molecules were identified: No depolymerising, depolymerising and stabilizing.

### 6.8.3 Dose activity test and screening partial results: 3 stabilizing molecules and five depolymerizing molecules.

The dose-effect of the identified molecules allowed the establishment of the molecule concentration at which the molecule is active in the *in vitro* conditions. Colchicine was chosen as the control molecule in the test, as mentioned before no positive control is possible due to the lack of a reported XMAP215/ch-TOG inhibitor.

From the 14,000 molecules analyzed, we selected eight with an *in vitro* effect on the tubulin-aster formation (Fig-61). The resultant effect is far away of the predicted effect for an XMAP215 inhibitor, were the expected number of MT anchored by bead would be reduced as the concentration of the molecule rises.



**Figure 61. Dose - activity test for a candidate molecule (b) in relation to a known molecule such as Colchicine (a) at different concentrations. (c), Diagram of the effect of a depolymerizant molecule in comparison to an expected effect of a XMAP215 inhibition on its MT anchoring activity (d).**

The wished inhibiting effect on the MT anchoring to Ni-NTA-XMAP215-his7 complex was not found, however eight molecules shown an effect that could result of our future interest (Table. XI).

	Reference	Structure	Formula	<i>In vitro</i> effect	Similar compounds/ activity
DIVERSet™	305 (E8) 5312262		$C_{13}H_7Cl_3N_2O_2$ <b>Mw.</b> 329.57	MT weak depolymerizant	<b>No patents found for similar structures</b>
	304 (C6) 5312565		$C_{15}H_{13}ClN_2O_2$ <b>Mw.</b> 288.74	MT weak depolymerizant	<b>No patents found for similar structures</b>
	308 (G8) 5319234		$C_{14}H_{10}ClN_3O_4$ <b>Mw.</b> 319,71	MT weak depolymerizant	<b>No patents found for similar structures</b>
	309 (C08) 5319344		$C_{15}H_{11}BrN_2O_2$ <b>Mw.</b> 331,17	MT weak depolymerizant	<b>No patents found for similar structures</b>
	295 (C3) 5262768		$C_9H_5ClO_2$ <b>Mw.</b> 340,12	MT weak depolymerizant	<b>No patents found for similar structures</b>
Curie Institut	H09	Chemical structure protected by intellectual property law.	$C_{17}H_{16}N_2O_3$ <b>Mw.</b> 180,592	MT stabilizant	<b>Two patents found for similar structures. No activity reported.</b>
	G5	Chemical structure protected by intellectual property law.	$C_{22}H_{25}NO_3$ <b>Mw.</b> 347,4641	MT stabilizant	<b>Four patents found for similar structures. Teratogens, antineoplastic</b>
	G02	Chemical structure protected by intellectual property law.	$C_{17}H_{10}O_5$ <b>Mw.</b> 294,2663	MT stabilizant	<b>No patents found for similar structures</b>
Known anti proliferatives	Nocodazole		$C_{14}H_{11}N_3O_3S$ <b>Mw.</b> 301.32044 <b>NCBI ID :</b> 4122	MT depolymerizant, antimitotic agent (1990).	<b>Used in cell biology experimentation</b>
	Taxol		$C_{47}H_{51}NO_{14}$ <b>Mw :</b> 853.90614 <b>NCBI ID :</b> 36314	MT stabilizant, antineoplastic agent used in chemotherapy (1995)	<b>Synonyms: Paclitaxel-Mepha® Paclitaxèle "Ebewe"® Paxene® Taxol®</b>
	Colchicine		$C_{22}H_{25}NO_6$ <b>Mw.</b> 399.437 <b>NCBI ID :</b> 6167	MT depolymerizant, antineoplastic agent	<b>Synonyms: Nocodazole, Oncodazole, Nocidazole</b>

**Table XI. Screening final list of active chemical compounds.** Nine molecules of interest were selected after the *in vitro* test. Structure comparison was made using the NCBI data base. **MT**, Microtubule; **MW**, Molecular Weigth.

Further structural comparison among the molecules structure and the molecules collection contained in public data bases did not show any similarity to the known anti-neoplastic molecules found in the pharmaceutical market. However, the stabilizing effect of the molecules could be seen as a highly positive result, if we think on the secondary effects and high toxicity reported for the commercially available molecule: Taxol.

The detailed XMAP215 structure domain could be involved in the attempt to find an inhibitor, further results based on the cellular functionality of the XMAP215 molecule could allow us to improve the quality of our *in vitro* test itself. This *in vitro* test was developed to restrain the MT anchoring and/or tubulin polymerization.

The MT anchoring is guaranteed by the XMAP215 N-terminal domain, but the anchoring to the centrosome is guaranteed by the C-terminal domain XMAP215. An XMAP215/ch-TOG inhibitor should be targeted to its C-terminal region; using this strategy the selectivity of the molecule activity would be limited to the actively mitotic cells, leaving the interphasic cells untouched. Other technical considerations shall be taken in to account, such as the access and permeability of the cell membrane barrier, targeting mechanism to the centrosome and toxicity to the host.

## **DISCUSSION**



## DISCUSSION

The highly diverse and evolutionarily conserved MAP215/Dis1 family of related proteins has a well established root in the eukaryotes evolution. Based on their peptide sequences their evolution could be traced to the very origin of the eukaryotes differentiation. These proteins proved to be diverse enough to be distributed along the eukaryote “kingdom” going from the protists such as *Giardia lamblia*, *Entamoeba histolytica* and trypanosomes (*T. cruzi* and *T. brucei*) until the evolution tree reaches the *Homo sapiens*.

The so far characterized proteins of the XMAP215/Dis1 related family are **Saccharomyces pombe**, **Dis1** and **ALP14** (Garcia *et al.*, 2001; Nakaseko *et al.*, 2001); *Saccharomyces cerevisiae*, **Stu2** (Wang and Huffaker, 1997); *Arabidopsis thaliana*, **Mor1/Gem1** (Whittington *et al.*, 2001); *Nicotiana tabacum*, **TMBP200** (Yasuhara *et al.*, 2002); *Dyctyostelium discoideum*, **DdCP224** (Gräf *et al.*, 2000); *Caenorhabditis elegans*, **Zyg9** (Matthews *et al.*, 1998); *Drosophila melanogaster*, **MspS** (Matthews *et al.*, 1998); *Xenopus laevis*, **XMAP215** (Gard and Kirschner, 1987) and the *Homo sapiens*, **ch-TOG** (Charrasse *et al.*, 1995).

In 1987 Gard and Kirschner reported the isolation and preliminary characterization of a protein that exhibited the property to promote the elongation of MT plus-ends in centrosome-nucleated asters. This plus-end-specific, assembly-promoting factor from *Xenopus laevis* egg extract has been identified as a 228 kDa protein, having a 2065 amino acid sequence, the *Xenopus laevis* **XMAP215**. The importance of its activity has been proven through its depletion. Once 70% of the XMAP215 is removed from the egg extract, significant changes in MT lengths and catastrophe frequencies are produced (Tournebise *et al.*, 2000).

Years later, in 1995, Charrasse and collaborators reported the successful cloning and sequencing of cDNA encoding a human protein overexpressed in

tumors, during a screen for cytochrome p450. Thus, the XMAP215 human homologue had been described, the colon-hepatic tumor over expressed gene protein, **ch-TOG**. The gene was mapped on the short arm of the human chromosome 11, on the 11.2 band (11p11.2). The protein sequence is 1,972 aminoacids long, and posses a molecular weight of 218 kDa.

The characterization of the functional effects of these two proteins at the end of growing MTs has been established. **XMAP215** promotes MT assembly in an end specific manner: it increases the plus assembly rate approximately by **seven fold** while only increasing minus end assembly less than **two fold** (Gard and Kirschner, 1987; Vasquez *et al.*, 1994). In contrast, **ch-TOG** promotes faster MT elongation rates at both plus and minus ends by approximately **two fold** (Charrasse *et al.*, 1998).

Other functional effects have been taken in to account. For example, the addition of **XMAP215** to purified tubulin promotes of as much as a **10 fold increase in the rate of plus end elongation**, promotes two to three fold increase in the rate of rapid shortening, eliminate rescue, an do not suppress catastrophes (Vasquez *et al.*, 1994). XMAP215 is the only MAP (as a difference from other well characterized MAPs such as MAP2, MAP4 and Tau (Spittle *et al.*,2000) that is able to promote MT assembly at the plus end and increases their dynamic instability (Gard *et al.*, 1987; Cassimeris., 1993; Spittle *et al.*, 2000). However, **ch-TOG** can only **enhance by two fold the elongation rate** (Charrasse *et al.*, 1998), unfortunately complementary test to establish precisely the **ch-TOG** dynamics are not available considering the difficult technical approach.

But, what would be the reason to obtain such a different effect at the end of growing MTs for two proteins that share an 80% sequence identity? A few possibilities can be listed: For example, ch-TOG presents a less conserved C-terminal domain in comparison to XMAP215, and perhaps the difference in the



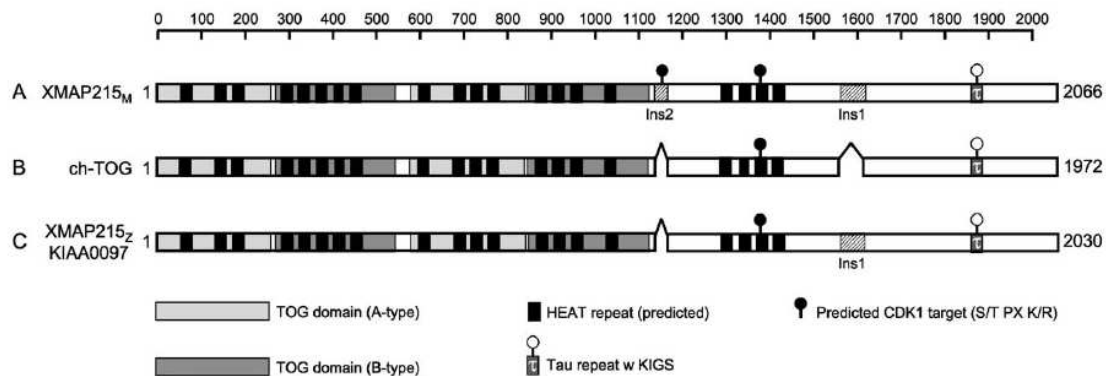
sequence could reflect a difference in the protein activity, a possibility already proposed by Gard in 2004.

Another remarkable difference among the two homologues is the **XMAP215** and **ch-TOG** proteins origin for the different experimentation test respectively. The **XMAP215** used for Gard and Kirschner in 1987 experiments was obtained from *Xenopus laevis* egg extract, a **mitotic** egg extract (with a heterogenic population of eggs arrested at different mitotic stages). However, the **ch-TOG** protein employed for Charrasse and collaborators in 1998 was purified from pig brains, clearly a **post-mitotic** tissue.

Structurally, these two homologues present a difference in the CDK1 predicted sequences. The ch-TOG single predicted target sequence for the CDK1-dependent phosphorylation (aa **1,361-1,364**) is located after the MT binding domain in the C-terminal region of the protein (for both ch-TOG isoforms, a and b) ([Fig. 62](#)). In contrast in the XMAP215 maternal isoform (**XMAP215<sub>M</sub>** - present in the mitotic egg extract), two predicted sites for the CDK1 phosphorylation are present, one at each side of the MT binding domain (aa **1,361-1,364** and **1,155-1,158**). It has been predicted that this second CDK1 target might play a role in regulating the function of XMAP215 during the rapid cell cycles of early *Xenopus* development (Gard *et al.*, 2004).

These differences take us right in to the cell cycle mechanism. Based on the structural information available, can we think that these proteins are able to have different activities on the MT dynamics upon the cell cycle?

One of the first theories concerning the **ch-TOG** activity was proposed by Charrasse *et al* in 1998. This report placed **ch-TOG** to the ER and spindle MTs and probed to find a high mRNA abundance in both non dividing tissues, i.e. Purkinje cells in brain tissue (Charrasse *et al.*, 1996) and tumors (Charrasse *et al.*, 1995), so at that time, it was already proposed that different ch-TOG functions could be dependent on the cell cycle.



**Figure 62. XMAP215/ch-TOG isoforms comparison.** Two isoforms have been reported for each homologue. The human **isoform a** (ch-TOG, 2032 aa) express the same insert (aa 1597-1656) than the frog **XMAP215<sub>Z</sub>** isoform, the zygotic form that is present later in the frog development. Both ch-TOG isoforms lack of a 36 aa insert (aa 1,136-1,171) present only in the XMAP215 maternal isoform (Gard *et al.*, 2004).

An **XMAP215** cell cycle-dependent regulated function has been also suggested. Gard and Kirschner established in 1987 that the protein is **hyperphosphorylated** during the **M phase** of the cell cycle. Additionally, the XMAP215 phosphorylation by **CDK1** *in vitro* reduces the assembly promotion without affecting MT binding (taxol stabilized MTs *in vitro*) (Vasquez *et al.*, 1999). Does that it means that the “assembly promotion” is assumed for a fraction of the XMAP215 population that is affected by the **CDK1** phosphorylation (described as a “*reduction of assembly promotion*”), while the other population fraction remains untouched (described as “*without affecting MT binding*”)? Are we facing the possibility of two **XMAP215** populations sharing the same sequence?

**XMAP215** and **ch-TOG** cellular localization has been subject of early studies since their very first reports. **ch-TOG** was localized to ER in interphasic cells and did not colocalize with MTs or centrosomes in interphase cells (Charrasse *et al.*, 1998). In contrast, **XMAP215** has been localized at the centrosome and interphasic network in cultured *Xenopus laevis* cells. However, both proteins share the same localization at the spindle pole and spindle MTs during the M phase (Tournébizet *et al.*, 2000; Popov *et al.*, 2001; Becker *et al.*, 2003; Gard *et al.*, 2004).

Further studies in the localization of the **XMAP215** related proteins have demonstrated the presence of some of the family members at the **+TIPs** of growing MTs. Imaging techniques have placed some of the XMAP215 orthologues at the MT +TIPs, it is the case for **MspS**, *Drosophila melanogaster* (Lee *et al.*, 2001); **Dis1**, *Schizosacharomyces pombe* (Nakaseko *et al.*, 2001); **Stu2**, *Saccharomyces cerevisiae* (van Breugel *et al.*, 2003) and **DdCP224**, *Dictoselium discoideum* (Herstermann and Graft, 2004). Also, *in vitro* the XMAP215 effects on MT dynamics have been an approach to its +TIP activity, because of its effects at the very tip of growing MTs in pure tubulin solutions (Gard and Kirshner, 1987; Spittle *et al.*, 2000). And finally, the XMAP215 expression in the *Xenopus laevis* early embryos, where it appears to be enriched at the MT + TIPs of interphasic blastomeres (Gard *et al.*, 2004).

Other approaches include the development of software-based simulators; these studies have placed XMAP215 in the MT + TIP environment, being part of a “guidance model effect”. Here XMAP215 joins the MT +TIP and furnish a surface to the tubulin dimers loading, at the same time it could provide support for longitudinal associations (van Buren *et al.*, 2005). Beyond these facts, the **XMAP215** localization at the growing MT tips *in vivo* has remained as a theory to be probed.

We have developed a set of **mcAB** anti **XMAP215**. The developed antibody recognizes an epitope contained in a region of the c-terminal fraction (aa **1,847-2,065**) of the XMAP215 protein. Its cross reactivity with other analyzed species has allow us to identify new cellular localizations for other members of the XMAP215 family members of proteins in fixed cells, such as *Xenopus laevis* (ATCC XL177, epithelial cell line), *Mus musculus* (ATCC 3T3, fibroblast) and *Homo sapiens* (Primary human fibroblast, PHF).

Images of fixed cells revealed the existence of two different **XMAP215 / ch-TOG** populations: Our confocal images have showed two populations that we denominate: “**microtubular XMAP215/ch-TOG**”, colocalizing with

**interphasic** MTs, and another one denominated “**+ TIP XMAP215/ch-TOG**” that localizes at the **growing end** of interphasic MTs. Additionally, the mitotic spindle in the mitotic cell and the centrosome in the interphasic cell are recognized by these antibodies.

XMAP215/ch-TOG is a protein that possesses a long list of potential activities. We can mention them in a non exhaustive list that could include: **MT regulators dynamics** (Spittle *et al.*, 2000; Tournebize *et al.*, 2000; Popov *et al.*, 2001; Kinoshita *et al.*, 2002), **tubulin addition** (Kerssemakers *et al.*, 2006; Slep *et al.*, 2007; Brouhard *et al.*, 2008), **RNA trafficking** (Kosturko *et al.*, 2005; Francone *et al.*, 2007), **MT nucleation to the centrosomes** (Popov *et al.*, 2002; Cassimeris *et al.*, 2004) and **spindle pole organization** (Gergely *et al.*, 2003).

Based on our fluorescence microscopy, electronic microscopy and TIRF results we will describe theories about the two different XMAP215/ch-TOG populations. We are interested in the possible biological interactions of each XMAP215/ch-TOG conformation; this strategy could produce a well coordinate biological activity going from the tubulin dimers addition to MT polymerization and MT structure, until its possible participation in cell translation.

## 7.1 XMAP215/ch-TOG, a new +TIP protein.

We have demonstrated the presence of a XMAP215/ch-TOG protein at the +TIPs of growing MTs *in vitro* and *in vivo*.

*In vitro* the images of fixed cells showed XMAP215/ch-TOG as the most distal protein at the MTs +TIP. The ch-TOG localization was compared not only with the MT growing end but also was compared to proteins such as EB1, CLIP170 and p150<sup>Glued</sup>. The XMAP215/ch-TOG structural localization could place its activity in the tubulin dimers addition as it has been suggested previously for other +TIP proteins (Arnal *et al.*, 2004; Vitre *et al.*, 2008; Coquelle *et al.*,

2009) or even could indicate the XMAP215/ch-TOG participation in the MT sheet closure (van Buren *et al.*, 2005).

The XMAP215 selective behaviour at the tips of MTs *in vitro* was probed through the observed changes in the MT tip architecture after our cryo-EM results. XMAP215 is able of speed MT elongation by delivering tubulin oligomers to the MT + end (Gard and Kirschner 1987; Spittle *et al.*, 2000). Additionally, the XMAP215 selective behaviour at the MT tips can be interpreted as an inhibition of the "pause" state, where it can be part of growing or shrinking mechanisms (Shirasu-Hiza *et al.*, 2003). Our results could support these XMAP215 model at the MT + TIP.

The cryo-EM revealed the *in vitro* MT tip ultrastructure as a result of XMAP215 activity. At the MT TIP XMAP215 form preferentially what we denominated a "sheet structure". We did not find any traceable XMAP215 (in terms of aggregates that could indicate the XMAP215 presence) at the TIP of growing MTs in any of the cryo-microscopy images, this observation make us thing that under the *in vitro* conditions XMAP215 is fully loaded by the tubulin dimers before joining the MT+TIP. These results could show the XMAP215 participation in the tubulin dimer addition only at the MTs very +TIP. This ultrastructural effect theory is contrary to other proposed theories previously where the XMAP215 activity is considered to be an antipause factor, where XMAP215 would deteriorate and/or prevent the MT sheet closure (Shirasu-Hiza *et al.*, 2003)

*In vivo*, XMAP215 showed to be present at the +TIP of mitotic MTs not only during MT polymerization but also during the MT depolymerization. In the egg extract system, the XMAP215 +TIPs comets probed to be dynamically exchanged from the +TIP of growing MTs. The specific XMAP215 conformation recognized by our 5D12 mcAB does exist *in vivo*. The +TIP XMAP215 conformation moves dynamically at the end of mitotic MTs perhaps playing an active role in the MT polymerization and depolymerization mechanism.

Several models can attempt to explain the mechanism involving the + **TIP XMAP215** activity. We have listed some models already proposed as an approaching theory to the tubulin dimers addition at the end of growing MTs.

A **first** model nominates that XMAP215 binds preferentially to the MT very end, providing a surface to the tubulin dimer addition along the 60 nm length of the molecule (van Buren *et al.*, 2005; Kerssemakers *et al.*, 2006) (**Fig. 63a**).

A **second** model, the “guidance model” was suggested. In this model XMAP215 binds to MTs and allows the tubulin dimer loading on the XMAP215 surface, been away from the leading edge of the MT tip (Gard and Kirschner, 1987; Gard *et al.*, 2004; Spittle *et al.*, 2000; van Buren *et al.*, 2005) (**Fig. 63b**). Along our cryo-EM experiments we did not observed any traceable “partially bounded” XMAP215 at the MTs +TIPs, as could be expected to support experimentally these first two models.

One **third** model proposes that XMAP215 is previously charged with its tubulin dimers cargo to finally deliver the complex at the growing tip of the MTs (Gard and Kirschner, 1987, van Buren *et al.*, 2005; Kerssemakers *et al.*, 2006), a model that fits with our *in vitro* observations due to the absence of a traceable XMAP215 on the MT images and the statistically significant changes on the tip conformation (**Fig. 63c**).

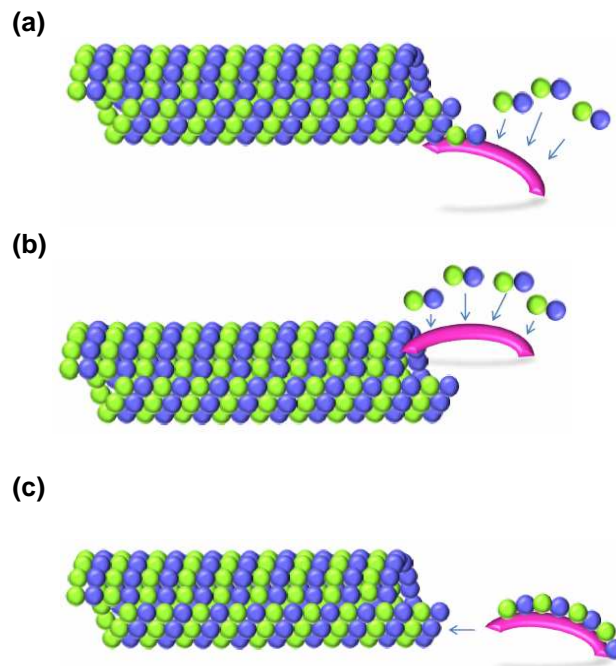
One **fourth** model has been proposed recently. Here the stoichiometry interaction among some of the XMAP215/Dis1 family members and tubulin has been studied. **Stu2**, the dimerized *Sacharomyces cerevisiae* XMAP215 homologue, is considered to be required for carrying one tubulin dimer (2:1). The same stoichiometry realized for XMAP215 is considered to be 1:1, where a XMAP215 protein would wrap the tubulin dimer with its first four TOG domains to accomplish the potential +TIP tracking. Using its MT binding domain

contained in its C-terminal region, the XMAP215 molecule delivers the tubulin dimer to the MT growing end. As the tubulin dimer is delivered, the protein releases itself from the MT structure and the mechanism becomes cyclic. It is considered to be a processive translocation along the MT (**Fig. 63d**) (Slep *et al.*, 2007).

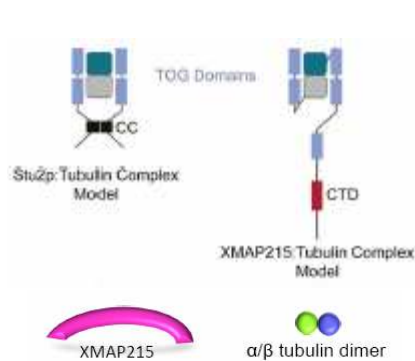
The processive mechanism contrasts with previous proposed XMAP215 activity models, where the protein would remain linear. This strategy could explain the polymerization-depolymerization characteristics reported for its remarkable *in vitro* activity. Our cryo-electron microscopy images did not show any traces of a XMAP215 being part of a processive created structure, our images show a processive XMAP215 molecules along the MT lattice and a XMAP215 that increases 3.5 times the sheet length when it is present during the tubulin dimers addition. A processive translocation would be traceable through the structure, and is not the case under our experimental conditions.

Based on our results and taking into account the proposed third XMAP215 activity model, the functionality mechanism could be provided by a polarized orientation due to the XMAP215 structural domains organization and length. XMAP215 is a long, flexible monomer with a contour length of ~60nm (Gard and Kirschner, 1987; Cassimeris *et al.*, 2001), with a predicted colinear structure thanks to a high HETA repeats content (Cassimeris *et al.*, 2001). This finding supports the XMAP215/ch-TOG colinear activity theory.

The **colinear interaction theory** among XMAP215/ch-TOG and the MT can be predicted from the absence of changes in the MT rigidity, when the polymerizations were realized in absence or presence of XMAP215. In contrast, the MT rigidity can be altered when the interaction includes the cross-linking among MAP-tubulin subunits of adjacent protofilaments. This is the particular case of MAP2, MAP4, and tau (Spittle *et al.*, 2000; Al-Bassam *et al.*, 2002).



**Figure 63. Different + TIP XMAP215 activity models.** XMAP215 activity has produced several activity models. **(a)** Free XMAP215 joins the MT growing end through its MT-binding domain near the C-terminus. Thus, the tubulin dimers are loaded on the entire XMAP215 surface. **(b)** XMAP215 joins the MT +TIP without following the MT leading edge. **(c)** XMAP215 uses its surface to load the tubulin dimers, finally joining the Mt leading edge. **(d)** Schematic proposed mechanism for some of the XMAP215/Dis1 family members, Stu2 and XMAP215 (Slep, 2010)



All these predictions are directed to produce activity models in an attempt to describe XMAP215 promotion of elongation. The potential list of activities could include among the +TIP activities: tubulin dimer addition, participation in tubulin oligomers addition, construction of protofilaments-like structures and participation in the construction, sealing and stabilization of the MT lattice. Also the destabilization of the MT growing end and rapid shortening promotion could be involved among its functions (Gard and Kirschner, 1987; Spittle *et al.*, 2000; Cassimeris *et al.*, 2001; Gard *et al.*, 2004).

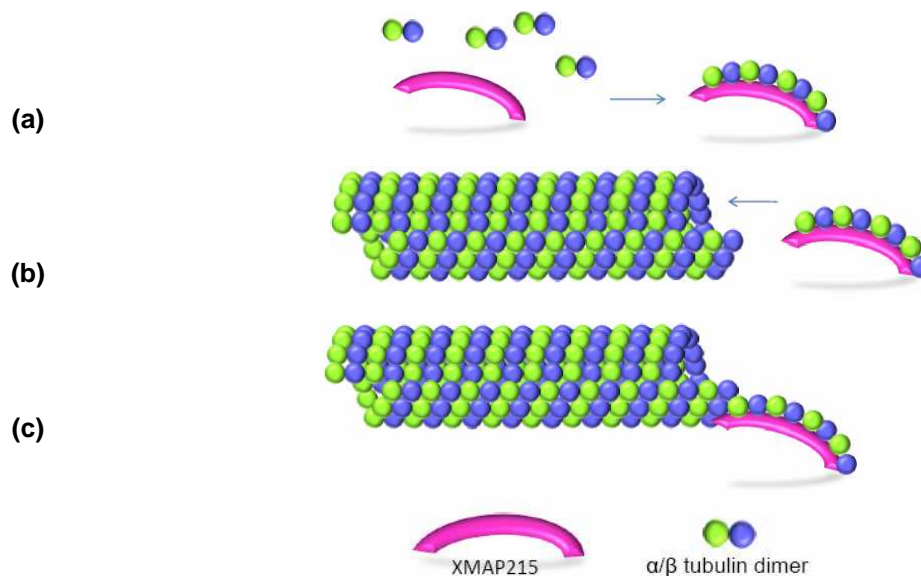
The XMAP215/ch-TOG experimental description as a 60 nm long molecule that is able to charge 6-8 tubulin dimers (Cassimeris *et al.*, 2001). This



finding fits with the experimental data were XMAP215 polymerized MTs are not assembled in a “regular size” instead, they are assembled by portions of 40-60 nm length, corresponding to the XMAP215/tubulin dimers adding (Kerssemakers *et al.*, 2006). This finding corresponds to the absence of XMAP215/ch-TOG dimerization. That makes possible the +TIP activity could be realized by addition of XMAP215 single and linear molecules.

Additionally, the *in vitro* interaction among XMAP215 and a recognized +TIP protein such as EB1 has been proposed. This interaction would work as an XMAP215 regulation mechanism where EB1 would promote the XMAP215 binding (Kronja *et al.*, 2009). Is the XMAP215 “comet like-structure” a transitory population ready to be loaded with tubulin dimers that will be deliver to the MT +TIP in just one step process?.

Based in our results, we proposed a general mechanism to describe the **+ TIP XMAP215** activity that could be structured as it follows. We propose that free XMAP215 is previously charged with its tubulin cargo where seven to eight tubulin dimers can be loaded on a linear XMAP215 molecule (Cassimeris *et al.*, 2001) (**Fig. 64a**), the bigger cargo among all of the studied +TIPs, considering that the molecule has not shown any dimerization activity. The resulted interaction among the ch-TOG domains and the tubulin dimers produces a 60 nm protofilament-like structure that is delivered at the tip of growing MTs (**Fig. 64b**). At this point the multimerization of the TOG domains represents an advantage in the general mechanism of the tubulin dimers addition. Once the fully loaded XMAP215 joins the MT growing end to become a +TIP XMAP215 (**Fig. 64c**). This functional conception could explain the MT velocity growth, enhancement only observed previously in the presence of XMAP215 in pure tubulin solutions. It has even been postulated that perhaps the XMAP215-tubulin complex could express a higher affinity for the MT end that the tubulin dimers themselves (Kerssemakers *et al.*, 2006).



**Figure 64. Hypothetical model of +TIP XMAP215/ch-TOG participation in complex protein formation.** In an *in vitro* solution XMAP215 is loaded with 7-8 tubulin dimers (a). The tubulin – charged XMAP215 reach the MT +TIP to delivers its cargo (b). The MT sheet conformation changes and the MT is closed to become a hollow and linear structure (c).

The functionality of the XMAP215 structure provides an orientation of its own. In our **XMAP215 +TIP activity model**, the linearity of XMAP215 on the MT lattice can be traduced in terms of the different domains contained in its sequence. The XMAP215 polarity could be giving by its MT-binding domain contained in the C terminal region of the protein, and who would allow the “landing” of the molecule at the MT growing end. The N terminal domain, containing the TOG domains could allow the tubulin dimer loading, transport and adding to the final structure.

## 7.2 The N-terminal domain related activity

The XMAP215 **N-terminal** ch-TOG domain participates in the MT dynamics directing the molecule towards the MT growing end, being part of the polymerization mechanism. Using this strategy, the XMAP215 N-terminal domain has probed that it could stimulate MT growth at the MT + TIP (Popov *et al.*, 2001).

Also, at the MT +TIP, XMAP215 could stabilize the MT from depolymerization by KXCM1. Some authors propose the possibility that

XMAP215 “overhangs” the MT +TIP, using its MT binding domain 1 (aa ~250-800), a domain with a moderate affinity for the MT lattice. Using this strategy the molecule could anchor to the MT lattice and facilitate the tubulin dimers addition (Cassimeris *et al.*, 2001; Ohkura *et al.*, 2001; Shirasu, Hiza *et al.*, 2003, Gard *et al.*, 2004). However, our results take us to hypothesise that the XMAP215 molecule is previously fully loaded to be added to the MT lattice. At this cellular localization XMAP215 could interact with other structures such as chromosomes (kinetochores), cell cortex and other end binding proteins.

The N-terminal fragment of the XMAP215 contains two TOG domains, **TOG1A** (aa 1-263) and **TOG1B** (aa 264-543). Each domain predicted isoelectrical point (pI), is negative at physiological pH for **TOG1A**, in contrast to the **TOG1B** that posses a positive charge under the same conditions (Slep and Vale, 2007).

Keeping in mind these physico-chemical characteristics it is very likely that the domain **TOG1A** would present a higher affinity for the  **$\alpha$ -tubulin** monomer of the free dimers preferentially, while the  **$\beta$ -tubulin** would be loaded at the domain **TOG1B** (Al-Bassam *et al.*, 2007). The electrical affinity presented by the protein could produce it self a selected mechanism for the tubulin dimers loading and addition, giving origin to an already well structured and polarized protofilament-like structure ready to be added to the MT. Many of the MT binding domains studied so far have a chemical characteristic: they are basic, because they are enriched in basic amino acids. This observation could suggest that the MT binding is dependent on chemical interactions of the binding domain, rather than in the sequence it self (Gard *et al.*, 2004).

The electrostatic interaction among XMAP215 and the C-terminal domains of  $\alpha/\beta$ -tubulin (known as E-hook) has been proposed as the mechanism used by XMAP215 to remain attached to the MT growing end (Brouhard *et al.*, 2008). However, the ch-TOG N-terminal domain has probed not to have a MT-related activity dependent on the tubulin E-hook (Spittle *et al.*,

2000). In consequence another kind of interaction tubulin-XMAP215/ch-TOG must be considered.

In the TOG domain subject, there is particularity. In 2001 Popov *et al.* reported the colocalization with MT for one of the XMAP215 fragments in the mitotic egg extract but not in the living cell: the **N-terminal fragment**. Already the N-terminal fragment of XMAP215 has been implicated in the MT dynamics and in the suppression of catastrophes by kinesins (Popov *et al.*, 2001). In the egg extract the N-terminal fragment success to be recognized and be part of the “local” machinery. This region contains two TOG domains and a MARK kinase sequence (aa 353 KFGS 356).

### 7.3 Our plus end hierarchy complex hypothesis

The XMAP215 +TIP affinity can find an explanation through the protein evolution itself. But, beyond a wise evolution method, many other proteins function at the same environment, expressing an affinity for a region that after our measurements has an average of 1.17 $\mu$ m length. What make of this tiny region of the MT so attractive to the +TIPs?

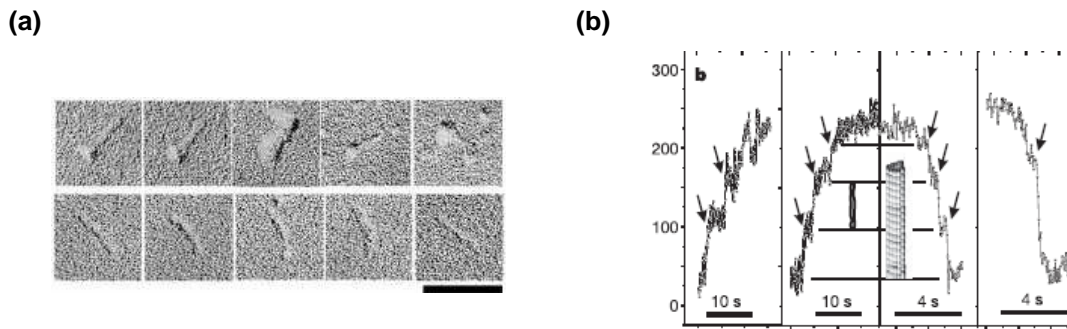
The key of the targeted activity could find an explanation through a mixed reaction involving structural features, chemical affinities and physical interactions. The composition of the XMAP215/ch-TOG protein itself constitutes already in an affinity advantage. XMAP215 fragments express a particular affinity for the MT structure showing kDs among 1 and 20 $\mu$ M up on the analyzed domain. In this context the C-ter domain expresses the minimal kD (>20 $\mu$ M) and the whole protein the maximal one <1  $\mu$ M (Gard *et al.*, 2004). In general, the +TIPs proteins express lows kD in their affinities with tubulin or MT up on the case: 0.067  $\mu$ M for CLIP170/MT and 0.26  $\mu$ M CLIP170/tubulin (Tirnauer *et al.*, 2002); 403  $\mu$ M for p150<sup>Glued</sup>/tubulin, and 0.51  $\mu$ M for CLIP170/tubulin (Mishima *et al.*, 2007). Eventhough EB1 do not bind to unpolymerized tubulin, it can bind to the MT structure with a kD of 0.44  $\mu$ M

(Tirnauer *et al.*, 2002; Slep and Vale, 2007). In all cases the dissociation constant is weak, showing the evidence of the transitory state of the interaction among each one of them and tubulin or the MT.

In a physical context XMAP215 could provide the structural support for the MT sheet closure. The conformational changes observed for MT structures in the cryo-electronic micrographs showed an “architectonical effect” at the tips of MTs when XMAP215 participates in the MT polymerization. The MT tip become “linear”, an activity that could facilitate the MT sheet closure. In contrast, when the XMAP215 activity is limited at the MT tips, these MT tips show a tendency to create a curved conformation, compatible perhaps with the tubulin oligomer addition or the MT depolymerization taking the structure to a blunt end (the transition structure).

The XMAP215/ch-TOG has been previously described experimentally as a long thin molecule 60 nm long able to charge 6-8 tubulin dimers (**Fig.65a**) (Cassimeris *et al.*, 2001). Also, XMAP215 polymerized MTs are not assembled in a “regular size”, they are assembled by portions of 40-60 nm length, corresponding to the tubulin dimers adding (Kerssemakers *et al.*, 2006) (**Fig.65b**). No dimerization of XMAP215/ch-TOG has been showed, so it is possible addition at the very tip of the MT could be realized by addition of XMAP215 single and linear molecules.

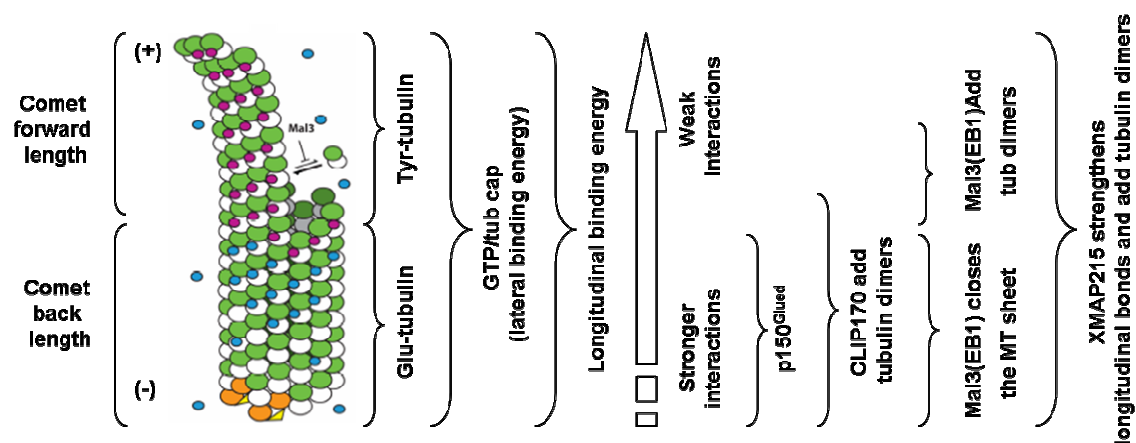
Once our +TIPs hierarchy was established based on imaging obtained data (**Figure 47**) In the results chapter, the next step is the potential explanation to the general comet-like hierarchy observed. It is important to keep in mind that for this study we divided the comet like structure in two regions: **the back-length comet**, defined as the region of the comet that remains on the MT surface; and the **forward length comet**, that is the region of the comet that remains outside the MT surface (**Fig. 66**).



**Figure 65. in vitro XMAP215 behaviour . (a)** XMAP215 is a long rod shaped molecule that remains as a 60 nm monomer, scale bar 100 nm (Cassimeris *et al.*, 2001) **(b)** High resolution of tubulin polymerization in presence of XMAP215. Arrows indicate the length changes during growth (left) and shrinkage (right) (Kerssemakers *et al.*, 2006)

Starting the analysis from the back length of the comet we found that EB1 shows the longest back length comet. The explanation could be addressed to the potential EB1 activity in the MT sheet closure, as has been shown for Mal3, the *Schizosaccharomyces pombe* EB1 homolog (Sandblad *et al.*, 2006). Thus, and using its structural and physicochemical skills, EB1 could be able to leadership the comet +TIP back length closing the formed MT lattice, and remaining on the MT structure (des Georges *et al.*, 2008).

Additionally, the interaction among XMAP215 and EB1 have been proposed as an XMAP215 regulation made by EB1, where EB1 would promote the XMAP215 binding (Kronja *et al.*, 2009) Could this indicate the presence of a linear XMAP215/ch-TOG protein ready to “accept” its tubulin cargo at the MT tip? Or is the XMAP215 “comet like-structure” a transitory population of XMAP215 ready to be loaded by tubulin dimers and to deliver them to the MT +TIP in just one step process?



**Figure 66-. +TIPs hierarchy theory.** The MT +TIP has been divided for its analysis: the **comet back length and forward length**. Tubulin post translational modifications are considered as two different populations present at the +TIP. The freshly added Tyr-tubulin builds the MT sheet and the Glu-tubulin is part of the already sealed MT tube. The GTP-CAP could provide the lateral binding interactions that reduce the distance among tubulin subunits. As the tubulin dimer addition takes place, the new created protofilaments express a longitudinal binding energy, being stronger in the closed MT structure than in the freshly added tubulin dimers. (Piette *et al.*, 2008). Finally each +TIP protein respond to its own structure and collective affinity to accomplish their final task: polymerize the MT under safety measures. **White**,  $\alpha$ -tubulin subunits; **Green**,  $\beta$ -tubulin subunit; **Magenta**, Mal3 tightly bound to tubulin; **Blue**, Mal3 free or weakly bound to tubulin; **Orange**,  $\gamma$ -tubulin complexes. Modified from de Georges *et al.*, 2008.

In contrast,  $p150^{Glued}$ , CLIP170 and ch-TOG share the same departing point (-1.16; -1.26 and -1.24  $\mu\text{m}$  respectively **Figure 47** of the results chapter). The recognition of related sequences among each protein could explain not only the independent interaction +TIP protein/tubulin or +TIP protein/MT. This almost collective departing point could show at what point the interactions could be shared/dependent among each other.

From the other side, the forward length of the comet is a ch-TOG privilege.  $p150^{Glued}$  comet starts where the MT sheet is closed. CLIP170 and EB1 follow the sequence. A few differences can be listed among the back length and the forward length of the comet as an attempt to explain the events. At this structural point of the MT the forward region of the comet is constituted by Tyr-tubulin as part of the most recently added dimers, being less stable than the Glu-tubulin that forms the sealed MT. This structural/post-translational difference might select the access to the CAP-Gly armed proteins.

Previous findings shown that CAP-Gly proteins do not bind to MTs that are composed of tubulin heterodimers lacking of the C-terminal Tyr of EEY/F (Peris *et al.*, 2006) Now, and if the tubulin tyrosination takes place preferentially on the free tubulin subunits, the freshly added tubulin dimers would form a transitory structure at the +TIP that would be enriched in Tyr-tubulin, being perhaps the region were the four +TIPs proteins of this study confluence. But, there is still a remaining issue about the TTL activity targeting: EB1 and  $\alpha$ -tubulin contain each an EEY motif and that CLIP170 requires EB1 to the +TIP tracking, is the TTL regulator of the +TIP tracking mechanisms through the modification of  $\alpha$ -tubulin or EB1 or both? (Slep, 2010).

The MT +TIP is also a region were the GTP is doing its work. The GTP-CAP strengths the lateral bounds among dimers ( $\alpha$ -tubulin/ $\beta$ -tubulin) that is weak due to the curved MT +TIP geometry at the MT growing end. However, the GTP hydrolysis is not required for XMAP215 to promote MT growth (Brouhard *et al.*, 2008).

In conclusion the observed changes at the MT growing end could require structural help to support and seal the structure during the tubulin dimers addition. Here the different MAPs develop a highly specialized role each. CLIP and p150<sup>Glued</sup> could be EB1 regulated to add tubulin dimers at the MT tip. Additionally, EB1 could not only add tubulin dimers but also could close the MT sheet acting as a zipper in the structure. Finally, XMAP215 join the team, using its size and domains to add a huge quantity of tubulin dimers in one step only and at the same time strengthening the protofilament longitudinal bonds.



## 7.4 Microtubular XMAP215/ch-TOG: RNA trafficking and other cellular activities. Another protein-protein interaction?

Functionally, the +TIP XMAP215 conformation can be associated to the tubulin dimers loading, but based on the subcellular localizations, the microtubular XMAP215 (**MT-XMAP215**) might be associated to the MT stabilization and other cellular activities in which could be involved such as RNA trafficking (Lee *et al.*, 2001; Mohr *et al.*, 2001; Lopez *et al.*, 2004; Slep *et al.*, 2007; Siegrist *et al.*, 2008). We propose that after the tubulin dimers addition is made by the **+ TIP XMAP215** conformation, the **MT-XMAP215** molecule keep its interaction with the MT lattice, remaining on it playing different roles.

Our theory is based on the observation realized for the RNAi depletion in *Xenopus laevis* cells and PHF 24 and 48 hours after the transfection the mitotic cells expressed the already reported phenotype: multispindle pole cells with the consequent mitotic arrest. But, as the depletion went on the interphasic cells started a cell death process after 72 and 96 hours post transfection.

How could be the ch-TOG partial depletion take an interphasic cell to its death?. We think the answer relay in our XMAP215/ch-TOG model, where once the tubulin dimers have been delivered at the MT growing end, the XMAP215 remains not longer as a **+TIP XMAP215/ch-TOG**, they assume a new task as a **MT-XMAP215/ch-TOG**. Once the depletion is produced as a result of the RNAi transfection, the remaining TOG is not enough to accomplish the 100% of its microtubular task, restraining the microtubular traffic activity, taking the cell to death.

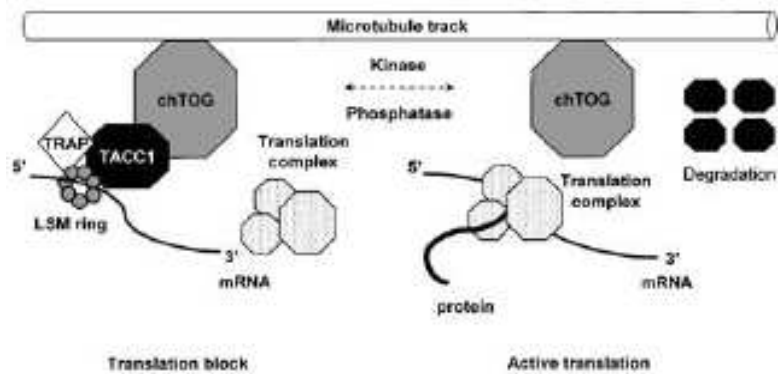
The **MT-XMAP215/ch-TOG** model has been previously described as part of a protein-protein interaction mechanism responsible for the mRNA trafficking, this mechanism is able to target the translation at cell competent sites. This specific traffic involves the recognition of mRNA by RNA binding proteins forming a RNA-protein complex known as RNA granules. Then, RNA granules

are transported to the target area using cytoskeletal and motor proteins (Kosturko *et al.*, 2005).

For example, colocalization of **ch-TOG** and **hnRNP A2** (heterogenous nuclear protein A2) in oligodendrocytes and neurons has been showed in 90% of the studied RNA granules, these results suggest that ch-TOG is part of the RNA transport granules. Briefly, HnRNP A2 binds a particular sequence termed A2RE (A2 response element). Molecules of A2RE RNA and hnRNP A2 protein assemble into large ribonucleoprotein complexes, termed **RNA granules**. These granules are composed by related RNA-binding proteins, components of the translational machinery, and molecular motors. Finally, RNA granules are transported along **MTs** to distal dendrites where RNA is localized and translation is activated (Kosturko *et al.*, 2006).

Another possible member of the mRNA trafficking mechanism could involve the activity of the taxin proteins (**TACC**), which forms a complex TACC/ch-TOG through the coiled-coil domain contained in the TACC C-terminus. This time the RNA granules anchorage would depend on the kinases or phosphatases activity. A kinase might “release” the complex, and the phosphatases could “join” the complex back again.

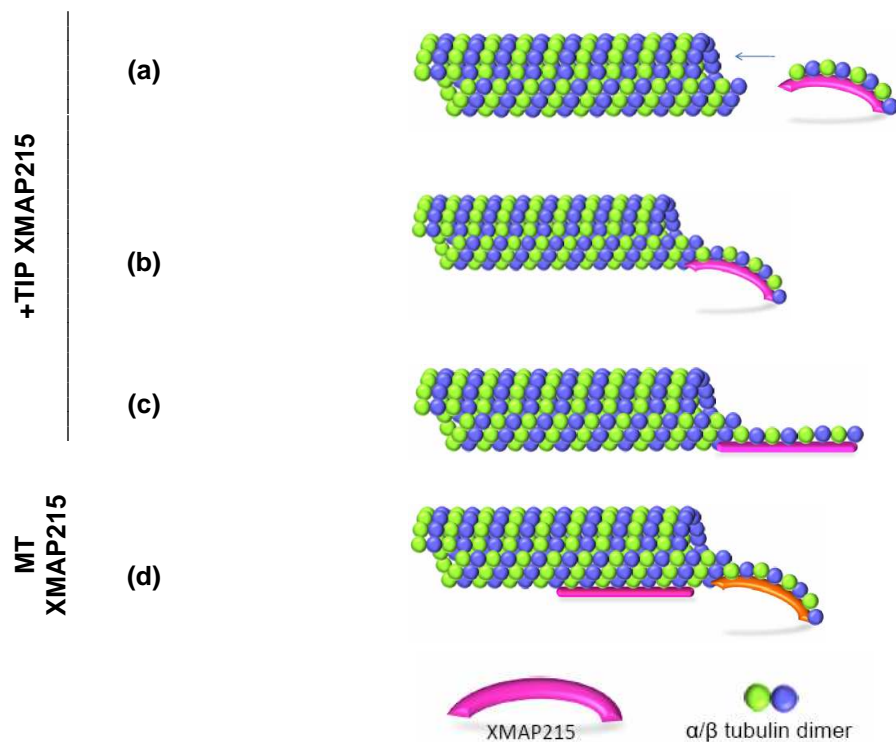
The presence of the MT-XMAP215/ch-TOG under the kinases or phosphatases activity might result in the anchoring of the mRNA granules at translation competent sites along the MT. Several functions can be attributed to these complexes such as their intervention during cell division and the establishment or maintenance of cell polarity (**Fig. 67**) (Conte *et al.*, 2002, 2003; Francone *et al.*, 2007).



**Figure 67. Hypothetical model of MT- XMAP215/ch-TOG participation in complex protein formation.** The complex is formed by **ch-TOG**, **TACC1** (transforming acid coiled-coil protein), **TRAP** (tudor repeat associator with PCTAIRE2, an adaptor protein), the **LSM ring** (Like-Sm protein 7, a mRNA regulator) and a mitotic serine/threonine **kinase** (Aurora A kinase). In the model the required mRNA (e.g. Cyclin B) is transported to a specialized site (e.g. spindle pole) where the complex is located through movements along the MT lattice. During transport the translation is blocked. The precise role of the LSM ring is not known. After arrival the complex is liberated due to kinases phosphorylation (e.g. Aurora A or others) and /or degradation of TACC1. Conte *et al.*, *Oncogene* 2003

To accomplish its potential microtubular task XMAP215 must remain after the tubulin dimers addition and the MT sealing. We propose a general mechanism where XMAP215/ch-TOG binds the MT in a polarized orientation (**Fig. 68**).

The free XMAP215/ch-TOG allows the tubulin dimers loading in solution, becoming a protofilament-like structure (**Fig. 68a**). Next and using its C-terminal MT binding domain, the XMAP215/tubulin dimers complex anchors the MT + TIP (**Fig. 68b**). Then, the protofilaments-like structure is added and the tubulin dimers addition at the + TIP has place, at this point the MT structure has gained 40-60nm length (**Fig. 68c**). As a result of the XMAP215/ch-TOGp addition, the + TIP change mechanically from a curved structure to a more linear one, allowing the sealing of the MT sheet in to a hollow structure (**Fig. 68d**). As the MT+ TIP is growing the longitudinal + TIP XMAP215/ch-TOGp that was at the very tip keep moving within the MT lattice, leaving behind the MT + TIP and becoming a microtubular-XMAP215/ch-TOGp (**Fig. 68e**) (Cassimeris *et al.*, 2001 ; van Buren *et al.*,2005).



**Figure 68. Model for XMAP215/ch-TOG activity in the microtubular environment.** XMAP215 is loaded by 6-7 tubulin dimers (a). Then the protofilament-like structure created by the XMAP215-tubulin dimers reach the + TIP of the MT (b). The tubulin dimers addition has place, leaving XMAP215 at the MT +TIP (c). XMAP215 presence transforms the MT+ TIP from a deeply curved structure in to a linear one, allowing the MT closure (d). A “new” XMAP215 molecule is added giving origin to a “+ TIP XMAP215”, making of the precedent a MT-XMAP215 (e).

## 7.5 Centrosomal XMAP215/chTOG and MT anchoring

It has been proved that the MT anchoring to the centrosomes is an XMAP215 dependent mechanism (Tournebize *et al.*, 2000; Popov *et al.*, 2002) and its co-localization with MTs has been already described. The two XMAP215/ch-TOG populations identified by two different mcAB are present in the cell centrosome of fixed cells. Could it be possible that each XMAP215/ch-TOG population is also present at the cell centrosome having each one an activity of their own?

Two different roles It have been attributed for the particular XMAP215/ch-TOG localization at the mitotic centrosomes: to anchor the minus end of MTs,

and to stabilize the minus ends counteracting the effects from the catastrophe factor XKCM1/MCAK kinesin (Cassimeris and Morabito, 2004; Holmfeldt *et al.*, 2004).

The XMAP215 preferential targeting to the centrosome has been associated to the C-terminal domain of the protein. The centrosome targeting domain is enclosed at the **C-terminal** region of the XMAP215 protein (aa 1,167-2,065). The sequence contains a double domain and function: the MT binding domain and the centrosomal targeting domain towards the MT minus ends (Spittle *et al.*, 2000; Popov *et al.*, 2001; Al-Bassam *et al.*, 2007; Slep and Vale, 2007). The presence of the sequence that codes for the Tau repeat (aa 1,866-1,883 of the XMAP215 sequence, and aa 1,833-1,850 of the KIAA0097 ch-TOG sequence) has been identified as a MT binding motif that could be by itself part of the mechanism for the centrosome targeting. The Tau repeat is present in other MAPs such as tau, MAP2 and MAP4 (Gard *et al.*, 2004).

Additionally to the tau sequence, the C-terminal fragment contains a 175 aa length sequence (aa ~1,150-1,325) with a high MT binding affinity ( $K_d < 1 \mu\text{M}$ ). The potential functionality of this sequence could be related to the protein anchoring to the MT lattice, anchor the MT to the centrosome and even could participate in the stabilization of the MT free minus ends by counteracting the KinI catastrophe factor (Gard *et al.*, 2004).

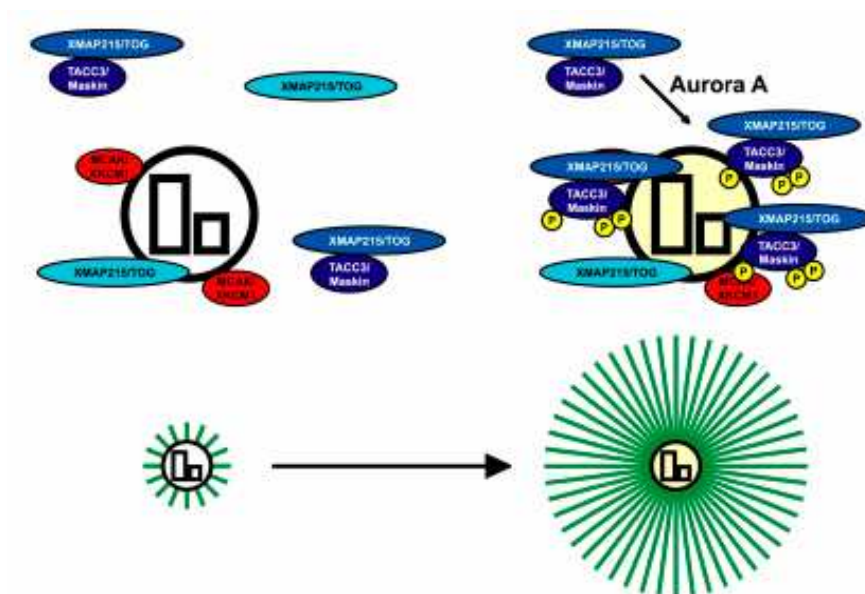
In the cellular model, the ch-TOG cellular RNAi depletion showed a reduced length and density of spindle MTs by ~20%, produced **multipolar spindle** formation and **centrosome fragmentation** (multiple  $\gamma$ -tubulin foci), (Gergely *et al.*, 2003; Cassimeris *et al.*, 2004; Basto *et al.*, 2007). ch-TOG has probed to be necessary for the structure and bipolar organization of the mitotic spindle. The multiple centrosome fragments probes the role of the ch-TOG in the cell centrosome integrity.

Additionally, in the *in vitro* conditions a XMAP215 depletion produces the absence of MT nucleation by centrosomes in the *Xenopus laevis* egg extract, but the nucleation of MT asters by recombinant XMAP215 loaded on NiNTA beads shows the XMAP215 ability to anchor MTs in pure tubulin solutions, these experiences suggest that XMAP215 cooperates with  $\gamma$ -tubulin to nucleate MTs in the cytoplasm, perhaps by stabilizing protofilament interactions, anchoring MTs organizing them into asters (Popov *et al.*, 2002).

Other interactions have probed for XMAP215. Members of the XMAP215/chTOG family interact with members of the Transforming Acidic Coiled-Coil family (**TACC** family), who through its COOH terminal coiled-coil domain (TACC domain) targets the protein to the centrosomes and, at the same time interacts with the XMAP215/TOG family members (Gergely *et al.*, 2002).

Based than the fact that MT are anchored from centrosomes and requires the presence of XMAP215 (Tournebize *et al.*, 2000). Immunoprecipitation (IP) experiments showed that XMAP215 coprecipitates with **Maskin** (*Xenopus* homologue of the human **TACC**) and **Eg2** (homologue of the human **Aurora A kinase**) in the *Xenopus* egg extract (Peset *et al.*, 2005). On the other hand, **Maskin** is considered to be important for MT stabilization and growing but not for the anchoring (Peset *et al.*, 2005). **TACC-3** depleted cells showed a loss of ch-TOG from the mitotic spindle but not from the centrosome (Gergely *et al.*, 2003; Cassimeris and Morabito, 2004).

Targeting of the Maskin-XMAP215 complex to mitotic centrosomes overcomes the high MT-destabilizing activity of **MCAK**. In this context, XMAP215 is required to protect spindle MTs from MCAK activity at centrosomes. Targeting of Maskin-XMAP215 would enhance its activity at centrosomes; stabilizing nascent plus ends (**Fig. 69**) (Holmfeldt 2004, 2005; Kinoshita *et al.*, 2005; Noetzel *et al.*, 2005; O'Brien *et al.*, 2005).



**Figure 69. A XMAP215 activity at the centrosome in M phase.** Centrosome nucleated MTs (green) are not stabilized by XMAP215/ch-TOG (light blue) due to the XKCM1/MACK (red) presence, left side of the image. TACC3/Maskin (dark blue) phosphorylation by Aurora A kinase (yellow circles indicate the phosphorylated serine residues) targets the complex XMAP215/ch-TOG – TACC3/maskin to centrosomes. The result is an enhanced XMAP215 activity, stabilizing and allowing the MT growth from centrosomes (right side of the image). Modified from Kinoshita *et al.*, 2005.

## 7.6 ch-TOG, from the functional theory to the fact theory.

ch-TOG was described for first time in 1995 as a colon hepatic tumor overexpressed gene. So far we have described an experimental functionality of the protein: from the tubulin dimers addition to the RNA granules and the centrosomal activities, but the real fact is: what is the ch-TOG real part in to cell tumorigenesis? Is it playing the main role in the uncontrolled cell proliferation or is just having a secondary part in the disease? Is the ch-TOG overexpression the responsible protein for a cellular strong invasive mechanism? Could it be considered as an innovative useful tool in the fight against cancer?

For the time of the **ch-TOG** first report, its chromosomal localization (**11p11.2**) was not associated to a disease. However an association existed among the 11p11 locus and the neoplastic events. For example genes such as the **Midkine** a gene that is transiently expressed in early stages of the

embryonal carcinoma and the **KAI1** gene, a metastasis suppressor gene for cancer of the prostate, they were both mapped in the 11p11.2 band. In fact, it had been previously suggested that the inactivation of one or more tumor suppressor genes on 11p were at the origin of several cancers. The short arm of chromosome 11 (11p, **petit**) could contain genes involved in tumor development (Charrasse *et al.*, 1995).

Already, Charrasse *et al.* (1998) hypothesized that the high levels of ch-TOG and OP18/stathmin may result from a micro-evolutionary process, a process that involved the cell de-differentiation. The resulting product is the survival group of cells that are able to make rapid mitosis MT-rearrangements, key elements necessary for the cell cycle. This cell dedifferentiation hypothesis represents a limited chance to find embryo-specific expressed sequences, which could be re-expressed in cancer cells. This is a possibility that so far remains related to genes located in chromosomes 3 (3q13.13, 3p25.2) and 8 (8p23.1) (Monk *et al.*, 2001).

If ch-TOG participates or is de-differentiated during the neoplastic processes is an interesting biological event that remains to be probed. XMAP215 and ch-TOG are able to produce at least two splicing variant form products each. The **XMAP215** protein express the **XMAP215<sub>M</sub>** isoform, a shorter form of the protein, present only during early embryogenesis; and the **XMAP215<sub>Z</sub>**, is the expressed form starting at the embryo gastrulation until the adult life of the frog. In the human case, the **ch-TOG isoform a** is known as the **KIAA0097** sequence (NCBI accession number NP\_001008938.1), is 2,032 aa length and a mRNA 6,714 bp (transcript variant 1), **the isoform b** (NCBI accession number 055571.2) is 1972 aa length and mRNA of 6534 pb (transcript variant 2). Both sequences are composed for 44 exons and the difference among them consist of a 180 bp insert present in the isoform a, but not in b ([Fig. 62](#)).



There are five CKAP5 reported sequences in the NCBI database. Three of them were reported from pathological tissues or cell lines, and the remaining two were reported from blastic tissue. For example the KIAA0097 sequence was derived from an **acute myeloid leukaemia** (AML) cell line (a myeloblast, a unipotent stem cell that will differentiate in to a granular cell. Nagase *et al.*, 1995), a second sequence belongs to **primary lung cystic fibrosis** epithelial cells (damaged tissue due to inflammation and hypoxia, reported by Bonaldo *et al.*, 1996), a third sequence is originated from **erythroid precursor cells** (a precursor of a red blood cell. Gubin *et al.*, 2002, NIH unpublished), a fourth sequence is derived from **germinal center B cells** (lymph nodules containing mature B lymphocytes. Strausberg *et al.*, 1999, NIH-MGC unpublished) and finally, the fifth and last was obtained from **human tumoral brain** (ch-TOG sequence. Charasse *et al.*, 1995). Could this “differential expression” be interpreted as a biological trace of the ch-TOG de-differentiation in certain pathological or blastic events? Does this finding means that the ch-TOG protein could participate in a cancer event?

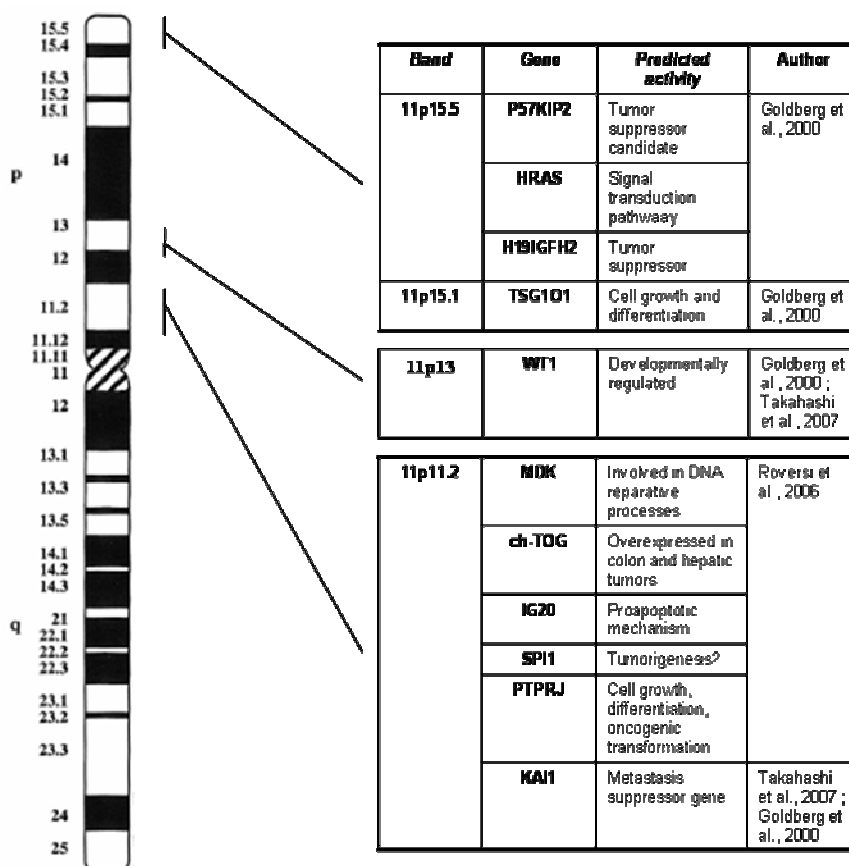
The ch-TOG de-differentiation at certain pathological states has remained as a possibility. Previous studies searched ch-TOG mRNA expression in human tumoral brain tissue using reverse transcription polymerase chain reaction (RT-PCR). The assays amplified a 593 bp fragment belonging to the C-terminal region of the ch-TOG mRNA sequence, but also a lighter product was amplified (~375 bp). The lighter product expression was proportionally related to the anatomic tissue localization (tumor, surrounding tissue or peritumoral), where the stronger expression was related to the tumor tissue. The possible explanation could relay on the presence of two ch-TOG messengers as the product of a differential splicing (Charrasse *et al.*, 1996).

Even though the ch-TOG expression in pathological human tissues could allow us to produce theories directed to its participation in the disease mechanism, the *in vitro* test presents serious disadvantages.

During the ch-TOG overexpression cell characterization, different cell lines were used, and a ch-TOG pattern was established. The human colonic adenocarcinoma cell line, Caco-2 expressed high levels of ch-TOG during their proliferative state (Charrasse *et al.*, 1995). After the ATCC (American Typing Culture Collection) technical information, this cell line has a characteristically 96 chromosomes, the polyploidy can explain the ch-TOG overexpression, but any other protein could be overexpressed with such a chromosomal overcharge.

If ch-TOG is related to tumor progression, its genomic localization can be a correlation among chromosome alteration and disease. **11p11** has been already implicated in the molecular pathogenesis of human cancer. Liver tumor suppressors loci were mapped to human chromosome **11p11.2-p12**, where one transcript in particular was lost or had a decreased expression, the **PIG11 gene**, a p53 induced protein. Other genes have been also mapped to the liver tumor suppressor, these genes code for guanine nucleotide binding protein gamma 3, the mitochondrial carrier homolog 2 and pRDI-BF1-rIZ1 domain containing 11 (Ricketts *et al.*, 2003). Then, a clinical correlation could have place, only if the genetics “statistics” are rich enough in accurate data.

In clinical cases, for example, the identification of genomic markers such as chromosomal lost or gains have become a key issue for the diagnostic, prognostic, therapeutics decisions and procedures to make. **Gliomas** are a frequent primary brain tumor, and despite de quality of the diagnosis or treatment, the prognosis remains poor. Studies have revealed the **gain** of the region **11p11.2-q13.2**. Among the genes contained in this band/region (**Fig. 70**) we can cite **DDB2**, a gene coding for a DNA repair protein, the DDB2 overexpression suppresses TNF mediated apoptosis. Another example is the **IG20** gene, encodes for a protein involved in the TNF-alpha signalling, its overexpression enhances resistance to vinblastine and  $\gamma$ -radiation among others (Roversi *et al.*, 2006).



**Figure 70. Identified genes in chromosome 11p and its possible implication in cancer evolution.** Charrasse *et al.*, 1995; Takahashi *et al.*, 2007; Goldberg *et al.*, 2000

Alterations in 11p chromosome have been reported in the progression of lung cancer, being particularly present in the metastatic cases (11p15 and **11p11-13** regions) (Takahashi *et al.*, 2007). These alterations are possibly associated to a worse prognosis due to the invasiveness observed for small-sized lung adenocarcinomas (**11p11-p12** region) (Nakanishi *et al.*, 2009), they are also present in human prostatic cancer progression (Dong *et al.*, 1995). The chromosomal imbalance where the 11p arm is involved, is related mostly of the time to its partial chromosomal lost. Some of the reported pathologies where it is associated include: hepatocellular adenoma and hepatocellular carcinoma (Boerman *et al.*, 1996; Cai *et al.*, 2009), acute lymphoblastic leukaemia (ALL) (Gorello *et al.*, 2010), acute promyelocytic leukaemia (APL) (Akagi *et al.*, 2009), acute myeloid leukaemia (Gupta *et al.*, 2008; Sweetser *et al.*, 2001), chronic

myeloid leukaemia (Phan *et al.*, 2006), chronic lymphoid leukaemia (Dighiero *et al.*, 2002), and megakaryoblastic leukemias (Alvarez *et al.*, 2001),

All this characteristically chromosomal abnormalities that become constant in a population are considered to be a “**prognosis marker**”, a molecular foot print of cancer progression. This means that this marker could indicate the tumor state (primary or metastatic), possible treatment to avoid resistance, the therapy recommended and even more important the attended patient prognosis. Could we think in a ch-TOG as a prognosis marker?

The ch-TOG localization at the 11p11.2 break point leaves untouched the coded protein, but with the lost chromosome fragment the cell is losing several genes that are potentially related to the suppression of tumour progression, cell growth and differentiation mechanisms. Losing the “tumour control genes” contained in the region 11p12-11p15, the cell lose its cell division control capacity, but keeps the highly advantageous mitotic skills through the ch-TOG intact activity. The ch-TOG overexpression due to the “lack of control” might provide a good marker of the potential metastatic and lethal characteristics of a primary tumour. The early diagnosis through the sample analysis of a primary tumour could accelerate and change deeply the prognosis and treatment in a patient. The right and early diagnosis could prevent the tumour metastasis spread; here the “**clonal evolution theory**” takes its place.

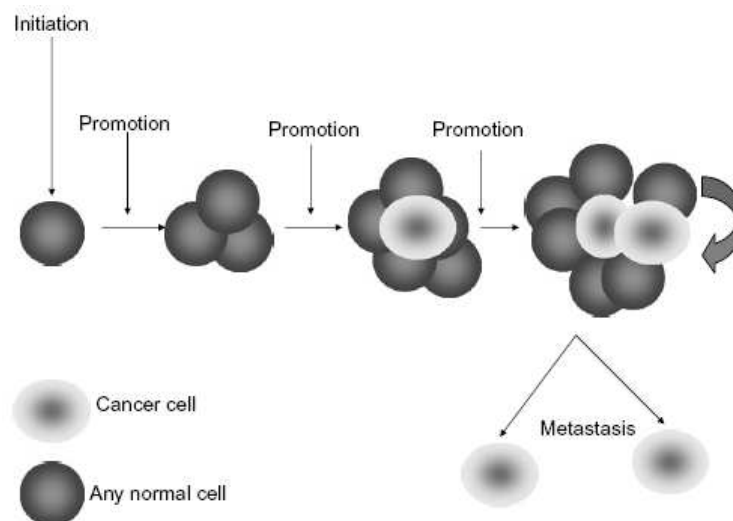
In a **primary tumour** only the more malignant cells with selective genetics alterations will survive to the difficult nutritional and highly oxidative conditions (**Fig. 71**). Among a genetically diverse primary cell tumour population (**polyclonal**), only the cells possessing metastatic abilities will survive (e.g. a cell expressing a deletion 11p11.2). If a cell with these characteristics succeeds to escape and to establish in another tissue, it will be able to form a **metastatic tumour**, now we are talking about a **clonal** tumour, that express common selective genetic alterations that were not detected in the primary one. These alterations will be responsible for providing cell of skills such as detachment,

invasion, survival in circulation, attachment extravasation, proliferation, neovasculature induction and evasion of host defences (Takahashi *et al.*, 2007)

## 7.7 The XMAP215/ch-TOG future

The fight against cancer is not a new issue. The ch-TOG main role during cell division and ubiquitous localization in human tissues make of this protein a good target in a battle against a disease that took over 7,6 million lives around the world in 2007 and estimations arrive to predict that more than 12 million people will die because of cancer in 2030 (source WHO).

Innovation is always a human challenge, no matter what discipline are we talking about. In the cancer case, innovation becomes a survival issue. The complex and mostly unknown origin of the cancer disease makes a call to innovation, innovation to improve the patient quality of life, innovation to fight and succeed against the cancer resistance, innovation to diminish secondary effects, innovation to provide an alternative treatment to those people that are desperate waiting and searching for one.



**Figure 71. Clonal mechanism of Cancer.** Image from Argyle *et al.*, 2008

The XMAP215/ch-TOG key activity during cell division provides a singular tool to break down the cell proliferation; the tumor growth and metastasis. These punctual characteristics make of this protein a potential target for the biotechnological industry in the constant research of intelligent designed antiproliferative molecules.

This strategy presents several advantages and disadvantages at the same time. For example, we could hypothesize that the designed ch-TOG inhibitor must be highly specific, not only to target and potentialize its effect but also to avoid any secondary effect.

Keeping in mind the observed ch-TOG localization and activity, the designed molecule should be directed against the **ch-TOG +TIP**. Targeting the tubulin dimers addition at the MT **+TIP**, the C-ter centrosome targeting domain or even better the MT nucleation to the centrosome (all of them XMAP215/ch-TOG mediated), the possibility of arriving to a highly effective and mitotic selective effect in the cell proliferation is almost guaranteed. But on the contrary, if the molecule has an effect on the **MT-XMAP215**, the “selectivity” of the effect would be lost and the undesirable effects would be expressed in the non-mitotic cells, which in principle shall not be targeted.

Due to the ch-TOG ubiquitary location in the human tissues, the inhibitor biochemical properties do not admit any mistake; beyond the secondary effects the main objective is to protect the cancer non touched tissues. Ch-TOG presence in brain regions such as cerebellum demands an anti-proliferative inhibitor that won't be able to cross the hematoencephalic barrier, with one interesting exception only: brain tumors and their particular difficult anatomic access to other forms of treatment. The ch-TOG mRNA presence has been detected in several different kinds of tumoral tissues, mostly of them with a poor prognosis. At this point the secondary effects and the irreversible or reversible effect of the treatment shall be considered.

The bone marrow is one of the tissues that could be considered as “sensitive” to a ch-TOG inhibitor. Two of the sequences reported for first time for ch-TOG used blastic blood cells: the erythroblast primary culture (red cells precursors) and the acute myelogenous leukaemia (**AML**) cell line, the KG-1 cells that gave origin to the CKAP5 **KIAA0097** sequence. Having both the bone marrow for origin, the potential activity of an inhibitor could present a high toxicity for this tissue. However, if the patient is facing a leukemia diagnosis, perhaps the secondary effect could be considered as positive and even highly useful.

Science has provided good examples in the development of molecules product of the **rational drug design**. This is the case of **Gleevec®** (Novartis), a molecule developed to inhibit the activity of a fusion protein, the product of a translocation fragment from the chromosome 22 to chromosome 9, giving origin to the known Philadelphia chromosome, a classic marker of the **chronic myelogenous leukemia**. The fusion product is an aberrant protein, the bcr-abl protein (breaking point cluster - Abelson proto-oncogene) for which Gleevec is specific for the TK domain in the abl fragment of the protein; it occupies the TK active site, leading to a decrease in the protein activity and cell proliferation.

XMAP215/ch-TOG structural complexity furnish a protein with many cell vital activities, if we arrive to influence wisely the subtle balance among its different activities, we could count on awesome clinical and biotechnological possibilities.





## **CONCLUSION**



## CONCLUSION

The XMAP215/Dis1 family of proteins has evolved primarily to regulate the MT cytoskeleton. Their functions have been associated to several mitotic activities such as: centrosome integrity, MT anchoring and mitotic spindle morphology. Thus these cellular localizations are considered to be a classical feature for this group of proteins. **XMAP215** was isolated from the *Xenopus laevis* eggs, the african frog. XMAP215 was reported as a protein that promoted dramatically and specifically the elongation of MTs plus ends, having perhaps a role in the rapid assembly and organization of MTs during the fertilization and rapid division cycles of the early embryo (Gard and Kirshner, 1987). Its human homolog, the colon-hepatic Tumor Overexpressed Gene protein (**ch-TOG**) was found to be expressed at low levels in all cells, but being abundant in brain and tumoral tissues. Then, and based in the peptide sequences, ch-TOG was proposed as a new human microtubule associated protein, the XMAP215 human homolog (Charrasse *et al.*, 1998).

However, some of the members of this particular family have been reported at the tip of growing MTs: **Dis1** (*Schizosacharomyces pombe*); **Stu2** (*Saccharomyces cerevisiae*); **DdCP224** (*Dictoselium discoideum*) and **MspS** (*Drosophila melanogaster*); interestingly this range covers a long way of the evolution tree, going from fungi through nematodes until it reaches the insects. Departing from the concept that different species of the XMAP215/Dis1 family have shown to possess an orthologue that is located at different cellular localizations, we developed a series of **mcAB** to identify the potential different populations present in two of the higher eukaryotes described so far for the family: **XMAP215** and **ch-TOG**.

We provide the first description of two different XMAP215/ch-TOG cellular localizations. Using the confocal images we can identify one population, the one that classically colocalizes with MTs, a microtubular XMAP215 (**MT-XMAP215**). The other XMAP215 population localizes at the MT growing end, a

plus tip XMAP215 (**+TIP XMAP215**). The +TIP XMAP215/ch-TOG conformation is the most distal of the analyzed +TIPs proteins. Further studies of the confocal microscopy images revealed that XMAP215/ch-TOG was at the head of the +TIPs proteins hierarchy, a hierarchy obtained from the image analysis of the most known +TIP proteins such as EB1, CLIP170 and p150<sup>Glued</sup>.

Further *in vivo* experimentation allows us to confirm the presence of XMAP215 at the MT +TIPs. In the *Xenopus laevis* mitotic egg extract, the TRIF acquired images showed a XMAP215 at the growing end of Ni-NTA based polymerizing MTs. The +TIP XMAP215 was detectable as the MT polymerization took place, surprisingly, the +TIP XMAP215 signal is detectable also during the depolymerization events. These series of facts probe the existence of an *in vivo* +TIP XMAP215 that joins polymerization at the mitotic +TIP.

The step that follows drives us to the MT tip architecture. XMAP215 is actively present at the MT TIP structure. The Cryo-EM images showed dramatic changes in the MT architecture, all these changes are related to the XMAP215 activity through its potential tubulin dimers addition. In pure tubulin solutions XMAP215 is able to increase the presence of sheet structures conformation more than twice in comparison to the control conditions.

Based on our results we propose a model for the XMAP215 activity. XMAP215 could use its five TOG repeats to be potentially allow the free tubulin dimers loading. Using this mechanism, the complex tubulin-XMAP215 reaches the MT growing end, using the XMAP215 C-terminal domain as the link among the MT structure and the protein. Once the filament-like structure has joined the structure, XMAP215 could participate of the mechanisms that drive to the final MT closure. As the MT structure continues to polymerize the +TIP XMAP215 do not leaves the MT surface, it evolves to a MT-related MAP protein, it evolves to a MT-XMAP215.

## **BIBLIOGRAPHY**



## Bibliography

**Akagi T, Shih LY, Kato M, Kawamata N, Yamamoto G, Sanada M, Okamoto R, Miller CW, Liang DC, Ogawa S, Koeffler HP.** 2009. Hidden abnormalities and novel classification of t(15;17) acute promyelocytic leukemia (APL) based on genomic alterations. *Blood*. Feb 19;113(8):1741-8.

**Akhmanova A, Hoogenraad CC.** 2005. Microtubule plus-end-tracking proteins: mechanisms and functions. *Curr Opin Cell Biol*. Feb;17(1):47-54.

**Akhmanova A, Steinmetz MO.** 2008. Tracking the ends: a dynamic protein network controls the fate of microtubule tips. *Nat Rev Mol Cell Biol*. Apr;9(4):309-22.

**Al-Bassam J, Ozer RS, Safer D, Halpain S, Milligan RA.** 2002. MAP2 and tau bind longitudinally along the outer ridges of microtubule protofilaments. *J Cell Biol*. Jun 24;157(7):1187-96.

**Al-Bassam J, van Breugel M, Harrison SC, Hyman A.** 2006. Stu2p binds tubulin and undergoes an open-to-closed conformational change. *J Cell Biol*. Mar 27;172(7):1009-22.

**Al-Bassam J, Larsen NA, Hyman AA, Harrison SC.** 2007. Crystal structure of a TOG domain: conserved features of XMAP215/Dis1-family TOG. *Structure*. Mar;15(3):355-62.

**Albee AJ, Tao W, Wiese C.** 2006. Phosphorylation of maskin by Aurora-A is regulated by RanGTP and importin beta. *J Biol Chem*. Dec 15;281(50): 38293-301.

**Alvarez S, MacGrogan D, Calasanz MJ, Nimer SD, Jhanwar SC.** 2001. Frequent gain of chromosome 19 in megakaryoblastic leukemias detected by comparative genomic hybridization. *Genes Chromosomes Cancer*. Nov;32(3):285-93.

**Amos LA, Baker TS.** 1979. The three-dimensional structure of tubulin protofilaments. *Nature*. Jun 14; 279(5714):607-12.

**Amos LA, Löwe J.** 1999. How Taxol stabilises microtubule structure. *Chem Biol*. Mar;6(3):R65-9.

**Andersen SS, Buendia B, Domínguez JE, Sawyer A, Karsenti E.** 1994. Effect on microtubule dynamics of XMAP230, a microtubule-associated protein present in *Xenopus laevis* eggs and dividing cells. *J Cell Biol*. Dec;127(5):1289-99.

- Andersen SS, Karsenti E.** 1997. XMAP310: a *Xenopus* rescue-promoting factor localized to the mitotic spindle. *J Cell Biol.* Nov 17;139(4):975-83.
- Andersen SS.** 1998. *Xenopus* interphase and mitotic microtubule-associated proteins differentially suppress microtubule dynamics in vitro. *Cell Motil Cytoskeleton.*; 41(3):202-13.
- Andersen SS.** 2000. Spindle assembly and the art of regulating microtubule dynamics by MAPs and Stathmin/Op18. *Trends Cell Biol.* Jul;10(7):261-7.
- Anderson P, Kedersha N.** 2006. RNA granules. *J Cell Biol.* Mar 13;172(6):803-8. Epub 2006 Mar 6.
- Anderson P, Kedersha N.** 2008. Stress granules: the Tao of RNA triage. *Trends Biochem Sci.* Mar;33(3):141-50.
- Andrade MA, Perez-Iratxeta C, Ponting CP.** 2001. Protein repeats: structures, functions, and evolution. *J Struct Biol.* May-Jun;134(2-3):117-31.
- Argyle DJ, Blacking T.** 2008. From viruses to cancer stem cells: dissecting the pathways to malignancy. *Vet J.* Sep;177(3):311-23.
- Arnal I, Karsenti E, Hyman AA.** 2000. Structural transitions at microtubule ends correlate with their dynamic properties in *Xenopus* egg extracts. *J Cell Biol.* May 15;149(4):767-74.
- Arnal I, Heichette C, Diamantopoulos GS, Chrétien D.** 2004. CLIP-170/tubulin-curved oligomers coassemble at microtubule ends and promote rescues. *Curr Biol.* Dec 14;14(23):2086-95.
- Asbury CL.** 2008. XMAP215: a tip tracker that really moves. *Cell.* Jan 11;132(1): 19-20
- Askham JM, Vaughan KT, Goodson HV, Morrison EE.** 2002. Evidence that an interaction between EB1 and p150(Glued) is required for the formation and maintenance of a radial microtubule array anchored at the centrosome. *Mol Biol Cell.* Oct;13(10):3627-45.
- Baker TS, Amos LA.** 1978. Structure of the tubulin dimer in zinc-induced sheets. *J Mol Biol.* Jul 25;123(1):89-106.
- Barnard DC, Cao Q, Richter JD.** 2005. Differential phosphorylation controls Maskin association with eukaryotic translation initiation factor 4E and localization on the mitotic apparatus. *Mol Cell Biol.* Sep;25(17):7605-15.
- Barr FA, Gruneberg U.** 2007. Cytokinesis: placing and making the final cut. *Cell.* Nov 30;131(5):847-60.



**Barros TP, Kinoshita K, Hyman AA, Raff JW.** 2005. Aurora A activates D-TACC-Msps complexes exclusively at centrosomes to stabilize centrosomal microtubules. *J Cell Biol.* Sep 26;170(7):1039-46.

**Basto R, Gergely F, Draviam VM, Ohkura H, Liley K, Raff JW.** 2007. Hsp90 is required to localise cyclin B and Msps/ch-TOG to the mitotic spindle in *Drosophila* and humans. *J Cell Sci.* Apr 1;120(Pt 7):1278-87.

**Becker BE, Gard DL.** 2000. Multiple isoforms of the high molecular weight microtubule associated protein XMAP215 are expressed during development in *Xenopus*. *Cell Motil Cytoskeleton.* Dec;47(4):282-95.

**Becker BE, Romney SJ, Gard DL.** 2003. XMAP215, XKCM1, NuMA, and cytoplasmic dynein are required for the assembly and organization of the transient microtubule array during the maturation of *Xenopus* oocytes. *Dev Biol.* Sep 15;261(2):488-505.

**Belmont LD, Hyman AA, Sawin KE, Mitchison TJ.** 1990. Real-time visualization of cell cycle-dependent changes in microtubule dynamics in cytoplasmic extracts. *Cell.* Aug 10;62(3):579-89.

**Blasius TL, Cai D, Jih GT, Toret CP, Verhey KJ.** 2007. Two binding partners cooperate to activate the molecular motor Kinesin-1. *J Cell Biol.* Jan 1;176(1):11-7.

**Bloom K.** 2004. Microtubule composition: cryptography of dynamic polymers. *Proc Natl Acad Sci U S A.* May 4;101(18):6839-40.

**Boerman RH, Anderl K, Herath J, Borell T, Johnson N, Schaeffer-Klein J, Kirchhof A, Raap AK, Scheithauer BW, Jenkins RB.** 1996. The glial and mesenchymal elements of gliosarcomas share similar genetic alterations. *J Neuropathol Exp Neurol.* Sep;55(9):973-81.

**Bonaldo MF, Lennon G, Soares MB.** 1996. Normalization and subtraction: two approaches to facilitate gene discovery. *Genome Res.* Sep;6(9):791-806.

**Bouchet-Marquis C, Zuber B, Glynn AM, Eltsov M, Grabenbauer M, Goldie KN, Thomas D, Frangakis AS, Dubochet J, Chrétien D.** 2007. Visualization of cell microtubules in their native state. *Biol Cell.* Jan;99(1):45-53.

**Brittle AL, Ohkura H.** 2005. Mini spindles, the XMAP215 homologue, suppresses pausing of interphase microtubules in *Drosophila*. *EMBO J.* Apr 6;24(7):1387-96.

**Brouhard GJ, Stear JH, Noetzel TL, Al-Bassam J, Kinoshita K, Harrison SC, Howard J, Hyman AA.** 2008. XMAP215 is a processive microtubule polymerase. *Cell.* Jan 11;132(1):79-88.

- Bu W, Su LK.** 2003.Characterization of functional domains of human EB1 family proteins. *J Biol Chem.* Dec 12;278(50):49721-31.
- Budde PP, Desai A, Heald R.**2006.Analysis of microtubule polymerization in vitro and during the cell cycle in *Xenopus* egg extracts. *Methods.* Jan;38(1):29-34.
- Cai YR, Gong L, Teng XY, Zhang HT, Wang CF, Wei GL, Guo L, Ding F, Liu ZH, Pan QJ, Su Q.** 2009. Clonality and allelotype analyses of focal nodular hyperplasia compared with hepatocellular adenoma and carcinoma. *World J Gastroenterol.* Oct 7;15(37):4695-708.
- Carson JH, Blondin N, Korza G.** 2006. Rules of engagement promote polarity in RNA trafficking. *BMC Neurosci.* Oct 30;7 Suppl 1:S3.
- Carvalho P, Tirnauer JS, Pellman D.** 2003.Surfing on microtubule ends. *Trends Cell Biol.* May;13(5):229-37.
- Cassimeris L.** 1993. Regulation of microtubule dynamic instability. *Cell Motil Cytoskeleton.*;26(4):275-81.
- Cassimeris L.** 1999. Accessory protein regulation of microtubule dynamics throughout the cell cycle. *Curr Opin Cell Biol.* Feb;11(1):134-41.
- Cassimeris L, Gard D, Tran PT, Erickson HP.** 2001. XMAP215 is a long thin molecule that does not increase microtubule stiffness. *J Cell Sci.* Aug;114(Pt 16):3025-33.
- Cassimeris L, Morabito J.** 2004. TOGp, the human homolog of XMAP215/Dis1, is required for centrosome integrity, spindle pole organization, and bipolar spindle assembly. *Mol Biol Cell.* Apr;15(4):1580-90.
- Charrasse S, Mazel M, Taviaux S, Berta P, Chow T, Larroque C.** 1995. Characterization of the cDNA and pattern of expression of a new gene over-expressed in human hepatomas and colonic tumors. *Eur J Biochem.* Dec 1;234(2):406-13.
- Charrasse S, Coubes P, Arrancibia S, Larroque C.** 1996. Expression of the tumor over-expressed ch-TOG gene in human and baboon brain. *Neurosci Lett.* Jul 12;212(2):119-22.
- Charrasse S, Schroeder M, Gauthier-Rouviere C, Ango F, Cassimeris L, Gard DL, Larroque C.** 1998. The TOGp protein is a new human microtubule-associated protein homologous to the *Xenopus* XMAP215. *J Cell Sci.* May;111 (Pt 10):1371-83.
- Charrasse S, Lorca T, Dorée M, Larroque C.** 2000.The *Xenopus* XMAP215 and its human homologue TOG proteins interact with cyclin B1 to target p34cdc2 to microtubules during mitosis. *Exp Cell Res.* Feb 1;254(2):249-56.

- Cheeseman IM, Desai A.** 2008. Molecular architecture of the kinetochore-microtubule interface. *Nat Rev Mol Cell Biol.* Jan;9(1):33-46.
- Chen C, Okayama H.** 1987. High-efficiency transformation of mammalian cells by plasmid DNA. *Mol Cell Biol.* Aug;7(8):2745-52.
- Chen P, Shen WZ, Karnik P.** 2004. Suppression of malignant growth of human breast cancer cells by ectopic expression of integrin-linked kinase. *Int J Cancer.* Oct 10;111(6):881-91.
- Chesnel F, Vignaux F, Richard-Parpaillon L, Huguet A, Kubiak JZ.** 2005. Differences in regulation of the first two M-phases in *Xenopus laevis* embryo cell-free extracts. *Dev Biol.* Sep 15;285(2):358-75.
- Chrétien D, Fuller SD, Karsenti E.** 1995. Structure of growing microtubule ends: two-dimensional sheets close into tubes at variable rates. *J Cell Biol.* Jun;129(5):1311-28.
- Coleman WB, Esch GL, Borchert KM, McCullough KD, Reid LH, Weissman BE, Smith GJ, Grisham JW.** 1997. Localization of a putative liver tumor suppressor locus to a 950-kb region of human 11p11.2-p12 using rat liver tumor microcell hybrid cell lines. *Mol Carcinog.* Aug;19(4):267-72.
- Collins CA, Vallee RB.** 1989. Preparation of microtubules from rat liver and testis: cytoplasmic dynein is a major microtubule associated protein. *Cell Motil Cytoskeleton.* 14(4):491-500.
- Conte N, Charafe-Jauffret E, Delaval B, Adélaïde J, Ginestier C, Geneix J, Isnardon D, Jacquemier J, Birnbaum D.** 2002. Carcinogenesis and translational controls: TACC1 is down-regulated in human cancers and associates with mRNA regulators. *Oncogene.* Aug 15;21(36):5619-30.
- Conte N, Delaval B, Ginestier C, Ferrand A, Isnardon D, Larroque C, Prigent C, Séraphin B, Jacquemier J, Birnbaum D.** 2003. TACC1-chTOG-Aurora A protein complex in breast cancer. *Oncogene.* Nov 6;22(50):8102-16.
- Coquelle FM, Vitre B, Arnal I.** 2009. Structural basis of EB1 effects on microtubule dynamics. *Biochem Soc Trans.* Oct;37(Pt 5):997-1001
- Cullen CF, Deák P, Glover DM, Ohkura H.** 1999. mini spindles: A gene encoding a conserved microtubule-associated protein required for the integrity of the mitotic spindle in *Drosophila*. *J Cell Biol.* Sep 6;146(5):1005-18.
- Cullen CF, Ohkura H.** 2001. Msps protein is localized to acentrosomal poles to ensure bipolarity of *Drosophila* meiotic spindles. *Nat Cell Biol.* Jul;3(7):637-42.
- Culver-Hanlon TL, Lex SA, Stephens AD, Quintyne NJ, King SJ.** 2006. A microtubule-binding domain in dynactin increases dynein processivity by skating along microtubules. *Nat Cell Biol.* Mar;8(3):264-70.

**Dammermann A, Desai A, Oegema K.** 2003. The minus end in sight. *Curr Biol.* Aug 5;13(15):R614-24.

**Desai A, Mitchison TJ.** 1997. Microtubule polymerization dynamics. *Annu Rev Cell Dev Biol.*;13:83-117.

**De Robertis E, Schmitt FO.** 1948. An electron microscope analysis of certain nerve axon constituents. *J Cell Physiol.* Feb;31(1):1-23.

**des Georges A, Katsuki , Drummond DR, Osei M, Cross RA, Amos LA.** 2008. Mal3, the *Schizosaccharomyces pombe* homolog of EB1, changes the microtubule lattice. *Nat Struct Mol Biol.* Oct;15(10):1102-8

**Dighiero G.** 2002. Chronic lymphoid leukemia: a single disease or 2 distinct diseases? *Bull Acad Natl Med.*;186(7):1251-66; discussion 1266-8.

**Dong JT, Lamb PW, Rinker-Schaeffer CW, Vukanovic J, Ichikawa T, Isaacs JT, Barrett JC.** 1995. KAI1, a metastasis suppressor gene for prostate cancer on human chromosome 11p11.2. *Science.* May 12;268(5212):884-6.

**Dragestein KA, van Cappellen WA, van Haren J, Tsibidis GD, Akhmanova A, Knoch TA, Grosveld F, Galjart N.** 2008. Dynamic behavior of GFP-CLIP-170 reveals fast protein turnover on microtubule plus ends. *J Cell Biol.* Feb 25;180(4):729-37.

**Drewes G, Ebneith A, Preuss U, Mandelkow EM, Mandelkow E.** 1997. MARK, a novel family of protein kinases that phosphorylate microtubule-associated proteins and trigger microtubule disruption. *Cell.* Apr 18;89(2):297-308.

**Erck C, Peris L, Andrieux A, Meissirel C, Gruber AD, Vernet M, Schweitzer A, Saoudi Y, Pointu H, Bosc C, Salin PA, Job D, Wehland J.** 2005. A vital role of tubulin-tyrosine-ligase for neuronal organization. *Proc Natl Acad Sci U S A.* May 31;102(22):7853-8.

**Fielding AB, Dobрева I, Dedhar S.** 2008. Beyond focal adhesions: integrin-linked kinase associates with tubulin and regulates mitotic spindle organization. *Cell Cycle.* Jul;7(13):1899-906.

**Fielding AB, Dobрева I, McDonald PC, Foster LJ, Dedhar S.** 2008. Integrin-linked kinase localizes to the centrosome and regulates mitotic spindle organization. *J Cell Biol.* Feb 25;180(4):681-9.

**Folker ES, Baker BM, Goodson HV.** 2005. Interactions between CLIP-170, tubulin, and microtubules: implications for the mechanism of Clip-170 plus-end tracking behavior. *Mol Biol Cell.* Nov;16(11):5373-84.

**Fourest-Lieuvain A, Peris L, Gache V, Garcia-Saez I, Juillan-Binard C, Lantéz V, Job D.** 2006. Microtubule regulation in mitosis: tubulin

phosphorylation by the cyclin-dependent kinase Cdk1. *Mol Biol Cell*. Mar;17(3):1041-50.

**Francone VP, Maggipinto MJ, Kosturko LD, Barbarese E.** 2007. The microtubule-associated protein tumor Overexpressed gene/cytoskeleton-associated protein 5 is necessary for myelin basic protein expression in oligodendrocytes. *J Neurosci*. Jul 18;27(29):7654-62.

**Francone VP, Maggipinto MJ, Kosturko LD, Barbarese E.** 2007. The microtubule-associated protein tumor Overexpressed gene/cytoskeleton-associated protein 5 is necessary for myelin basic protein expression in oligodendrocytes. *J Neurosci*. Jul 18;27(29):7654-62.

**Frixione E.** 2000. Recurring views on the structure and function of the cytoskeleton: a 300-year epic. *Cell Motil Cytoskeleton*. Jun;46(2):73-94.

**Galjart N, Perez F.** 2003. A plus-end raft to control microtubule dynamics and function. *Curr Opin Cell Biol*. Feb;15(1):48-53.

**Galjart N.** 2005. CLIPs and CLASPs and cellular dynamics. *Nat Rev Mol Cell Biol*. Jun;6(6):487-98.

**Ganem NJ, Compton DA.** 2006. Functional roles of poleward microtubule flux during mitosis. *Cell Cycle*. Mar;5(5):481-5.

**Gangisetty O, Lauffart B, Sondarva GV, Chelsea DM, Still IH.** 2004. The transforming acidic coiled coil proteins interact with nuclear histone cetyltransferases. *Oncogene*. Apr 1;23(14):2559-63.

**Garcia MA, Vardy L, Koonrugsa N, Toda T.** 2001. Fission yeast ch-TOG/XMAP215 homologue Alp14 connects mitotic spindles with the kinetochore and is a component of the Mad2-dependent spindle checkpoint. *EMBO J*. Jul 2;20(13):3389-401.

**Gard DL, Kirschner MW.** 1987. Microtubule assembly in cytoplasmic extracts of *Xenopus* oocytes and eggs. *J Cell Biol*. Nov;105(5):2191-201.

**Gard DL, Kirschner MW.** 1987. A microtubule-associated protein from *Xenopus* eggs that specifically promotes assembly at the plus-end. *J Cell Biol*. Nov;105(5):2203-15.

**Gard DL, Becker BE, Josh Romney S.** 2004. MAPping the eukaryotic tree of life: structure, function, and evolution of the MAP215/Dis1 family of microtubule-associated proteins. *Int Rev Cytol*;239:179-272.

**Gardner MK, Hunt AJ, Goodson HV, Odde DJ.** 2008. Microtubule assembly dynamics: new insights at the nanoscale. *Curr Opin Cell Biol*. Feb;20 (1):64-70.

**Gardner MK, Hunt AJ, Goodson HV, Odde DJ.** 2008. Microtubule assembly dynamics: new insights at the nanoscale. *Curr Opin Cell Biol.* Feb;20(1):64-70.

**Gergely F, Karlsson C, Still I, Cowell J, Kilmartin J, Raff JW.** 2000. The TACC domain identifies a family of centrosomal proteins that can interact with microtubules. *Proc Natl Acad Sci U S A.* Dec 19;97(26): 14352-7.

**Gergely F.** 2002. Centrosomal TACCtics. *Bioessays.* Oct;24(10):915-25.

**Gergely F, Draviam VM, Raff JW.** 2003. The ch-TOG/XMAP215 protein is essential for spindle pole organization in human somatic cells. *Genes Dev.* Feb 1;17(3):336-41.

**Gill SR, Schroer TA, Szilak I, Steuer ER, Sheetz MP, Cleveland DW.** 1991. Dynactin, a conserved, ubiquitously expressed component of an activator of vesicle motility mediated by cytoplasmic dynein. *J Cell Biol.* Dec;115(6):1639-50.

**Gimona M, Djinovic-Carugo K, Kranewitter WJ, Winder SJ.** 2002. Functional plasticity of CH domains. *FEBS Lett.* Feb 20;513(1):98-106.

**Gorello P, La Starza R, Varasano E, Chiaretti S, Elia L, Pierini V, Barba G, Brandimarte L, Crescenzi B, Vitale A, Messina M, Grammatico S, Mancini M, Matteucci C, Bardi A, Guarini A, Martelli MF, Foà R, Mecucci C.** 2010. Combined interphase fluorescence in situ hybridization elucidates the genetic heterogeneity of T-cell acute lymphoblastic leukemia in adults. *Haematologica.* Jan;95(1):79-86.

**Gräf R, Dauderer C, Schliwa M.** 2000. Dictyostelium DdCP224 is a microtubule-associated protein and a permanent centrosomal resident involved in centrosome duplication. *J Cell Sci.* May;113 ( Pt 10):1747-58.

**Green RA, Wollman R, Kaplan KB.** 2005. APC and EB1 function together in mitosis to regulate spindle dynamics and chromosome alignment. *Mol Biol Cell.* Oct;16(10):4609-22.

**Groisman I, Huang YS, Mendez R, Cao Q, Theurkauf W, Richter JD.** 2000. CPEB, maskin, and cyclin B1 mRNA at the mitotic apparatus: implications for local translational control of cell division. *Cell.* Oct 27;103(3): 435-47.

**Gupta M, Raghavan M, Gale RE, Chelala C, Allen C, Molloy G, Chaplin T, Linch DC, Cazier JB, Young BD.** 2008. Novel regions of acquired uniparental disomy discovered in acute myeloid leukemia. *Genes Chromosomes Cancer.* Sep;47(9):729-39.

**Hainfeld JF, Liu W, Halsey CM, Freimuth P, Powell RD.** 1999. Ni-NTA-gold clusters target His-tagged proteins. *J Struct Biol.* Sep;127(2):185-98.

**Hammond JW, Cai D, Verhey KJ.** 2007. Tubulin modifications and their cellular functions. *Curr Opin Cell Biol.* Feb;20(1):71-6.

**Hayashi I, Ikura M.** 2003. Crystal structure of the amino-terminal microtubule-binding domain of end-binding protein 1 (EB1). *J Biol Chem.* Sep 19;278(38):36430-4.

**Hayashi I, Plevin MJ, Ikura M.** 2007. CLIP170 autoinhibition mimics intermolecular interactions with p150Glued or EB1. *Nat Struct Mol Biol.* Oct;14(10):980-1.

**Hannak E, Heald R.** 2006. Investigating mitotic spindle assembly and function in vitro using *Xenopus laevis* egg extracts. *Nat Protoc.*;1(5) :2305-14.

**Heald R.** 2000. A dynamic duo of microtubule modulators. *Nat Cell Biol.* Jan;2(1): E11-2.

**Helenius J, Brouhard G, Kalaidzidis Y, Diez S, Howard J.** 2006. The depolymerizing kinesin MCAK uses lattice diffusion to rapidly target microtubule ends. *Nature.* May 4;441(7089):115-9.

**Hestermann A, Gräf R.** 2004. The XMAP215-family protein DdCP224 is required for cortical interactions of microtubules. *BMC Cell Biol.* Jun 8;5:24.

**Holzbaur EL, Hammarback JA, Paschal BM, Kravit NG, Pfister KK, Vallee RB.** 1991. Homology of a 150K cytoplasmic dynein-associated polypeptide with the *Drosophila* gene Glued. *Nature.* Jun 13;351(6327):579-83.

**Holmfeldt P, Stenmark S, Gullberg M.** 2004. Differential functional interplay of TOGp/XMAP215 and the KinI kinesin MCAK during interphase and mitosis. *EMBO J.* Feb 11;23(3):627-37.

**Holmfeldt P, Zhang X, Stenmark S, Walczak CE, Gullberg M.** 2005. CaMKIIγ-mediated inactivation of the Kin I kinesin MCAK is essential for bipolar spindle formation. *EMBO J.* Mar 23;24(6):1256-66.

**Holzbaur EL, Hammarback JA, Paschal BM, Kravit NG, Pfister KK, Vallee RB.** 1991. Homology of a 150K cytoplasmic dynein-associated polypeptide with the *Drosophila* gene Glued. *Nature.* Jun 13;351(6327):579-83.

**Honnappa S, Okhrimenko O, Jaussi R, Jawhari H, Jelesarov I, Winkler FK, Steinmetz MO.** 2006. Key interaction modes of dynamic +TIP networks. *Mol Cell.* Sep 1;23(5):663-71.

**Howard J, Hyman AA.** 2003. Dynamics and mechanics of the microtubule plus end. *Nature.* Apr 17;422(6933):753-8.

**Hughes JR, Meireles AM, Fisher KH, Garcia A, Antrobus PR, Wainman A, Zitzmann N, Deane C, Ohkura H, Wakefield JG.** 2008. A microtubule

interactome: complexes with roles in cell cycle and mitosis. *PLoS Biol.* Apr 22;6(4):e98.

**Ishikawa K, Kamohara Y, Tanaka F, Haraguchi N, Mimori K, Inoue H, Mori M.** 2008. Mitotic centromere-associated kinesin is a novel marker for prognosis and lymph node metastasis in colorectal cancer. *Br J Cancer.* Jun 3;98(11):1824-9.

**Joglekar AP, Bouck DC, Molk JN, Bloom KS, Salmon ED.** 2006. Molecular architecture of a kinetochore-microtubule attachment site. *Nat Cell Biol.* Jun;8(6):581-5.

**Jordan MA, Wilson L** 2004. Microtubules as a target for anticancer drugs. *Nat Rev Cancer.* Apr;4(4):253-65.

**Kaname T, Kuwano A, Murano I, Uehara K, Muramatsu T, Kajii T.** 1993. Midkine gene (MDK), a gene for prenatal differentiation and neuroregulation, maps to band 11p11.2 by fluorescence in situ hybridization. *Genomics.* Aug;17(2):514-5.

**Kardon JR, Reck-Peterson SL, Vale RD.** 2009. Regulation of the processivity and intracellular localization of *Saccharomyces cerevisiae* dynein by dynactin. *Proc Natl Acad Sci U S A.* Apr 7;106(14):5669-74.

**Kawai J, Shinagawa A, Shibata K, Yoshino M, Itoh M, Ishii Y, Arakawa T, Hara A.** 2001. Functional annotation of a full-length mouse cDNA collection. *Nature.* Feb 8;409(6821):685-90.

**Kazazian HH, Junien C.** 1987. Report of the committee on the genetic constitution of chromosomes 10, 11, and 12. *Cytogenet Cell Genet.* 46(1-4):188-212.

**Kerssemakers J, Howard J, Hess H, Diez S.** 2006. The distance that kinesin-1 holds its cargo from the microtubule surface measured by fluorescence interference contrast microscopy. *Proc Natl Acad Sci U S A.* Oct 24;103(43):15812-7.

**Kerssemakers JW, Munteanu EL, Laan L, Noetzel TL, Janson ME, Dogterom M.** 2006. Assembly dynamics of microtubules at molecular resolution. *Nature.* Aug 10;442(7103):709-12.

**Kikkawa M, Metlagel Z.** 2006. A molecular "zipper" for microtubules. *Cell.* Dec 29;127(7):1302-4.

**Kinoshita K, Arnal I, Desai A, Drechsel DN, Hyman AA.** 2001. Reconstitution of physiological microtubule dynamics using purified components. *Science.* Nov 9;294(5545):1340-3.



**Kinoshita K, Habermann B, Hyman AA.** 2002. XMAP215: a key component of the dynamic microtubule cytoskeleton. *Trends Cell Biol.* Jun;12(6):267-73.

**Kinoshita K, Noetzel TL, Pelletier L, Mechtler K, Drechsel DN, Schwager A, Lee M, Raff JW, Hyman AA.** 2005. Aurora A phosphorylation of TACC3/maskin is required for centrosome-dependent microtubule assembly in mitosis. *J Cell Biol.* Sep 26;170(7):1047-55.

**Komarova Y, Lansbergen G, Galjart N, Grosveld F, Borisy GG, Akhmanova A.** 2005. EB1 and EB3 control CLIP dissociation from the ends of growing microtubules. *Mol Biol Cell.* Nov;16(11):5334-45.

**Kosturko LD, Maggipinto MJ, D'Sa C, Carson JH, Barbarese E.** 2005. The microtubule-associated protein tumor overexpressed gene binds to the RNA trafficking protein heterogeneous nuclear ribonucleoprotein A2. *Mol Biol Cell.* Apr;16(4):1938-47.

**Kosturko LD, Maggipinto MJ, Korza G, Lee JW, Carson JH, Barbarese E.** 2006. Heterogeneous nuclear ribonucleoprotein (hnRNP) E1 binds to hnRNP A2 and inhibits translation of A2 response element mRNAs. *Mol Biol Cell.* Aug;17(8):3521-33.

**Kronja I, Kruljac-Letunic A, Caudron-Herger M, Bieling P, Karsenti E.** 2009. XMAP215-EB1 interaction is required for proper spindle assembly and chromosome segregation in *Xenopus* egg extract. *Mol Biol Cell.* Jun 1 (20): 2684-2696.

**Lansbergen G, Komarova Y, Modesti M, Wyman C, Hoogenraad CC, Goodson HV, Lemaitre RP, Drechsel DN, van Munster E, Gadella TW Jr, Grosveld F, Galjart N, Borisy GG, Akhmanova A.** 2004. Conformational changes in CLIP-170 regulate its binding to microtubules and dynactin localization. *J Cell Biol.* Sep 27;166(7):1003-14.

**Lansbergen G, Akhmanova A.** 2006. Microtubule plus end: a hub of cellular activities. *Traffic.* May;7(5):499-507.

**Lappin TR, Mullan RN, Stewart JP, Morgan NA, Thompson A, Maxwell AP.** 2002. AINT/ERIC/TACC: an expanding family of proteins with C-terminal coiled coil domains. *Leuk Lymphoma.* Jul;43(7):1455-9.

**Lauffart B, Howell SJ, Tasch JE, Cowell JK, Still IH.** 2002. Interaction of the transforming acidic coiled-coil 1 (TACC1) protein with ch-TOG and GAS41/NuBI1 suggests multiple TACC1-containing protein complexes in human cells. *Biochem J.* Apr 1;363(Pt 1):195-200.

**Le Breton M, Cormier P, Bellé R, Mulner-Lorillon O, Morales J.** 2005. Translational control during mitosis. *Biochimie.* Sep-Oct;87(9-10):805-11.

- Lee MJ, Gergely F, Jeffers K, Peak-Chew SY, Raff JW.** 2001. Msps/XMAP215 interacts with the centrosomal protein D-TACC to regulate microtubule behaviour. *Nat Cell Biol.* Jul;3(7):643-9.
- Lee T, Langford KJ, Askham JM, Brüning-Richardson A, Morrison EE.** 2008. MCAK associates with EB1. *Oncogene.* Apr 10;27(17):2494-500.
- Lehnert S, Götz C, Kartarius S, Schäfer B, Montenarh M.** 2008. Protein kinase CK2 interacts with the splicing factor hPrp3p. *Oncogene.* Apr 10;27(17):2390-400.
- Ligon LA, Shelly SS, Tokito M, Holzbaur EL.** 2003. The microtubule plus-end proteins EB1 and dynactin have differential effects on microtubule polymerization. *Mol Biol Cell.* Apr;14(4):1405-17.
- Ligon LA, Shelly SS, Tokito MK, Holzbaur EL.** 2006. Microtubule binding proteins CLIP-170, EB1, and p150Glued form distinct plus-end complexes. *FEBS Lett.* Feb 20;580(5):1327-32.
- Lohka MJ, Maller JL.** 1985. Induction of nuclear envelope breakdown, chromosome condensation, and spindle formation in cell-free extracts. *J Cell Biol.* Aug;101(2):518-23.
- López de Heredia M, Jansen RP.** 2004. mRNA localization and the cytoskeleton. *Curr Opin Cell Biol.* Feb;16(1):80-5.
- Lothe RA, Peltomäki P, Tommerup N, Fosså SD, Stenwig AE, Børresen AL, Nesland JM.** 1995. Molecular genetic changes in human male germ cell tumors. *Lab Invest.* Nov;73(5):606-14.
- Mandelkow EM, Thies E, Trinczek B, Biernat J, Mandelkow E.** 2004. MARK/PAR1 kinase is a regulator of microtubule-dependent transport in axons. *J Cell Biol.* Oct 11;167(1):99-110.
- Mandelkow EM, Mandelkow E, Milligan RA.** 1991. Microtubule dynamics and microtubule caps: a time-resolved cryo-electron microscopy study. *J Cell Biol.* Sep;114(5):977-91.
- Manna T, Honnappa S, Steinmetz MO, Wilson L.** 2008. Suppression of microtubule dynamic instability by the +TIP protein EB1 and its modulation by the CAP-Gly domain of p150glued. *Biochemistry.* Jan 15;47(2):779-86.
- Manning AL, Compton DA.** 2008. Structural and regulatory roles of non motor spindle proteins. *Curr Opin Cell Biol.* Feb;20(1):101-6.
- Matthews LR, Carter P, Thierry-Mieg D, Kempfues K.** 1998. ZYG-9, a *Caenorhabditis elegans* protein required for microtubule organization and function, is a component of meiotic and mitotic spindle poles. *J Cell Biol.* Jun 1;141(5):1159-68.

- May KM, Hardwick KG.** 2006. The spindle checkpoint. *J Cell Sci.* Oct 15;119 (Pt 20):4139-42.
- McNally F.** 2003. Microtubule dynamics: new surprises from an old MAP. *Curr Biol.* Aug 5;13(15):R597-9.
- Mili S, Moissoglu K, Macara IG.** 2008. Genome-wide screen reveals APC-associated RNAs enriched in cell protrusions. *Nature.* May 1;453(7191):115-9.
- Mimori-Kiyosue Y, Grigoriev I, Lansbergen G, Sasaki H, Matsui C, Severin F, Galjart N, Grosveld F, Vorobjev I, Tsukita S, Akhmanova A.** 2005. CLASP1 and CLASP2 bind to EB1 and regulate microtubule plus-end dynamics at the cell cortex. *J Cell Biol.* Jan 3;168(1):141-53.
- Mishima M, Maesaki R, Kasa M, Watanabe T, Fukata M, Kaibuchi K, Hakoshima T.** 2007. Structural basis for tubulin recognition by cytoplasmic linker protein 170 and its autoinhibition. *Proc Natl Acad Sci U S A.* Jun 19;104 (25):10346-51.
- Mishima M, Pavicic V, Grüneberg U, Nigg EA, Glotzer M.** 2004. Cell cycle regulation of central spindle assembly. *Nature.* Aug 19;430(7002):908-13.
- Mohr E, Richter D.** 2001. Messenger RNA on the move: implications for cell polarity. *Int J Biochem Cell Biol.* Jul;33(7):669-79.
- Monk M, Holding C.** 2001. Human embryonic genes re-expressed in cancer cells. *Oncogene.* Dec 6;20(56):8085-91.
- Morrison EE, Wardleworth BN, Askham JM, Markham AF, Meredith DM.** 1998. EB1, a protein which interacts with the APC tumour suppressor, is associated with the microtubule cytoskeleton throughout the cell cycle. *Oncogene.* Dec 31;17(26):3471-7.
- Morrison EE.** 2006. Action and interactions at microtubule ends. *Cell Mol Life Sci.* Feb;64(3):307-17.
- Musacchio A, Salmon ED.** 2007. The spindle-assembly checkpoint in space and time. *Nat Rev Mol Cell Biol.* May;8(5):379-93.
- Nagase T, Seki N, Tanaka A, Ishikawa K, Nomura N.** 1995. Prediction of the coding sequences of unidentified human genes. IV. The coding sequences of 40 new genes (KIAA0121-KIAA0160) deduced by analysis of cDNA clones from human cell line KG-1. *DNA Res.* Aug 31;2(4):167-74, 199-210.
- Nakamura T, Nagao K, Nakaseko Y, Yanagida M.** 2002. Cut1/separase C-terminus affects spindle pole body positioning in interphase of fission yeast: pointed nuclear formation. *Genes Cells.* Nov;7(11):1113-24.

**Nakanishi H, Matsumoto S, Iwakawa R, Kohno T, Suzuki K, Tsuta K, Matsuno Y, Noguchi M, Shimizu E, Yokota J.** 2009. Whole genome comparison of allelic imbalance between noninvasive and invasive small-sized lung adenocarcinomas. *Cancer Res.* Feb 15;69(4):1615-23.

**Nakaseko Y, Goshima G, Morishita J, Yanagida M.** 2001. M phase-specific kinetochore proteins in fission yeast: microtubule-associating Dis1 and Mtc1 display rapid separation and segregation during anaphase. *Curr Biol.* Apr 17;11(8):537-49.

**Niethammer P, Kronja I, Kandels-Lewis S, Rybina S, Bastiaens P, Karsenti E.** 2007. Discrete states of a protein interaction network govern interphase and mitotic microtubule dynamics. *PLoS Biol.* Feb;5(2):e29.

**Noetzel TL, Drechsel DN, Hyman AA, Kinoshita K.** 2005. A comparison of the ability of XMAP215 and tau to inhibit the microtubule destabilizing activity of XKCM1. *Philos Trans R Soc Lond B Biol Sci.* Mar 29;360(1455):591-4.

**O'Brien LL, Albee AJ, Liu L, Tao W, Dobrzyn P, Lizarraga SB, Wiese C.** 2005. The *Xenopus* TACC homologue, maskin, functions in mitotic spindle assembly. *Mol Biol Cell.* Jun;16(6):2836-47.

**O'Connell CB, Khodjakov AL.** 2007. Cooperative mechanisms of mitotic spindle formation. *J Cell Sci.* May 15;120(Pt 10):1717-22.

**Ohkura H, Adachi Y, Kinoshita N, Niwa O, Toda T, Yanagida M.** 1988. Cold-sensitive and caffeine-supersensitive mutants of the *Schizosaccharomyces pombe* *dis* genes implicated in sister chromatid separation during mitosis. *EMBO J.* May;7(5):1465-73

**Ohkura H, Garcia MA, Toda T.** 2001. Dis1/TOG universal microtubule adaptors - one MAP for all?. *J Cell Sci.* Nov;114 (Pt 21):3805-12.

**Pascreau G, Delcros JG, Cremet JY, Prigent C, Arlot-Bonnemains Y.** 2005. Phosphorylation of maskin by Aurora-A participates in the control of sequential protein synthesis during *Xenopus laevis* oocyte maturation. *Biol Chem.* Apr 8;280(14):13415-23.

**Perez F, Diamantopoulos GS, Stalder R, Kreis TE.** 1999. CLIP-170 highlights growing microtubule ends in vivo. *Cell.* Feb 19;96(4):517-27.

**Peris L, Thery M, Fauré J, Saoudi Y, Lafanechère L, Chilton JK, Gordon-Weeks P, Galjart N, Bornens M, Wordeman L, Wehland J, Andrieux A, Job D.** 2006. Tubulin tyrosination is a major factor affecting the recruitment of CAP-Gly proteins at microtubule plus ends. *J Cell Biol.* Sep 11;174 (6):839-49.

**Peset I, Seiler J, Sardon T, Bejarano LA, Rybina S, Vernos I.** 2005. Function and regulation of Maskin, a TACC family protein, in microtubule growth during mitosis. *J Cell Biol.* Sep 26;170(7):1057-66.

**Pfeiffer DC, Gard DL.** 1999. Microtubules in *Xenopus* oocytes are oriented with their minus-ends towards the cortex. *Cell Motil cytoskeleton*; 44 (1):34-43.

**Phan TX, Hoang AV, Huynh VM, Nguyen KT, Nguyen TB, Huynh N, Pham QT, Tran VB, Tran VB, Tokunaga K, Sato Y.** 2006. Unique secondary chromosomal abnormalities are frequently found in the chronic phase of chronic myeloid leukemia in southern Vietnam. *Cancer Genet Cytogenet.* Jul 1;168(1):59-68.

**Pierre P, Scheel J, Rickard JE, Kreis TE.** 1992. CLIP-170 links endocytic vesicles to microtubules. *Cell.* Sep 18;70(6):887-900.

**Piette BM, Liu J, Peeters K, Smertenko A, Hawkins T, Deeks M, Quinlan R, Zakrzewski WJ, Hussey PJ.** 2009. A thermodynamic model of microtubule assembly and disassembly. *PLoS One.* Aug 11;4(8):e6378

**Pollard TD.** 2003. The cytoskeleton, cellular motility and the reductionist agenda. *Nature.* Apr 17;422(6933):741-5.

**Popov, A., Pozniakovsky, A., Arnal, I., Antony, C., Ashford, A., Kinoshita, K., Tournebise, R., Hyman, A., Karsenti, E.** 2001. XMAP215 regulates microtubule dynamics through two distinct domains. *EMBO J.* 20 (2) :397-410.

**Popov, A., Severin, S., Karsenti, A.** 2002. XMAP215 is required for the microtubule-nucleating activity of centrosomes. *Curr Biol.* 2002 Aug 6;12(15):1326-30.

**Popov AV, Karsenti E.** 2003. Stu2p and XMAP215: turncoat microtubule associated proteins?. *Trends Cell Biol.* Nov;13(11):547-50.

**Ricketts SL, Carter JC, Coleman WB.** 2003. Identification of three 11p11.2 candidate liver tumor suppressors through analysis of known human genes. *Mol Carcinog.* Feb;36(2):90-9.

**Rogers SL, Rogers GC, Sharp DJ, Vale RD.** 2002. Drosophila EB1 is important for proper assembly, dynamics, and positioning of the mitotic spindle. *J Cell Biol.* Sep 2;158(5):873-84.

**Ross JL, Ali MY, Warshaw DM.** 2008. Cargo transport: molecular motors navigate a complex cytoskeleton. *Curr Opin Cell Biol.* Feb;20(1):41-7.

**Rosenbaum J.** 2000. Cytoskeleton: functions for tubulin modifications at last. *Curr Biol.* Nov 2;10(21):R801-3.

**Roversi G, Pfundt R, Moroni RF, Magnani I, van Reijmersdal S, Pollo B, Straatman H, Larizza L, Schoenmakers EF.** 2006. Identification of novel genomic markers related to progression to glioblastoma through genomic profiling of 25 primary glioma cell lines. *Oncogene.* Mar 9;25(10):1571-83.

- Sadek CM, Pelto-Huikko M, Tujague M, Steffensen KR, Wennerholm M, Gustafsson JA.** 2003. TACC3 expression is tightly regulated during early differentiation. *Gene Expr Patterns*. May;3(2):203-11.
- Sandblad L, Busch KE, Tittmann P, Gross H, Brunner D, Hoenger A.** 2006. The Schizosaccharomyces pombe EB1 homolog Mal3p binds and stabilizes the microtubule lattice seam. *Cell*. Dec 29;127(7):1415-24.
- Sankaran S, Parvin JD.** 2006. Centrosome function in normal and tumor cells. *J Cell Biochem*. Dec 1;99(5):1240-50.
- Schek HT 3rd, Gardner MK, Cheng J, Odde DJ, Hunt AJ.** 2007. Microtubule assembly dynamics at the nanoscale. *Curr Biol*. Sep 4;17(17):1445-55.
- Schliwa M, Woehlke G.** 2003. Molecular motors. *Nature*. Apr 17;422(6933):759-65.
- Schneider L, Essmann F, Kletke A, Rio P, Hanenberg H, Wetzel W, Schulze - Osthoff K, Nürnberg B, Piekorz RP.** 2007. The transforming acidic coiled coil 3 protein is essential for spindle-dependent chromosome alignment and mitotic survival. *J Biol Chem*. Oct 5;282(40):29273-83
- Scholey JM, Brust-Mascher I, Mogilner A.** 2003. Cell division. *Nature*. Apr 17;422(6933):746-52.
- Schroer TA.** 2004. Dynactin. *Annu Rev Cell Dev Biol*.;20:759-79.
- Schwartz K, Richards K, Botstein D.** 1997. BIM1 encodes a microtubule-binding protein in yeast. *Mol Biol Cell*. Dec;8(12):2677-91.
- Severin F, Hyman AA, Piatti S.** 2001. Correct spindle elongation at the metaphase/anaphase transition is an APC-dependent event in budding yeast. *J Cell Biol*. Nov 26;155(5):711-8.
- Shiina N, Tsukita S.** 1999. Regulation of microtubule organization during interphase and M phase. *Cell Struct Funct*. Oct;24(5):385-91.
- Shirasu-Hiza M, Coughlin P, Mitchison T.** 2003. Identification of XMAP215 as a microtubule-destabilizing factor in Xenopus egg extract by biochemical purification. *J Cell Biol*. Apr 28;161(2):349-58.
- Siegrist SE, Doe CQ.** 2007. Microtubule-induced cortical cell polarity. *Genes Dev*. Mar 1;21(5):483-96.
- Sihag RK, Inagaki M, Yamaguchi T, Shea TB, Pant HC.** 2007. Role of phosphorylation on the structural dynamics and function of types III and IV intermediate filaments. *Exp Cell Res*. Jun 10;313(10):2098-109.

**Sillen A, Barbier P, Landrieu I, Lefebvre S, Wieruszeski JM, Leroy A, Peyrot V, Lippens G.** 2007. NMR investigation of the interaction between the neuronal protein tau and the microtubules. *Biochemistry*. Mar 20;46(11):3055-64.

**Simon JR, Salmon ED.** 1990. The structure of microtubule ends during the elongation and shortening phases of dynamic instability examined by negative-stain electron microscopy. *J Cell Sci*. Aug;96 ( Pt 4):571-82.

**Slautterback DB.** 1963. Cytoplasmic microtubules. I. HYDRA. *J Cell Biol*. Aug;18:367-88.

**Slep KC, Vale RD.** 2007. Structural basis of microtubule plus end tracking by XMAP215, CLIP-170, and EB1. *Mol Cell*. Sep 21;27(6):976-91.

**Slep KC.** 2010. Structural and mechanistic insights into microtubule end-binding proteins. *Curr Opin Cell Biol*. 22:88-95

#### Source WHO

**Spittle C, Charrasse S, Larroque C, Cassimeris L.** 2000. The interaction of TOGp with microtubules and tubulin. *J Biol Chem*. Jul 7;275(27):20748-53.

**Still IH, Vettaikorumakankauv AK, DiMatteo A, Liang P.** 2004. Structure-function evolution of the transforming acidic coiled coil genes revealed by analysis of phylogenetically diverse organisms. *BMC Evol Biol*. Jun 18;4:16.

**Su LK, Burrell M, Hill DE, Gyuris J, Brent R, Wiltshire R, Trent J, Vogelstein B, Kinzler KW.** 1995. APC binds to the novel protein EB1. *Cancer Res*. Jul 15;55(14):2972-7.

**Sweetser DA, Chen CS, Blomberg AA, Flowers DA, Galipeau PC, Barrett MT, Heerema NA, Buckley J, Woods WG, Bernstein ID, Reid BJ.** 2001. Loss of heterozygosity in childhood de novo acute myelogenous leukemia. *Blood*. Aug 15;98(4):1188-94.

**Takahashi K, Kohno T, Matsumoto S, Nakanishi Y, Arai Y, Yamamoto S, Fujiwara T, Tanaka N, Yokota J.** 2007. Clonal and parallel evolution of primary lung cancers and their metastases revealed by molecular dissection of cancer cells. *Clin Cancer Res*. Jan 1;13(1):111-20.

**Tan AL, Rida PC, Surana U.** 2005. Essential tension and constructive destruction: the spindle checkpoint and its regulatory links with mitotic exit. *Biochem J*. Feb 15;386(Pt 1):1-13.

**Tassan JP, Le Goff X.** 2004. An overview of the KIN1/PAR-1/MARK kinase family. *Biol Cell*. Apr;96(3):193-9.

**Tirnauer JS, Canman JC, Salmon ED, Mitchison TJ** . 2002. EB1 targets to kinetochores with attached, polymerizing microtubules. *Mol Biol Cell*. Dec;13(12):4308-16.

**Tirnauer JS, Grego S, Salmon ED, Mitchison TJ**. 2002. EB1-microtubule interactions in *Xenopus* egg extracts: role of EB1 in microtubule stabilization and mechanisms of targeting to microtubules. *Mol Biol Cell*. Oct;13(10):3614-26.

**Tournebize R, Popov A, Kinoshita K, Ashford AJ, Rybina S, Pozniakovskiy A, Mayer TU, Walczak CE, Karsenti E, Hyman AA**. 2000. Control of microtubule dynamics by the antagonistic activities of XMAP215 and XKCM1 in *Xenopus* egg extracts. *Nat Cell Biol*. Jan;2(1):13-9.

**Tsvetkov AS, Samsonov A, Akhmanova A, Galjart N, Popov SV**. 2007. Microtubule-binding proteins CLASP1 and CLASP2 interact with actin filaments. *Cell Motil Cytoskeleton*. Jul;64(7):519-30.

**Ulisse S, Baldini E, Toller M, Delcros JG, Guého A, Curcio F, De Antoni E, Giacomelli L, Ambesi-Impiombato FS, Bocchini S, D'Armiento M, Arlot-Bonnemains Y**. 2007. Transforming acidic coiled-coil 3 and Aurora-A interact in human thyrocytes and their expression is deregulated in thyroid cancer tissues. *Endocr Relat Cancer*. Sep;14(3):827-37.

**Usui T, Maekawa H, Pereira G, Schiebel E**. 2003. The XMAP215 homologue Stu2 at yeast spindle pole bodies regulates microtubule dynamics and anchorage. *EMBO J*. Sep 15;22(18):4779-93.

**Valentine MT, Perlman ZE, Mitchison TJ, Weitz DA**. 2005. Mechanical properties of *Xenopus* egg cytoplasmic extracts. *Biophys J*. Jan;88(1): 680-9.

**Vallee RB, Höök P**. 2006. Autoinhibitory and other autoregulatory elements within the dynein motor domain. *J Struct Biol*. Oct;156(1):175-81.

**van Breugel M, Drechsel D, Hyman A**. 2003. Stu2p, the budding yeast member of the conserved Dis1/XMAP215 family of microtubule-associated proteins is a plus end-binding microtubule destabilizer. *J Cell Biol*. Apr 28;161(2):359-69.

**van Buren V, Odde DJ, Cassimeris L**. 2002 Estimates of lateral and longitudinal bond energies within the microtubule lattice. *Proc Natl Acad Sci U S A*. Apr 30;99(9):6035-40.

**van Buren V, Cassimeris L, Odde DJ**. 2005. Mechanochemical model of microtubule structure and self-assembly kinetics. *Biophys J*. Nov;89(5):2911-26.

**Vanderslice R, Hirsh D**. 1976. Temperature-sensitive zygote defective mutants of *Caenorhabditis elegans*. *Dev Biol*. Mar;49(1):236-49.



**Vasquez RJ, Gard DL, Cassimeris L.** 1994. XMAP from *Xenopus* eggs promotes rapid plus end assembly of microtubules and rapid microtubule polymer turnover. *J Cell Biol.* Nov;127(4):985-93.

**Vasquez RJ, Gard DL, Cassimeris L.** 1999. Phosphorylation by CDK1 regulates XMAP215 function in vitro. *Cell Motil Cytoskeleton.*;43(4):310-21.

**Vaughan PS, Miura P, Henderson M, Byrne B, Vaughan KT.** 2002. A role for regulated binding of p150(Glued) to microtubule plus ends in organelle transport. *J Cell Biol.* Jul 22;158(2):305-19.

**Vaughan KT.** 2004. Surfing, regulating and capturing: are all microtubule-tip-tracking proteins created equal? *Trends Cell Biol.* Sep;14(9):491-6.

**Vaughan KT.** 2005. TIP maker and TIP marker; EB1 as a master controller of microtubule plus ends. *J Cell Biol.* Oct 24;171(2):197-200.

**Vée S, Lafanechère L, Fisher D, Wehland J, Job D, Picard A.** 2001. Evidence for a role of the (alpha)-tubulin C terminus in the regulation of cyclin B synthesis in developing oocytes. *J Cell Sci.* Mar;114(Pt 5):887-98.

**Verde F, Labbé JC, Dorée M, Karsenti E.** 1990. Regulation of microtubule dynamics by cdc2 protein kinase in cell-free extracts of *Xenopus* eggs. *Nature.* Jan 18;343(6255):233-8.

**Verhey KJ, Gaertig J.** 2007. The tubulin code. *Cell Cycle.* Sep 1;6(17): 2152-60.

**Vitre B, Coquelle FM, Heichette C, Garnier C, Chrétien D, Arnal I.** 2008. EB1 regulates microtubule dynamics and tubulin sheet closure in vitro. *Nat Cell Biol.* Apr;10(4):415-21. Epub 2008 Mar 23

**Walczak CE, Heald R.** 2008. Mechanisms of mitotic spindle assembly and function. *Int Rev Cytol.*;265:111-58.

**Wang PJ, Huffaker TC.** 1997. Stu2p: A microtubule-binding protein that is an essential component of the yeast spindle pole body. *J Cell Biol.* Dec 1;139(5): 1271-80.

**Waterman-Storer CM, Karki S, Holzbaur EL.** 1995. The p150Glued component of the dynactin complex binds to both microtubules and the actin-related protein centractin (Arp-1). *Proc Natl Acad Sci U S A.* Feb 28;92(5):1634-8.

**Watson P, Stephens DJ.** 2006. Microtubule plus-end loading of p150 (Glued) is mediated by EB1 and CLIP-170 but is not required for intracellular membrane traffic in mammalian cells. *J Cell Sci.* Jul 1;119(Pt 13):2758-67.

**Weisbrich A, Honnappa S, Jaussi R, Okhrimenko O, Frey D, Jelesarov I, Akhmanova A, Steinmetz MO.** 2007. Structure-function relationship of CAP-Gly domains. *Nat Struct Mol Biol.* Oct;14(10):959-67.

**Westermann S, Weber K.** 2003. Post-translational modifications regulate microtubule function. *Nat Rev Mol Cell Biol.* Dec;4(12):938-47.

**Whittington AT, Vugrek O, Wei KJ, Hasenbein NG, Sugimoto K, Rashbrooke MC, Wasteneys GO.** 2001. MOR1 is essential for organizing cortical microtubules in plants. *Nature.* May 31;411(6837):610-3.

**Wilde A, Zheng Y.** 1999. Stimulation of microtubule aster formation and spindle assembly by the small GTPase Ran. *Science.* May 21;284(5418):1359-62.

**Wu X, Xiang X, Hammer JA 3rd.** 2006. Motor proteins at the microtubule plus-end. *Trends Cell Biol.* Mar;16(3):135-43.

**Yasuhara H, Muraoka M, Shogaki H, Mori H, Sonobe S.** 2002. TMBP200, a microtubule bundling polypeptide isolated from telophase tobacco BY-2 cells is a MOR1 homologue. *Plant Cell Physiol.* Jun;43(6):595-603.

**Zheng Y, Tsai MY.** 2006. The mitotic spindle matrix: a fibro-membranous lamin connection. *Cell Cycle.* Oct;5(20):2345-7.

**Zovko S, Abrahams JP, Koster AJ, Galjart N, Mommaas AM.** 2008. Microtubule plus-end conformations and dynamics in the periphery of interphase mouse fibroblasts. *Mol Biol Cell.* Jul;19(7):3138-46.

**Zumbrunn J, Kinoshita K, Hyman AA, Näthke IS.** 2001. Binding of the adenomatous polyposis coli protein to microtubules increases microtubule stability and is regulated by GSK3 beta phosphorylation. *Curr Biol.* Jan 9;11(1):44-9.

## **APPENDIX**



Table of solutions, buffers, and chemicals I

<b>Method</b>	<b>Buffers</b>	<b>Specification / Composition</b>		<b>Provider</b>	
<b>Tubulin purification</b>	<b>DP</b> (Depolymerisation buffer)	MES	50 mM	Sigma	
		CaCl <sub>2</sub>	1 mM		
	<b>HMPB</b> (High molarity PIPES)	pH: 6.6 with HCl			
		PIPES	1 M		
		MgCl	10 mM		
		EGTA	20 mM		
pH: 6.9 with KOH					
<b>BRB80</b> (Brinkley Buffer 1980)	PIPES	80 mM			
	MgCl <sub>2</sub>	1 mM			
	EGTA	1 mM			
pH: 6.8 with KOH					
	<b>ATP</b>	100 mM			
	<b>GTP</b>	200 mM			
<b>Rhodamine conjugation to tubulin</b>	<b>TAMRA</b>	(5-(and 6)-carboxytetramethylrhodamine, succinimidyl ester)		Molecular Probes	
	<b>High pH cussion</b>	MgCl <sub>2</sub>	1 mM	Sigma	
		EGTA	1 mM		
		Glycerol	60%		
		NaHEPES	v/v		
pH: 8.6 with NaOH		0.1 M			
<b>Low pH cussion</b>	Glycerol	60%			
	In BRB80	v/v			
<b>Labelling buffer</b>	MgCl <sub>2</sub>	1 mM	Sigma		
	EGTA	1 mM			
	Glycerol	40%			
	NaHEPES	v/v			
pH: 8.6 with NaOH		0.1 M			
<b>Aster formation</b>	<b>NiNTA beads</b>		Dynabeads® TALON®		
	<b>GTP</b>	200mM stock, 1mM final	Sigma		
<b>Human and mouse cell culture</b>	<b>RPMI 1640</b>		Gibco®		
	<b>Penicilin/streptomycin</b>	100 U/μg			
	<b>Foetal calf serum</b>	10%			

Table of solutions, buffers, and chemicals II

<i>Method</i>	<i>Buffers</i>	<i>Description</i>	<i>Provider</i>	
Hybridoma Cell culture	<b>RPMI 1640</b>		Gibco®	
	<b>Foetal calf serum</b>	10%		
	<b>Penicillin/ streptomycin</b>	100 U/μg		
	<b>Sodium piruvate</b>	50 μM		
	<b>Non essential amino acids</b>	1%		
	<b>2 Mercaptoethanol</b>	50 μM		
Cell fixing	<b>Methanol</b>		Carlo Erba	
	<b>PBS</b> (Phosphate Buffered Saline)	NaCl 150mM KCl 2.7 nM Na <sub>2</sub> PO <sub>4</sub> 20 mM KH <sub>2</sub> PO <sub>4</sub> 1.8 mM pH: 7.4 with KOH	Gibco®	
	<b>PBS/Triton 100</b>	Triton 100 0.1% in PBS	Sigma	
	<b>PFA 4%</b>	Paraformaldehyde 4% in BRB80		
	Egg Extract obtention	<b>PMSG</b>	Pregnant Mare Serum Gonadotropin, 100 units	Intervet
		<b>HCG</b>	Human Chorionic Gonadotropin	
<b>Protease inhibitors</b>		Leucepeptine Pepstatine A 10 mg/ml Aprotinine		
<b>Cytocholastine B</b>		10 mg/ml		
<b>MMR</b>		NaCl 100 mM KCl 2 mM MgCl <sub>2</sub> 1 mM CaCl <sub>2</sub> 2 mM EDTA 0.1 mM HEPES 5 mM pH: 7.8 with NaOH	Sigma	
<b>Dejelling</b>		Cysteine 2% EGTA 1 mM In distilled water pH: 7.8		

Table of solutions, buffers, and chemicals III

<i>Method</i>	<i>Buffers</i>	<i>Description</i>		<i>Provider</i>
<b>Egg Extract obtention... cont</b>	<b>XB</b>	KCl	100 mM	Sigma
		MgCl <sub>2</sub>	1 mM	
		CaCl <sub>2</sub>	0,1 mM	
		K-HEPES	10 mM	
		Sucrose	50 mM	
		pH: 7.7 with KOH		
	<b>CSF-XB</b>	MgCl <sub>2</sub>	2 mM	
		EGTA	5 mM	
		In XB buffer pH: 7.7 with KOH		
<b>XMAP215 depletion</b>	<b>Protein A beads</b>			Dynabeads®
	<b>PBS/Tx 0,1%</b>	Triton 100 in PBS	0,1%	
<b>Electrophoresis</b>	<b>SDS-PAGE</b>	<b>SDS-PAGE:</b>		
	<b>Molecular weight markers</b>	Precision Plus Protein™ Standards. All blue		Biorad
	<b>Migration buffer</b>	Tris	50 mM	
		SDS	1%	
		Glycine	384 mM	
		pH: 6.8		
	<b>Loading Buffer (Laemmli 5X)</b>	Tris	50 mM	Sigma
		SDS	2%	
		Glycerol	10%	
		β-mercaptoethanol	10%	
		Bromophenol blue	10%	
	<b>Comassie Blue</b>	Comassie brilliant blue R	0,5% 40%	
		Methanol	7%	
		Acetic Acid		
<b>Western Blot</b>	<b>Transfert buffer</b>	Tris	25 mM	Sigma
		Methanol	20%	
		Glycine	192%	

**Table of solutions, buffers, and chemicals IV**

<i>Method</i>	<i>Buffers</i>	<i>Description</i>	<i>Provider</i>
<b>Western Blot... cont</b>	<b>Red Ponceau</b>	Red ponceau S Trichloroacetic acid Methanol	1% 0.3% 50% Sigma





## ABSTRACT

**XMAP215** and **ch-TOG** are the *Xenopus laevis* and human members of an evolutionary conserved family of microtubule-associated proteins. In all studied species, proteins related to XMAP215/ch-TOG play multiple roles in the regulation of the microtubule cytoskeleton. In this work we developed a panel of monoclonal antibodies (**mcABs**) to reveal that at the tips of polymerizing microtubules XMAP215/ch-TOG adopts a distinct conformation, which is different from that all along the rest of the microtubule. Using these mcABs, we compared ch-TOG localization with that of EB1, p150<sup>Glued</sup> and CLIP170 - known microtubule plus-end tracking proteins (**+TIPs**) - and established a hierarchy of their respective “comet”- like staining. Analysis showed that ch-TOG (**+TIP XMAP215/ch-TOG**) occupies the most distal relative to microtubules tips position. Using fluorescently-labelled anti +TIP XMAP215/ch-TOG mcAB in *Xenopus* egg extracts as a conformational sensor to track (+) ends of microtubules, we showed that the +TIP XMAP215 specific conformation of XMAP215 capped the ends of both growing and shrinking microtubules. Cryo-electron microscopy study of growing microtubules assembled in pure tubulin solution indicated that XMAP215 promoted the formation of outwardly curved tubulin sheets. Based on our results we propose a model according to which: (i) XMAP215 allows the tubulin dimmers loading on its surface, forming a protofilament-like structure. (ii) XMAP215 is continuously recruited to the tips of growing microtubules, promoting an outwardly curved sheet structures as the tubulin dimmers are added and possibly, the MT structure is closed.

Keywords: XMAP215, ch-TOG, microtubules, microtubule dynamics, cell cycle